**Title**
Aspects of Holography And Quantum Error Correction



**Author**
Rath, Pratik

**Publication Date**
2020

Peer reviewed|Thesis/dissertation

# Aspects of Holography And Quantum Error Correction

by

Pratik Rath

A dissertation submitted in partial satisfaction of the

requirements for the degree of

Doctor of Philosophy

in

Physics

in the

Graduate Division

of the

University of California, Berkeley

Committee in charge:

Professor Yasunori Nomura, Chair
Professor Raphael Bousso
Professor Richard Borcherds

Summer 2020

Aspects of Holography And Quantum Error Correction

Abstract

Aspects of Holography And Quantum Error Correction

by

Pratik Rath

Doctor of Philosophy in Physics

University of California, Berkeley

Professor Yasunori Nomura, Chair

The holographic principle has been a central theme in most of the progress in the field of quantum gravity in recent years. Our understanding of the AdS/CFT duality, the best known embodiment of the holographic principle, has taken a quantum leap in the last decade. A key role in the elucidation of how the holographic duality functions has been played by ideas from quantum information theory. In particular, the modern understanding of the holographic dictionary is that it works as a quantum error correcting code.

In this dissertation, we focus on a two-pronged approach to developing a deeper insight into the framework of quantum gravity. Firstly, despite the fact that we have learnt a lot about quantum gravity from AdS/CFT, it is not directly applicable to our universe which is an accelerating cosmological spacetime. Taking inspiration from the holographic principle and formulating ideas from AdS/CFT in the abstract language of quantum error correction, we take some preliminary steps in freeing ourselves from the crutches of AdS spacetimes and understanding features of holography in a wider class of spacetimes. We develop a framework for holography in general spacetimes using the Ryu-Takayanagi formula as a postulate and discuss conditions for bulk reconstruction, the existence of a bulk dual and qualitative features of putative holographic theories in arbitrary spacetimes.

Secondly, the holographic dictionary is not completely understood even within the realm of AdS/CFT. We clarify some aspects and propose novel entries to the AdS/CFT dictionary which shed light on how a gravitational description of a quantum mechanical system emerges holographically. In particular, this includes an understanding of how the holographic computation of Renyi entropy arises from a general feature of quantum error correction, supplemented by the special property that gravitational states have maximally mixed edge modes. Further, we resolve a long standing conjecture about the nature of tripartite entanglement of holographic states. Finally, we propose novel holographic duals to the reflected entropy in the presence of entanglement islands, and the Connes cocycle flow.

To my parents,

Bratati Dash and Pradyot Kumar Rath,

for their limitless trust in my passion and eternal support in my endeavour,

and

to my wife,

Shoan Jain,

for her vital role in this often arduous process.

# Contents

# List of Figures

## Acknowledgments

I am indebted to my research advisor, Yasunori Nomura, for his support, guidance and encouragement through my experience at graduate school. Collaborating with him and seeing his passion for research has inspired me to strive for excellence. Time and again he went out of his way to help me in my pursuits and I'm very grateful for the freedom he gave me in exploring collaborations with other researchers.

I am also very grateful to Raphael Bousso, who has been a great mentor throughout my graduate life. Collaborating with him and his group has been extremely enlightening, and these interactions have helped me guide my research interests.

I would also like to thank Richard Borcherds for agreeing to be on my dissertation committee and Marjorie Shapiro for agreeing to be a part of my qualifying exam committee.

I would like to especially thank Chris Akers who has had an extremely positive influence on my academic career and collaborating with whom has been a delightful experience. I would also like to thank all my previous and current collaborators - Nico Salzetta, Chitraang Murdia, Masamichi Miyaji, Ven Chandrasekaran, Arvin Shahbazi Moghaddam, Mudassir Moosa, Vincent Su, Thomas Faulkner and Simon Lin.

I have benefited enormously from a great research environment at BCTP and UC Berkeley. I would like to extend my heartfelt thanks to Ning Bao, Newton Cheng, David Dunsky, Bryce Kobrin, Illan Halpern, Stefan Leichenauer, Adam Levine, Francisco Machado, Hugo Marrochio, Grant Remmen, Evan Rule, Fabio Sanches, Christian Schmid, Reggie Caginalp, Tommy Schuster and Misha Usatyuk for valuable discussions.

I have also benefited tremendously from discussions with other researchers in the field of quantum gravity. I would like to extend my gratitude to Xi Dong, Daniel Harlow, Matt Headrick, Don Marolf, Rob Myers, Vasudev Shyam, Eva Silverstein, Ronak Soni and Aron Wall for useful discussions and positive feedback.

I would like to thank all my family members for constant encouragement and all the sacrifices they've made for me. A special thanks goes to my parents-in-law who have been extremely caring, considerate and supportive of my love for physics.

Last but not remotely the least, I would like to give a heartfelt thanks to all my friends who have been a constant source of support through my graduate school experience and who make this journey meaningful - Ayush Asthana, Mallika Bariya, Shashank Bhandari, Supranta Sarma Boruah, Sarthak Chandra, Swati Choudhary, Aanchal Jain, Akash Goel, Shashank Gupta, Varun Harbola, Monika Mahto, Sanjay Moudgalya, Arvind Singh Rathore, Anurag Sahay, Prateek Sahu, Nitica Sakharwade, Pratik Somani and Dhruv Kumar Yadav, among many others.

# Chapter 1

# Introduction

## 1.1 The Holographic Principle

Last century brought about deep insights into the way nature works, with the establishment of two of the founding pillars of modern physics - quantum mechanics and general relativity. Each of them have led to remarkable predictions that have been tested to a great accuracy and have helped unravel many mysteries of our universe. However, efforts to combine them into a unified theory of quantum gravity have faced various technical and fundamental issues. In a nutshell, we do not as yet have a concrete conceptual framework for quantum gravity, which we require to answer deep questions about, for instance, cosmology.

Since quantum gravity effects are often hard to test experimentally, we need theoretical principles to guide us in a bottom-up pursuit of a complete theory of everything. A theoretical window into a deeper understanding of quantum gravity comes from black holes, which arise as classical solutions to general relativity and nevertheless, also exhibit important quantum effects such as Hawking radiation [1, 2]. Some of the most important conceptual puzzles, the black hole information paradox and its modern variants like the firewall paradox, arise from requiring the consistency of the equivalence principle, a feature at the heart of general relativity, and unitarity, an equally important property of quantum mechanics [3, 4, 5]. Despite the fact that many of these problems haven't been resolved to a requisite degree of satisfaction, the physics of black holes from a low energy perspective often teaches us a great deal about the high energy physics of quantum gravity.

In particular, it is well understood that black holes behave like thermal objects, satisfying the well known laws of thermodynamics [6]. The crucial peculiarity that they demonstrate, however, is that the entropy of a black hole is given by the Bekenstein-Hawking formula [7]

$$S_{\rm BH} = \frac{\mathcal{A}}{4G_N}, \tag{1.1}$$

where $\mathcal{A}$ is the area of the black hole horizon. Most thermal systems, such as a box of gas, have an entropy that scales with the volume of the system. Thus, it is highly unusual that the entropy of the black hole in fact scales with its area.

Having associated an entropy to black holes, consistency with the second law of thermodynamics led Bekenstein to conjecture a bound on the amount of matter entropy content in a given region [8]. Namely, he proposed that the amount of entropy in a region $R$ can never exceed the entropy of a black hole fitting inside the region $R$, i.e., $\mathcal{A}(\partial R)/4G_N$. Although violations to the Bekenstein bound were found, a different version, the covariant entropy bound, has been consistent with all known examples and in fact, proved in certain regimes [9, 10, 11]. The covariant entropy bound states that

$$S_{\text{LS}} \leq \frac{\mathcal{A}(\partial R)}{4G_N}, \tag{1.2}$$

where $S_{\text{LS}}$ is the matter entropy on a light-sheet, a null hypersurface shot out from $\partial R$ in any one of the directions of negative expansion.

This holographic bound on the amount of entropy in a given gravitating region begs for an explanation. It was proposed that a satisfying explanation for this property would be that the quantum gravity degrees of a freedom in a given region $R$ in fact live on its boundary $\partial R$ as a hologram describing all the physics inside it [12, 13]. This idea, termed the holographic principle will be a driving force in much of the work described in this dissertation.

The holographic principle is in fact backed by evidence from some of the best understood top-down approaches to quantum gravity. String theory has been a leading candidate for a theory of quantum gravity which resolves many of the technical issues faced in quantizing gravity. Despite the fact that a complete understanding of non-perturbative string theory eludes us at the moment, it has given rise to the most concrete realization of the holographic principle, the AdS/CFT correspondence. The AdS/CFT correspondence is a duality between quantum gravity in anti-de Sitter (AdS) spacetime, a solution to Einstein's equations with a negative cosmological constant, and a conformal field theory (CFT) living on the boundary of the spacetime [14, 15, 16]. This duality is a perfect embodiment of the holographic principle, an ordinary non-gravitational theory living on the holographic boundary of spacetime, in one lesser dimension, that describes the gravitational physics in the spacetime [17]. Inspired by this, we will take seriously the possibility that quantum gravity is described by such a holographic theory more generally, beyond just the example of the AdS/CFT correspondence.

## 1.2 AdS/CFT and Quantum Error Correction

A big step in understanding holography came in 2006, when Ryu and Takayanagi realized that the Bekenstein-Hawking entropy formula, Eq. (1.1), was in fact a special case of a much more general formula for the entanglement entropy of subregions in the CFT [18, 19],

$$S(R) = \frac{\mathcal{A}(\gamma_R)}{4G_N}, \tag{1.3}$$

where $R$ is a subregion of the CFT and $\gamma_R$ is the Ryu-Takayanagi (RT) surface, a bulk surface of minimal area anchored to the entangling surface $\partial R$. This entry to the AdS/CFT

dictionary was soon updated to include time dependence and quantum corrections [20, 21, 22], and currently reads

$$S(R) = \frac{\mathcal{A}(\gamma_R)}{4G_N} + S_{\text{bulk}}(\text{EW}(R)), \tag{1.4}$$

where $\gamma_R$ is the quantum extremal surface (QES) found by extremizing the quantity on the right hand side. EW($R$), termed the entanglement wedge, is the domain of dependence of a partial Cauchy slice $\Sigma_R$ in the bulk such that $\partial\Sigma_R = R \cup \gamma_R$.

The QES formula in turn implied that the AdS/CFT dictionary has the feature of subregion duality, i.e., the boundary subregion $R$ has access to all the information about the bulk in its associated entanglement wedge EW($R$) [23, 24, 25]. Although subregion duality initiall led to some naive paradoxes, it was beautifully explained by thinking of semiclassical states of the bulk gravitational theory as being encoded in the boundary theory via the mechanism of quantum error correction [26]. More precisely, the Hilbert space of semiclassical bulk states $\mathcal{H}_{\text{bulk}}$ is unitarily mapped to a subspace $\mathcal{H}_{\text{code}}$ of the boundary Hilbert space $\mathcal{H}_{\text{CFT}}$. This mapping is such that the action of bulk operators in the region EW($R$) can be faithfully represented by boundary operators in the subregion $R$.

Moreover, it was shown that a version of the RT formula holds in any quantum error correcting code [27]. Thus, the existence of an RT formula goes hand in hand with the property of subregion duality. Remarkable examples of quantum error correcting codes where subregion duality and a geometric RT formula hold are tensor networks (TNs), which serve as toy models for holography [28, 29]. Interestingly, TNs, whose graph structure can be thought of as a discretized version of the bulk geometry it represents, are not bound to be hyperbolic as they would in cases relevant to AdS/CFT. This makes it seem plausible that Eq. (1.4) and the feature of subregion duality could hold quite broadly in quantum gravity. In this dissertation, we will take the RT formula as a guiding principle for the framework of quantum gravity and utilize it in general non-AdS spacetimes.

## 1.3 Holography in General Spacetimes

Part I of this dissertation focuses on applying ideas inspired from AdS/CFT to more general spacetimes. In order to do so, we first need to understand where the holographic description of the spacetime lives, i.e., what is the analogue of the boundary of AdS in an arbitrary spacetime. Using the covariant entropy bound, it was proposed that "holographic screens" provide the natural location for a holographic theory describing a general spacetime [30]. Holographic screens are hypersurfaces foliated by marginally trapped/anti-trapped surfaces which provide the most optimal bound on the entropy in a spacetime. In AdS, the holographic screen approaches the boundary as expected. More generally, holographic screens are highly non-unique, perhaps suggesting different holographic descriptions for different patches of spacetime.

A framework for understanding holography in general spacetimes based on the above principles was laid out in [31]. Given a choice of holographic screen $H$ in a spacetime $\mathcal{M}$, we postulate that states living on constant time surfaces of $H$ describe the gravitational physics of the interior of $H$. Importantly, as described before, we postulate that such states satisfy the RT formula, Eq. 1.4. We then derive various consequences of these postulates to probe whether this is a reasonable hypothesis. We now briefly summarize the contents of this part of the dissertation.

In Chapter 2, we argue that classical spacetimes represent information that is amplified by a redundant encoding in the holographic theory of quantum gravity. In general, classicalization of a quantum system involves making this information robust at the cost of exponentially reducing the number of observables. In quantum gravity, the geometry of spacetime must be the analogously amplified information. Bulk local semiclassical operators probe this information without disturbing it; these correspond to logical operators acting on code subspaces of the holographic theory. From this viewpoint, we study how local bulk operators may be realized in a holographic theory of general spacetimes, which includes AdS/CFT as a special case, and deduce its consequences. In the first half of this chapter, we ask what description of the bulk physics is provided by a holographic state dual to a semiclassical spacetime. In particular, we analyze what portion of the bulk can be reconstructed as spacetime in the holographic theory. We characterize the set of points reconstructable by dressing local operators to the intersection of entanglement wedges, which allows us to go beyond entanglement shadows. The analysis also indicates that when a spacetime contains a quasi-static black hole inside a holographic screen, the theory provides a description of physics as viewed from the exterior. In the second half, we study how and when a semiclassical description emerges in the holographic theory. We find that states representing semiclassical spacetimes are non-generic in the holographic Hilbert space. If there are a maximal number of independent microstates, semiclassical operators must be given state-dependently; we elucidate this point using the stabilizer formalism and tensor network models. We also discuss possible implications of the present picture for the black hole interior. This chapter is based on Ref. [32].

In Chapter 3, we attempt to unravel the fascinating relationship between entanglement and emergent spacetime. It was broadly understood that entanglement between holographic degrees of freedom is crucial for the existence of bulk spacetime [33]. We examine this connection from the other end of the entanglement spectrum and clarify the assertion that maximally entangled states in fact have no reconstructable spacetime. To do so, we first define the conditions for bulk reconstructability. Under these terms, we scrutinize two cases of maximally entangled holographic states. One is the familiar example of AdS black holes, which are dual to thermal states of the boundary CFT. Sending the temperature to the cutoff scale makes the state maximally entangled and the respective black hole consumes the spacetime. We then examine the de Sitter limit of FRW spacetimes. This limit is maximally entangled if one formulates the boundary theory on the holographic screen. Paralleling the AdS black hole, we find the resulting reconstructable region of spacetime vanishes. Motivated by these results, we prove a theorem showing that maximally entangled states have no

reconstructable spacetime. Evidently, the emergence of spacetime requires intermediate entanglement. By studying the manner in which intermediate entanglement is achieved, we uncover important properties about the boundary theory of FRW spacetimes. With this clarified understanding, our final discussion elucidates the natural way in which holographic Hilbert spaces may house states dual to different geometries. This paper provides a coherent picture clarifying the link between spacetime and entanglement and develops many promising avenues of further work. This chapter is based on Ref. [34].

In Chapter 4, we introduce a novel, covariant bulk object—the holographic slice. This construction is motivated by the ability to consistently apply the RT prescription for general convex surfaces and is inspired by the relationship between entanglement and geometry in tensor networks. The holographic slice is found by considering the continual removal of short range information in a boundary state. It thus provides a natural interpretation as the bulk dual of a series of coarse-grained holographic states. The slice possesses many desirable properties that provide consistency checks for its boundary interpretation. These include monotonicity of both area and entanglement entropy, uniqueness, and the inability to probe beyond late-time black hole horizons. Additionally, the holographic slice illuminates physics behind entanglement shadows, as minimal area extremal surfaces anchored to a coarse-grained boundary may probe entanglement shadows. This lets the slice flow through shadows. To aid in developing intuition for these slices, many explicit examples of holographic slices are investigated. Finally, the relationship to tensor networks and renormalization (particularly in AdS/CFT) is discussed. This chapter is based on Ref. [35].

## 1.4 Holographic Dictionary

Part II of this dissertation focuses on a better understanding of the holographic dictionary within the realm of AdS/CFT. A particular emphasis is laid on the abstract understanding of holography as quantum error correction, so that most of the ideas discussed could also apply in general spacetimes. This includes a detailed understanding of the entanglement structure of holographic states and proposals for the holographic duals of various information theoretic quantities. We now briefly summarize the contents of this part of the dissertation.

In Chapter 5, we discuss the applicability of the RT formula in a limited regime beyond the realm of AdS/CFT. A concrete step towards understanding holography in general spacetimes is to first understand the emergence of sub-AdS locality in AdS/CFT. The $T\bar{T}$ deformation, proposed to be dual to finite cutoff holography, serves as a rare, solvable irrelevant deformation and thus, gives tractable QFT tools to approach the problem of sub-AdS locality. In this chapter, we explain the success of the RT formula in $TT$ deformed theories based on an argument similar to the proof of the RT formula in AdS/CFT [36]. We emphasize general arguments that justify the use of the RT formula in general holographic theories that obey a GKPW-like dictionary [15, 16]. In doing so, we clarify subtleties related to holographic counterterms and discuss the implications for holography in general spacetimes. This chapter is based on Ref. [37].

In Chapter 6, we study Renyi entropies $S_n$ in quantum error correcting codes and compare the answer to the cosmic brane prescription for computing $\widetilde{S}_n \equiv n^2\partial_n(\frac{n-1}{n}S_n)$. We find that general operator algebra codes have a similar, more general prescription. Notably, for the AdS/CFT code to match the specific cosmic brane prescription, the code must have maximal entanglement within eigenspaces of the area operator. This gives us an improved definition of the area operator, and establishes a stronger connection between the Ryu-Takayanagi area term and the edge modes in lattice gauge theory. We also propose a new interpretation of existing holographic tensor networks as fixed area eigenstates instead of smooth geometries. This interpretation would explain why tensor networks have historically had trouble modeling the Renyi entropy spectrum of holographic CFTs, and it suggests a method to construct holographic networks with the correct spectrum. This chapter is based on Ref. [38].

In Chapter 7, we argue that holographic CFT states require a large amount of tripartite entanglement, in contrast to the conjecture that their entanglement is mostly bipartite [39]. Our evidence is that this mostly-bipartite conjecture is in sharp conflict with two well-supported conjectures about the entanglement wedge cross section surface $EW$ [40, 41, 42]. If $EW$ is related to either the CFT's reflected entropy or its entanglement of purification, then those quantities can differ from the mutual information at $\mathcal{O}(\frac{1}{G_N})$. We prove that this implies holographic CFT states must have $\mathcal{O}(\frac{1}{G_N})$ amounts of tripartite entanglement. This proof involves a new Fannes-type inequality for the reflected entropy, which itself has many interesting applications. In doing so, we also show that random stabilizer tensor networks, although a promising, analytically tractable model for various purposes, in fact are inconsistent with holography. This chapter is based on Ref. [43].

In Chapter 8, we propose a new formula for the reflected entropy that includes contributions from entanglement islands. Contributions from entanglement islands have recently been understood to be crucial when computing the entanglement entropy in QFT states coupled to regions of semiclassical gravity [44, 45, 46, 47, 48, 49, 50]. Inspired by this, we derive this new formula for the reflected entropy from the gravitational path integral by finding additional saddles that include generalized replica wormholes. We also demonstrate that our covariant formula satisfies all the inequalities required of the reflected entropy. We use this formula in various examples that demonstrate its relevance in illustrating the structure of multipartite entanglement that are invisible to the entropies. This chapter is based on Ref. [51].

In Chapter 9, we define the "kink transform" as a one-sided boost of bulk initial data about the Ryu-Takayanagi surface of a boundary cut. For a flat cut, we then conjecture that the resulting Wheeler-DeWitt patch is the bulk dual to the boundary state obtained by Connes cocycle (CC) flow across the cut. The bulk patch is glued to a precursor slice related to the original boundary slice by a one-sided boost. This evades ultraviolet divergences and distinguishes our construction from one-sided modular flow. We verify that the kink transform is consistent with known properties of operator expectation values and subregion entropies under CC flow. CC flow generates a stress tensor shock at the cut, controlled by a shape derivative of the entropy; the kink transform reproduces this shock holographically

by creating a bulk Weyl tensor shock. We also go beyond known properties of CC flow by deriving novel shock components from the kink transform. This chapter is based on Ref. [52].

# Part I

# Holography in General Spacetimes

# Chapter 2

# Classical Spacetimes as Amplified Information in Holographic Quantum Theories

## 2.1 Introduction

Emergence of classical spacetimes from the fundamental theory of quantum gravity is an important problem. In general, classicalization of a quantum system involves a large reduction of possible observables. Suppose the final state of a scattering experiment is $c_A|A\rangle + c_B|B\rangle$, where $|A\rangle$ and $|B\rangle$ are two possible particle states. In principle, one can measure this state in any basis in the space spanned by $|A\rangle$ and $|B\rangle$. Classicalization caused by the dynamics, however, makes this state evolve into a superposition of two classical worlds of the form $c_A|AAA\cdots\rangle + c_B|BBB\cdots\rangle$, in which the information about the final particles is amplified in each branch [53, 54, 55]. In these classicalized worlds, the appropriate observable is only a binary question, $A$ or $B$, instead of continuous numbers associated with $c_A$ and $c_B$. At the cost of this reduction of observables, however, the information $A$ and $B$ is now robust—it can be probed by many physical entities of the system, and hence is classical. We note that the information amplified may depend on the state, e.g. the configuration of a detector. (You can imagine $|A\rangle$ and $|B\rangle$ being the spin up and down states of a spin-1/2 particle.) Given a state, however, the amount of information amplified is only an exponentially small subset of the whole microscopic information.

In quantum gravity, the information of the semiclassical spacetimes must be analogously amplified. At the level of a semiclassical description, this information appears in the two-point functions of quantum field operators (a class of operators defined in code subspaces of the holographic theory [26, 28, 27]). At the fundamental level, this arises mainly from entanglement entropies between the holographic degrees of freedom [18, 20, 36]. Note that entanglement entropies are numbers, so they comprise only an exponentially small fraction of the whole quantum information that the fundamental degrees of freedom may have, and

hence the corresponding information may appear multiple times, e.g., in the propagators of different low energy fields. This implies, in particular, that spacetime exists only to the extent that we can erect the corresponding code subspace in which the notion of local bulk operators can be defined.

In this paper, we pursue this picture in the context of a holographic theory for general spacetimes developed in Ref. [31] (which includes AdS/CFT as a special case). Key assumptions in our analyses are

(i) The holographic theory has degrees of freedom that appear local at lengthscales larger than a cutoff $l_c$. When a semiclassical description is available, the effective density of these degrees of freedom is 1/4 in units of the bulk Planck length.

(ii) If a holographic state represents a semiclassical spacetime, the area of the minimal area extremal surface (the HRT surface [20]) anchored to the boundary of a region $\Gamma$ on a leaf $\sigma$ of a holographic screen gives the entanglement entropy of $\Gamma$ in the holographic theory [56].

(iii) A quantum mechanical version of the statement (ii) above, analogous to those obtained/conjectured in the AdS/CFT case [21, 22], is valid.

In Ref. [31], a few possible structures for the holographic Hilbert space have been discussed, consistent with these assumptions. Our analyses in this paper, however, do not depend on the details of these structures, so we will be mostly agnostic about the structure of the holographic Hilbert space beyond (i)–(iii) above.

We emphasize that the items listed above, especially (ii) and (iii), are assumptions. They are motivated by bulk reconstruction in AdS/CFT, but for general spacetimes their basis is weaker. However, the structures in (ii) and (iii) do not seem to be particularly tied to the asymptotic AdS nature [27, 29], and there are analyses suggesting that they may indeed apply to more general spacetimes [56, 57]. Our philosophy here is to adopt them as guiding principles in exploring the structure of the (putative) holographic theory of general spacetimes. In particular, we investigate what bulk spacetime picture the general holographic theory provides and how it may arise from the fundamental microscopic structure of the theory.

Our analyses of these issues are divided into two parts. In the first part, we study the question: given a holographic state that represents a semiclassical spacetime,[1] what description of the bulk physics does it provide? For this purpose, we employ the tool developed by Sanches and Weinberg in AdS/CFT [58], which allows us to identify the region in the bulk described by a local semiclassical field theory. To apply it in our context, however, we need an important modification. To describe a general spacetime, it is essential to fix a reference frame, which corresponds to choosing a gauge for the holographic redundancy [55]. In the

[1] By a semiclassical spacetime, we mean a curved manifold on which a low energy effective field theory can be erected. A holographic state representing a semiclassical spacetime, however, does not necessarily describe the whole spacetime region in the interior of the holographic screen.

bulk picture, this amounts to erecting a specific holographic screen with definite time slicing. In fact, this time slicing has a special significance [59]: it is the preferred time foliation in the sense that other foliations of the same holographic screen do not lead to equal-time hypersurfaces that satisfy the defining characteristic of leaves (i.e. marginal surfaces).

This leads us to propose that the holographic description of a general spacetime in a given reference frame provides a local field theoretic description in the region consisting of a point $p$ that can be written as

$$p = \bigcap_{\Gamma} \mathrm{EW}(\Gamma), \tag{2.1}$$

where $\mathrm{EW}(\Gamma)$ is the entanglement wedge [60, 61] of $\Gamma$, and $\Gamma$ must be chosen from spatial regions on leaves of the holographic screen in the given reference frame. We find that this criterion allows us to reconstruct most of the region inside the holographic screen for regular spacetimes, including some entanglement shadows: regions which the HRT surfaces do not probe. In AdS/CFT, the region reconstructable in this way seems to agree with the region obtained in Ref. [58] using the analogous criterion, in which $\Gamma$ is chosen from the set of all the codimension-one achronal submanifolds of the AdS boundary.[2]

We show that for a point $p$ to be reconstructable, it is sufficient that all the future-directed and past-directed light rays emanating from $p$ reach outside the entanglement shadow early enough. We also argue that for $p$ to be reconstructable, at least one future-directed *and* past-directed light ray from $p$ must escape the shadow region. This latter condition implies that the interior of a black hole cannot be reconstructed as local spacetime (except in transient periods, e.g., just after the formation), since the horizon of a quasi-static black hole serves as an extremal surface barrier [62]. On the other hand, the analyses of Refs. [23, 24] suggest that the information about the interior is somehow contained in the holographic state, since the entanglement wedges of leaf regions cover the interior. We interpret these to mean that the description of a black hole provided by the holographic theory is that of a distant picture: the information about the interior is contained in the stretched horizon degrees of freedom [63] whose dynamics is not described by local field theory in the bulk.

This does not exclude the possibility that there is an effective description that makes a portion of the interior spacetime manifest by appropriately rearranging degrees of freedom. We expect that such a description, if any, would be possible only at the cost of the local description in some other region, and it would be available only for a finite time measured with respect to the degrees of freedom made local in this manner. We will discuss possible implications of our picture for the issue of the black hole interior [4, 5, 64] at the end of this paper.

In the second part of our analyses, we study how and when a semiclassical description emerges in the holographic theory. We first argue that when the holographic space of volume

[2]This statement applies if the topology of the boundary space is simply connected as we focus on in this paper. If it is not, in particular if the boundary space consists of disconnected components as in the case of a two-sided black hole, then the two procedures lead to different physical pictures. This will be discussed in Ref. [34]

$\mathcal{A}$ is regarded as consisting of $N_{\mathcal{A}}$ cutoff-size cells, the number of degrees of freedom, $\ln k$, in each cell should be large. This is because entanglement between different subregions is robust only when many degrees of freedom are involved. When a semiclassical description is available, $\ln k$ is related to the strength of gravity in the bulk:

$$\ln k = \frac{\mathcal{A}}{4l_{\rm Pl}^{d-1}N_{\mathcal{A}}} \quad (\gg 1), \tag{2.2}$$

where $l_{\rm Pl}$ is the Planck length in the $(d+1)$-dimensional bulk. The large number of degrees of freedom in each cell implies that the holographic theory can encode information about the bulk in the configuration of these degrees of freedom, as well as in entanglement entropies between subregions. Given that local semiclassical operators in the reconstructable region carry the entanglement entropy information, we might expect that the information about the other regions of spacetime is encoded mostly in the degrees of freedom within the cells.

Including the degrees of freedom in each cell, the holographic space can accommodate up to $e^{\mathcal{A}/4}$ independent microstates for the same semiclassical spacetime. Our analysis indicates that a generic state in the holographic Hilbert space does not admit a semiclassical spacetime interpretation within the holographic screen. In other words, bulk gravitational spacetime emerges only as a result of non-genericity of states in the holographic Hilbert space. Suppose there is a spacetime $\mathcal{M}$ that has $e^{\mathcal{A}/4}$ independent microstates. Assumption (ii) above then tells us that the microstates for such a spacetime $\mathcal{M}$ cannot form a Hilbert space—if it did, a generic superposition of these states would still represent $\mathcal{M}$ and yet have an entanglement structure that is different from what is implied by (ii).

At the leading order in $1/\mathcal{A}$, the space of microstates is *at most* the group space of $U(k)^{\mathcal{N}_{\mathcal{A}}}$, which preserves the entanglement structure between local degrees of freedom in the holographic theory. This space is tiny compared with $\mathcal{H}_{\mathcal{A}}$, i.e. the group space of $U(k^{\mathcal{N}_{\mathcal{A}}})$: $\|U(k)^{\mathcal{N}_{\mathcal{A}}}\| \lll \|U(k^{\mathcal{N}_{\mathcal{A}}})\|$. The actual space for the microstates, however, can be even smaller.

If the microstates comprise the elements of $U(k)^{\mathcal{N}_{\mathcal{A}}}$, then it has $e^{\mathcal{A}/4}$ independent microstates. In this case, the semiclassical operators associated with these microstates must be state-dependent as argued by Papadodimas and Raju for the interior of a large AdS black hole [65, 66]. This is because the code subspaces relevant for these microstates have nontrivial overlaps in the holographic Hilbert space.

What happens if microstates comprise (essentially) only a discrete $e^{\mathcal{A}/4}$ "axis" states? In this case, different code subspaces can be orthogonal, so that one might think that semiclassical operators can be defined state-independently without any subtlety. However, we argue that semiclassical operators still cannot be state-independent in this case. This is because a semiclassical operator is represented redundantly on subregions of the holographic space as a result of amplifying the information about spacetime. The necessity of state-dependence, therefore, is robust if any given spacetime $\mathcal{M}$ has $e^{\mathcal{A}/4}$ independent microstates.

The organization of this paper is as follows. In Section 2.2, we review our framework of the holographic theory of general spacetimes. In Section 2.3, we discuss the role of information amplification in classicalization. In Section 2.4, we present the first part of our

analyses. We study what portion of the bulk is directly reconstructable from a holographic state, for spacetimes without an entanglement shadow, with reconstructable shadows, and with non-reconstructable shadows. In Section 2.5, we present the second part, in which we study how and when a semiclassical description emerges. We discuss general features of the holographic encoding of spacetimes and non-genericity of semiclassical states. In Section 2.6, we conclude with remarks on possible implications of our picture for the black hole interior.

Throughout the paper, we adopt the unit in which the length $l_{\rm Pl}$—which corresponds to the bulk Planck length when the semiclassical picture is available—is set to unity.

## 2.2 Framework

The holographic degrees of freedom live in a holographic space, which can be identified as a leaf of the holographic screen [67] when the state admits a semiclassical interpretation. For definiteness, we assume that the holographic redundancy is fixed in the observer centric manner [68, 55]—the future-directed ingoing light rays emanating orthogonally from the leaf meet at a spacetime point (associated with the origin of a freely falling reference frame), unless these light rays hit a singularity before this happens.

The size (volume) of the holographic space changes as a function of time. The Hilbert space relevant for the holographic degrees of freedom can thus be regarded as[3]

$$\mathcal{H} = \bigoplus_{\mathcal{A}} \mathcal{H}_{\mathcal{A}}, \tag{2.3}$$

where $\mathcal{H}_{\mathcal{A}}$ is the Hilbert space for the states of the degrees of freedom living in the holographic space of volume between $\mathcal{A}$ and $\mathcal{A}+\delta\mathcal{A}$; namely, we have grouped classically continuous values of $\mathcal{A}$ into a discrete set by regarding the values between $\mathcal{A}$ and $\mathcal{A}+\delta\mathcal{A}$ as the same and labeling them by $\mathcal{A}$. As in standard statistical mechanics, the precise way this grouping is done is not important (unless $\delta\mathcal{A}$ is taken exponentially small in $\mathcal{A}$, which is equivalent to resolving microstates and hence is not a meaningful choice).

The dimension of $\mathcal{H}_{\mathcal{A}}$ is given by

$$\ln \dim \mathcal{H}_{\mathcal{A}} = \frac{\mathcal{A}}{4}\left\{1 + O\left(\frac{1}{\mathcal{A}^{q>0}}\right)\right\}. \tag{2.4}$$

This gives the upper bound of $e^{\mathcal{A}/4}$ on the number of independent semiclassical states having the leaf area $\mathcal{A}$. (The original covariant entropy bound of Ref. [9] only says that the number of independent semiclassical states is bounded by $e^{\mathcal{A}/2}$, since the number in each side of the leaf is separately bounded by $e^{\mathcal{A}/4}$. In Ref. [31], it was argued that the actual bound might be stronger: $e^{\mathcal{A}/4}$ for states representing both sides of the leaf. Our discussions in this paper do not depend on this issue.)

[3]It is possible that the direct sum structure arises only effectively at the fundamental level. It is also possible that the Hilbert space of quantum gravity contains states that cannot be written as elements of $\mathcal{H}_{\mathcal{A}}$. These issues, however, do not affect our arguments.

For the purposes of this paper, we focus on holographic spaces which have the topology of $\mathbb{S}^{d-1}$ with a fixed $d$, although we do not see a difficulty in extending this to other cases.[4] This implies that the holographic theory lives in $d$-dimensional (non-gravitational) spacetime, and we are considering the emergence of $(d+1)$-dimensional gravitational spacetime. Following assumption (i) in the introduction, we divide the holographic space of volume $\mathcal{A}$ into $N_{\mathcal{A}} = \mathcal{A}/l_{\rm c}^{d-1}$ cutoff-size cells and consider that each cell can take $k = e^{l_{\rm c}^{d-1}/4}$ different states:

$$\mathcal{H}_{\mathcal{A}} = \mathcal{H}_{\rm c}^{\otimes N_{\mathcal{A}}}, \tag{2.5}$$

where $\mathcal{H}_{\rm c}$ is a $k$-dimensional Hilbert space associated with each cutoff cell. Below, we focus on the regime

$$\mathcal{A} \gg l_{\rm c}^{d-1}, \qquad \frac{l_{\rm c}^{d-1}}{4} \geq \ln 2, \tag{2.6}$$

so that the setup is meaningful.

In the AdS/CFT case, $k \sim e^c$, where $c$ is the central charge of the CFT, which is taken to be large. This implies that $l_{\rm c}$ is large in units of the bulk Planck length. Indeed, the whole physics in a single AdS volume near the cutoff surface corresponds to physics of the $c$ degrees of freedom in a single cell of volume $l_{\rm c}^{d-1}$. This, however, does not mean that physics in a single AdS volume in the central region is confined to a description within a single boundary cell. It is, in fact, delocalized over the holographic space, (mostly) encoded in the entanglement between the degrees of freedom in different cells.

## 2.3 Classicalization and Spacetime

In this section, we present a heuristic discussion on amplification of information and its relation to the emergence of spacetime.

As discussed in the introduction, classicalization of a quantum system involves amplification of information at the cost of reducing the amount of accessible information. To illustrate this, consider that a detector interacts with a quantum system

$$|\Psi_{\rm s}\rangle = c_A|A\rangle + c_B|B\rangle. \tag{2.7}$$

The configuration of the detector can be such that it responds differently depending on whether the system is in $|A\rangle$ or $|B\rangle$. The state of the system and detector after the interaction is then

$$|\Psi_{\rm s+d}\rangle = c_A|A\rangle|d_A\rangle + c_B|B\rangle|d_B\rangle, \tag{2.8}$$

where $|d_A\rangle$ and $|d_B\rangle$ represent the states of the detector. Now suppose that an observer reads the detector. The observer's mental state will then be correlated with the state of the detector:

$$|\Psi_{\rm s+d+o}\rangle = c_A|A\rangle|d_A\rangle|o_A\rangle + c_B|B\rangle|d_B\rangle|o_B\rangle, \tag{2.9}$$

[4] An interesting case is that the holographic space consists of two $\mathbb{S}^{d-1}$ with a CFT living on each of them [69].

where $|o_A\rangle$ and $|o_B\rangle$ are the observer's mental states. The observer may then write the result of the experiment on a note:

$$|\Psi_{\text{s+d+o+n}}\rangle = c_A|A\rangle|d_A\rangle|o_A\rangle|n_A\rangle + c_B|B\rangle|d_B\rangle|o_B\rangle|n_B\rangle, \tag{2.10}$$

where $|n_A\rangle$ and $|n_B\rangle$ are the states of the note after this is done. We find that the information about the result is amplified in each term, i.e. it is redundantly encoded. This implies that a physical entity can learn the result of the experiment by accessing any factor, e.g. $|o_X\rangle$ or $|n_X\rangle$ $(X = A, B)$, without fully destroying the information about it in the world. This signifies that the relevant information, i.e. $A$ or $B$, is classicalized—it can be shared by multiple entities in the system or accessed multiple times by a single physical object.

The above process of classicalization is accompanied by a reduction of the number of observables. The original state of the system contains a qubit of information, given by two parameters $(\theta, \phi)$ spanning the Bloch sphere. This manifests in the fact that depending on the configuration of the detector, one could have amplified the information in a basis other than $\{|A\rangle, |B\rangle\}$. Once a state is chosen, however, the amplification occurs only for a limited amount of information; in the above case, the only observable about the system in a classicalized world is a binary question, $A$ or $B$:

$$\text{qubit: } (\theta, \phi) \longrightarrow \text{ bit: } A \text{ or } B. \tag{2.11}$$

This exponential reduction of the number of observables is the cost of making the information robust and is a consequence of the no-cloning theorem [70]. We note that there is no issue of ambiguity of measurement basis in Eq. (2.10): the basis is determined by amplification.

Another example of classicalized states, analogous to each term in Eq. (2.10), is given by coherent states in a harmonic oscillator of frequency $\omega$

$$|\alpha\rangle = e^{-\frac{1}{2}|\alpha|^2} \sum_{n=0}^{\infty} \frac{\alpha^n}{\sqrt{n!}} |n\rangle, \tag{2.12}$$

where $\alpha = |\alpha|e^{i\varphi}$ is a complex number with $|\alpha| \gg 1$, and $|n\rangle$ are the energy eigenstates: $H|n\rangle = (n + 1/2)\omega|n\rangle$. The information in $\alpha$ is amplified in the sense that it is robust under measurements, i.e. actions of creation and annihilation operators, up to corrections of order $1/|\alpha|^2$. For example, the action of a creation operator to $|\alpha\rangle$, $|\tilde{\alpha}\rangle \propto a^\dagger|\alpha\rangle$, does not affect the phase space trajectory of the oscillator at the leading order in $1/|\alpha|^2$:

$$\langle\tilde{\alpha}(t)|\mathcal{O}_\pm|\tilde{\alpha}(t)\rangle = \langle\alpha(t)|\mathcal{O}_\pm|\alpha(t)\rangle\left\{1 + O\left(\frac{1}{|\alpha|^2}\right)\right\}. \tag{2.13}$$

Here, $|\alpha(t)\rangle = e^{-iHt}|\alpha\rangle$ and similarly for $|\tilde{\alpha}(t)\rangle$, while $\mathcal{O}_+ = (a + a^\dagger)/2$ and $\mathcal{O}_- = (a - a^\dagger)/2i$, giving

$$\langle\alpha(t)|\mathcal{O}_+|\alpha(t)\rangle = |\alpha|\cos(\omega t - \varphi), \tag{2.14}$$

$$\langle\alpha(t)|\mathcal{O}_-|\alpha(t)\rangle = -|\alpha|\sin(\omega t - \varphi). \tag{2.15}$$

Thus, the information in $|\alpha|$ and $\varphi$ can be said to be classicalized. It is an exponentially small subset of the information that a generic microstate in the Hilbert space of the harmonic oscillator may carry.

The above example illustrates that the information amplification need not occur in real space. It also suggests that the resulting classical states are generally overcomplete (for more complete discussion, see, e.g., Ref. [71]). Specifically, the space formed—not spanned—by $|\alpha\rangle$ is larger than that of $|n\rangle$. Nevertheless, for $|\alpha| \gg 1$, the coherent states can be viewed as forming (approximate) basis states: they are nearly orthogonal

$$|\langle\alpha|\alpha'\rangle|^2 = e^{-|\alpha-\alpha'|^2} \lll 1, \tag{2.16}$$

and complete

$$\frac{1}{\pi}\int d^2\alpha\, |\alpha\rangle\langle\alpha| = \hat{I}, \tag{2.17}$$

so that an arbitrary state $|\psi\rangle$ may be expanded as

$$|\psi\rangle = \int d^2\alpha\, c_\alpha |\alpha\rangle, \tag{2.18}$$

where $c_\alpha = \langle\alpha|\psi\rangle/\pi$. We note, again, that there is no basis ambiguity here because of the amplification. Interpreted in terms of operators whose matrix elements between $|\alpha\rangle$ and $|\alpha'\rangle$ ($\alpha \neq \alpha'$) are suppressed, such as $\mathcal{O}_\pm$ giving $\langle\alpha|\mathcal{O}_\pm|\alpha'\rangle = |\alpha' \pm \alpha^*|^2 e^{-|\alpha-\alpha'|^2}/4$, the state in Eq. (2.18) appears as a superposition of different classical worlds.

In quantum gravity, we deal with the issue of classicalization in two steps. We first deal with classicalization of the major degrees of freedom in the fundamental theory while leaving the rest as quantum degrees of freedom. This can be done in each basis state, e.g. a single term in Eq. (2.10) and Eq. (2.18). The classicalized degrees of freedom correspond to background spacetime while the remaining ones are excitations on it (which we call matter, but also includes gravitons). The resulting theory—the theory of quantum degrees of freedom on classical spacetime—is what we call semiclassical theory. Since the way amplification occurs depends on the dynamics, what spacetime picture emerges may depend on the time evolution operator. In this language, the reference frame dependence of formulating the holographic theory arises because there are multiple equivalent ways of describing the system using different time evolution operators.

Since classicalization leading to semiclassical theory is only partial, observables in the semiclassical theory are still quantum operators. The information classicalized in this process, i.e. background spacetime, appears in the two-point functions of these operators. From the microscopic point of view, the semiclassical operators are defined by their actions in the code subspace [26, 28, 27], and their two-point functions encode entanglement entropies between the fundamental holographic degrees of freedom [18, 20, 36]. (This structure is visible clearly, e.g., in tensor network models [72, 28, 29].) The information in entanglement entropies, and in more general entanglement structures, may be viewed as amplified; for

instance, a maximally entangled state between two systems $A$ and $B$ is given by

$$|\Psi\rangle \propto \left(\prod_i e^{a_i^\dagger b_i^\dagger}\right)|0\rangle, \tag{2.19}$$

where $a_i|0\rangle = b_i|0\rangle = 0$, and gross features of entanglement between the two systems, including the entanglement entropy, are robust with respect to (a class of) measurements, i.e. operations of a limited number of creation and annihilation operators. It is this robustness that allows us to take the probe approximation, and hence consider models adopting this approximation (e.g. tensor network models).

While classicalized information is amplified, it cannot be probed an infinite number of times (unless the system is infinitely large). For example, if quantum measurements are performed to all the entities in Eq. (2.10), the information about the experimental result would be lost from the state. In gravity, information about background spacetime can be probed by excitations in the semiclassical theory. Their existence, however, necessarily affects the spacetime, so that having too many of them alters it completely. It is interesting that two seemingly unrelated statements that probing geometry necessarily backreacts on spacetime and that quantum information is fragile under measurements are in fact related. (A similar consideration also applies to the measurement of electric/magnetic fields.)

The precise way in which a semiclassical state and the code subspace associated with it emerge in the holographic theory is not yet understood. Various aspects of this issue have been studied, e.g., in Refs. [65, 66, 73, 31, 74, 75], including the dependence of the code subspace on a semiclassical state and the possible overcomplete nature of the semiclassical states. This issue will be the subject of our study in Section 2.5.

We stress that since the amplified information appears only in correlators of semiclassical operators, microscopic information about the holographic degrees of freedom is said to be measured only if it is probed by semiclassical operators, i.e. transferred to excitations represented by these operators. This implies that any "gravitational thermal radiation," e.g. the thermal atmosphere within the zone of a black hole, is not "physical" (does not have a semiclassical meaning) unless it is probed by matter degrees of freedom, e.g. detected by a physical apparatus or converted into Hawking radiation in the asymptotic region (outside the zone). This is, in fact, a key element of a proposed solution to (the entanglement argument of) the firewall paradox [76, 77, 78] and the Boltzmann brain problem [79] (see also [80]).

## 2.4 Reconstructing Spacetime

In a holographic theory for general spacetimes, it is important to choose a reference frame to obtain a description in which the redundancy associated with holography (and complementarity) is fixed. As we will see below, reconstructing spacetime through our method generally requires knowledge about the holographic state at different times. (For an analysis of spacetime regions reconstructed from a single leaf, see the appendix.) Suppose that the state represents a semiclassical spacetime, at least for a sufficiently long time period. We

are interested in knowing what portion of the spacetime is directly reconstructable from such a state. In other words, we want to know what kind of bulk spacetime description the holographic theory provides.

For this purpose, we first define the entanglement wedge [60, 61, 56] in the form applicable to general spacetimes. Let $\Gamma$ be a (not necessarily connected) region on a leaf, and let $E(\Gamma)$ be the HRT surface (appropriately generalized to include higher order effects): the bulk codimension-two surface anchored to the boundary of $\Gamma$, $\partial E(\Gamma) = \partial\Gamma$, extremizing the generalized entropy [22].[5] The entanglement wedge of $\Gamma$ is defined as the bulk domain of dependence of any achronal bulk surface $\Sigma$ whose boundary is the union of $\Gamma$ and $E(\Gamma)$:

$$\mathrm{EW}(\Gamma) = D_\Sigma, \qquad \partial\Sigma = \Gamma \cup E(\Gamma). \tag{2.20}$$

In the AdS/CFT case, the entanglement wedge can be defined either associated with a spatial region $\Gamma$ or its boundary domain of dependence, which are equivalent if we know the conditions imposed at the boundary. In general spacetimes, it is important to define the entanglement wedge associated with a spatial region on a leaf (a preferred time slice in the holographic theory), since the theory on the holographic screen is in general not Lorentz invariant. In the AdS/CFT case, this implies that we only consider spatial regions $\Gamma$ on equal-time hypersurfaces in a fixed time foliation (although different $\Gamma$'s can be regions at different times).

We note that if we change a reference frame, the set of $\Gamma$ we consider changes from the bulk point of view. In general spacetimes, changing the reference frame corresponds to choosing a different time evolution operator—in the bulk language, this ends up choosing a different holographic screen, and hence different leaves, from which $\Gamma$'s are selected. In the AdS/CFT case, changing the reference frame does not affect the time evolution operator, i.e. CFT Hamiltonian, because of the high symmetry of the system—it only changes the time foliation to another one related by a conformal transformation. This, however, does not mean that we can choose $\Gamma$ to be an arbitrary spacelike region. In any fixed reference frame, $\Gamma$ should be restricted to spatial regions on equal-time hypersurfaces of the given time foliation.

Going back to the issue of reconstructing spacetime, the analyses of Refs. [23, 24], together with our assumption (iii) in the introduction, suggest that the information in $\mathrm{EW}(\Gamma)$ is in general contained in the density matrix of $\Gamma$ in the holographic theory. This, however, does not mean that all of this information can be arranged directly in the form represented by local operators in the bulk effective theory. Indeed, we will argue below that the portion of spacetime reconstructed in this way is generally smaller than the union of $\mathrm{EW}(\Gamma)$ for all $\Gamma$. This is, in fact, consonant with the picture of Ref. [63]. Suppose a black hole is formed dynamically. The region $\cup_\Gamma \mathrm{EW}(\Gamma)$ then contains the region inside the black hole, as can be seen by considering $\Gamma$ comprising the entire holographic screen at a late time. This implies that the information about the interior is contained in the holographic theory in some form,

[5] We do not expect that a homology constraint [81, 61] plays an important role in our discussion, since we consider the microscopic description of pure states.

but—as we will argue—not as local excitations in semiclassical spacetime (while keeping locality in the entire exterior region). We claim that this information corresponds to what we call excitations on the stretched horizon in the bulk picture.

We now assert that semiclassical spacetime as viewed from a fixed reference frame is composed of the set of points $p$ that can be written as

$$p = \bigcap_{\Gamma \in \tilde{\mathcal{G}}} \mathrm{EW}(\Gamma), \tag{2.21}$$

where $\tilde{\mathcal{G}}$ is a subset of the collection of all the spatial regions on all leaves, $\tilde{\mathcal{G}} \subset \mathcal{G} = \{\Gamma\}$.

There are two recent papers that used similar constructions [82, 58]. In Ref. [82], a local bulk operator in AdS was constructed in CFT using bulk HRT surfaces intersecting at that point. This, however, does not allow us to construct operators in an entanglement shadow: the spacetime region which the HRT surfaces do not probe (see below). Our criterion is more along the lines of the construction in Ref. [58], in which entanglement wedges associated with all the $(d-1)$-dimensional achronal submanifolds of the AdS boundary were considered to construct local operators in the AdS bulk (including those in an entanglement shadow). In fact, the criterion of Eq. (2.21) can be obtained by the logic analogous to that given in Ref. [58]. We claim, however, that to obtain a physical description in a fixed reference frame, the regions to which entanglement wedges are associated must be restricted to those on equal-time hypersurfaces *in the given time foliation*. In the case of AdS/CFT with simply connected boundary space, we have not found an example in which the region given by Eq. (2.21) and the localizable region of Ref. [58] differ. In general spacetimes, however, one must choose the set of regions $\Gamma$ as described here (spatial regions on leaves). This issue is also important in AdS/CFT if the boundary consists of multiple disconnected components [34].

Below, we demonstrate that the criterion given in Eq. (2.21), with $\Gamma$ restricted to spatial regions on leaves, allows us to reconstruct almost the entire spacetime, except for certain special regions determined by the causal structure, e.g. the interior of a black hole. We focus our analysis to the interior of the holographic screen, $\mathcal{M} \equiv \cup_\sigma F_\sigma$, whose information is encoded (mostly) in entanglement between subregions in the holographic theory [31]. Here, $F_\sigma$ is the union of all interior achronal hypersurfaces whose only boundary is $\sigma$ and which does not intersect with the holographic screen except at $\sigma$. The exterior of the holographic screen will be commented on in Section 2.5. Throughout, we assume that holographic states are pure.

## Spacetime without a Shadow

We first note that if a bulk point is at the intersection of $d$ HRT surfaces $E(\Gamma_i)$ $(i = 1, \cdots, d)$, then it satisfies the condition of Eq. (2.21). This is because for each HRT surface, we can include $\Gamma_i$ and its complement on the leaf, $\bar{\Gamma}_i$, in $\tilde{\mathcal{G}}$, so that $\mathrm{EW}(\Gamma_i) \cap \mathrm{EW}(\bar{\Gamma}_i) = E(\Gamma_i)$.

This implies that we can reconstruct the whole spacetime in $\mathcal{M}$ if the HRT surface $E(\Gamma)$ behaves continuously under a change of $\Gamma$ (i.e. if there is no entanglement shadow). To show this explicitly, let us choose a leaf $\sigma(0)$ on the holographic screen. We can introduce the

angular coordinates $\phi_{1,\cdots,d-1}$ on it. Let us now introduce the coordinates $x_j$ $(j = 1, \cdots, d)$ with $\sum_{j=1}^{d} x_j^2 = 1$:

$$x_1 = \cos(\phi_1), \tag{2.22}$$
$$x_2 = \sin(\phi_1)\cos(\phi_2), \tag{2.23}$$
$$\vdots \tag{2.24}$$
$$x_{d-1} = \sin(\phi_1)\cdots\sin(\phi_{d-2})\cos(\phi_{d-1}), \tag{2.25}$$
$$x_d = \sin(\phi_1)\cdots\sin(\phi_{d-2})\sin(\phi_{d-1}). \tag{2.26}$$

This allows us to consider spatial regions on the leaf

$$\Gamma_i^{(s)}(0) = \{\sigma(0) \,|\, x_i \leq s\}, \tag{2.27}$$

specified by a discrete index $i = 1, \cdots, d$ and a continuous number $-1 \leq s \leq 1$. Because of the continuity assumption, for each $i$ the corresponding HRT surfaces $E_i^{(s)}(0)$ sweep an interior achronal hypersurface bounded by $\sigma(0)$:

$$\Sigma_i(0) \equiv \bigcup_s E_i^{(s)}(0). \tag{2.28}$$

In general, the resulting $d$ hypersurfaces $\Sigma_i(0)$ $(i = 1, \cdots, d)$ are different, and the HRT surfaces contained in them do not intersect; see Fig. 2.1.

We can, however, repeat the same procedure for all different leaves $\sigma(\tau)$. Here, $\tau$ is the time parameter on the holographic screen. The coordinates $x_j$ on different leaves can be defined from those on $\sigma(0)$ by following the integral curves of a vector field on the holographic screen which is orthogonal to every leaf. (Such a vector field was used [83] to prove that the area theorem of Refs. [59, 84] is local.)

The continuity assumption then implies that for each $i$ the hypersurfaces $\Sigma_i(\tau)$ sweep the entire spacetime region inside the holographic screen, $\mathcal{M}$, as $\tau$ varies:[6]

$$\mathcal{M} = \bigcup_\tau \Sigma_i(\tau). \tag{2.29}$$

This in turn implies that for any bulk point $p$ inside the holographic screen, we can find the values of $s$ and $\tau$ for each $i$, $(s_i, \tau_i)$, such that the corresponding HRT surface $E_i^{(s_i)}(\tau_i)$ goes through $p$ (see Fig. 2.1). Therefore, by choosing

$$\tilde{\mathcal{G}} = \left\{ \Gamma_i^{(s_i)}(\tau_i), \bar{\Gamma}_i^{(s_i)}(\tau_i) \,\middle|\, i = 1, \cdots, d \right\}, \tag{2.30}$$

the point $p$ can be written as in Eq. (2.21).

We note that in general, $\tau_i$ for different $i$ need not be the same. And yet, the region giving each entanglement wedge is on a single leaf.

[6] In the case that the holographic screen is spacelike, it seems logically possible that $\Sigma_i(\tau)$ for some $i$ does not sweep the entire spacetime. We do not consider such a possibility.

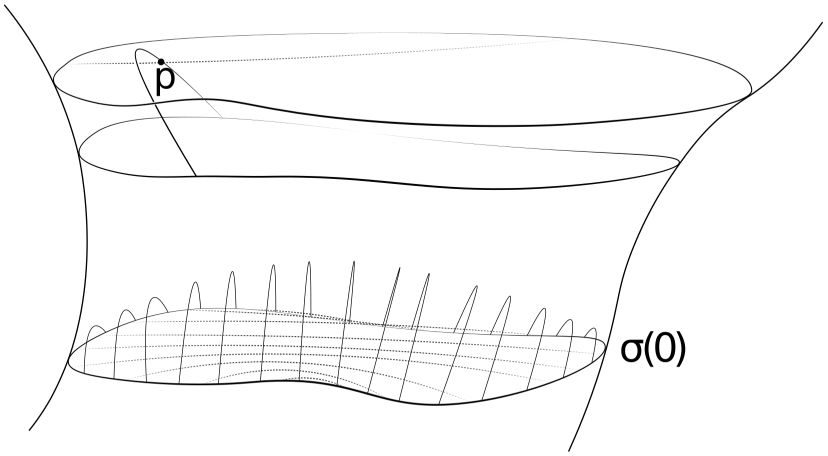


Figure 2.1: If the HRT surface $E(\Gamma)$ behaves continuously under a change of $\Gamma$, we can reconstruct the entire spacetime region inside the holographic screen, $\mathcal{M}$, despite the fact that $d$ families of HRT surfaces all anchored on a single leaf $\sigma(0)$ do not in general span the same hypersurface.

## Reconstructable Shadow

The construction described above does not apply if there is an entanglement shadow $\mathcal{S}$: a spacetime region which the HRT surfaces do not probe. This phenomenon occurs rather generally, for example in spacetimes with a conical deficit [85] or a dense star [86]. Here we show that a point $p \in \mathcal{S}$ may still be written as in Eq. (2.21) if certain conditions are met. An important point is that while an HRT surface $E(\Gamma)$ is always outside the shadow, the other part of the boundary of the entanglement wedge $\mathrm{EW}(\Gamma)$ can go into the shadow region.

Consider the future light cone of $p$, which we define as the subset of $\mathcal{M}$ covered by the set of future-directed light rays, $L^+(\Omega)$, emanating from $p$ in all directions parameterized by angles $\Omega = (\varphi_1, \cdots, \varphi_{d-1})$. Similarly, we can consider the set of past-directed light rays $L^-(\Omega)$, emanating from $p$ in all directions. Suppose all future (past) directed light rays escape the shadow region by the time the first future (past) directed light ray intersects the

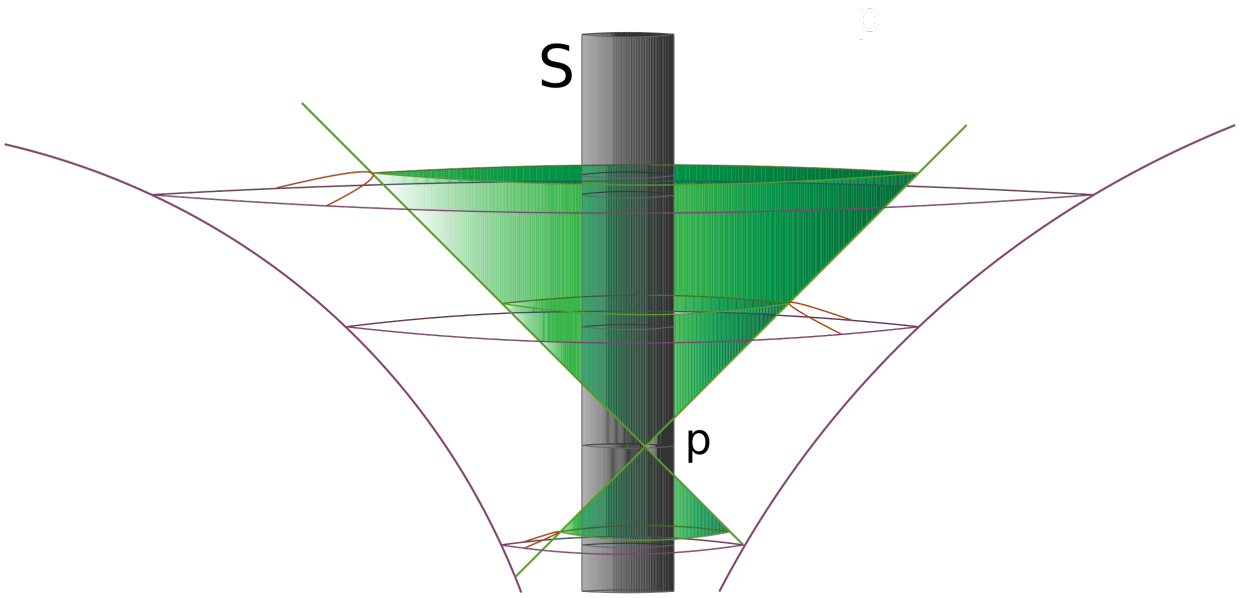


Figure 2.2: A point $p$ in an entanglement shadow $\mathcal{S}$ can be reconstructed as an intersection of entanglement wedges associated with spatial regions on leaves if all the future-directed and past-directed light rays emanating from $p$ reach outside the entanglement shadow early enough. Here we see that all past-directed light rays escape the shadow before the first of them intersects the holographic screen.

holographic screen (if at all), i.e. they all enter $\mathcal{M} \setminus \mathcal{S}$ early enough.[7] We now show that point $p \in \mathcal{S}$ can then be reconstructed as in Eq. (2.21). A sketch of the procedure is given in Fig. 2.2.

Let us take a point $q^+(\Omega)$ on the portion of $L^+(\Omega)$ in $\mathcal{M} \setminus \mathcal{S}$. We can then find an HRT surface, $E^+(\Omega)$, that goes through $q^+(\Omega)$, tangent to the light cone there, and anchored on some leaf of the holographic screen. An argument is the following. As in the previous subsection, we consider families of HRT surfaces anchored on $\sigma(0)$; see Eq. (2.28). In the previous subsection, we considered $d$ such sets $E_i^{(s)}(0)$, but now we consider an infinite number of sets parameterized by the angular coordinates $\Phi = (\phi_1, \cdots, \phi_{d-1})$ on $\sigma(0)$: $E_\Phi^{(s)}(0)$. (The corresponding spatial region $\Gamma_\Phi^{(s)}(0)$ can be taken to enlarge from the point specified by $\Phi$ toward its antipodal point as $s$ increases from $-1$ to 1.) Because of the entanglement shadow, these surfaces, $E_\Phi^{(s)}(0)$ $(-1 \le s \le 1)$, do not cover the entire interior achronal

[7] We assume that these light rays enter $\mathcal{M} \setminus \mathcal{S}$ while their congruences are still expanding. This is generally true for small shadow regions.

surface bounded by $\sigma(0)$; there will be some hole(s). However, by extending this to all possible leaves $\sigma(\tau)$, $E_\Phi^{(s)}(\tau)$ for each $\Phi$ will sweep the entire region outside the shadow:

$$\mathcal{M} \setminus \mathcal{S} = \bigcup_{s,\tau} E_\Phi^{(s)}(\tau). \tag{2.31}$$

This implies that we have a set of HRT surfaces parameterized by $\Phi$ that all go through $q^+(\Omega)$:

$$E_\Phi^{(s(\Phi))}(\tau(\Phi)) \quad \big(\ni q^+(\Omega)\big). \tag{2.32}$$

From these, we can choose one that is tangent to the light cone at $q^+(\Omega)$ because this imposes $d-1$ conditions on the $d-1$ parameters $\phi_1, \cdots, \phi_{d-1}$.

We therefore have the appropriate HRT surface $E^+(\Omega)$ for $q^+(\Omega)$, which is anchored on leaf $\sigma(\tau(\Phi))$. There are two regions on this leaf that can be associated with $E^+(\Omega)$, which are complement with each other on the leaf. We take the one such that the boundary of its entanglement wedge contains $L^+(\Omega)$, and we call it $\Gamma^+(\Omega)$. We then find that the intersection of the entanglement wedges of $\Gamma^+(\Omega)$ for all $\Omega$ gives a region that is a subset of the causal future of $p$ and contains $p$:

$$p \in \bigcap_\Omega \mathrm{EW}\big(\Gamma^+(\Omega)\big) \subseteq J^+(p). \tag{2.33}$$

Repeating the same construction for the past light cone, we obtain the analogous region with $+ \to -$. Since the intersection of $J^+(p)$ and $J^-(p)$ is just $p$, we find that by taking

$$\tilde{\mathcal{G}} = \big\{\Gamma^+(\Omega),\, \Gamma^-(\Omega) \,\big|\, \forall\Omega\big\}, \tag{2.34}$$

we can write $p$ in the form of Eq. (2.21). Note that each region $\Gamma^+(\Omega)$ or $\Gamma^-(\Omega)$ is on a single leaf.

We conclude that to reconstruct $p$ through Eq. (2.21), it is sufficient that all the future-directed and past-directed light rays emanating from $p$ reach outside the entanglement shadow early enough. This condition, however, appears too strong as a necessary condition for the reconstruction.

In general, the bulk portion of the boundary of an entanglement wedge consists of three elements: (i) the HRT surface, (ii) null surfaces generated by light rays emanating orthogonally from the HRT surface, and (iii) caustics developed by the congruence of these light rays. To reconstruct a point $p$ through Eq. (2.21), one of these elements must go through $p$. For a point in an entanglement shadow, (i) is not available. In the construction above, we have used (ii). We can, however, also use (iii).

Consider a spatial region $\Gamma$ on a leaf. Suppose that $\Gamma$ is chosen such that a caustic developed by a congruence of *past*-directed light rays emanating from $E(\Gamma)$ passes through $p$. Suppose also that we can find $d$ such regions, $\Gamma_i$ $(i = 1, \cdots, d)$, which seems possible generically based on parameter counting. Then, the intersection of $\mathrm{EW}(\Gamma_i)$,

$$K^+(p) = \bigcap_i \mathrm{EW}(\Gamma_i), \tag{2.35}$$

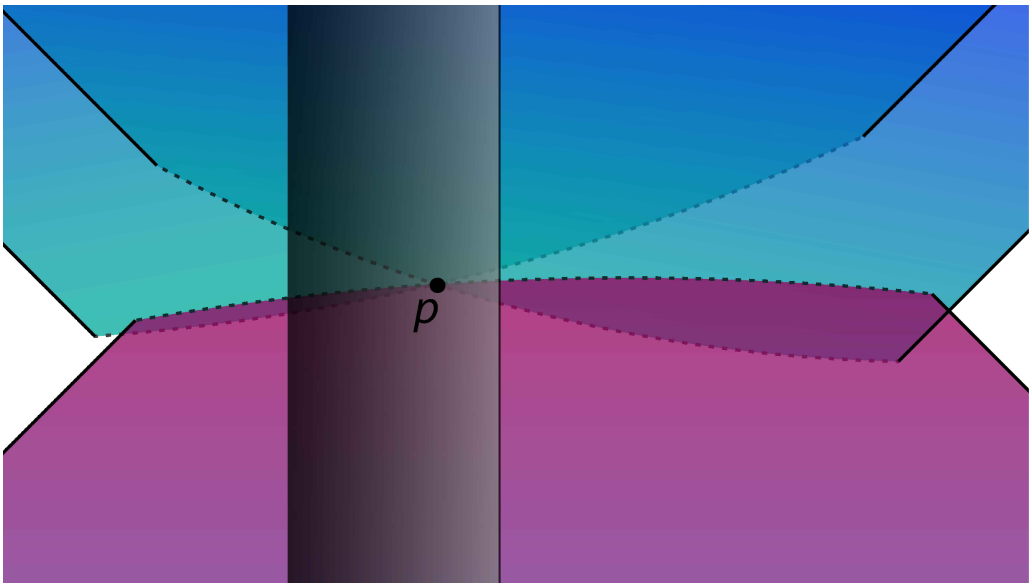


Figure 2.3: A point $p$ in an entanglement shadow may be reconstructed as the intersection of a finite number of entanglement wedges if it is on caustics of these entanglement wedges (denoted by the dotted lines).

forms a region which has a "tip" at $p$. It therefore seems possible to find a region $\Gamma'$ such that a caustic developed by a congruence of *future*-directed light rays emanating from $E(\Gamma')$ passes through $p$, and that

$$\tilde{\mathcal{G}} = \{\Gamma_i, \Gamma'\}, \tag{2.36}$$

gives $p$ through Eq. (2.21); see Fig. 2.3. This would allow us to reconstruct $p$ without requiring that all the light rays emanating from $p$ reach outside the entanglement shadow.

In all the reconstruction procedures we could consider, however, it seems necessary that at least one future-directed *and* past-directed light ray from $p$ escapes the entanglement shadow region. We thus require this as a necessary condition for $p$ to be reconstructable. (This is, in fact, a very weak requirement. In every case we considered, we actually needed a stronger condition.)

## Non-reconstructable Shadow

The necessary condition described above has important implications. Suppose a black hole is formed in $\mathcal{M}$. After a sufficiently long time, the black hole becomes quasi-static. For any such black hole, HRT surfaces anchored on leaves cannot penetrate the horizon [87, 62]. The condition described above then implies that the interior of a quasi-static black hole cannot be reconstructed directly in the holographic theory.

Two comments are in order. First, the entanglement shadow around a black hole in general extends beyond the horizon (except for a large black hole in AdS) [86]. This region, however, is reconstructable as described in the previous subsection. Second, HRT surfaces may probe the interior of the event horizon shortly after a black hole is formed [88], which allows us to reconstruct the region as described in Section 2.4. After the black hole is stabilized, however, no HRT surface can penetrate the horizon (at least by any macroscopic distance). The interior of a stabilized black hole, therefore, still cannot be reconstructed.

We interpret this non-reconstructability to mean that in the given reference frame the black hole interior is not described in terms of local operators in semiclassical spacetime (at least a priori; see below). Suppose we (try to) represent a bulk point $p$ as in Eq. (2.21) with some $\tilde{\mathcal{G}}$. Let us call the element of $\tilde{\mathcal{G}}$ on the latest (earliest) leaf $\Gamma_+$ ($\Gamma_-$) and the corresponding time parameter on the holographic screen $\tau_+$ ($\tau_-$). Let us define $\Delta\tau$ as the smallest value of $\tau_+ - \tau_-$ over the possible choices of $\tilde{\mathcal{G}}$:

$$\Delta\tau = \min_{\tilde{\mathcal{G}}}\{\tau_+ - \tau_-\}. \tag{2.37}$$

The analyses in the previous subsections imply that for a reconstructable bulk point, $\Delta\tau$ is finite. On the other hand, for a non-reconstructable point, we may view that $\Delta\tau$ is infinite (as the relevant light ray fails to escape the shadow region in a finite time). This implies that using operators that probe (only) entanglement entropies between subregions, it takes an infinite time to resolve a point in the non-reconstructable region. In other words, the effective theory for the degrees of freedom represented by these operators describe physics in this region as a "vacuum degeneracy," condensed in the energy interval of $\Delta E \sim 1/\Delta\tau \to 0$.

This strongly suggests that the description obtained in the holographic theory is that of a distant picture for the black hole. (Recall that it is the entanglement entropy structure between subregions that local bulk operators under consideration are mainly sensitive to.) This, however, does not necessarily mean that there can be no *effective* description that makes (a portion of) the interior spacetime manifest by appropriately rearranging degrees of freedom. Based on intuition from Ref. [63], and more recent analysis in Ref. [89], we expect that such a description—if any—cannot keep locality in all the original spacetime region (in particular, outside the causal patch of a single infalling geodesic). In fact, we expect that any such effective description is applicable only for a finite time, measured with respect to the degrees of freedom made local in this way, reflecting the fact that the corresponding spacetime has a singularity. The issue of the black hole interior will be discussed further in Section 2.6.

We finally present another example of spacetime with a non-reconstructable region: an isotropic AdS cosmology. Through a coordinate transformation, the interior of a future light cone $L$ in global AdS space can be written as an open FRW universe with the metric

$$ds^2 = -dt^2 + a^2(t)\big(d\chi^2 + \sinh^2\chi\, d\Omega\big). \tag{2.38}$$

Any small perturbation makes this universe end with a big-crunch collapse at some time $t_*$ ($> 0$), so that

$$a(0) = a(t_*) = 0, \tag{2.39}$$

where the $t = 0$ hypersurface is taken to be on $L$. In Ref. [62], it was shown that HRT surfaces anchored to the AdS boundary cannot probe the region

$$t > t_{\rm turn}, \tag{2.40}$$

where $t_{\rm turn}$ is the time at which $a(t)$ becomes maximum. Since any future-directed light ray emanating from a point in this region hits the singularity, our criterion says that this region is not reconstructable. (The region $t < t_{\rm turn}$ is reconstructable as it is probed by HRT surfaces.)

In fact, it seems that any non-reconstructable region in realistic spacetimes is associated with a collapsing region (region in which time runs backwards in the language of Ref. [59]) whose future ends in a singularity. (We have excluded the region inside a past light cone in the isotropic AdS cosmology, which we consider "unrealistic," analogous to the white hole region.) This may be viewed as a quantum gravity version of cosmic censorship, although the surface "hiding" a singularity, i.e. that dividing reconstructable and non-reconstructable regions, is not necessarily null here.

## 2.5 Spacetime Is Non-Generic

We have discussed what description the holographic theory provides when a holographic state represents semiclassical spacetime. Here we discuss how such states are embedded in the holographic Hilbert space.

### Holographic Encoding of Spacetime

Consider the holographic space $\Xi_{\mathcal{A}}$ of volume $\mathcal{A}$, which consists of $\mathcal{N}_{\mathcal{A}}$ cutoff-size cells containing $\ln k$ degrees of freedom. If a state on this space (an element of $\mathcal{H}_{\mathcal{A}}$) represents a semiclassical spacetime (or more precisely a snapshot of it in the holographic theory), then the von Neumann entropy $S(\Gamma)$ of a subregion $\Gamma \subset \Xi_{\mathcal{A}}$ is related to the area of the HRT surface $E(\Gamma)$ as [56]

$$S(\Gamma) = \frac{1}{4}\|E(\Gamma)\|, \tag{2.41}$$

ignoring the bulk matter contribution, which does not play a role in the discussion below. Here, $\|x\|$ represents the volume of the object $x$ (often called the area for a codimension-two surface in spacetime).

Suppose we take an entanglement structure $S_{\mathcal{A}} \equiv \{S(\Gamma)\,|\,\forall\Gamma \subset \Xi_{\mathcal{A}}\}$ on $\Xi_{\mathcal{A}}$ implied by some semiclassical spacetime. Since any unitary transformation acting within a single cell does not change entanglement entropies between subregions, this allows us to have a set of states labeled by the group elements of $U(k)^{\mathcal{N}_{\mathcal{A}}}$

$$|\psi_z^{S_{\mathcal{A}}}\rangle, \quad z \in U(k)^{\mathcal{N}_{\mathcal{A}}}, \tag{2.42}$$

all having the same entanglement structure $S_{\mathcal{A}}$. We expect that some (but not necessarily all) of these states are microstates of the corresponding spacetime.

In general, we expect that $k$ is large because entanglement between different subregions is robust (only) when many degrees of freedom are involved; see, e.g., Eq. (2.19).[8] In the case of AdS/CFT, i.e. $L_{\rm AdS}^{d-1} \ll \mathcal{A}$ where $L_{\rm AdS}$ is the AdS length, $k$ is related to the ratio of $L_{\rm AdS}$ to the bulk Planck length $l_{\rm Pl}$ (which we restore here):

$$\ln k \sim \left(\frac{L_{\rm AdS}}{l_{\rm Pl}}\right)^{d-1} \gg 1. \tag{2.43}$$

For more general spacetimes, which one may view as the case $L_{\rm AdS}^{d-1} \gg \mathcal{A}$, the meaning of $k$ is not clear, but one possibility is

$$\ln k \sim \left(\frac{l_{\rm s}}{l_{\rm Pl}}\right)^{d-1} \sim N, \tag{2.44}$$

where $l_{\rm s}$ and $N$ are the string length and the number of species in the low energy bulk effective theory, respectively. We then expect that $k$ is also large in this case.

The degrees of freedom in $z \in U(k)^{\mathcal{N}_{\mathcal{A}}}$ corresponding to the microstates of the spacetime may contain a large amount of information, especially for $k \gg 1$. Such information cannot be captured by entanglement between different subregions on $\Xi_{\mathcal{A}}$. In Section 2.4, we have seen that semiclassical physics in a non-reconstructable region cannot be captured by entanglement entropies between subregions, so it is natural to conjecture that this physics (e.g. physics of the excitations of the stretched horizon) is encoded in these degrees of freedom. We might suspect that physics outside the holographic screen may also be encoded in these degrees of freedom. If this is true, the logarithmic dimension of the Hilbert space describing both the interior and exterior regions of the holographic screen is $\mathcal{A}/4$ [31]. An alternative possibility is that the degrees of freedom describing the exterior region is not captured by those discussed here. (They may not even be arranged locally in any space.) In this case, the system we discuss here should be regarded as that responsible only for the interior region.

## Semiclassical States Are Special

The number of independent states within the space of $U(k)^{\mathcal{N}_{\mathcal{A}}}$ is $k^{\mathcal{N}_{\mathcal{A}}} = e^{\mathcal{A}/4}$. This implies that there can be up to $e^{\mathcal{A}/4}$ independent microstates for the same semiclassical spacetime, within the uncertainties associated with the coarse-graining $\delta\mathcal{A}$, although this does not mean that all, or even any, semiclassical spacetimes must have that many independent microstates.

[8] Later, we consider perfect tensor network models, which do not a priori require large bond dimensions (which one might think are analogous to $k$ here). For small bond dimensions, however, perfect tensors are finely tuned: small perturbations would destroy their absolutely maximally entangled nature. Models with these tensors can be used (only) to simulate coarse-grained structures of the fundamental theory. For large bond dimensions, this issue of stability does not arise.

If a semiclassical spacetime has $e^{\mathcal{A}/4}$ independent microstates, however, it leads to the following puzzling situation.[9] Suppose there are $e^{\mathcal{A}/4}$ independent microstates $|\psi_i\rangle$ ($i = 1, \cdots, e^{\mathcal{A}/4}$) which all correspond to (a holographic snapshot of) a single semiclassical spacetime $\mathcal{M}$ and hence have the same entanglement structure $S_{\mathcal{M}} = \{S_{\mathcal{M}}(\Gamma) \,|\, \forall \Gamma \subset \Xi_{\mathcal{A}}\}$.[10] Suppose we take a superposition of $e^n$ such states

$$|\Psi\rangle = \sum_{i=1}^{e^n} c_i |\psi_i\rangle, \tag{2.45}$$

with comparable coefficients. Here, $\sum_i |c_i|^2 = 1$. If we compute the holographic entanglement entropy of this state in a subregion $\Gamma$, we generally obtain

$$S(\Gamma) \neq S_{\mathcal{M}}(\Gamma). \tag{2.46}$$

For small $n \ll V_\Gamma$, where

$$V_\Gamma \equiv \min\left\{\|\Gamma\|, \|\bar{\Gamma}\|\right\}, \tag{2.47}$$

we find

$$S(\Gamma) = S_{\mathcal{M}}(\Gamma) - \sum_{i=1}^{e^n} |c_i|^2 \ln |c_i|^2, \tag{2.48}$$

so that the second term (classical Shannon entropy) is of order $n$, which is negligible compared with the first term (typically of order $V_\Gamma$). If we superpose a sufficiently large number of microstates with $n \sim \mathcal{A}$, however, the entanglement structure of $|\Psi\rangle$, $S_\Psi \equiv \{S(\Gamma) \,|\, \forall \Gamma \subset \Xi_{\mathcal{A}}\}$, can take a form unrelated with $S_{\mathcal{M}}$, since $|\psi_i\rangle$ form (approximately) a basis of $\mathcal{H}_{\mathcal{A}}$. Indeed, for a generic superposition with $n \approx \mathcal{A}/4$, we expect from Page's argument [91] that $S(\Gamma) = V_\Gamma/4$ to a high degree.

On the other hand, one might expect that the state $|\Psi\rangle$ still describes semiclassical spacetime $\mathcal{M}$, since it is simply a superposition of microstates that all describe the same semiclassical spacetime $\mathcal{M}$. If this were true, then we would find that a generic state describing spacetime $\mathcal{M}$, i.e. a generic state of the form of Eq. (2.45), has an entanglement structure that has nothing to do with $S_{\mathcal{M}}$. This would violate assumption (ii) in the introduction.

We are, therefore, led to the conclusion that if a semiclassical spacetime has $e^{\mathcal{A}/4}$ independent microstates, then these states do not form a Hilbert space. In fact, the space of microstates for a fixed semiclassical spacetime is *at most* the $z$ space (see Eq. (2.42)), whose volume is tiny compared with that of $\mathcal{H}_{\mathcal{A}}$:

$$\|U(k)^{\mathcal{N}_{\mathcal{A}}}\| \lll \|U(k^{\mathcal{N}_{\mathcal{A}}})\|. \tag{2.49}$$

[9] One might expect that given standard de Sitter entropy [90], the de Sitter FRW universe provides an example of such spacetime, with $e^{\mathcal{A}/4}$ independent microstates. This is, however, not the case, since spacetime "disappears" in the de Sitter limit of the holographic FRW theory [34].

[10] We expect this basis of microstates to be uncorrelated with the position space basis states in holographic space and take this to be the case.

In fact, the actual space of microstates can be smaller. Note that taken at face value, the space of microstates given by Eq. (2.49) is measure zero in $\mathcal{H}_{\mathcal{A}}$. Our expressions, however, apply only at the leading order in $1/\mathcal{A}$, so we expect that the space has a nonzero "width" at subleading order in $1/\mathcal{A}$. This, however, does not affect our conclusion that an arbitrary superposition of the form of Eq. (2.45) cannot be interpreted as a semiclassical state representing $\mathcal{M}$.

If the microstates of a spacetime comprise the entire $\|U(k)^{\mathcal{N}_{\mathcal{A}}}\|$ space, then what happens? We can use tensor network models to simulate this situation.[11] For example, consider a tensor network obtained by contracting perfect tensors with some bulk legs left dangling. By varying the perfect tensor chosen at each node, while keeping the network structure unaltered, we can generate a class of quantum error correcting codes represented in the holographic space. This generates the code subspaces for all the geometry microstates satisfying the condition that $S(\Gamma) = S_{\mathcal{M}}(\Gamma)$ for all $\Gamma$. The semiclassical (logical) operators obtained in this way are state-dependent, because different semiclassical states in different code subspaces have nontrivial overlaps in the holographic Hilbert space. The same conclusion is obtained using random tensor networks, rather than perfect tensor networks.

A similar observation about state-dependence has been made recently in Ref. [75] which considered overlaps of code subspaces corresponding to different geometries realized in the same holographic space. On the other hand, our discussion here concerns microstates corresponding to the same semiclassical geometry, which does not require different matter configurations at the semiclassical level. The basic outcome for the purpose of the present discussion, however, is that the two situations can be treated similarly.[12]

The fact that the space of microstates for a fixed semiclassical spacetime is bounded from above by $\|U(k)^{\mathcal{N}_{\mathcal{A}}}\|$ ($\ll \|U(k^{\mathcal{N}_{\mathcal{A}}})\|$) has an important implication. Consider a generic state in $\mathcal{H}_{\mathcal{A}}$. In such a state, the entanglement entropy of a region $\Gamma$ is given by

$$S(\Gamma) = \frac{1}{4} V_{\Gamma}, \tag{2.50}$$

where $V_{\Gamma}$ is defined by Eq. (2.47). This is because for a typical state, the reduced density matrix of a subsystem smaller than a half of the whole system is maximally mixed to a high degree [91]. If this state is interpreted through Eq. (2.41), we have

$$\forall \Gamma \quad \|E(\Gamma)\| = V_{\Gamma}. \tag{2.51}$$

An essentially unique way in which this happens is that the HRT surface anchored to $\partial\Gamma$ is $\Gamma$ itself (or $\bar{\Gamma}$, whichever is smaller). The corresponding geometry in $\mathcal{M}$ then must have a

[11] Strictly speaking, the models discussed in this and next subsections apply only to the situation in which the holographic space is approximately time independent, but we expect that the conclusions are more general, since the time independence does not play a particularly important role.

[12] This is consonant with the picture of Refs. [76, 77, 92] that different microstates for the "same" spacetime (e.g. a single classical black hole) can/should actually be viewed as states with slightly different spacetimes (black holes with slightly different masses).

horizon just inside the leaf, which serves as an extremal surface barrier. Since the description of the holographic theory is that of the exterior picture, this state does not have any semiclassical spacetime inside $\mathcal{M}$.[13]

We conclude that a generic state in the holographic Hilbert space does not represent a semiclassical spacetime inside the holographic screen. Specifically, if the initial state of a system is generic in $\mathcal{H}_{\mathcal{A}_0}$ and if the dynamics of the holographic theory is such that the state keeps being generic in $\mathcal{H}_{\mathcal{A}}$ throughout the evolution, where $\mathcal{A} > \mathcal{A}_0$, then the system does not admit a semiclassical spacetime interpretation within the holographic screen. In this sense, we can say that bulk gravitational spacetime emerges only as a result of non-genericity of the state in the holographic Hilbert space.

We emphasize, though, that non-genericity here refers to that in the holographic Hilbert space without a constraint. In particular, our argument does not exclude the possibility that with a specification of an energy range which is sufficiently lower than the cutoff, semiclassical states are generic among the states in that energy range. This is indeed the case in standard AdS/CFT. Similarly, it is possible that imposing a constraint on some other quantity makes semiclassical states typical within the specified class. Further discussion on this issue is given in Ref. [34].

## State-dependence and Many Microstates

We have learned that a semiclassical spacetime inside the holographic screen appears only as a result of non-genericity of the holographic state. We have also argued that if a semiclassical spacetime has $e^{\mathcal{A}/4}$ independent microstates, then the semiclassical operators are state-dependent. This latter argument has been made by considering that the semiclassical microstates occupy the $U(k)^{\mathcal{N}_{\mathcal{A}}}$ space. Here we show that the necessity of state-dependence for a spacetime having $e^{\mathcal{A}/4}$ independent microstates is even more robust.

The smallest possible space containing $e^{\mathcal{A}/4}$ independent microstates consists of discrete $e^{\mathcal{A}/4}$ "axis" states (with some small "width" around them). In this case, all the different code subspaces can be exactly orthogonal:

$$\forall a, b \quad \langle \psi_a^{(i)} | \psi_b^{(j)} \rangle = 0 \quad \text{for } i \neq j, \tag{2.52}$$

where $|\psi_a^{(i)}\rangle$ $(a = 1, \cdots, e^{S_{\text{code}}})$ represents the elements of the code subspace $\mathcal{H}_{\text{code},i}$ associated with microstate $i$. One might then think that any semiclassical operator $\mathcal{O}_X$ can be represented state-independently as

$$\tilde{\mathcal{O}}_X = \bigoplus_i \mathcal{O}_X^{(i)}, \tag{2.53}$$

[13]The relation in Eq. (2.51) can be obtained in a different way (only) if a leaf and the HRT surfaces can be mapped on an extremal surface using a (infinitely) large boost transformation; then the HRT surfaces lie on a null hypersurface associated with the leaf. Spacetime also disappears in this case [34]. (This indeed occurs in the de Sitter limit of flat FRW universes.)

without any subtlety. Here, $\mathcal{O}_X^{(i)}$ act "correctly" on elements of $\mathcal{H}_{\text{code},i}$ but annihilate all the other states:

$$\forall X, a \quad \mathcal{O}_X^{(i)}|\psi_a^{(j)}\rangle = 0 \quad \text{for } i \neq j. \tag{2.54}$$

Indeed, if these operators are represented in the whole holographic space $\Xi_{\mathcal{A}}$, then there is no obstacle in defining them as in Eq. (2.54), so that we can build any semiclassical operator state-independently through Eq. (2.53).

However, an important feature—or rather a defining property—of semiclassical operators is that they are represented in multiple different regions in the holographic space $\Xi_{\mathcal{A}}$. Unlike the case of measuring a standard physical object, in quantum gravity there is no large external environment in which information can be amplified, and hence the amplification must occur "internally" within the holographic degrees of freedom given by the system. The holographic theory achieves this by utilizing quantum error correction, amplifying information of entanglement entropies between the holographic degrees of freedom (which makes this information—the geometry—robust under operations in code subspaces). A consequence of this is that operators in code subspaces, i.e. semiclassical operators, are represented in multiple subregions on $\Xi_{\mathcal{A}}$.

We now argue that the requirement of a semiclassical operator being represented redundantly on subregions of $\Xi_{\mathcal{A}}$ in the present setup prevents us from defining the operator in the form of Eq. (2.53) acting universally on all the microstates. To see this, we use models given by the stabilizer formalism, which describes a broad class of quantum error correcting codes. In this formalism, the logical states are those living in the simultaneous eigenspace of an abelian subgroup of the Pauli group. For $n$ physical qubits, the Pauli group $G_n$ is comprised of Pauli operators which are a tensor product of $n$ Pauli matrices: $G_n = \pm\{\boldsymbol{I}, \boldsymbol{X}, \boldsymbol{Y}, \boldsymbol{Z}\}^{\otimes n}$. For qudits of higher dimensions, this can be appropriately generalized.

We consider that the degrees of freedom of the holographic theory are $n$ physical qudits. Let $\mathcal{H}$ be the physical (holographic) Hilbert space and $T$ be an abelian subgroup of the Pauli group, which we consider to be *fixed*. Then the states in the code subspace $\mathcal{H}_{\text{code}}$ can be defined as

$$|\psi\rangle \in \mathcal{H}_{\text{code}} \ \text{ iff } \ t|\psi\rangle = |\psi\rangle \ \ \forall t \in T. \tag{2.55}$$

The group $T$ is called the stabilizer of the code. We regard this code subspace as the Hilbert space of the semiclassical theory built on one of the microstates. A class of operators that have particular significance are logical operators. These operators have nontrivial action on the states in the code subspace and are given by elements of the Pauli group that commute with $T$ but are not elements of $T$.

Now, instead of Eq. (2.55), we could have chosen any other of the simultaneous eigenspaces (with eigenvalues not all $+1$) to be our code subspace. These eigenspaces are orthogonal and completely cover the full physical Hilbert space; we say that they "tile" $\mathcal{H}$. We identify these eigenspaces to be code subspaces $\mathcal{H}_{\text{code},i}$ associated with microstates $i = 1, \cdots, e^{S_{\text{micro}}}$. In this setup, each code subspace has elements $|\psi_a^{(i)}\rangle$ ($a = 1, \cdots, e^{S_{\text{code}}}$), so that

$$S_{\text{micro}} \approx \frac{\mathcal{A}}{4}, \quad S_{\text{code}} \ll \mathcal{A}, \tag{2.56}$$

and

$$S_{\text{micro}} + S_{\text{code}} = \ln \dim \mathcal{H}. \tag{2.57}$$

It is, in fact, simple to build tensor network models realizing this framework. For example, we may consider perfect tensor networks discussed in the previous subsection; but instead of choosing an arbitrary perfect tensor at each node, we now choose a tensor from simultaneous eigenstates of some *fixed* stabilizer group. This leads to quantum error correcting codes that have a particular entanglement structure $S_{\mathcal{M}}$ and correspond to $\mathcal{H}_{\text{code},i}$ discussed above.

The quantum error correcting nature of the codes allows us to represent a semiclassical operator $\mathcal{O}_X$ for each microstate $i$ in various subregions $\Gamma$ in $\Xi_{\mathcal{A}}$, which we denote by $\mathcal{O}_X^{(i)}(\Gamma)$. Note that in general

$$\mathcal{O}_X^{(i)}(\Gamma) \neq \mathcal{O}_X^{(j)}(\Gamma) \quad \text{for } i \neq j, \tag{2.58}$$

although these operators act identically on states in their own code subspaces:

$$\langle \psi_a^{(i)} | \mathcal{O}_X^{(i)}(\Gamma) | \psi_b^{(i)} \rangle = X_{ab}, \tag{2.59}$$

where $X_{ab}$ do not depend on $i$ or possible choices of $\Gamma$. We regard that the operators obtained in this way are essentially the only semiclassical operators. This realizes the situation in which the space of microstates consists of $e^{\mathcal{A}/4}$ discrete basis states (with some possible small "widths").

By construction, the operators $\mathcal{O}_X^{(i)}(\Gamma)$ all commute with the stabilizer generators

$$\left[t, \mathcal{O}_X^{(i)}(\Gamma)\right] = 0, \quad t \in T, \tag{2.60}$$

where $\mathcal{O}_X^{(i)}(\Gamma)$ are interpreted to be defined on the whole holographic space $\Xi_{\text{A}}$, acting trivially on $\bar{\Gamma}$. This implies that actions of these operators do not send a state out of the code subspace it belongs to

$$\mathcal{O}_X^{(i)}(\Gamma) \, |\psi_a^{(j)}\rangle \in \mathcal{H}_{\text{code},j}, \tag{2.61}$$

so that the matrix elements of these operators are nonzero only between states in the same code subspace

$$\langle \psi_a^{(j)} | \mathcal{O}_{X_1}^{(i_1)}(\Gamma) \cdots \mathcal{O}_{X_m}^{(i_m)}(\Gamma) | \psi_b^{(k)} \rangle \propto \delta_{jk}. \tag{2.62}$$

We also find that the matrix elements involving states and operators of different code subspaces have $O(1)$ entries but only with the probability of $e^{-S_{\text{code}}}$:

$$\langle \psi_a^{(j)} | \mathcal{O}_{X_1}^{(i_1)}(\Gamma) \cdots \mathcal{O}_{X_m}^{(i_m)}(\Gamma) | \psi_b^{(j)} \rangle \sim O(1) \quad \text{with } P \sim e^{-S_{\text{code}}}, \tag{2.63}$$

where we have normalized operators such that nonvanishing $X_{ab}$ in Eq. (2.59) are $O(1)$.

The property of Eq. (2.63) follows because the quantum error correcting code corresponding to each microstate $i$ can be viewed as a single large tensor having logical qudits and physical qudits as its indices. The set of tensors corresponding to all the microstates can

then be viewed as the simultaneous eigenstates of some fixed (stabilizer) generators acting on all these indices. This structure guarantees that Eq. (2.63) is satisfied.[14]

We now see how the properties in Eqs. (2.61 – 2.63) prevents us from having state-independent semiclassical operators. In order for exactly state-independent semiclassical operators to be defined, $\mathcal{O}_X^{(i)}(\Gamma)$ must satisfy

$$\langle\psi_a^{(j)}|\mathcal{O}_{X_1}^{(i_1)}(\Gamma)\cdots\mathcal{O}_{X_m}^{(i_m)}(\Gamma)|\psi_b^{(j)}\rangle \neq 0 \quad \text{only for } i_1=\cdots=i_m=j, \tag{2.64}$$

at least for small values of $m$. In this case, the operators represented in subregion $\Gamma$

$$\tilde{O}_X(\Gamma) = \sum_{i=1}^{e^{S_{\rm micro}}} \mathcal{O}_X^{(i)}(\Gamma), \tag{2.65}$$

would become the direct sum form of Eq. (2.53) and act correctly on all possible states of the form

$$|\Psi_a\rangle = \sum_{i=1}^{e^n} c_i|\psi_a^{(i)}\rangle. \tag{2.66}$$

However, for $\Gamma \neq \Xi_{\mathcal{A}}$, the conditions in Eq. (2.64) are not satisfied for all operators; see Eq. (2.63).

In fact, nonzero entries in Eq. (2.63) do not allow for even approximately state-independent operators. To see this, consider the matrix elements

$$\begin{aligned}\langle\psi_a^{(j)}|\tilde{O}_X(\Gamma)|\psi_b^{(j)}\rangle &= \sum_{i=1}^{e^{S_{\rm micro}}} \langle\psi_a^{(j)}|\mathcal{O}_X^{(i)}(\Gamma)|\psi_b^{(j)}\rangle \\ &= X_{ab} + \sum_{i=1;i\neq j}^{e^{S_{\rm micro}}} \langle\psi_a^{(j)}|\mathcal{O}_X^{(i)}(\Gamma)|\psi_b^{(j)}\rangle,\end{aligned} \tag{2.67}$$

where we have used Eq. (2.59) and $\sum_i |c_i|^2 = 1$. The first term is what we want, but the second term gives a much larger contribution $\sqrt{e^{S_{\rm micro}}e^{-S_{\rm code}}} \gg |X_{ab}| \sim O(1)$, where the square root in the leftmost expression arises because of random phases. This implies that we cannot define state-independent semiclassical operators even approximately.

Note that the origin of the state-dependence is not the overlap between different code subspaces. In fact, different code subspaces are orthogonal, Eq. (2.52), in the present (extreme) setup of discrete microstates. Semiclassical operators, however, still must be defined

[14]Instead of adopting the exact stabilizer formalism as we did here, we could use random tensor network models to simulate the setup in which the microstates comprise $e^{\mathcal{A}/4}$ axis states. To do so, we can choose generic $e^{\mathcal{A}/4}$ codes from those obtained by randomly varying the tensor at each node of a fixed network; these $e^{\mathcal{A}/4}$ codes then approximately tile $\mathcal{H}$. In these models, essentially all the elements in the left-hand side of Eq. (2.63) are nonzero, but they are uniformly suppressed as $e^{-S_{\rm code}/2}$. This does not change the conclusion of our analysis here.

state-dependently because of the requirement of being represented redundantly in the holographic space. We find that the necessity of state-dependence is robust in the holographic theory if there are $e^{\mathcal{A}/4}$ independent microstates for a semiclassical spacetime.

We thus conclude either that semiclassical states are special or that bulk operators are state-dependent, in which case semiclassical states can be generic.

## 2.6 Black Hole Interior

We finally discuss the issue of the black hole interior within our framework. A simple description of the interior would arise if a portion of the holographic screen enters inside the black hole horizon. However, we find this is unlikely to occur in a realistic setup in which the second law of thermodynamics, $d\mathcal{A}/d\tau > 0$, is obeyed. First, the holographic screen cannot approach close to the singularity, since then the area of the leaf would decrease in time, contradicting the assumption of $d\mathcal{A}/d\tau > 0$. This leaves the possibility that a portion of a leaf enters the black hole and then exits or terminates. Even in this case, however, we would still encounter the strange situation where the portion of a leaf inside the black hole has a larger area than the corresponding part of the black hole horizon. We therefore assume that the holographic screen does not enter inside the black hole horizon (except possibly in transient periods), though a general proof is lacking.

This only leaves the possibility that the black hole interior can be described effectively by rearranging the degrees of freedom of the theory (which include the stretched horizon degrees of freedom identified in Section 2.4). Such a description would make approximate locality in a portion of the interior manifest at the cost of the local description in some other region (the complementarity picture [63]).[15] We note that this rearrangement of the degrees of freedom would have a different nature than just changing the reference frame, e.g., by boosting the origin of a freely falling reference frame with respect to which the holographic screen is erected. In fact, we expect that any effective description of the black hole interior is applicable only for a finite time (measured with respect to the degrees of freedom made local) reflecting the existence of the singularity, while the reference frame change would give another description of the system which does not have such a restriction.

What about the arguments of Refs. [4, 5, 64] then, which seem to exclude even the possibility of this kind of (effective) description? These arguments can essentially be summarized into two classes:

> *Entanglement argument.* Consider an outgoing mode localized in the zone, corresponding to a Hawking quanta just emitted from the stretched horizon. Unitarity requires this mode to be entangled with a mode representing Hawking radiation emitted earlier, while the smoothness of the horizon requires it to be entangled with the pair

[15] In AdS/CFT, this might be done along the lines of Refs. [65, 66]. We suspect that the requirement of the same interior region being represented redundantly, associated with amplification, might address the question of why the specific set of operators considered in Refs. [65, 66] has a special physical significance.

mode inside the horizon. These two cannot both be true because of monogamy of entanglement.

*Typicality argument.* Suppose we calculate the average of the number operator $\hat{a}^\dagger\hat{a}$ in the dual field theory over states having energies in a chosen range, with $\hat{a}$ corresponding to an infalling mode in the bulk. The resulting number is at least of order unity, because one can choose a basis for these states such that they are all eigenstates of the number operator $\hat{b}^\dagger\hat{b}$ with $\hat{b}$ corresponding to a mode localized in the zone (and because the expectation value of $\hat{a}^\dagger\hat{a}$ in any eigenstate of $\hat{b}^\dagger\hat{b}$ is at least of order unity). This implies that the expectation value of $\hat{a}^\dagger\hat{a}$ is of order unity or larger, giving firewalls, in a typical state in this energy range.

The former, entanglement argument was addressed in Refs. [76, 77]. At the level of a semiclassical description, the Bekenstein-Hawking entropy, $S_{\rm BH} = \mathcal{A}/4$, can be interpreted as the logarithm of the number of independent black hole states of masses between $M$ and $M+\Delta M$, where $\Delta M$ can be taken naturally as the inverse of the Hawking emission timescale. Interpreted in terms of semiclassical operators, this information is distributed according to the thermodynamic entropy associated with the blue-shifted Hawking temperature. This implies that while most of the information is concentrated near the stretched horizon, it has some spread over the zone. In particular, an $O(1)$ amount of information—which is an $O(1/\mathcal{A})$ fraction of the full Bekenstein-Hawking entropy—is at the edge of the zone.

From the semiclassical viewpoint, Hawking emission is a process in which the black hole information (and energy), stored in spacetime, is converted into that of semiclassical excitations *at the edge of the zone* (more precisely, the region around the edge of the zone with the radial width of order the wavelength of emitted Hawking quanta). Note that in the semiclassical viewpoint it is natural that the process occurs in this particular region; it is where the two static geometries—the near horizon, Rindler-like space and asymptotic, Minkowski-like space—are "patched" to obtain the full geometry. This implies that it is incorrect to view that Hawking emission (and the associated information transfer) occurs through outgoing semiclassical excitations in the zone as envisioned in Refs. [4, 5, 64]. In fact, the transfer of energy and information must be viewed as occurring through the flux of negative energy and negative entropy, defined with respect to the static, Hartle-Hawking vacuum.

The typicality argument does not apply when semiclassical operators are given state-dependently [65, 66]. Moreover, if the black hole microstates comprise only a subset of the space spanned by the independent microstates, as contemplated in Section 2.5, then the argument may become irrelevant because the black hole microstates would indeed be non-generic. If this is the case, then smooth black hole states would have to be selected dynamically.

Finally, the fact that the holographic screen does not enter the black hole may allow us to take the attitude that the black hole interior need not be described, since a measurement performed in the interior cannot be communicated to an external observer described directly

in the holographic theory. Of course, what "happened inside" is encoded indirectly in the final Hawking radiation (and in the configuration of the stretched horizon degrees of freedom at intermediate stages), which can be described appropriately in the holographic theory.

# Chapter 3

# Spacetime from Unentanglement

## 3.1 Introduction

It is believed that dynamical spacetime described by general relativity is an emergent phenomenon in the fundamental theory of quantum gravity. Despite this pervasive idea, the materialization of spacetime itself is not fully understood. Holography posits that a fundamental description of quantum gravity resides in a non-gravitational spacetime whose dimension is less than that of the corresponding bulk spacetime [12, 13, 30]. In this paper, we study the emergence of gravitational spacetime in the context of holography, using the renowned anti-de Sitter (AdS)/conformal field theory (CFT) correspondence [14] and a putative holographic theory of Friedmann-Robertson-Walker (FRW) spacetimes [31].

In this paper, we expound on the intimate relationship between the emergence of spacetime and the lack of maximal entanglement in the boundary state. Through this, we see that the existence of spacetime is necessarily non-generic and that nature seizes the opportunity to construct local spacetime when states deviate from maximal entanglement. A reason why this viewpoint is not heavily emphasized (see, however, e.g. Refs. [32, 93]) in the standard context of AdS/CFT is that one almost always considers states with energy much lower than the cutoff (often sent to infinity). The restriction to these "low energy" states implicitly narrows our perspective to those automatically having non-maximal entropy. However, in a holographic theory with a finite cutoff scale (or a fundamentally nonlocal theory), the regime of maximal entropy is much more readily accessible. This happens to be the case in FRW holography, and perhaps holography in general. Through this lens, we analyze the emergence of spacetime both in the familiar setting of Schwarzschild-AdS spacetime with an infrared cutoff and in flat FRW universes. We explicitly see that the directly reconstructable region of spacetime [32, 58] emerges only as we deviate from maximally entangled states. This implies that a holographic theory of exact de Sitter space cannot be obtained as a natural limit of theories dual to FRW spacetimes by sending the fluid equation of state parameter, $w$, to $-1$. In addition to analyzing these two examples, we prove a theorem demonstrating the lack of directly reconstructable spacetime in the case that a boundary state is maximally

entangled.

After surveying the relationship between spacetime and (the lack of) entanglement, we then analyze the deviation from maximal entropy itself. The size of the subregions for which deviations occur reveals valuable information about the underlying holographic theory, and observing the corresponding emergence of spacetime in the bulk provides a glimpse into the mechanism by which nature creates bulk local degrees of freedom. In the case of Schwarzschild-AdS, reconstructable spacetime (the region between the horizon and the cutoff) appears as the temperature in the local boundary theory (the CFT) is lowered, and the resulting entanglement entropy structure (calculated holographically) is consistent with a local theory at high temperature. However, this entanglement structure is not observed in the case of FRW spacetimes as we adjust $w$ away from $-1$; additionally, the reconstructable region grows from the deepest points in the bulk outward. This suggests that the manner in which entanglement is scaffolded is unlike that of AdS/CFT. In fact, this aberrant behavior leads us to believe that the holographic theory dual to FRW spacetimes has nonlocal interactions.

The relationship between spacetime and quantum entanglement between holographic degrees of freedom is no secret [18, 20, 72, 33, 21, 22, 56], but what *is* spacetime? Undoubtedly, entanglement is a necessity for the existence of spacetime. But, it is indeed possible to have too much of a good thing. The analysis here exposes the inability to construct spacetime from maximally entangled boundary states. Since typical states in a Hilbert space are maximally entangled [91], this implies that states with bulk dual are not typical. We see that spacetime is an emergent property of non-generic states in the Hilbert space with both nonvanishing and non-maximal entanglement for subregions. The existence of entanglement allows for the construction of a code subspace of states [26] in which local, semi-classical bulk degrees of freedom can be encoded redundantly. Simultaneously, the lack of maximal entanglement allows for a code subspace with subsystem recovery—hence partitioning the bulk into a collection of local Hilbert spaces. With this perspective, we see that holographic theories are exceedingly enterprising—once deviating from maximal entanglement, nature immediately seizes the opportunity to construct spacetime. In this sense, spacetime is the byproduct of nature's efficient use of intermediate entanglement to construct codes with subsystem recovery.

For a given spacetime with a holographic boundary, one can calculate the von Neumann entropies for all possible subregions of the boundary via the Hubeny-Rangamani-Ryu-Takayanagi (HRRT) prescription [18, 20, 56]. The corresponding entanglement structure heavily constrains the possible boundary states, but by no means uniquely specifies it. In fact, given an entanglement structure and a tensor product Hilbert space, one can always find a basis for the Hilbert space in which all basis states have the desired entanglement structure. If one considers each of these basis states to be dual to the spacetime reproducing the entanglement, then by superpositions one could entirely change the entanglement structure, and hence the spacetime. This property naturally raises the question of how the boundary Hilbert space can accommodate states dual to different semiclassical geometries. Fortunately, for generic dynamical systems, the Hilbert space can be binned into energy

bands, and canonical typicality provides us with the result that generic states *within these bands* have the same entanglement structure, regardless of the energy band's size. This allows the holographic Hilbert space to contain states dual to many different spacetimes, each of which can have bulk excitations encoded state independently. Importantly, this is contingent on the result that typical states have no spacetime.

**Outline**

Section 3.2 walks through the statement that maximally entangled (and hence typical) states have no reconstructable spacetime. This is broken down into parts. First, we must define what we mean by reconstructable; this is detailed in Section 3.2, and is very important toward understanding the framework of the rest of the paper. We then use this construction in Section 3.2 to investigate the reconstructable region of AdS with a black hole. We see the expected behavior that the reconstructable region of spacetime vanishes as the temperature of the black hole reaches the cutoff scale, making the state typical. In Section 3.2, we show that de Sitter states are maximally entangled by finding their HRRT surfaces. In Section 3.2, we combine numerical results for flat FRW universes and use the additional property that de Sitter's HRRT surfaces lie on a null cone to show that the reconstructable region vanishes in the de Sitter limit of FRW spacetimes. Motivated by these results, in Section 3.2 we prove a theorem showing that if a state is maximally entangled, then its HRRT surfaces either wrap the holographic space or live on the null cone. This is then used to present the general argument that maximally entangled states have no spacetime.

Section 3.3 compares the emergence of spacetime in the two theories we are considering. Sections 3.3 and 3.3 present results comparing the entanglement structure of AdS black holes and FRW spacetimes, respectively. Section 3.3 interprets these results and argues that the appropriate holographic dual of FRW spacetimes is most likely nonlocal.

In Section 3.4, we put together all of the previous results and explain how one Hilbert space can contain states dual to many different semiclassical spacetimes. Here we discuss the lack of a need for state dependence when describing the directly reconstructable region.

In Appendix A.2, we analyze two-sided black holes within our construction and discuss how a version of complementarity works in this setup. Appendices A.3 and A.4 collect explicit calculations for Schwarzschild-AdS and the de Sitter limit of FRW spacetimes, respectively.

## 3.2 Maximally Entropic States Have No Spacetime

In this section, we see that maximally entangled states in holographic theories do not have directly reconstructable spacetime. First we lay out the conditions for reconstructability in general theories of holographic spacetimes. Then we examine the familiar example of a large static black hole in AdS and determine its reconstructable region. We then discuss the de Sitter limit of flat FRW spacetimes. Finally, we prove a theorem establishing that maximally entropic holographic states have no reconstructable spacetime.

## Holographic reconstructability

In order to argue that typical states have no reconstructable region, we must first present the conditions for a region of spacetime to be reconstructed from the boundary theory. We adopt the formalism presented first in Ref. [58] but appropriately generalized in Ref. [32] to theories living on holographic screens [67] (which naturally includes the boundary of AdS as in the AdS/CFT correspondence).

The question to answer is: "given a boundary state and its time evolution with a known gravitational bulk dual, what regions of the bulk can be reconstructed?" This may sound tautological, but it is not. Settings in which this question is nontrivial include spacetimes with black holes and other singularities. From entanglement wedge reconstruction [23, 24], we know that the information of a pure black hole is contained in the boundary theory but whether or not the interior is reconstructable is unknown. In holographic theories of general spacetimes, we are interested in describing spacetimes with big bang singularities and a natural question is whether or not the theory reconstructs spacetime arbitrarily close to the initial singularity.

To answer this question, Ref. [58] proposed that reconstructable points in a spacetime are precisely those that can be localized at the intersection of entanglement wedges. This is similar to the proposal in Ref. [82] which advocates that reconstructable points are those located at the intersection of HRRT surfaces anchored to arbitrary achronal subregions of the AdS conformal boundary. However, this construction lacks the ability to localize points in entanglement shadows, which can form in rather tame spacetimes (e.g. a neutron star in AdS), while using the intersection of entanglement wedges allows us to probe these regions.

In order to generalize this to theories living on holographic screens, an essential change is that one can only consider HRRT surfaces anchored to the leaves of a given holographic screen (usually associated to a fixed reference frame) [32]. This is because holographic screens have a unique foliation into leaves that corresponds to a particular time foliation of the holographic theory. Thus the von Neumann entropy of subregions in the holographic theory only makes sense for subregions of a single leaf. Note that despite the lack of a unique time foliation of the conformal boundary, this subtlety is also present in AdS/CFT. Namely, one should consider only a single time foliation of the boundary and the HRRT surfaces anchored to the associated equal time slices even in asymptotically AdS spacetimes [32].[1] This issue becomes manifest when the boundary contains multiple disconnected components, as we discuss in Appendix A.2.

Thus we define the reconstructable region of a spacetime as the union of all points that can be localized at the boundary of entanglement wedges of all subregions of leaves of the holographic screen. Henceforth, we will refer to the regions of spacetime constructed in this way as the directly reconstructable regions (or simply the reconstructable regions when the context is clear), and our analysis will primarily focus on these regions. For a more detailed study of directly reconstructable regions in general spacetimes, see Ref. [32]. In particular,

[1] This is related to the work in Ref. [94], which studied the breakdown of the HRRT formula in certain limits of boundary subregions. These breakdowns correspond to disallowed foliations of the boundary theory.

this definition only allows for the reconstruction of points outside the horizon for a quasi-static one-sided black hole, since such a horizon acts as an extremal surface barrier [62].[2] This also prevents the direct reconstruction of points near singularities such as big bang singularities and the black hole singularity of a two-sided black hole.

Now that we have detailed the conditions for regions of spacetime to be directly reconstructable, we must determine a measure of "how much" spacetime is reconstructable. This will allow us to see the loss of spacetime in the limit of states becoming typical. In the context of quantum error correction [26], we are attempting to quantify the factorization of the code subspace, e.g. how many dangling bulk legs exist in a tensor network representation of the code [28, 29]. We expect the spacetime volume of the reconstructable region to be indicative to this property, and we will use it in our subsequent analyses. The bulk spacetime directly reconstructable from a single leaf depends on features of the bulk, for example, the existence of shadows and time dependence. In the case of $(d+1)$-dimensional flat FRW spacetimes, we find that a codimension-0 region can be reconstructed from a single leaf. On the other hand, in any static spacetime, all HRRT surfaces anchored to one leaf live in the same time slice in the bulk, and hence their intersections reconstruct a codimension-1 surface of the bulk. This is the case in an AdS black hole.

The discrepancy of the dimensions of the directly reconstructable regions for different spacetimes of interest may seem to cause issues when trying to compare the loss of spacetime in these systems. Namely, it seems difficult to compare the loss of reconstructable spacetime in Schwarzschild-AdS as we increase the black hole mass to the loss of spacetime in the $w \to -1$ limit of flat FRW spacetimes. However, in all cases, the spacetime region directly reconstructable from a small time interval in the boundary theory is codimension-0. We can then examine the relative loss of spacetime in both cases (black hole horizon approaching the boundary in AdS space and $w \to -1$ in FRW spacetimes) by taking the ratio of the volume of the reconstructable region to the reconstructable volume of some reference state (e.g. pure AdS and flat FRW with some fixed $w \neq -1$). In static spacetimes, this will reduce to a ratio of the spatial volumes reconstructed on a codimension-1 slice, allowing us to consider only the volume of regions reconstructed from single leaves.

## Large AdS black holes

Here we will see how spacetime disappears as we increase the mass of the black hole in static Schwarzschild-AdS spacetime, making the corresponding holographic state maximally entangled. We consider a holographic pure state living on the (single) conformal boundary of AdS. We introduce an infrared cutoff $r \leq R$ in AdS space and consider a $d+1$ dimensional large black hole with horizon radius $r = r_+$.

[2] This does not exclude the possibility that the holographic theory allows for some effective description of regions other than the directly reconstructable one, e.g. the black hole interior (perhaps along the lines of Ref. [66]). This may make the interior spacetime manifest, perhaps at the cost of losing the local description elsewhere, and may be necessary to describe the fate of a physical object falling into a black hole. We focus on spacetime regions that can be described by the boundary theory without resorting to such descriptions.

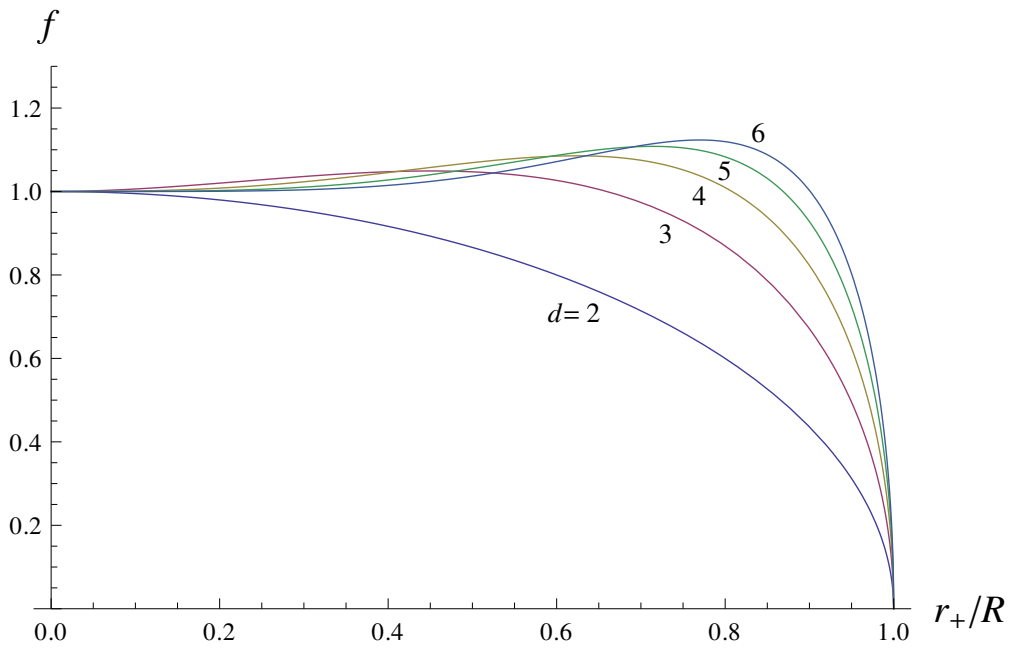


Figure 3.1: The volume $V(r_+, R)$ of the Schwarzschild-AdS spacetime that can be reconstructed from the boundary theory, normalized by the corresponding volume $V(R)$ in empty AdS space: $f = V(r_+, R)/V(R)$. Here, $R$ is the infrared cutoff of $(d+1)$-dimensional AdS space, and $r_+$ is the horizon radius of the black hole.

As discussed in Section 3.2, the size of the spacetime region directly reconstructable from the boundary theory is characterized by $V(r_+, R)$, the spatial volume between the black hole horizon and the cutoff. We normalize it by the volume of the region $r \leq R$ in empty AdS space, $V(R)$, to get the ratio

$$f\Big(\frac{r_+}{R}\Big) \equiv \frac{V(r_+, R)}{V(R)} = (d-1)\frac{r_+^{d-1}}{R^{d-1}} \int_1^{\frac{R}{r_+}} \frac{x^{d-2}}{\sqrt{1-\frac{1}{x^d}}}\, dx, \tag{3.1}$$

which depends only on $r_+/R$ (and $d$). As expected, it behaves as

$$f\Big(\frac{r_+}{R}\Big) \begin{cases} \simeq 1 & (r_+ \ll R) \\ \to 0 & (r_+ \to R), \end{cases} \tag{3.2}$$

in the two opposite limits. The details of this calculation can be found in Appendix A.3. Here, we plot $f(r_+/R)$ in Fig. 3.1 for various values of $d$.

In the limit $r_+ \to R$, the HRRT surface, $\gamma_A$, anchored to the boundary of subregion $A$ of a boundary space (a constant $t$ slice of the $r = R$ hypersurface) becomes the region $A$

itself or the complement, $\bar{A}$, of $A$ on the boundary space, whichever has the smaller volume.[3] This implies that the entanglement entropy of $A$, given by the area of the HRRT surface as $S_A = \|\gamma_A\|/4l_{\rm P}^{d-1}$, becomes exactly proportional to the smaller of the volumes of $A$ and $\bar{A}$ in the boundary theory:

$$S_A = \frac{1}{4l_{\rm P}^{d-1}} \min\{\|A\|, \|\bar{A}\|\}. \tag{3.3}$$

Here, $\|x\|$ represents the volume of the object $x$ (often called the area for a codimension-2 surface in spacetime), and $l_{\rm P}$ is the $(d+1)$-dimensional Planck length in the bulk. Via usual thermodynamic arguments, we interpret this to mean that the state in the boundary theory is generic, so that it obeys the Page law [91].[4] This in turn implies that the temperature of the system, which is identified as the Hawking temperature $T_{\rm H}$, is at the cutoff scale.[5] $T_{\rm H}$ is related to $r_+$ by

$$\frac{r_+}{R} = \frac{4\pi l^2}{dR} T_{\rm H}, \tag{3.4}$$

where $l$ is the AdS radius. Hence, the cutoff scale of the boundary theory is given by [17]

$$\Lambda = \frac{dR}{4\pi l^2}. \tag{3.5}$$

This allows us to interpret the horizontal axis of Fig. 3.1 as $T_{\rm H}/\Lambda$ from the viewpoint of the boundary theory.

We finally make a few comments. First, it is important to note that by the infrared cutoff, we do not mean that the spacetime literally ends there as in the scenario of Ref. [95]. Such termination of spacetime would introduce dynamical gravity in the holographic theory, making the maximum entropy of a subregion scale as the area, rather than the volume, in the holographic theory. Rather, our infrared cutoff here means that we focus only on the degrees of freedom in the bulk deeper than $r = R$, corresponding to setting the sliding renormalization scale to be $\approx R/l^2$ in the boundary theory. In particular, the boundary theory is still non-gravitational.

Second, to state that spacetime disappears in the limit where the holographic state becomes typical, it is crucial to define spacetime as the directly reconstructable region. This becomes clear by considering a large subregion $A$ on the boundary theory such that $A$ and its HRRT surface $\gamma_A$ enclose the black hole at the center. If we take the simple viewpoint of entanglement wedge reconstruction, this would say that spacetime does not disappear even if the black hole becomes large and its horizon approaches the cutoff surface, since the black hole interior is within the entanglement wedge of $A$ so that it still exists in the sense of

[3] We do not impose a homology constraint, since we consider a pure state in the holographic theory. Additionally, we only consider subregions larger than the cutoff size.

[4] Page's analysis tells us that for a generic state (a Haar random state) in a Hilbert space, the entanglement entropy of a reduced state is nearly maximal. In fact, at the level of the approximation we employ in this paper, $\|A\|/l_{\rm P}^{d-1} \to \infty$, such a state has the maximal entanglement entropy for any subregion, Eq. (3.3).

[5] When we refer to a high temperature state, we do not mean that the whole holographic state is a mixed thermal state. What we really mean is a high energy state, since we focus on pure states.

entanglement wedge reconstruction. We, however, claim that such a region does not exist as a localizable spacetime region, as explained in Section 3.2.

Third, the curves in Fig. 3.1 are not monotonically decreasing as $r_+$ increases for $d > 2$, despite the fact that

$$\frac{d}{dr_+}\left\{S_{A,\max} - S_{A,\mathrm{BH}}(r_+)\right\} < 0. \tag{3.6}$$

Here, $S_{A,\max}$ and $S_{A,\mathrm{BH}}(r_+)$ are the maximal entropy and the entropy corresponding to the black hole geometry of subregion $A$, given by

$$S_{A,\max} = \frac{\|A\|}{4l_{\mathrm{P}}^{d-1}}, \qquad S_{A,\mathrm{BH}}(r_+) = \frac{\|A\|}{4l_{\mathrm{P}}^{d-1}}\frac{r_+^{d-1}}{R^{d-1}}. \tag{3.7}$$

This increase in spacetime volume may be demonstrating that the additional entanglement in the boundary state allows for more bulk nodes in the code subspace. Alternatively, this may be a feature of using volume as our measure. Regardless, the decrease observed near the cutoff temperature is the main focus of our attention, and we expect any other reasonable measure to correspondingly vanish.

Finally, the statement that spacetime disappears as the holographic state approaches typicality persists for two-sided black holes. In this setup, there is a new issue that does not exist in the case of single-sided black holes: the choice of a reference frame associated with a relative time shift between the two boundaries. The discussion of two-sided black holes is given in Appendix A.2.

## de Sitter states are maximally entropic

We have seen that a large black hole in AdS with $r_+ \to R$ corresponds to CFT states at the cutoff temperature, and that the holographic states in this limit have the entanglement entropy structure of Eq. (3.3). Below, we refer to states exhibiting Eq. (3.3) as the *maximally entropic states*. Is there an analogous situation in the holographic theory of FRW spacetimes, described in Ref. [31]? Here we argue that the de Sitter limit ($w \to -1$) in flat FRW universes provides one.[6]

We first see that the holographic state becomes maximally entropic in the case that a universe approaches de Sitter space at late times [56]. This situation arises when the universe contains multiple fluid components including one with $w = -1$, so that it is dominated by the $w = -1$ component at late times. This analysis does not apply directly to the case of a single component with $w = -1 + \epsilon$ ($\epsilon \to 0^+$), which will be discussed later.

In the universe under consideration, the FRW metric approaches the de Sitter metric in flat slicing at late times

$$ds^2 = -dt^2 + e^{\frac{2t}{\alpha}}\left(dr^2 + r^2 d\Omega_{d-1}^2\right), \tag{3.8}$$

where $\alpha$ is the Hubble radius, and we have taken the spacetime dimension of the bulk to be $d + 1$. The Penrose diagram of this spacetime is depicted in Fig. 3.2, where constant time

[6]For a simple proof applicable to $2 + 1$ dimensions, see Appendix A.4.

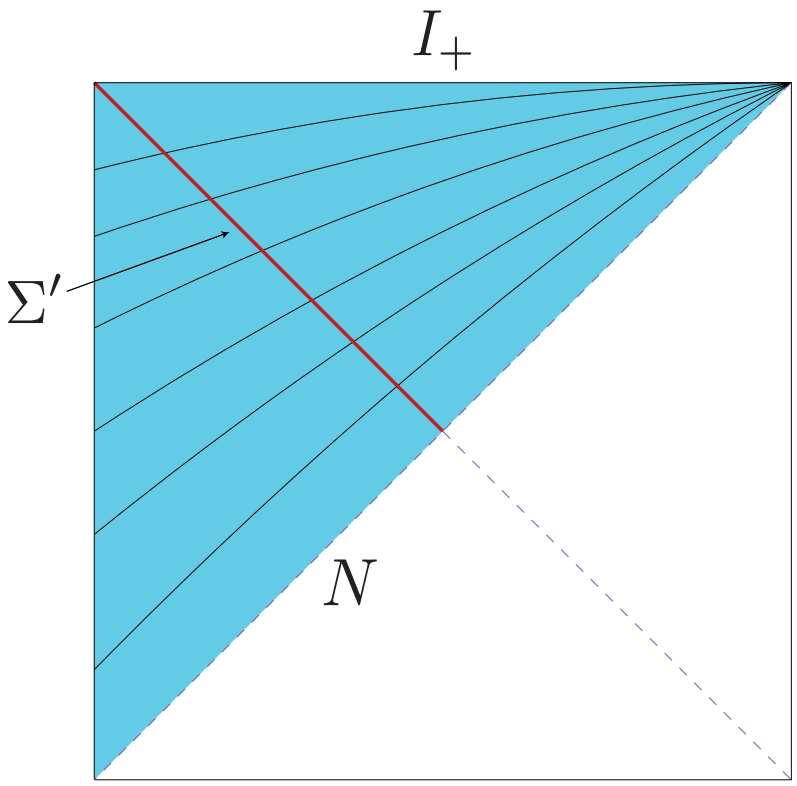


Figure 3.2: The Penrose diagram of de Sitter space. The spacetime region covered by the flat-slicing coordinates is shaded, and constant time slices in this coordinate system are drawn. The codimension-1 null hypersurface $\Sigma'$ is the cosmological horizon for an observer at $r = 0$, to which the holographic screen of the FRW universe asymptotes in the future.

slices are drawn and the region covered by the coordinates is shaded; future timelike infinity $I_+$ corresponds to $t = \infty$, while the null hypersurface $N$ corresponds to $t = -\infty$. At late times, the past holographic screen of the FRW universe asymptotes to the codimension-1 null hypersurface $\Sigma'$ depicted in the figure. This hypersurface is located at

$$r = \alpha\, e^{-\frac{t}{\alpha}}, \tag{3.9}$$

which corresponds to the cosmological horizon for an observer moving along the $r = 0$ geodesic.

We can now transform the coordinates to static slicing

$$ds^2 = -\left(1 - \frac{\rho^2}{\alpha^2}\right) d\tau^2 + \frac{1}{1 - \frac{\rho^2}{\alpha^2}} d\rho^2 + \rho^2 d\Omega_{d-1}^2. \tag{3.10}$$

In Fig. 3.3, we depict constant $\tau$ (red) and constant $\rho$ (blue) slices, with the shaded region being covered by the coordinates. This metric makes it manifest that the spacetime has a

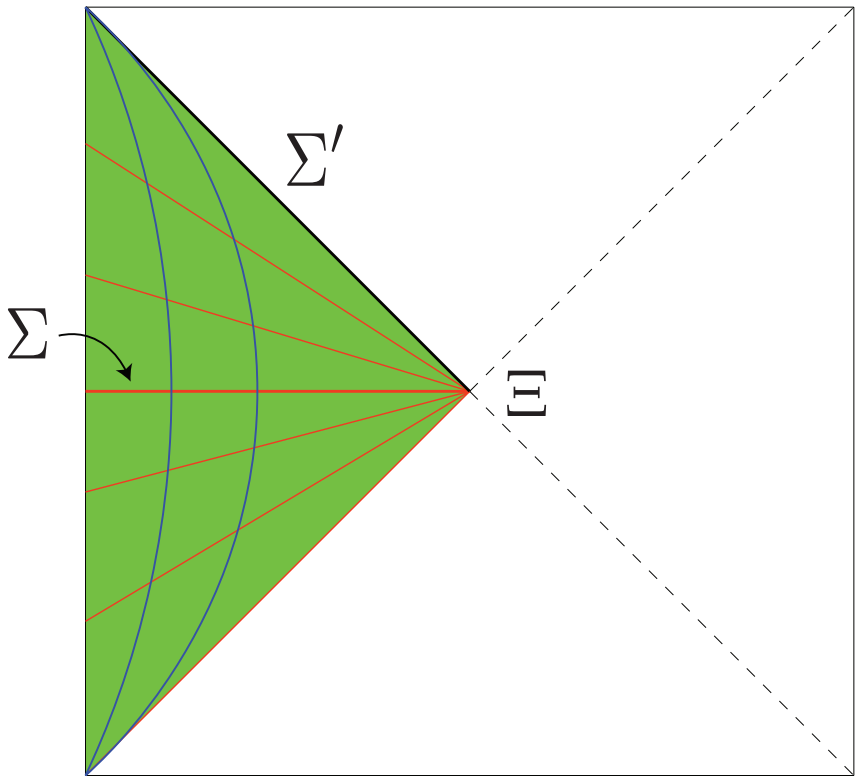


Figure 3.3: Constant time slices and the spacetime region covered by the coordinates in static slicing of de Sitter space. Here, $\Sigma$ is the $\tau = 0$ hypersurface, and $\Xi$ is the bifurcation surface, given by $\rho = \alpha$ with finite $\tau$.

Killing symmetry corresponding to $\tau$ translation. Using this symmetry, we can map a leaf of the original FRW universe to the $\tau = 0$ hypersurface, $\Sigma$. Since the leaf of the universe under consideration approaches arbitrarily close to Eq. (3.9) at late times, the image of the map, $\Xi'$, asymptotes to the bifurcation surface $\Xi$ at

$$\rho = \alpha, \tag{3.11}$$

for a leaf at later times.

Consider an arbitrary subregion $A$ on $\Xi'$ and the minimal area surface $\gamma_A$ on $\Sigma$ anchored to the boundary of $A$, $\partial A$. Since the geometry of $\Sigma$ is $S^d$ with $\Xi$ being an equator, the minimal area surface $\gamma_A$ becomes the region $A$ itself (or its complement on $\Xi'$, whichever is smaller) in the limit $\Xi' \to \Xi$. Strictly speaking, this statement does not apply for a small subset of subregions, since $\Xi'$ is not exactly $\Xi$ unless the leaf under consideration is at strictly infinite time. (For subregions in this subset, the minimal area surfaces probe $\rho \ll \alpha$. For spherical caps, these subregions are approximately hemispheres.) However, the fractional

size of the subset goes to zero as we focus on later leaves. Continuity then tells us that our conclusion persists for all subregions.

The surface $\gamma_A$ found above is in fact an extremal surface, since the bifurcation surface $\Xi$ is an extremal surface, so any subregion of it is also extremal. It is easy to show that this surface is indeed the HRRT surface, the minimal area extremal surface. Suppose there is another extremal surface $\gamma'_A$ anchored to $\partial A$. We could then send a null congruence from $\gamma'_A$ down to $\Sigma$, yielding another codimension-2 surface $\gamma''_A$ given by the intersection of the null congruence and $\Sigma$. Because $\gamma'_A$ is extremal, the focusing of the null rays implies $\|\gamma'_A\| > \|\gamma''_A\|$, and by construction $\|\gamma_A\| < \|\gamma''_A\|$. This implies that $\gamma_A$ is the HRRT surface, and hence

$$S_A = \frac{1}{4l_{\rm P}^{d-1}} \min\{\|A\|, \|\bar{A}\|\}. \tag{3.12}$$

Namely, the holographic state representing an FRW universe that asymptotically approaches de Sitter space becomes a maximally entropic state in the late time limit.

The global spacetime structure in the case of a single fluid component with $w \neq -1$ is qualitatively different from the case discussed above. For example, the area of a leaf grows indefinitely. However, for any finite time interval, the behavior of the system approaches that of de Sitter space in the limit $w \to -1$. In fact, the numerical analysis of Ref. [31] tells us that the holographic entanglement entropy of a spherical cap region becomes maximal in the $w \to -1$ limit. We show in Appendix A.4 that this occurs for an arbitrary subregion on a leaf.

## Spacetime disappears as $w \to -1$ in the holographic FRW theory

We have seen in our AdS/CFT example that as the holographic state approaches typicality, and hence becomes maximally entropic, the directly reconstructable region disappears. On the other hand, we have shown that the entanglement entropies for flat FRW universes approaches the maximal form as $w \to -1$. Does this limit have a corresponding disappearance of reconstructable spacetime? Here we will show that the answer to this question is yes.

From the analysis of Section 3.2, we see that a leaf at late times in universes approaching de Sitter space can be mapped to a surface on the $\tau = 0$ hypersurface $\Sigma$, which asymptotes to the bifurcation surface $\Xi$ in the late time limit. From the Killing symmetry, the HRRT surfaces anchored to this mapped leaf must all be restricted to living on $\Sigma$. Mapping the HRRT surfaces back to the original location, we see that they asymptote to living on the null hypersurface $\Sigma'$. Thus, we find that the HRRT surface for any subregion of a leaf $\sigma_*$ asymptote to the future boundary of the causal region $D_{\sigma_*}$, which we denote by $\partial D^{(+)}_{\sigma_*}$, as a universe approaches de Sitter space. A similar argument holds for universes where $w \to -1$. In Appendix A.4, we present some examples where we can see this behavior using analytic expressions for HRRT surfaces.

What does this imply for the reconstructable region in de Sitter space? Using the prescription outlined in Section 3.2, we find that spacetime points on the future causal boundary of a leaf, $\partial D^{(+)}_{\sigma_*}$, can be reconstructed. This is a codimension-1 region in spacetime. One

might then think that we can reconstruct a codimension-0 region by considering multiple leaves, as was the case in a Schwarzschild-AdS black hole. However, the holographic screen of de Sitter space is itself a null hypersurface, with future leaves lying precisely on the future causal boundary of past leaves. This means that even by using multiple leaves we cannot reconstruct any nonzero measure spacetime region in the de Sitter (and $w \to -1$) limit.

We will now compute the reconstructable region in $(2+1)$-dimensional flat FRW spacetimes. As discussed in Section 3.2, this region is comprised of points that can be localized as the intersection of edges of entanglement wedges. We will be considering the reconstructable region associated to a single leaf, and hence this prescription reduces to finding points located at the intersection of HRRT surfaces anchored to the leaf. This alone gives us a codimension-0 reconstructable region. In $(2+1)$-dimensional FRW spacetimes, HRRT surfaces are simply geodesics in the bulk spacetime, and this problem becomes tractable.

For a $(2+1)$-dimensional flat FRW universe filled with a single fluid component $w$, the leaf of the holographic screen at conformal time $\eta_*$ is located at coordinate radius

$$r_* = \frac{a}{\dot{a}}\bigg|_{\eta=\eta_*} = w\eta_*. \tag{3.13}$$

Let us parameterize the points on the leaf by $\phi \in [0, 2\pi)$. Consider an interval of the leaf at time $\eta_*$ centered at $\phi_0$ with half opening angle $\psi$. The HRRT surface of this subregion is simply the geodesic connecting the endpoints of the interval: $(\eta, \phi) = (\eta_*, \phi_0 - \psi)$ and $(\eta_*, \phi_0 + \psi)$. It is clear from the symmetry of the setup that if we consider a second geodesic anchored to an interval with the same opening angle but with a center $\phi_0' \in [\phi_0 - 2\psi, \phi_0 + 2\psi]$, then the two geodesics will intersect at a point, specifically where $\phi = (\phi_0 + \phi_0')/2$. Using these pairs of geodesics, it is clear that we can reconstruct all points on all geodesics anchored to the leaf. The union of these points gives us a codimension-0 region.

Can we get a larger region? In $(2+1)$-dimensional flat FRW spacetimes, the answer is no. In higher dimensions, knowing the HRRT surfaces for all spherical cap regions may not be sufficient to figure out reconstructable regions; for example, one may consider using disjoint regions in hopes that the new HRRT surfaces would explore regions inaccessible to the previous HRRT surfaces (although we do not know if this really leads to a larger reconstructable region). However, in $2+1$ dimensions, both connected and disconnected phases of extremal surfaces are constructed from the geodesics already considered, so we gain nothing from considering disconnected subregions. We thus find that the set of all points on HRRT surfaces anchored to arbitrary subregions on a leaf is exactly the reconstructable region from the state on the leaf.

In Fig. 3.4, we show a plot of the reconstructable spacetime volume as a function of $w$. It shows a qualitatively similar behavior to that of Fig. 3.1, where the reconstructable volume increases and then sharply declines to zero as the holographic state becomes maximally entropic.

We can also perform a similar analysis in higher dimensions. Due to the numerical difficulty in finding extremal surfaces, here we restrict ourselves to the region reconstructable

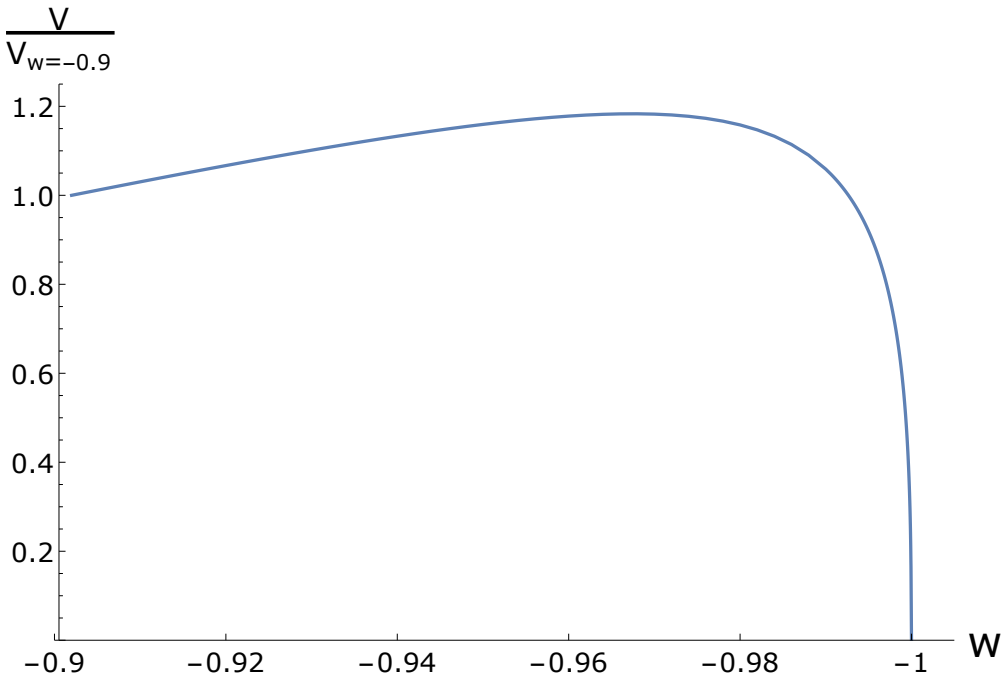


Figure 3.4: The spacetime volume of the reconstructable region in $(2+1)$-dimensional flat FRW universes for $w \in (-0.9, -1)$, normalized by the reconstructable volume for $w = -0.9$.

by spherical cap regions (which may indeed be the fully reconstructable region) and to only a few representative values of $w$. The results are plotted in Fig. 3.5 for $(3+1)$-dimensional FRW universes. These demonstrate the behavior that the extremal surfaces, and hence the reconstructable region, becomes more and more null as $w \to -1$.

The discussion in this subsection says that the reconstructable spacetime region disappears in the holographic theory of FRW spacetimes as the holographic state becomes maximally entropic in the de Sitter limit. While a microstate becoming maximally entropic does not directly mean that states representing the corresponding spacetime become typical in the holographic Hilbert space (since the number of independent microstates could still be small), we expect that the former indeed implies the latter as usual thermodynamic intuition suggests; see Section 3.4 for further discussion. In any event, since typical states in a holographic theory are maximally entropic, we expect that the reconstructable spacetime region disappears as the holographic state becomes typical.

An important implication of the analysis here is that a holographic theory of de Sitter space cannot be obtained by taking a limit in the holographic theory of FRW spacetimes. A holographic theory of exact de Sitter space, if any, would have to be formulated in a different manner.[7]

[7]Another instance in which spacetime disappears is when the holographic description changes from that based on a past holographic screen (foliated by marginally anti-trapped surfaces) to a future holographic

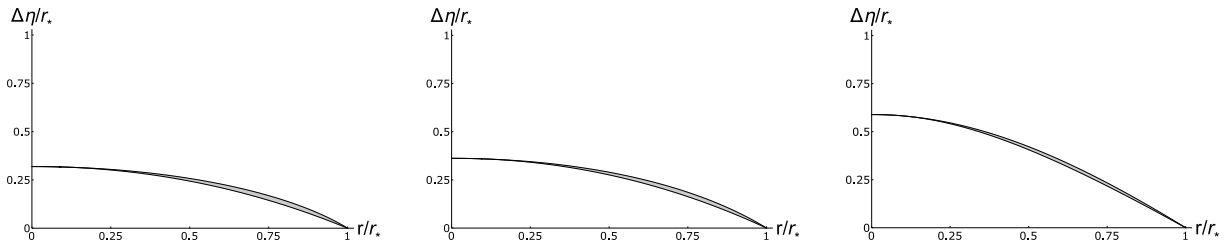


(a) $w = 1$, $\eta_* = 1$ (b) $w = 0$, $\eta_* = 1$ (c) $w = -4/5$, $\eta_* = -1$

Figure 3.5: Reconstructable spacetime regions for various values of $w$ in $(3+1)$-dimensional flat FRW universes. The horizontal axis is the distance from the center, normalized by that to the leaf. The vertical axis is the difference in conformal time from the leaf, normalized such that null ray from the leaf would reach 1. The full reconstructable region for each leaf would be the gray region between the two lines rotated about the vertical axis.

## Maximally entropic states have no spacetime

In this subsection, we provide a proof for the statement that the directly reconstructable region of a maximally entropic leaf is either the leaf itself or a subset of its null cone. We use this result to argue that maximally entropic states have no spacetime. This heavily utilizes the maximin techniques developed in Ref. [60].

**Theorem 1.** Consider a compact codimension-2 spacelike surface, $\sigma$, with area $\mathcal{A}$, living in a spacetime that satisfies $R_{ab}v^a v^b \geq 0$ for all null vectors $v^a$. Suppose HRRT surfaces can consistently be anchored to $\sigma$.[8] Let $m(\Gamma)$ denote the HRRT surface anchored to the boundary, $\partial\Gamma$, of a subregion $\Gamma$ of $\sigma$.

If $\|m(\Gamma)\| = \min\{\|\Gamma\|, \|\bar{\Gamma}\|\}, \forall \Gamma \subset \sigma$, then either $\sigma$ is a bifurcation surface or all of the HRRT surfaces of $\sigma$ lie on a non-expanding null hypersurface connected to $\sigma$.

*Proof.* If $\Gamma_1$ and $\Gamma_2$ are subregions of $\sigma$, we will abbreviate $\Gamma_1 \cup \Gamma_2$ as $\Gamma_1\Gamma_2$. Let $m(\Gamma)_\Sigma$ denote the representative of $m(\Gamma)$ on a complete achronal surface $\Sigma$, defined by the intersection of $\Sigma$ with a null congruence shot out from $m(\Gamma)$. From the extremality of $m(\Gamma)$, $R_{ab}v^a v^b \geq 0$, and the Raychaudhuri equation, $\|m(\Gamma)_\Sigma\| \leq \|m(\Gamma)\|$.

Consider three connected subregions $A$, $B$, $C$ of $\sigma$ such that $\partial A \cap \partial B \neq \emptyset$, $\partial B \cap \partial C \neq \emptyset$ where both such intersections are codimension-3, and $\|A \cup B \cup C\| \leq \|\sigma\|/2$; see Fig. 3.6

screen (marginally trapped surfaces). Such a change of description may occur in a spacetime with a late-time collapsing phase, e.g. in a closed FRW universe with the holographic screen constructed naturally in an observer-centric manner. (For an interpretation of such spacetime, see Ref. [31].) Since the leaf at the time of the transition is extremal, the analysis here indicates that the spacetime region reconstructable from a single leaf disappears at that time. This makes the necessity of the change of the description more natural.

[8] This requires the expansion of the two null hypersurfaces bounding $D(\sigma)$ to have $\theta \leq 0$, where $D(\sigma)$ is the interior domain of dependence of some achronal set whose boundary is $\sigma$. These HRRT surfaces are guaranteed to exist and satisfy basic entanglement inequalities; see Refs. [56, 57].

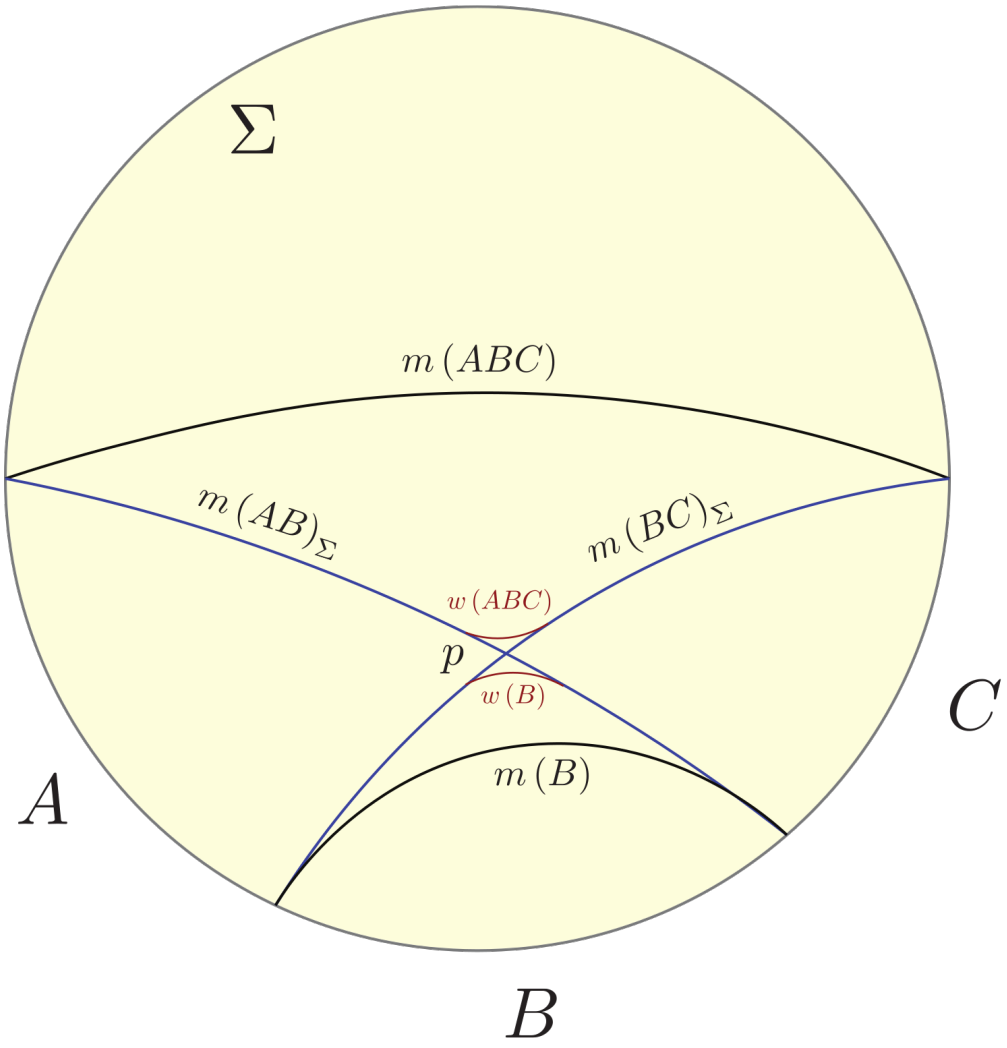


Figure 3.6: Diagrams representing the achronal surface $\Sigma$ in which two HRRT surfaces, $m(ABC)$ and $m(B)$, live. $m(AB)_\Sigma$ and $m(BC)_\Sigma$ are the representatives of $m(AB)$ and $m(BC)$, respectively. They are shown to be intersecting at $p$. On a spacelike $\Sigma$, one could deform around this intersection to create two new surfaces with smaller areas.

for a diagram. By Theorem 17.h of Ref. [60], take $m(ABC)$ and $m(B)$ to be on the same achronal surface, $\Sigma$. Now, consider the representatives $m(AB)_\Sigma$ and $m(BC)_\Sigma$. From the properties of representatives and maximin surfaces, we have

$$S(AB) + S(BC) \geq \frac{\|m(AB)_\Sigma\|}{4l_{\mathrm{P}}^{d-1}} + \frac{\|m(BC)_\Sigma\|}{4l_{\mathrm{P}}^{d-1}} \geq S(ABC) + S(B). \tag{3.14}$$

The assumption of maximal entropies then tells us that strong subadditivity is saturated,

and hence

$$\begin{aligned} \|m(AB)_\Sigma\| &= \|m(AB)\|, \\ \|m(BC)_\Sigma\| &= \|m(BC)\|. \end{aligned} \tag{3.15}$$

Additionally, $m(AB)_\Sigma \cap m(BC)_\Sigma \neq \emptyset$.

We have two cases depending on the nature of $\Sigma$.

Case 1: $m(ABC)$, $m(B)$, $m(AB)_\Sigma$, and $m(BC)_\Sigma$ live on $\Sigma$ which is a non-null hypersurface.

Suppose $m(AB)_\Sigma \cap m(BC)_\Sigma$ is a codimension-3 surface, meaning they intersect through some surface, $p$, depicted in Fig. 3.6. One could then smooth out the "corners" around $p$ to create new surfaces homologous to $ABC$ and $B$. This is depicted through the maroon lines in Fig. 3.6. By the triangle inequality, these new, smoothed out surfaces, $w(ABC)$ and $w(B)$, would have less total area than $m(ABC) \cup m(B)$ because $p \in \Sigma$, which is spacelike. However, this contradicts the minimality of $m(ABC)$ and $m(B)$:

$$\begin{aligned} (\|A\| + \|B\| + \|C\|) + \|B\| = \|m(ABC)\| + \|m(B)\| \leq \|w(ABC)\| + \|w(B)\| \\ < \|m(AB)_\Sigma\| + \|m(BC)_\Sigma\| = (\|A\| + \|B\|) + (\|B\| + \|C\|). \end{aligned} \tag{3.16}$$

Therefore, $m(AB)_\Sigma$ and $m(BC)_\Sigma$ cannot intersect through some codimension-3 surface, yet they must still intersect. This requires $m(AB)_\Sigma$ and $m(BC)_\Sigma$ to coincide somewhere, a neighborhood of $x$, and by Theorem 4.e of Ref. [60] these two surfaces must coincide at every point connected to $x$. This means that $m(AB) = m(A) \cup m(B)$ and $m(BC) = m(B) \cup m(C)$. The only way this can consistently occur for all possible $A$, $B$, and $C$ is for $m(\Gamma) \subset \sigma$. This means that $\sigma$ itself is extremal, and hence is a bifurcation surface.

Case 2: $m(ABC)$, $m(B)$, $m(AB)_\Sigma$, and $m(BC)_\Sigma$ live on hypersurface $\Sigma$ which is at least partially null.

Suppose $m(AB)_\Sigma \cap m(BC)_\Sigma$ is a codimension-3 surface, $p$. If at $p$, $\Sigma$ is null and non-expanding, then smoothing out the intersection will not result in new surfaces with smaller area. This is the condition that $\theta_u = 0$ on the null hypersurface, $\Sigma_u$, coincident with $\Sigma$ at $p$, where $u$ is the null vector generating $\Sigma_u$ at $p$. Hence, the representatives can intersect at $p$ and simultaneously saturate strong subadditivity. Additionally, because $\|m(BC)_\Sigma\| = \|m(BC)\|$, we know that $\theta_v = 0$ along the hypersurface generating the representatives of $m(BC)$, where $v$ is the null vector generating this hypersurface. Therefore at $p$, $\theta_u = \theta_v = 0$.

We can now scan across $m(BC)_\Sigma$ by considering its intersection with $m(AB')_\Sigma$ where $(B', C')$ is a bipartition of $B \cup C$ where $\partial B' \cap \partial A \neq \emptyset$, and then considering all such bipartitions. This is illustrated in Fig. 3.7 by splitting up $B \cup C$ at a few points labeled

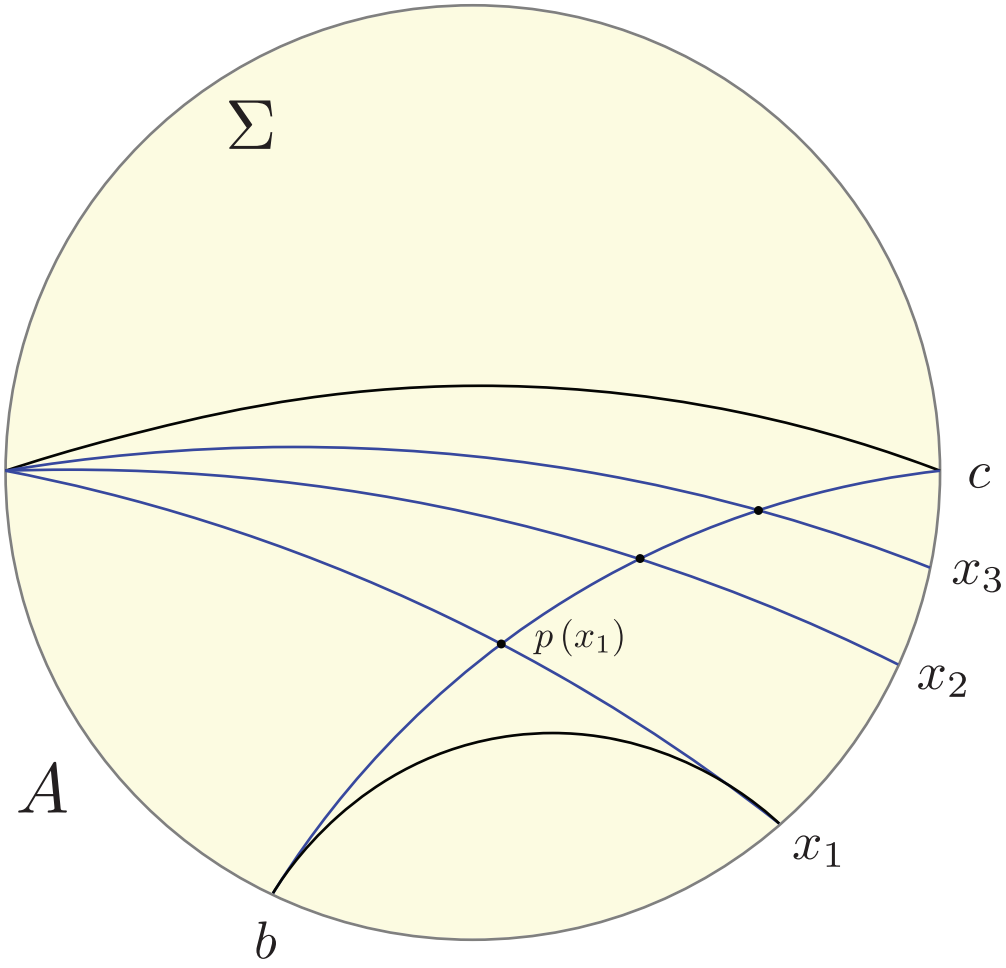


Figure 3.7: This depicts how one can scan across the representative $m(BC)_\Sigma$ by bipartitioning $BC$ on the achronal surface $\Sigma$. At each of these intersections, $p(x_i)$, $\theta_u = \theta_v = 0$ if the state on the leaf is maximally entropic and $\Sigma$ is null and non-expanding.

by $x_i$; for example, $B' = [b, x_3]$ and $C' = [x_3, c]$ is one such allowable bipartition. By continuity, all of $m(BC)_\Sigma$ will be scanned.[9]

By the argument in the previous paragraph, all intersection points along $m(BC)_\Sigma$ must then have $\theta_u = \theta_v = 0$. Assuming nondegeneracy, $m(BC)_\Sigma$ must therefore be the HRRT surface $m(BC)$. Additionally, every point of $m(BC)$ lives on some null, non-expanding hypersurface and at $\partial m(BC)$ this surface connects to $\sigma$. Hence, at $\partial m(BC)$, $\sigma$ must be marginal. This argument can be repeated for any set of

[9]We believe this is sufficient to scan over the whole surface assuming the spacetime is smooth. Additionally, Eq. (3.15) requires there to be no energy density between an HRRT surface and its representative, this will preclude jumps in the representatives due to entanglement shadows and the like.

appropriate subregions. This tells us that all HRRT surfaces have the previously stated properties.

Now, by Theorem 17.h of Ref. [60], we can construct an achronal surface, $\Sigma$, that is foliated by HRRT surfaces. Each point of $\Sigma$ must now be null and non-expanding. Additionally, the boundary of $\Sigma$, $\sigma$, must be marginal. Let $k$ denote the vector in this local marginal direction. This uniquely specifies $\Sigma$ as the null non-expanding hypersurface generated by $k$. This is true for all $\Sigma$ foliated by HRRT surfaces, and each HRRT surface can belong to some foliation of a $\Sigma$.[10] Hence all extremal surfaces anchored to $\sigma$ must belong to a non-expanding null hypersurface.

Back to the beginning, if the intersection of $m(AB)_\Sigma$ and $m(BC)_\Sigma$ is codimension-2, then the argument from Case 1 applies and $\sigma$ must be extremal.

This concludes the proof of Theorem 1. □

**Corollary 1.** Consider a codimension-2 surface, $\sigma$, with area $\mathcal{A}$, living in a spacetime satisfying $R_{ab}v^a v^b \geq 0$. Let $m(\Gamma)$ denote the HRRT surface anchored to $\partial\Gamma$.

If $\sigma$ is not marginal, then it cannot satisfy $\|m(\Gamma)\| = \min\{\|\Gamma\|, \|\bar{\Gamma}\|\}, \forall\Gamma \subset \sigma$.

*Proof.* The contrapositive of this statement is proven by Theorem 1. □

Consider the case that $\sigma$ is a leaf of a past holographic screen. If the leaf is extremal and the screen is not null, then the directly reconstructable spacetime is just the leaf itself. Additionally, this tells us the holographic screen must halt at this point. This indicates the end of a holographic description based on the past holographic screen. At this point, one can stitch the beginning of a new future holographic screen that starts at a bifurcation surface, patching together two holographic descriptions. This occurs in collapsing universes; see footnote 7.

In the other case, if all of the HRRT surfaces of $\sigma$ have area corresponding to the maximal entropy, then all of the extremal surfaces must lie on the future null cone of the leaf, where this null cone is non-expanding and compact. This cone itself is the limit of a past holographic screen because $\theta_k = 0$. Barring the existence of a continuum of compact, non-expanding, null hypersurfaces, the holographic screen then follows along this null surface from the leaf. Hence the directly reconstructable region will only be the screen itself, exactly as we observed in the case of de Sitter space. Again, we see that maximal entanglement corresponds to the end of a holographic description, but in this case the screen does not end; this corresponds to a stable final state.

In Section 3.2, we took the boundary to be at some large, fixed radius in AdS space. One may be concerned that this cutoff surface is not marginal, and hence Theorem 1 does not apply. However, in the limit that the black hole radius approaches the boundary, then the statement holds because the horizon of the black hole satisfies the needed properties. Note

[10] Under the assumption of the theorem, the HRRT surface of disconnected subregions will always be disconnected. This is because the disconnected surface is extremal.

that until this final limit, Corollary 1 tells us that the entanglement of the boundary cannot be maximal.

Finally we are prepared to make a statement about typicality. Typical boundary states are maximally entangled, and hence the argument shows us that for holographic theories living on screens (an instance of which is AdS/CFT), typical states have no directly reconstructable spacetime.

## 3.3 Spacetime Emerges through Deviations from Maximal Entropy

We have seen that when the holographic state becomes maximally entropic, spacetime defined as the directly reconstructable region disappears. Conversely, bulk spacetime emerges when we change parameters, e.g. the mass of the black hole or the equation of state parameter $w$, deviating the state from maximal entropy. In this section, we study how this deviation may occur and find qualitative differences between the cases of Schwarzschild-AdS and flat FRW spacetimes. This has important implications for the structures of holographic theories representing these spacetimes.

### CFT with subcutoff temperatures

Consider the setup discussed in Section 3.2: a large black hole in asymptotically AdS space. The holographic theory is then a local quantum (conformal) field theory. When the temperature of the system is at the cutoff scale, the holographic state has maximal entropies, Eq. (3.3). As we lower the temperature, the state deviates from a maximally entropic one, and correspondingly bulk spacetime emerges—the horizon of the black hole recedes from the cutoff surface, and the reconstructable spacetime region appears; see Fig. 3.1.

Suppose the temperature of the system $T$ is lower than the cutoff scale, $T < \Lambda$. We are interested in the behavior of von Neumann entropies of subregions of characteristic length $L$ in the boundary theory. These entropies are calculated holographically by finding the areas of the HRRT surfaces anchored to subregions of the cutoff surface $r = R$. We analyze this problem analytically for spherical cap regions in Appendix A.3. For sufficiently high temperature, $T \gg (\Lambda^{d-2}/l)^{1/(d-1)}$, we find that the entanglement entropy for a subregion $A$ behaves as

$$S_A \approx \begin{cases} cA_{d-2}L^{d-2}\Lambda^{d-2} & \text{for } L \ll L_*, \\ cA_{d-2}\frac{r_+^{d-1}L^{d-1}}{l^{2d-2}} \approx c\left(\frac{T}{\Lambda}\right)^{d-1} A_{d-2}L^{d-1}\Lambda^{d-1} & \text{for } L \gg L_*. \end{cases} \tag{3.17}$$

Here,

$$L_* \approx \frac{l^2 R^{d-2}}{r_+^{d-1}} \approx \frac{\Lambda^{d-2}}{T^{d-1}}, \tag{3.18}$$

$c \approx (l/l_{\rm P})^{d-1}$ is the central charge of the CFT, and $A_{d-2}$ is the area of the $(d-2)$-dimensional unit sphere. We find that the scaling of the entanglement entropy changes (smoothly) from an area law to a volume law as $L$ increases. For $T \ll (\Lambda^{d-2}/l)^{1/(d-1)}$, i.e. $L_* \gg l$, the entanglement entropy obeys an area law for all subregions. We note that the length in the boundary theory is still measured in terms of the $d$-dimensional metric at infinity with the conformal factor stripped off. The cutoff length is thus $1/\Lambda \approx O(l^2/R)$, and the size of the boundary space is $\approx O(l)$.

While we have analyzed spherical cap subregions, the behavior of the entanglement entropy found above is more general. When the temperature is lowered from the cutoff scale, the entanglement entropy $S_A$ deviates from the maximal value. Defining

$$Q_A = \frac{S_A}{S_{A,\max}} = \frac{S_A}{\|A\|/4l_{\rm P}^{d-1}}, \tag{3.19}$$

we find that

$$Q_A \approx \begin{cases} \frac{1}{L\Lambda} & \text{for } L \ll \frac{\Lambda^{d-2}}{T^{d-1}}, \\ \left(\frac{T}{\Lambda}\right)^{d-1} & \text{for } L \gg \frac{\Lambda^{d-2}}{T^{d-1}}. \end{cases} \tag{3.20}$$

Here, we have assumed that subregion $A$ is characterized by a single length scale $L$, and that the temperature is sufficiently high, $T \gg (\Lambda^{d-2}/l)^{1/(d-1)}$. (If $T \ll (\Lambda^{d-2}/l)^{1/(d-1)}$, $Q_A \approx 1/L\Lambda$ for all subregions.) This behavior is depicted schematically in Fig. 3.8.

We find that as the temperature is lowered from the cutoff scale, two things occur for entanglement entropies:

- For sufficiently large subregions, the entanglement entropies still obey a volume law, but the coefficient becomes smaller.
- The more the temperature is lowered, the further subregions have entanglement entropies obeying an area law. This occurs from shorter scales, i.e. subregions with smaller sizes.

These make the entanglement entropies deviate from the maximal value and lead to the emergence of reconstructable spacetime: the region between the black hole horizon and the cutoff surface, $r_+ < r \leq R$.

## FRW universes with $w > -1$

As spacetime emerges by reducing the mass of the black hole in the Schwarzschild-AdS case, a codimension-0 spacetime region that is reconstructable from a single leaf appears when $w$ is increased from $-1$. As in the AdS case, this appearance is associated with a deviation of entanglement entropies from saturation. However, the manner in which this deviation occurs is qualitatively different in the two cases.

To illustrate the salient points, let us consider flat FRW spacetimes with a single fluid component $w$ and a spherical cap region $A$ on a leaf parameterized by the half opening angle

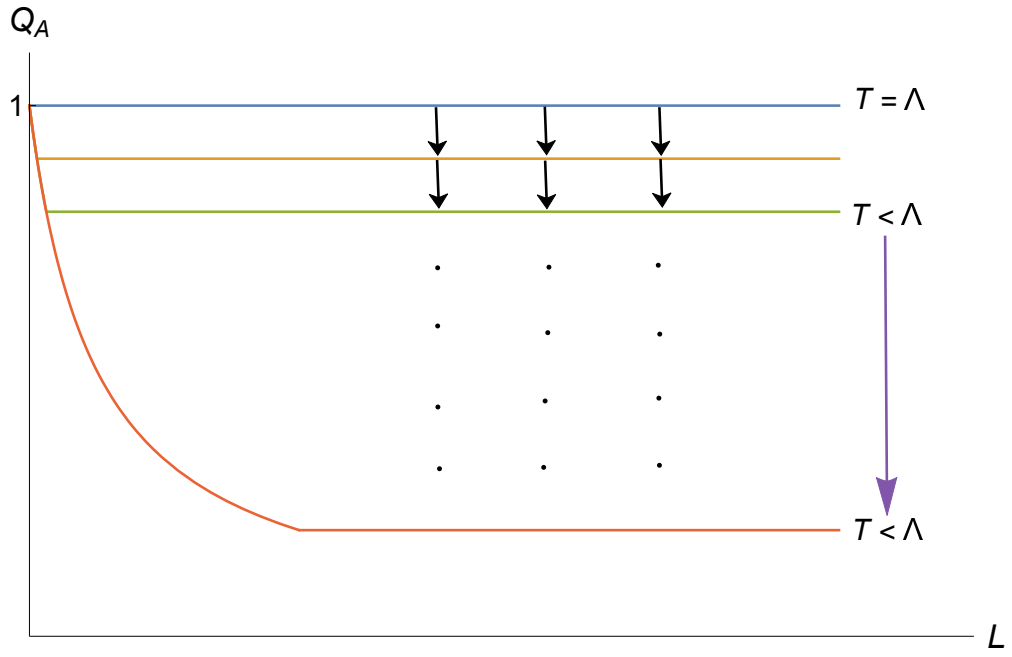


Figure 3.8: A schematic depiction of the entanglement entropy in the Schwarzschild-AdS spacetime, normalized by the maximal value of entropy in the subregion, $Q_A = S_A/S_{A,\max}$, and depicted as a function of the size $L$ of subregion $A$; see Eq. (3.20). The scales of the axes are arbitrary. As the mass of the black hole is lowered (the temperature $T$ of the holographic theory is reduced from the cutoff $\Lambda$), $Q_A$ deviates from 1 in a specific manner.

$\psi$. Below, we focus on entanglement entropies $S_w(\psi)$ of the regions with $\psi \leq \pi/2$. Those with $\psi > \pi/2$ are given by the relation $S_w(\psi) = S_w(\pi - \psi)$.

As before, we define

$$Q_w(\psi) = \frac{S_w(\psi)}{S_{\max}(\psi)} = \frac{S_w(\psi)}{\|A\|/4l_{\rm P}^{d-1}}. \tag{3.21}$$

This quantity was calculated in Ref. [31] in $3+1$ dimensions, which we reproduce in Fig. 3.9. The basic features are similar in other dimensions. In particular, $Q_w(\psi)$ satisfies the properties given in Eqs. (A.30, A.31) in Appendix A.4.

We find that the way $Q_w(\psi)$ deviates from 1 as $w$ is increased from $-1$ is qualitatively different from the way the similar quantity $Q_A$ deviates from 1 in the Schwarzschild-AdS case as the temperature is reduced from the cutoff scale. In particular, we find that in the FRW case

- The deviation from $Q_w(\psi) = 1$ occurs *from larger subregions*. Namely, as $w$ is raised from $-1$, $Q_w(\psi)$ is reduced from 1 first in the vicinity of $\psi = \pi/2$.

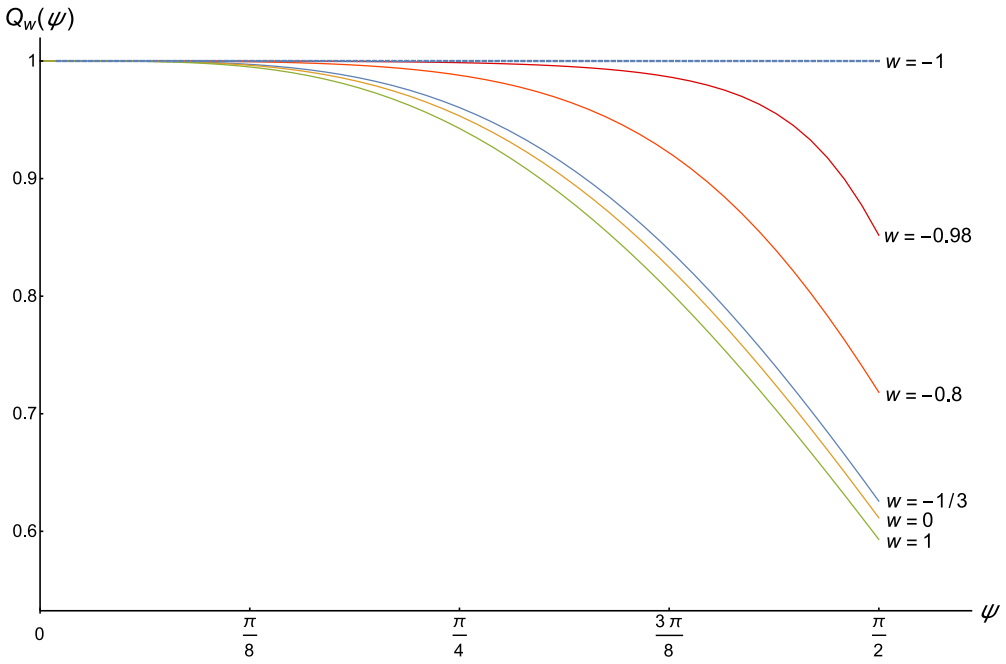


Figure 3.9: The entanglement entropy in the holographic theory of flat FRW spacetimes normalized by the maximal value of entropy in the subregion, $Q_w(\psi) = S_w(\psi)/S_{\max}(\psi)$, as a function of the size of the subregion, a half opening angle $\psi$. As the equation of state parameter $w$ is increased from $-1$, $Q_w(\psi)$ deviates from 1 in a way different from the Schwarzschild-AdS case.

- There is no regime in which the entanglement entropy obeys an area law, $Q_w(\psi) \sim 1/\psi$, or a volume law with a reduced coefficient, $Q_w(\psi) = \text{const.} < 1$.

As we will see next, these have profound implications for the nature of the holographic theory of FRW spacetimes.

## Locality vs nonlocality

In the following discussion, we assume that the dynamics in the holographic theory are chaotic and non-integrable as expected in a theory of quantum gravity; see, e.g. Ref. [96]. Such systems are expected to satisfy the eigenstate thermalization hypothesis (ETH) [97, 98], so generic high energy eigenstates reproduce the behavior of a thermal Gibbs density matrix. In addition, we note that the dimension of the holographic Hilbert space is large ($\mathcal{A}/4l_{\rm P}^{d-1} \gg 1$) and finite size effects causing deviations from the thermodynamic limit can be ignored.

We have already seen that one way to obtain a maximally entropic state is to look at high energy states in a local theory. In the context of AdS/CFT, this corresponds to examining

black holes with temperature near the cutoff scale. To deviate from maximal entropy, one can then simply lower the energy of the states being considered. For subregions beyond the correlation length, the reduced density matrix is well approximated by a Gibbs density matrix, and hence the entropy obeys a volume law but with a prefactor dependent on the temperature $T$. For length scales below the correlation length, the von Neumann entropy is dominated by the area law contribution. Together, these combine to give entanglement entropy curves that have the qualitative behavior shown in Fig. 3.8. Note that in a local theory, lowering the temperature shows deviation from thermal behavior originating at small length scales. Namely, the slope of $Q_A$ begins deviating from 0 at small scales. This entropy deviation at small scales is expected to be a general phenomenon of equilibrium states governed by a local Hamiltonian.

However, the entanglement entropy curves calculated for holographically FRW universes show drastically different behavior; see Fig. 3.9.[11] Namely, the deviations from maximal entropy originate at large length scales, and the entanglement entropy for small subregions is maximal regardless of the fluid parameter $w$. Additionally, these entropy curves are invariant under time translation. This behavior cannot be achieved by a local theory. One may think that a Lifshitz type theory with large $z$ may be able to accommodate such behavior due to large momentum coupling, but the leading order contribution to the entanglement entropy in $d$ dimensions is believed to be proportional to $(L/\epsilon)^{d-1-1/z}$ for weakly coupled theories [99], where $L$ is the characteristic length of the entangling region and $\epsilon$ is the cutoff length. Thus entanglement entropy is proportional to the volume only in the limit that $z \to \infty$, which would be a nonlocal field theory. Indeed, entanglement entropy being maximal for small subregions is observed in a number of nonlocal theories [100, 101, 102, 103, 104, 105] and is likely a generic phenomenon in such theories.

This leads us to believe that an appropriate holographic description of FRW universes would be nonlocal.[12] This provides us with a few possibilities of theories that have the desired qualitative features, all of which have a freedom to tune a parameter which corresponds to changing $w$ (and hence the entropy):

(I) a nonlocal theory with a characteristic length scale below the system size, changing the nonlocal length scale of the theory or energy of the state;

(II) a nonlocal theory coupling sites together at all length scales (like a long-range interacting spin chain or a variant of the Sachdev-Ye-Kitaev model [106, 107, 108] with

[11] It should be emphasized that we are calculating the entanglement entropy of the boundary state on the holographic screen, not the entropy associated with any bulk quantum fields. We refer to the degrees of freedom on the screen that govern the background gravitation dynamics as the gravitational degrees of freedom. Any low energy bulk excitations (which may include gravitons) are higher order corrections to the entanglement entropy and we do not discuss them.

[12] It is a logical possibility that a local theory could exhibit volume law entropy behavior due to open dynamics. Since the size of the leaf is constantly growing, there are degrees of freedom constantly being added to the system, which could already have long range entanglement. This seems to be an ad hoc solution, and we will not elaborate on this possibility further.

all-to-all random coupling between a fixed number, $q$, of sites, $\mathrm{SYK}_q$), changing the energy of the state;

(III) a nonlocal theory with a fundamental parameter controlling the coupling at all scales in which variations can change the entropy; for example, changing the number of sites coupled to each other in each term of the Hamiltonian (analogous to changing $q$ in $\mathrm{SYK}_q$).

The ground states of theories in case (I) are explored in Refs. [100, 101, 102] in string theory frameworks. This case can also be realized as a spin chain with interactions that couple all sites within a distance smaller than the characteristic nonlocal length scale. Above the nonlocal length scale an area law term starts to pick up and will eventually dominate. However, because of this eventual turn-on of an area law, the qualitative features of the entropy normalized by volume are different than those exhibited by FRW entropy curves. Namely, the concavity of the $Q_A$ plot beyond the nonlocal length scale is opposite to that observed in the FRW case. This is because beyond the nonlocal length scale the entropy approaches an area law, hence the second derivative of $Q_A$ will be positive, unlike that observed in the FRW case. Raising the temperature will only add an overall constant asymptotic value to $Q_A$. Hence, the concavity of $Q_A$ forbids the holographic theory of FRW spacetimes from being a theory with a characteristic nonlocal length scale smaller than the system size.

This reasoning leaves us with nonlocal theories with characteristic interaction lengths comparable to the system size—what does this mean? It simply means that a site can be coupled to any other site. For simplicity we will consider SYK-like theories but rather than being zero dimensional we split up the degrees of freedom to live on a lattice but keep the random couplings between them. At first thought, one may think that because of the random, all-to-all coupling the entanglement entropy for all subregions would always be maximal. However this is not the case. The entanglement entropy for small regions is indeed maximal, but then deviates at large length scales [104, 105]. One can intuitively understand this by thinking about the $\mathrm{SYK}_2$ model and Bell pairs. The SYK couplings are random, and some sites will have significantly higher coupling than average. In the ground state, these pairs have a high probability of being entangled, so if the subregion of interest contains only half of one of these special pairs, this will raise the entanglement with the outside. However, once the subregion becomes larger there is a higher probability that a complete Bell pair is contained, and this will drop the entanglement entropy.

From this intuition, one can see that the ground state of SYK-like theories have near maximal entanglement for small regions, which then deviates at large length scales. At higher energies, the probability of minimizing the term in the Hamiltonian coupling these special sites (and creating the effective Bell pair) will be lowered, and hence the entanglement entropy of all subregions will monotonically increase [105, 109]. This behavior is reminiscent of that observed in FRW entanglement entropy if we relate the fluid parameter, $w$, to the energy of the nonlocal state: the case (II) listed above. The limit of $T \to \infty$ would then correspond to $w \to -1$.

The third possibility (III) is similar to the one just discussed, but with the difference that $w$ is dual not to temperature but to a fundamental parameter dictating the "connectivity" of the boundary theory. In the language of $\text{SYK}_q$, this would correspond to changing $q$, where $q$ is the number of coupled fermions in each interaction term of the Hamiltonian. As $q$ increases, the ground state entanglement monotonically increases and as $q \to \infty$ becomes maximal. This would be the limit corresponding to $w \to -1$. However, any possibility like this, which employs a change of a fundamental parameter of the Hamiltonian, will require us to manufacture the whole Hilbert space of the boundary theory by considering the collection of only the low energy states for each value of $q$. We would like one related class of spacetimes to be dual to one boundary theory, which is not the case in this option. We thus focus on option (II) as the best candidate, but we cannot logically exclude option (III).

It is interesting to observe the relationship between where the deviation from volume law entropy occurs and where the corresponding spacetime emerges. In the Schwarzschild-AdS case, $Q_A$ drops from 1 immediately at small subregions, and the spacetime that emerges is precisely that which is reconstructed from small subregions. Hence the directly reconstructable region appears at the boundary and grows inwards as the temperature of the state is lowered. The converse is true in the case of FRW spacetimes. As we move away from $w = -1$, the entanglement entropy drops from maximal at large subregions and the corresponding spacetime that emerges is constructed by intersecting large surfaces. This is because the HRRT surfaces of small subregions of leaves with $w$ near $-1$ all lie on the same codimension-1 surface, the future causal boundary of the leaf, analogous to the small surfaces in Fig. A.4 in Appendix A.4. The HRRT surfaces for large subregions deviate from this and hence allow for reconstructing a codimension-0 region starting with points deepest in the bulk.

The language of quantum error correction [26] and tensor networks [72, 28, 29] allows for a nice interpretation of this phenomenon. The loss of entanglement in pure gravitational degrees of freedom affords nature the opportunity to redundantly encode local bulk degrees of freedom in the boundary. In AdS, short range entanglement is lost first, and hence there is "room" for the information of local bulk degrees of freedom to be stored. In the case of FRW, long range entanglement is lost first, and subsequently points in the bulk that require large subregions to reconstruct emerge first.

## 3.4 Holographic Hilbert Spaces

The analysis of the previous sections brings us to a suitable position to discuss the structure of holographic Hilbert spaces. In this section, we propose how a single theory can host states with different spacetime duals while keeping geometric operators linear in the space of microstates for a fixed semiclassical geometry. We use intuition gathered from quantum thermodynamic arguments to guide us. Similar ideas have been discussed in Ref. [110]. Here we present a slightly generalized argument to emphasize its independence of dynamics, and explain its application to our framework.

Let us assume that the entanglement entropy of subregions of a boundary state dual to a semiclassical geometry is calculated via the HRRT prescription. Given a bulk spacetime, one can then find the corresponding entanglement entropies for all subregions of the boundary. Note that here we consider the "classical limit." Namely, all the subregions we consider contain $O(\mathcal{N})$ degrees of freedom, where

$$\mathcal{N} = \frac{\mathcal{A}}{4l_{\mathrm{P}}^{d-1}}, \tag{3.22}$$

with $\mathcal{A}$ being the volume of the holographic space. The collection of all boundary subregions and their corresponding entanglement entropies will be referred to as the entanglement structure of the state, which we denote by $S(|\psi\rangle)$.

From here, it is natural to ask whether or not all states with the same entanglement structure are dual to the same bulk spacetime. This might indeed be the case, but it leads to some undesirable features. These primarily stem from the fact that given a particular entanglement structure, one can find a basis for the Hilbert space in which all basis states have the specified entanglement structure. For a Hilbert space with a local product structure, one can do this by applying local unitaries to a state—these will retain the entanglement structure and yet generate orthogonal states. This would imply that by generically superposing $e^{O(\mathcal{N})}$ of these states, one could drastically alter the entanglement structure and create a state dual to a completely different spacetime. Hence, geometric quantities could not be represented by linear operators, even in an approximate sense. If this were the case, a strong form of state dependence would be necessary to make sense of dynamics in the gravitational degrees of freedom [32].

However, it is not required that every state in the holographic Hilbert space with the same entanglement structure is dual to the same spacetime. How can this consistently happen? Given an entanglement structure, $S(|\phi\rangle)$, we expect the existence of a subspace in which generic states (within this subspace) have this same entanglement structure up to $O(\mathcal{N}^p)$ corrections with $p < 1$. The existence of a subspace with a unique entanglement structure is not surprising if the dimension of the subspace is $e^{O(\mathcal{N}^p)}$ with $(p < 1)$, since we generally expect

$$S\left(\sum_{i=1}^{e^M} c_i|\psi_i\rangle\right) = S(|\psi\rangle) + O(M), \tag{3.23}$$

where $S(|\psi_i\rangle) = S(|\psi\rangle)$ for all $i$.

However, we argue further that there exist such subspaces with dimension $e^{O(\mathcal{N})}$, spanned by some basis states $|\psi_i\rangle$ $(i = 1, \cdots, e^{Q\mathcal{N}})$, with

$$S\left(\sum_{i=1}^{e^{Q\mathcal{N}}} c_i|\psi_i\rangle\right) = S(|\psi\rangle) + O(\mathcal{N}^p;\, p < 1), \tag{3.24}$$

where $Q \leq 1$ does not scale with $\mathcal{N}$. The existence of these subspaces with entanglement structures invariant under superpositions is expected from canonical typicality (also referred

to as the general canonical principle) [111, 112]. This provides us with the powerful result that generic states in subspaces have the same reduced density matrix for small subsystems (up to small corrections). The proof of this statement is purely kinematical and hence applies generally. In fact, from canonical typicality the correction term in Eq. (3.24) is exponentially small, $O(e^{-Q\mathcal{N}/2})$.

Canonical typicality is a highly nontrivial statement because the size of the subspaces in question is large enough that one would naively think that superpositions would ruin the entanglement structure at $O(\mathcal{N})$.[13] Therefore, even if one considers an exponentially large superposition of microstates (so long as they are generic states from the same subspace), geometric operators can be effectively linear within this subspace. We propose that states dual to semiclassical geometries are precisely generic states within their respective subspaces.

An example of one of these subspaces would be an energy band of an SYK theory. These harbor an exponentially large number of states, and yet from canonical typicality any superposition of generic states within this band will have the same entanglement entropy. Another example would be states that have energy scaling with the central charge, $c$, in AdS/CFT. These are dual to large black holes and there are also an exponentially large number of states within the energy band. Despite this, generic states within this energy band will have the same entanglement entropy structure. Essentially, canonical typicality proves the existence of exponentially large subspaces that have entanglement structures preserved under superpositions of just as many states.

We need this strengthened statement because the entanglement entropy calculations for FRW suggest the size of subspaces dual to identical spacetimes are exponentially large. This is because the quantity $Q$ in Eq. (3.24) is related with von Neumann entropies characterizing the whole state, e.g. $Q_A$ in Section 3.3 with $A$ being the half boundary space and $Q_w(\pi/2)$ in Section 3.3. This intuition stems from the statement that the thermal entropy density and entanglement entropy density for states in the thermodynamic limit are approximately equal. For generic states within some energy interval subspace, this holds by canonical typicality. The statement also results from assuming the system satisfies the ETH (like in AdS/CFT). SYK models, however, do not strictly satisfy the ETH; nevertheless, it remains true that $Q_A$ at half system size gives a good approximation for the thermal entropy density, and the discrepancy vanishes as the energy of the states is increased. For these reasons, we expect $Q_w(\pi/2)$ to well approximate the thermal entropy density of states dual to an FRW spacetime with fluid parameter $w$.

We can now address the properties of typical states within an entire Hilbert space. Consider a holographic Hilbert space of a given theory, e.g. a CFT with a finite cutoff or the holographic theory of FRW spacetimes. If there are multiple superselection sectors in a given theory, then we focus on one of them. In such a Hilbert space, the effective subspace with $Q = 1$ corresponds to typical states. Applying Page's analysis, we can then conclude that the only entanglement structure consistent with Eq. (3.24) where $Q = 1$ must be that of

[13] Note that if one fine-tunes coefficients and selects states in this subspace carefully, one could construct a state with lower entanglement via superposition.

maximal entropy. For example, the number of microstates for a large black hole approaches the dimension of the boundary Hilbert space as $T \to \Lambda$, and these states are maximally entangled. Similarly, using the argument in the previous paragraph, the number of independent microstates in the de Sitter limit approaches the dimension of the boundary Hilbert space, and these states are maximally entangled. As shown in Section 3.2, the directly reconstructable spacetime region vanishes in these cases—an effective subspace with $Q = 1$ does not have reconstructable spacetime. It is in this sense that typical states in the *whole* Hilbert space have no reconstructable spacetime.

On the other hand, if $Q < 1$, the corresponding entanglement structure $S(|\psi\rangle)$ can be non-maximal, and generic states in this subspace may be dual to some bulk spacetime. As discussed in Section 3.3, we expect that dynamics of the boundary theory can naturally select these subspaces, for example by simply lowering the energy of the system in the case of the boundary CFT.

The structure discussed here allows for a single holographic Hilbert space to harbor effective subspaces dual to different geometries, allows for a "generically linear" spacetime operator, and hence eliminates the need for any strong form of state dependence.[14] Because this "spacetime operator" is identical for states of a given entanglement, it will obviously act linearly on generic superpositions of states within one of these dynamically selected, entanglement-invariant subspaces. We suspect that it is only in this thermodynamic sense that classical spacetime emerges from the fundamental theory of quantum gravity.

## 3.5 Conclusion

### Discussion

Our understanding of the relationship between spacetime and entanglement seems to be converging. The necessity of entanglement between boundary degrees of freedom for the existence of spacetime has been known for some time, but this fact may have mistakenly established the intuition that the fabric of spacetime itself is purely this entanglement. However, this cannot be the case. A one-to-one mapping between the entanglement structure of a boundary state and the directly reconstructable bulk spacetime cannot be upheld in a state independent manner. In addition, we see that as boundary entanglement approaches maximality the reconstructable region of the bulk vanishes.

[14] By strong state dependence, we mean a theory that would require state dependence to describe bulk excitations in the directly reconstructable region of a boundary state which is a generic superposition of states dual to a given spacetime. For a more detailed analysis of this statement, we refer the reader to Ref. [32]. The main result is that requiring linearity for the multiple boundary representations of a bulk operator is impossible if the number of geometry microstates is $e^{\mathcal{N}}$. This prohibits the existence of a directly reconstructable region for typical states. Note that the directly reconstructable region does not probe behind black hole horizons, and hence we are not addressing the possibility that state dependence is necessary to recover the black hole interior.

In hindsight, this should not be too surprising. Let us recall Van Raamsdonk's discussion [33] relating spacetime to entanglement by examining the link between mutual information and correlations in a system. The mutual information between two boundary subsystems $A$ and $B$ is defined as

$$I(A,B) = S(A) + S(B) - S(A \cup B). \tag{3.25}$$

This quantity bounds the correlations in a system between operators $\mathcal{O}_A$ and $\mathcal{O}_B$, supported solely on $A$ and $B$ via the relation

$$I(A,B) \geq \frac{(\langle \mathcal{O}_A \mathcal{O}_B \rangle - \langle \mathcal{O}_A \rangle \langle \mathcal{O}_B \rangle)^2}{2|\mathcal{O}_A|^2 |\mathcal{O}_B|^2}. \tag{3.26}$$

Hence, when the mutual information between two subregions $A$ and $B$ vanishes, the correlation between local operators supported within the subregions must also vanish. Assuming that subregion duality holds, this implies that correlation functions of bulk fields vanish. Generally, correlators between two bulk fields go as

$$\langle \mathcal{O}_1(x_1) \mathcal{O}_2(x_2) \rangle \sim a f(L), \tag{3.27}$$

where $L$ is the distance of the shortest geodesic connecting $x_1$ and $x_2$, $a$ is some theory dependent constant, and $f(z)$ is a decreasing function of $z$. One can then make the argument that decreasing entanglement between regions will drop the mutual information between the regions, and hence make $L$ effectively infinite. This implies that the spacetime regions dual to subregions $A$ and $B$ are disconnected when the entanglement (and hence mutual information) vanishes. For intuition's sake, one can imagine two subregions of the AdS boundary which are in a connected entanglement phase—increasing the distance between these two subregions will drop the mutual information. This is an argument demonstrating the need for entanglement in a holographic theory dual to spacetime, so long as the holographic theory has subregion duality.

However, there is a different (quite the opposite) way to make the mutual information between small (less than half of the system) subregions vanish, and consequently kill the bulk correlations. This is by considering maximally entropic boundary states—in these, the mutual information will vanish for any pair of subregions. This is the case both in cutoff temperature AdS black holes and in the de Sitter limit of the holographic theory of FRW universes. In these, the boundary states are maximally entropic and hence the bulk correlators must vanish; however, there exist finite length geodesics in the bulk (even if restricted only to the directly reconstructable region) which connect all points on the boundary. This means that the prefactor, $a$, of Eq. (3.27) must vanish, making the bulk theory ultralocal. In these cases, the maximal entropy implies that there cannot be an extra emergent bulk dimension. This is because the ground state of any quantum field theory quantized on spacelike hypersurfaces must be entangled at arbitrarily short scales, which is violated by the assumption that $a = 0$. However, this is not necessarily unexpected—in

both de Sitter space and cutoff temperature black holes, the directly reconstructable regions are codimension-1 null surfaces of the bulk (the de Sitter horizon and black hole horizon respectively). A natural description of the fields on this surfaces would be through null quantization, which is known to be ultralocal [113]. Accordingly, we see a breakdown in the holographic description.

From the above arguments one can convince themselves that it is not entanglement itself which allows for the construction of spacetime, but rather something related to intermediate entanglement.

How can this be better understood? The framework of tensor networks provides some intuition behind this. Here, a maximally entropic boundary state is most naturally represented by a single bulk node with one bulk leg and multiple boundary legs.[15] Hence the "spacetime" is just one non-localizable bulk region, a "clump" as defined in Ref. [58]. This bulk point can be reconstructed once a subregion of the boundary contains more than half of the boundary legs. Here it is clear that a maximally entropic boundary state has no dual "spacetime," and yet it is possible to encode a bulk code subspace with full recovery once more than half of the boundary is obtained. Note that these typical states will all satisfy (in fact saturate) the holographic entropy cone inequalities [114] simply because a random tensor network accurately describes the state, but this does not mean that there is a reconstructable region of the spacetime.

Additionally, if maximally entropic states did have reconstructable spacetime, then state dependence would be necessary in order to describe bulk excitations in these states, under the assumption that subregion duality holds. This is because the number of microstates with maximal entropy is approximately the dimension of the full boundary Hilbert space, and by the argument in Section V.C. of Ref. [32], it is impossible to find a boundary representation of a bulk operator that has support only on a subregion of the boundary *and* acts approximately linearly on all microstates of a given spacetime. Intuitively, this is because the operator will be over-constrained by insisting it both have support on a subregion of the boundary and act linearly on $D$ microstates, when the dimension of the full boundary space is $D$. This means that if we require state independence, then the only possible boundary operators representing bulk excitations for a maximally entropic state must have support on the full boundary space.[16] Therefore, the minimum possible subregion in which bulk excitations can be encoded state independently is the whole boundary space; hence there is no directly reconstructable spacetime. This directly highlights the tension between reconstructing spacetime for maximally entropic states (in any manner), and requiring both subregion duality and state independence.

But what happens if we lower the entanglement of the boundary state while keeping the

[15] Any attempt to create a bulk by artificially including more nodes with extremely large bulk bond dimension can be reduced to the case of one bulk node.

[16] This is not contradicting the statement in the previous paragraph that the sole bulk node's state in a random tensor can be recovered with just more than half of the boundary. In that case, only the recovery of the bulk code subspace for one microstate was considered. State independence would require us to have an operator that acts linearly on *all* microstates of a given spacetime.

dimension of the boundary Hilbert space constant? Again, we turn to tensor networks for intuition. In these situations, a natural way to encode sub-maximal entanglement (while fixing the bulk leg dimension) is by including more bulk nodes. Therefore, by reducing the boundary entanglement, it is possible to create a bulk code subspace in which subsystem recovery is possible. It seems that quantum gravity naturally utilizes this sub-maximal entanglement in order to encode information via subregion duality. This suggests that perhaps entanglement is not the fundamental constituent of spacetime per se, but rather the avenue by which subregion duality manifests.

## Future directions

This paper has attempted to clarify the nature of spacetime in holographic theories and it naturally raises interesting questions to be investigated in future work.

### Reconstructability and generalized holographic renormalization

The analysis of this paper utilized the condition for reconstructable spacetime presented in Ref. [58], but appropriately generalized for use in the context of holographic screens [32]. This paper illuminated some highly desirable properties of the directly reconstructable region defined in this manner—namely that one can describe this region state independently. It would be extremely beneficial to attempt to find an explicit way to construct bulk operators using this method, perhaps uniting it with the methods of entanglement wedge reconstruction [115, 116].

It would also be interesting to try and develop new tools for reconstructing the bulk. The relationship between the depth in the bulk and the scale in the boundary theory in AdS/CFT suggests that it may be possible to define the reconstructable region of spacetime as that which is swept through a renormalization procedure. How this manifests in general holography is not clear, but it is suggestive that there exists at least one foliation where one can "pull" the leaf inward while retaining the ability to consistently apply the HRRT prescription. Because the area of these renormalized leaves are monotonically decreasing, it is natural that this "pulling" may correspond to some renormalization procedure. The decrease in area also happens locally, which can be seen by generalizing the spacelike monotonicity theorem of Ref. [31].

One guess as to how to construct the renormalized leaf is to first pick the coarse graining scale of the boundary, and then define the new leaf as the collection of all of the deepest points of the extremal surfaces anchored to subregions with the size of the coarse graining scale. In AdS/CFT this will pull the boundary in along the $z$ direction as expected, while in FRW spacetimes this will pull the leaf along the null direction if the coarse graining scale is small. Using this method, one can renormalize to a given scale in a number of different ways. For example, one could perform many small renormalization steps or one large one. The renormalized leaves in the two cases will generically differ, and this may correspond to the difference between one-shot renormalization and a renormalization group

method. The collection of all renormalized leaves may then determine the reconstructable region.[17] Theorem 1 tells us that once the renormalized state becomes maximally entropic, the renormalization procedure must halt. Furthermore, because extremal surfaces for non-maximally entropic states probe the bulk, this renormalization procedure will continue until the leaf becomes maximally entangled. Thus, this renormalization group flow will halt only once a bifurcation surface or a null non-expanding surface is reached. In this language, maximally entropic states correspond to fixed points. This is speculation, but may shed some light on the nature of renormalization in general holographic theories.

### Cosmic equilibration

In Section 3.2, we proved that maximally entropic states have no directly reconstructable spacetime. Additionally, we argued that if one desires a state on a holographic screen to be maximally entropic and evolve in time, then the holographic screen is a null non-expanding surface and the directly reconstructable region is no more than the screen itself. This suggests that in a holographic theory of cosmological spacetimes, if a state becomes maximally entropic and the screen does not halt, then the holographic description approaches that of de Sitter space. Consequently, the area of the screen is constant. It would be interesting to investigate the result from the other direction. By first assuming that the screen approaches a constant area, one may be able to argue that the leaves would then approach maximal entropy, and hence the holographic description approaches that of de Sitter space. This could provide another way to consider equilibrating to de Sitter type solutions; see Ref. [117].

### Complementarity

In Appendix A.2, we highlighted the dependence of the reconstructable region on the frame of reference. In the case of the two-sided AdS black hole, we considered different reference frames corresponding to different time slicings in the same boundary theory—as one shifts the difference in the two boundary times, one recovers more and more of the black hole interior. This is an example of complementarity. It would be interesting to pursue this idea further and investigate the directly reconstructable region of a two-sided black hole.

One intriguing aspect of the two-sided black hole is that the directly reconstructable region does not extend beyond the extremal surface barrier; this is a *macroscopic* distance away from the future singularity, regardless of the boundary frame. Does this mean that the boundary CFT cannot describe semiclassical physics behind this barrier, even where curvature is small? Perhaps this means that there is a different description for the interior, living on a different holographic space.

[17] Using this construction, it is not possible to extend reconstruction beyond horizons, but it is possible to reach behind entanglement shadows.

### Fundamentality of subregion duality

In many of the discussions throughout this paper, we either required subregion duality or saw that it naturally arose from other considerations. This seems to suggest that subregion duality is a fundamental characteristic of general holography. Investigating the manner in which subregion duality arises in AdS/CFT may shed light on holography in general spacetimes.

### Holographic theory of flat FRW spacetimes

One of the most obvious open problems is that of finding an effective holographic theory applicable beyond asymptotically AdS spacetimes. In this paper and throughout previous work, we have focused on the case of flat FRW universes and assumed that a theory exists on the holographic screen in which the generalized HRRT prescription holds. Investigations into this has led to a deeper understanding of the nature of entanglement in constructing spacetime, along with (the lack of) state dependence in holographic theories.

It seems that a consistent theory is possible, and the most promising candidate for a theory describing the gravitational degrees of freedom is a theory with long-range interactions in which the energy of the states are dual to the fluid parameter of the FRW universe. We know that it cannot be entirely nonlocal because this would prohibit the existence of entanglement phase transitions. A theory with long range interactions would accurately reproduce the entanglement entropy structure we observe for FRW universes and would allow for a universal theory describing the single class of spacetimes. Beyond this, we have some additional data about the properties of the boundary theory.

We know that a code subspace of states manifests, and these states are dual to bulk excitations. Assuming subregion duality holds, one can ask the question of whether or not nonlocality/very long-range interactions in the gravitational degrees of freedom prohibits the local propagation of bulk excitations in the boundary theory. We expect that the operators dual to bulk excitations are weakly coupled to the gravitational degrees of freedom, and that a local description of these bulk operators exists in the boundary. In fact, this is what happens when one renormalizes the AdS boundary down to a single AdS volume [118]. This renormalization induces an infinite set of interactions which makes the resulting theory on the renormalized boundary nonlocal. Despite this, the renormalized theory still describes bulk physics through subregion duality. Hence, the nonlocality of the boundary theory does not seem to be a fundamental obstacle in describing low energy excitations using local dynamics in the boundary theory.[18] The dynamics of boundary operators dual to bulk excitations in flat FRW spacetimes was studied in Ref. [119] and it was determined that regardless of dimension and fluid parameter, the spread of these operators was characteristic of a theory with $z = 4$ Lifshitz scaling. This provides extra constraints for finding a candidate theory.

[18] It would be interesting to study this effective boundary theory, induced in AdS/CFT by renormalizing all the way down to the AdS scale. The holographic theory capturing sub-AdS locality could be very closely related to the theory on holographic screens.

### Holographic theory for general spacetimes

It might appear that defining quantum gravity using holography, as envisioned here, is background dependent. Namely, the holographic theory is given for each class of background spacetimes, e.g. asymptotically AdS spacetimes and flat FRW spacetimes. This situation is analogous to defining string theory on the worldsheet, which is defined separately on each target space background. From the perspective of the worldsheet, different backgrounds correspond to different theories living on the two dimensional spacetime. Nevertheless, we believe there exists some unified framework encompassing all these possibilities. Similarly, in the case of holographic theories, it is plausible that the resultant theories for different background spacetimes correspond to different sectors described within a single framework.

# Chapter 4

# Pulling the Boundary into the Bulk

## 4.1 Introduction

The holographic duality between asymptotically Anti-de Sitter (AdS) spacetimes in $d+1$ dimensions and conformal field theories (CFTs) in $d$ dimensions is perhaps the closest realization of a complete theory of quantum gravity [14, 16, 15]. One of the most intriguing results stemming from this correspondence is the renowned Ryu-Takayanagi formula relating entanglement entropy in time independent CFTs to the area of minimal surfaces in the bulk spacetime [18]. The covariant extension of this formula to include time dependent cases was obtained by Hubeny-Rangamani-Takayanagi and uses extremal bulk surfaces (henceforth referred to as the HRRT prescription) [20]. Remarkably, by including quantum corrections to this formula, one obtains entanglement wedge reconstruction [23, 24]. These investigations have shed light on the deep connection between entanglement in the boundary and emergent gravitational physics in the bulk.

However, there is reason to believe that these results extend beyond the scope of AdS/CFT. The Bekenstein-Hawking formula [7, 2] and the covariant entropy bound [9] provide us with holographic bounds on entropy in general spacetimes. These suggest that gravitational physics may inherently be holographic [12, 13]. Furthermore, the areas of extremal surfaces anchored to any convex boundaries satisfy all known entropic inequalities [57, 114, 56, 120]. In isometric tensor networks, calculating the entanglement entropy of a subregion of boundary sites reduces to finding the minimum cut across the network [121]. A version of entanglement wedge reconstruction also holds in perfect and random tensor networks [28, 29]. This evidence seems to indicate that the HRRT prescription may in fact generalize to spacetimes outside of AdS.

It is with this perspective that we have pursued investigations of quantum gravity beyond AdS/CFT. We postulate that the HRRT prescription (with quantum corrections [21, 22] to allow for entanglement wedge reconstruction) applies to general convex boundaries. In particular, we assume the existence of a quantum state that "lives" on the convex boundary and encodes the bulk geometry of the interior. Our previous work [31, 32, 34] has focused pri-

marily on investigating this assumption applied to holographic screens [67], but holographic screens are only special in the sense that they are the largest surfaces in which we can apply the HRRT prescription in general spacetimes. In this paper, we have relaxed this condition and look at general convex surfaces—in particular this allows us to consider asymptotically AdS spacetimes.

We emphasize that the postulate we adopt here is falsifiable. At any point in the analysis, had the geometric properties of general relativity prohibited a consistent boundary interpretation, the program would have failed. Through the present, however, no such roadblock has presented itself. In fact, we can view the self-consistency of this work as further evidence that the relationship between entanglement and geometry prevails in general spacetimes.

The present framework allows us to consider a nested family of convex surfaces each of which contains less bulk information than the previous. Taking a natural continuum version of these convex surfaces yields a surface which we dub the *holographic slice*. As has proved historically useful, studying covariantly defined geometric objects yields insights into holographic theories, and the holographic slice is such an object. In particular, the slice allows us to visualize the coarse-graining of holographic states and provides us with a method to categorize bulk regions as being "more IR" than others.

The construction of the slice is purely perturbative, and thus does not allow us to analyze complex quantum gravitational states formed as superpositions of many geometries. It is inherently tied to one background geometry, but this is no more restrictive than the HRRT prescription itself. For a simply connected boundary, the slice seems to sweep the maximal bulk region that can be perturbatively reconstructed, i.e. it pulls the boundary in through shadows all the way to black hole horizons, and contracts no further. It was the study of extremal surfaces in maximally entangled pure states that initiated this work, where it was realized that maximally entangled states were fixed points of flow in the direction of small HRRT surfaces [34].[1]

## Overview

In Section 4.2, we offer the intuitive motivation for the construction of the holographic slice. This reveals the connection to coarse-graining and provides a basic definition for the object. In Section 4.3, we geometrically define the object rigorously and then illustrate some of its most important properties. These properties must necessarily be satisfied for a consistent interpretation as coarse-graining of a boundary state. Section 4.4 goes through multiple explicit examples of the slice in different spacetimes.

After introducing the holographic slice as a geometric object, we are poised to analyze its boundary interpretation in Section 4.5. Here we delve into its relationship to coarse-graining and emphasize that the slice encodes a sequence of codimension-0 bulk regions, not merely the codimension-2 bulk convex surfaces. We also describe the relationship to tensor

[1] By maximally entangled, we mean that the von Neumann entropy of any subregion saturates the Page curve [91]. This was referred to as maximally entropic in Ref. [34].

networks, particularly continuous tensor networks [122]. Because the holographic slice is constructed from one boundary time slice, it can be used as a novel gauge fixing of the bulk—this is discussed in the final subsection of Section 4.5. Since the slice grants us a way to uniquely pull in the boundary, it is natural to consider its connection to renormalization. This is explored in Section 4.6. We conclude with discussing the slice's place in the wider view of quantum gravity in Section 4.7. The appendices contain proofs of various geometric statements made in the body of the text.

### Preliminaries

This paper will work in the framework of holography for general spacetimes proposed in Ref. [31]. We will highlight the applications to AdS/CFT but use language from generalized holography. In particular, the term "boundary" will refer to the holographic screen, which reduces to the conformal boundary of AdS. Additionally, holographic screens have a unique time foliation into codimension-2 surfaces called leaves [59]. This uniqueness is lost in the case of AdS because of the asymptotic symmetries, but to remain consistent within the generalized framework we must choose a particular time foliation of the boundary of AdS [32]. We will then refer to a time slice of this foliation as a leaf.

For a subregion, $A$, of a leaf, we will denote its HRRT surface as $\gamma(A)$ and its entanglement wedge as $\mathrm{EW}(A)$. $\mathrm{EW}(A)$ is defined as the domain of dependence of any closed, compact, achronal set with boundary $A \cup \gamma(A)$.[2] Throughout this paper, we will work at the lowest order in bulk Newton's constant. In particular, we will only consider extremal surfaces found by extremizing the area, not the generalized entropy. We expect that by making appropriate modifications, along the lines of Refs. [21, 22, 123], our results can be extended to higher orders.

For an achronal codimension-2 surface $\omega$, we denote the domain of dependence of any achronal set with boundary $\omega$ as $D(\omega)$. Wherever $G_{\mathrm{N}} = l_{\mathrm{P}}^{d-1}$ appears, it represents Newton's constant in the bulk spacetime.

## 4.2 Motivation

Amongst other things, the concept of subregion duality in holographic theories allows us to address questions regarding where bulk information is stored in the boundary theory [124, 125, 126, 127, 128, 60, 61, 23, 24]. This line of inquiry has provided us with the intuition that bulk geometric information is encoded redundantly in the boundary theory. In particular, a bulk local operator can be represented in multiple different regions of the boundary, a

[2] In standard AdS/CFT, reflective boundary conditions are imposed at the conformal boundary. This extends the domain of dependence of $A \cup \gamma(A)$ to include the boundary domain of dependence of $A$. However, for holographic screens there are no such impositions on the screen (they can even be spacelike), and thus $\mathrm{EW}(A)$ generally does not include any portion of the screen other than $A$ itself. In particular, there is no generalization of causal wedges to holographic screens.

special case being the whole boundary space. However, despite this seemingly democratic distribution of bulk information throughout boundary degrees of freedom, lack of access to a boundary region necessarily prohibits the reconstruction of a corresponding bulk region. Namely, if one removes a subregion $A$ from a leaf $\sigma$, the maximum possible bulk region reconstructed from the remaining region, $\overline{A}$, will be the entanglement wedge of $\overline{A}$, $\mathrm{EW}(\overline{A})$. This implies that indispensable information of the region $\mathrm{EW}(A)$ is stored in $A$.

Suppose one were to coarse-grain over all boundary subregions of balls of radius $\delta$. From the logic above, the bulk region whose information can remain is given by

$$R(B_\delta) = \bigcap_{p\in\sigma} \mathrm{EW}\big(\overline{B_\delta(p)}\big), \tag{4.1}$$

where $B_\delta(p)$ is a ball of radius $\delta$ centered at point $p$ on the boundary leaf $\sigma$. Because the intersection of domains of dependence is itself a domain of dependence,[3] $R(B_\delta)$ is a domain of dependence of some achronal set, and thus has a unique boundary, $\sigma(B_\delta)$.

Motivated by ideas of holographic renormalization in AdS/CFT [129, 130, 118, 131, 132], surface state correspondence [57], and previous work on holographic screens [56, 31, 32, 34], we conjecture that there exists a holographic state living on $\sigma(B_\delta)$ which encodes aspects of the bulk geometry to its interior. A check of this proposal is that the HRRT prescription can be consistently applied, in the sense that the areas of these HRRT surfaces obey the known holographic entropy inequalities. Given this consistency check, we conjecture that "coarse-grained subregion duality" holds—namely that entanglement wedge reconstruction holds on this new leaf.

Now suppose one wants to coarse-grain over some scale on this new leaf, $\sigma(B_\delta)$. This will produce a new leaf even deeper in the bulk. Repeating this process will in turn produce a series of new leaves, henceforth called renormalized leaves. Sending the coarse-graining scale at each step to zero in a consistent manner will produce a continuous family of renormalized leaves that sweep out a smooth surface through the bulk, $\Upsilon$. The manner in which $\Upsilon$ is constructed naturally reveals its relationship to holographic coarse-graining. This prompts us to assert that the continuous coarse-graining of a holographic state pulls the boundary slice in along the slice $\Upsilon$.

## 4.3 Holographic Slice

The geometric object $\Upsilon$ is what we will refer to as the holographic slice. In this section, we give a more rigorous definition of holographic slices and highlight some of the salient properties of them.

[3] We could not find a proof of this statement, so we have included one in Appendix A.5.

## Definition

Consider a closed codimension-2 achronal surface $\sigma$ living in a $(d+1)$-dimensional spacetime $M$. Denote the two future-directed null orthogonal directions as $k$ and $l$. Suppose the null expansions along these directions satisfy $\theta_k \leq 0$ and $\theta_l > 0$.[4] For concreteness, one could imagine $\sigma$ to be a leaf of a past holographic screen ($\theta_k = 0$, $\theta_l > 0$) or a time slice of the (regularized) boundary of AdS. Borrowing this language, we will call $\sigma$ a leaf. From Ref. [56], we know that the boundary of the domain of dependence of $\sigma$, $D(\sigma)$, is an extremal surface barrier for HRRT surfaces anchored to $\sigma$. In addition, the boundary of an entanglement wedge of a subregion $\Gamma$ on $\sigma$ serves as an extremal surface barrier for all extremal surfaces anchored within $\mathrm{EW}(\Gamma)$.

Now, on $\sigma$, consider a family of open, codimension-0 (within the leaf) smooth subregions, with an injective mapping from points on the leaf, $p$, to subregions, $C(p)$, with the constraint that $p \in C(p)$ and that $C(p)$ varies continuously with $p$. For example, one may take $C(p)$ to be open balls of radius $\delta$ centered at $p$, $B_\delta(p)$. Now, let

$$R(C) = \bigcap_{p\in\sigma} \mathrm{EW}\big(\overline{C(p)}\big), \tag{4.2}$$

where $\overline{C(p)}$ is the complement of $C(p)$ in $\sigma$. From Appendix A.5, we know that $R(C)$ itself is a domain of dependence of some achronal sets, all of which share a unique boundary, $\sigma_C^1$, called a renormalized leaf; see Fig. 4.1.

Provided the characteristic scale of $\mathrm{EW}(C(p))$ is sufficiently smaller than the extrinsic curvature scale of $\sigma$, we can identify all points on $\sigma_C^1$ with those on $\sigma$. At each point on $\sigma$, consider the plane generated by $k$ and $l$. This will intersect $\sigma_C^1$ at one point so long as adjacent planes do not intersect at a caustic before hitting $\sigma_C^1$, which is guaranteed if we take $C(p)$ to be sufficiently small. We now have a natural identification of the points on $\sigma$ with points on $\sigma_C^1$. In particular, we can identify the length scale $\delta$ on $\sigma$ to the appropriate scale on $\sigma_C^1$. Moreover, since $\sigma_C^1 \subseteq \mathrm{EW}(\overline{C(p)})\ \forall p$ and $\mathrm{EW}(\overline{C(p)})$ serves as an extremal surface barrier for all surfaces anchored within $\mathrm{EW}(\overline{C(p)})$, all extremal surfaces anchored to $\sigma_C^1$ are contained within $R(C) = D(\sigma_C^1)$. If we interpret the area of these extremal surfaces as entanglement entropies for the associated subregions, convexity of $R(C)$ and the null energy condition ensure that all known holographic entanglement inequalities are satisfied. This allows us to interpret these extremal surfaces as HRRT surfaces.

Utilizing coarse-grained subregion duality, we can repeat the construction above but with new subregions, $C^1(p)$, on the renormalized leaf, $\sigma_C^1$. This yields a new leaf $\sigma_C^2$. We can associate points on $\sigma_C^2$ with those on $\sigma_C^1$, and hence on $\sigma$, as was done above. All we require of the new subregions is that the size scale of $C^i(p)$ match with that of $C(p)$ under the natural identification described previously. This procedure can be repeated until stringy effects become important, i.e. when the size of the renormalized leaf is $O(l_\mathrm{s})$.

In the limit of sending the size of $C(p)$ to 0 for all $p$, the collection of all renormalized leaves in $M$, $\Upsilon = \{\sigma_C^i\}$ sweeps out a continuous surface. This is a holographic slice. Note

[4] Appropriate modifications can be made to extend to surfaces where $\theta_k \geq 0$ and $\theta_l < 0$.

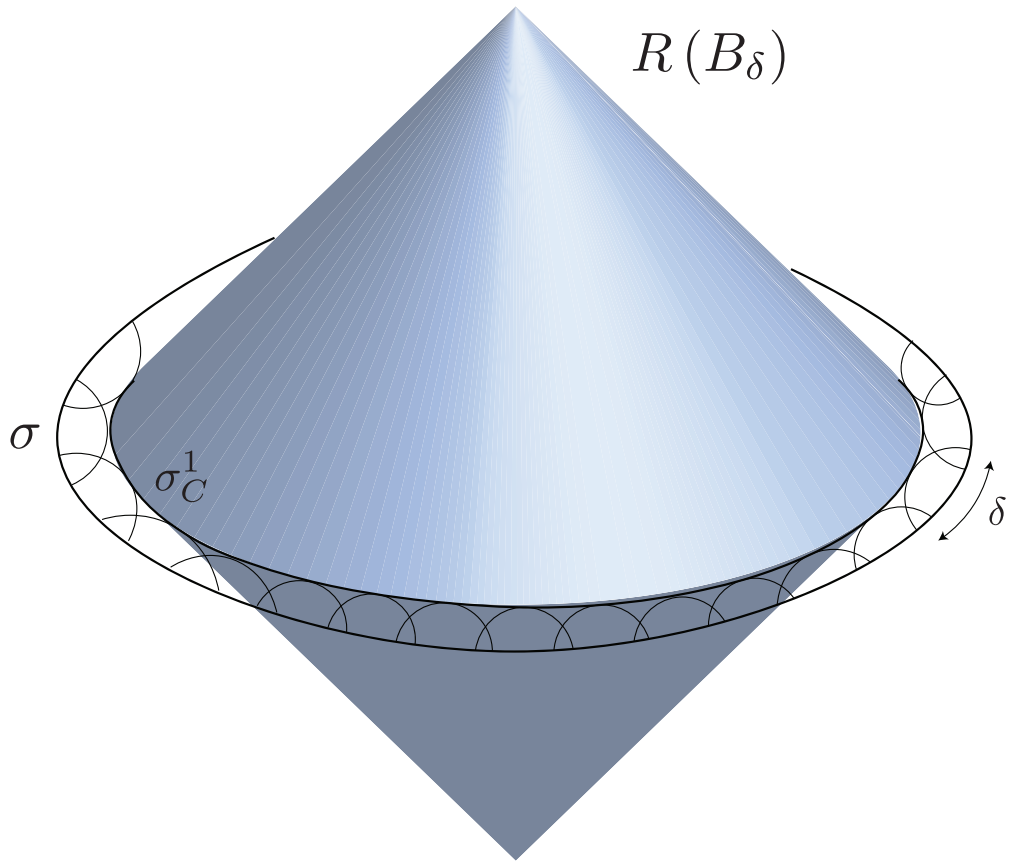


Figure 4.1: $R(B_\delta)$ is the entanglement wedge associated with the new leaf $\sigma_C^1$, where we have taken $C(p) = B_\delta(p)$. It is formed by intersecting the entanglement wedges associated with the complements of spherical subregions of size $\delta$ on the original leaf $\sigma$.

that we can take the $G_N \to 0$ limit in discussing classical spacetime, so we may take $C(p) \to 0$ thus making $\Upsilon$ continuous in this limit. We can then label the renormalized leaves of $\Upsilon$ by some continuous parameter $\lambda$, corresponding to the depth of the renormalized leaf, i.e. $\sigma(\lambda)$ is some $\sigma_C^i$ and $\sigma(0) = \sigma$. Below we take $\lambda$ to decrease as $i$ increases, so that $\lambda \leq 0$.

## Properties

### Uniqueness

$\Upsilon$ is dependent on an extraordinary number of degrees of freedom, namely the shape $C(p)$ at each point on $\sigma$. Despite this freedom, we find that $\Upsilon$ is unique provided some mild assumptions hold.

In particular, imposing homogeneity and isotropy on $C(p)$ (and each subsequent $C^i(p)$) yields a unique holographic slice. For example, one can restrict themselves to the case where

$C^i(p)$ are composed of the same shape and with random orientations. These all reduce to the slice formed by considering balls of constant radius for $C(p)$ and mapping these balls to the subsequent renormalized leaves. We will focus on this preferred slice for the remainder of the paper.

A full discussion of uniqueness is provided in Appendix A.6. However, one of the primary results is that the vector $s$, which is tangent to $\Upsilon$ and radially evolves the leaf inward is given by

$$s = \frac{1}{2}(\theta_k l + \theta_l k). \tag{4.3}$$

This tells us that for a (non-renormalized) leaf of a holographic screen, $s \propto k$ and $\theta_s = 0$. In these situations, the holographic slice initially extends in the null direction and the leaf area remains constant.

In fact, the $s$ vector coincides with the Lorentzian generalization of the mean curvature vector of the leaf [133, 134]. This preferred holographic slice is then realized as the mean curvature flow of the initial leaf.

### Monotonicity of Renormalized Leaf Area

One of the most important features of the holographic slice is that the area of the renormalized leaves decreases monotonically as $\lambda$ decreases. This is crucial to the interpretation as coarse-graining. This property can be shown in a manner similar to Ref. [83], but only after showing that $\theta_k \leq 0$ and $\theta_l \geq 0$ for each renormalized leaf. This is proved in Appendix A.7.

Armed with this knowledge, consider a point $p$ on $\sigma$ and the $s$ vector (defined in the previous section) orthogonal to the leaf $\sigma$ at $p$. The integral curves of $s$ passing through $p$ provide a mapping of $p$ to a unique point on each $\sigma(\lambda)$. Now consider an infinitesimal area element $\delta A$ around $p$. The rate at which this area changes as one flows along $s$ is measured by the expansion

$$\theta_s = \theta_k \theta_l \leq 0, \tag{4.4}$$

as found in Appendix A.6.

Since the area for all infinitesimal area elements decreases on flowing along $s$, the total leaf area also decreases. In fact, this property holds locally. For any subregion of a renormalized leaf, as one flows inward along the holographic slice the area of the subregion decreases monotonically.

### Monotonicity of Entanglement Entropy

Along with the fact that the renormalized leaf area shrinks, the entanglement entropy of subregions also decreases monotonically. This must necessarily happen for a consistent interpretation that the coarse-graining procedure continuously removes short range entanglement.

This is precisely the spacelike monotonicity theorem of Ref. [31], so we will only sketch the idea.[5]

Consider a leaf $\sigma = \sigma(\lambda_0)$ and a renormalized leaf obtained after some small amount of radial evolution, $\sigma' = \sigma(\lambda_0 + \delta\lambda)$, where $\delta\lambda < 0$. A subregion $A$ of $\sigma$ is mapped to subregion $A'$ of $\sigma'$ by following the integral curves of $s$.

Suppose the HRRT surface $\gamma(A')$ anchored to $A'$ is the minimal surface on a spacelike slice $\Sigma'$. Now extend $\Sigma'$ by including the portion of the holographic slice between $\sigma$ and $\sigma'$, such that $\Sigma'$ is now an achronal slice with boundary $\sigma$. Now consider the minimal surface $\Xi(A)$ anchored to $A$ on this extended $\Sigma'$. $\Xi(A)$ has a portion in the exterior of $\sigma'$ which can be projected down to $\sigma'$ using the normal vector $s$. This projection, denoted by $\Xi(A) \to \pi(\Xi(A))$, decreases the area of $\Xi(A)$ due to the spacelike signature of $\Sigma'$. This projection results in a surface anchored to $A'$, which must have an area greater than that of $\gamma(A')$. On the other hand, due to the maximin procedure [60], $\Xi(A)$ must also have an area less than the area of the HRRT surface $\gamma(A)$ anchored to $A$. In summary,

$$\|\gamma(A')\| \leq \|\pi(\Xi(A))\| \leq \|\Xi(A)\| \leq \|\gamma(A)\|, \tag{4.5}$$

where $\|x\|$ represents the volume of the object $x$ (often called the area for a codimension-2 surface in spacetime). The inequalities arise from minimization, projection, and maximization, respectively.

### Subregion Flow Contained within Entanglement Wedge

Suppose one were given access to a finite subregion $A$ on the leaf $\sigma$ and chose to apply the holographic slice construction only to this subregion. The result would be a sequence of renormalized leaves given by $\sigma(\lambda) = A(\lambda) \cup \overline{A}$, with $A(\lambda)$ denoting the sequence of subregions that result from radially evolving $A$ as illustrated in Fig. 4.2.

An interpretation of this procedure as coarse-graining requires that it should not add any further information than what was already available. Thus, it should not allow one to reconstruct points in the bulk beyond what was already accessible from $A$, i.e. $\mathrm{EW}(A)$. This is ensured by the fact that the boundary of $\mathrm{EW}(A)$ acts as an extremal surface barrier for HRRT surfaces anchored to points inside $\mathrm{EW}(A)$, and thus, at no step does $A(\lambda)$ cross outside $\mathrm{EW}(A)$. In fact, if there were a non-minimal extremal surface anchored to $A$ which is contained within $\mathrm{EW}(A)$, the holographic slice would not be able to go beyond this. This would be the case if one were to consider $A$ to be a large subregion of the boundary dual to an AdS black hole.

### Probes Directly Reconstructable Region

Using the definition of Ref. [32], we define the directly reconstructable region of spacetime as the set of bulk points which can be localized by the intersections of some set of boundary

[5] This interpretation may in fact be the most natural explanation of why the spacelike monotonicity theorem holds.

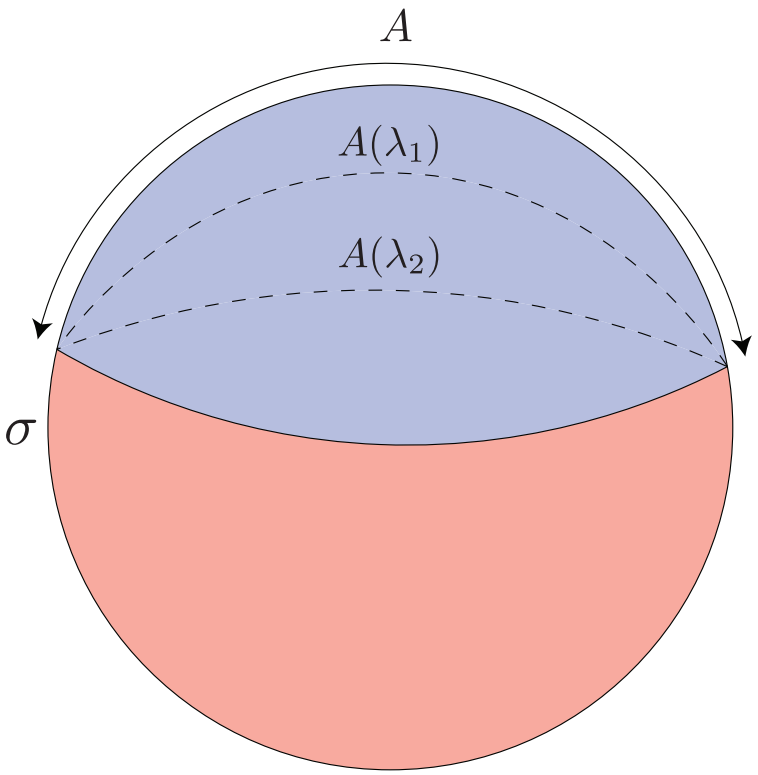


Figure 4.2: The radial evolution procedure when restricted to a subregion $A$ results in a new leaf $\sigma(\lambda) = A(\lambda) \cup \overline{A}$, where $A$ is mapped to a subregion $A(\lambda)$ contained within EW($A$) (blue). The figure illustrates this for two values of $\lambda$ with $\lambda_2 < \lambda_1 < 0$ (dashed lines).

anchored HRRT surfaces and the boundary of their entanglement wedges. Boundary operators corresponding to the maximally localizable bulk operators are dual to local operators in the directly reconstructable region [58].

As argued in Ref. [32], the interior of an equilibrated black hole cannot be reconstructed using the intersection of entanglement wedges. Since the horizon acts as a barrier for all extremal surfaces anchored to points outside the black hole, $\sigma(\lambda)$ stays outside the horizon at each step. Thus, the holographic slice cannot enter the black hole interior. This implies that bulk regions that are not directly reconstructable using the entire holographic screen are inaccessible to any holographic slice.

In fact, as long as $\sigma(\lambda)$ does not become extremal, the holographic slice procedure can continue moving the leaf spatially inward. This is a consequence of Theorem 1 in Ref. [34]. As we will see later, the radial evolution will only halt once the boundary state on the renormalized leaf no longer has distillable local correlations. This can happen in two ways. The first is that the surface closes off to zero area (corresponding to the vanishing of the coarse-grained Hilbert space). The second is if the surface asymptotes to a bifurcation surface

or Killing horizon (corresponding to a maximally entangled state).

Holographic slices probe entanglement shadows, the spacetime regions which cannot be probed by HRRT surfaces anchored to a non-renormalized leaf $\sigma$. The extremal surfaces anchored to $\sigma$ that probe the shadow regions are non-minimal. This prevents the reconstruction of points in these regions by using intersection of HRRT surfaces anchored to $\sigma$. However, the set of HRRT surfaces used for constructing subsequent renormalized leaves need not be minimal on $\sigma$; they need only be minimal on the renormalized leaf at hand. Since non-minimal surfaces anchored to $\sigma$ become minimal when anchored to an appropriately renormalized leaf $\sigma(\lambda)$, the holographic slice can flow through entanglement shadows. We will see an example of this in the next section.

Not only will the holographic slice itself flow through entanglement shadows, HRRT surfaces anchored to a renormalized leaf will probe regions behind shadows of the original leaf. Again, this is because the minimal extremal surfaces anchored to renormalized leaves need not be portions of minimal extremal surface anchored to the original leaf. In fact, one immediately starts recovering portions of shadow regions once the boundary is pulled in. This is what occurs in dense stars and conical AdS. In these cases, more and more of the shadow is recovered as the boundary is pulled in, and the entire shadow is only recovered once the slice contracts to a point.[6]

Because the holographic slices pass through shadows, it seems that the collection of all holographic slices anchored to boundary leaves will sweep out the directly reconstructable region. However, this breaks down if one considers a disconnected boundary. Consider the case of a two-sided AdS black hole. The directly reconstructable region can include regions behind the horizon if one picks a foliation of the left and right boundaries with an offset in time (see Appendix A of Ref. [34]). The intersection of HRRT surfaces anchored to large subregions with support on both boundaries allow for the reconstruction of points behind the horizon. On the other hand, the holographic slice is built from infinitesimal HRRT surfaces anchored to individual boundaries and hence cannot recover regions built from these long range correlations. In the two-sided black hole (no matter what the offset in boundary times), the holographic slice will always connect through the bifurcation surface and never probe behind the horizon; Section 4.4 explains this in detail.

## 4.4 Examples

In this section, we illustrate salient properties of the holographic slice using a few example spacetimes.

[6]This will be explored in future work. This is similar to how entanglement of purification probes portions of shadow regions [135]. However, to recover the entire shadow region using entanglement of purification, one must impose additional conditions on the purification [136, 137].

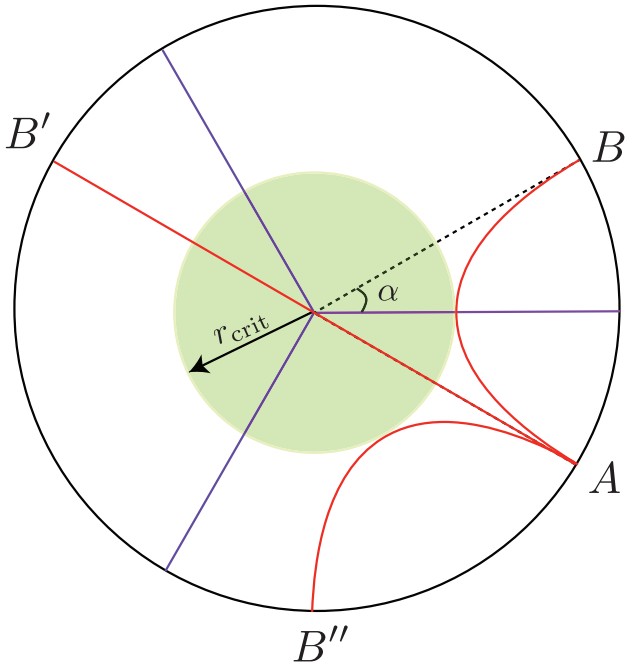


Figure 4.3: The case of conical $AdS_3$ with $n = 3$. The points $B$, $B'$, and $B''$ are identified. There are 3 geodesics from $A$ to $B$, of which generically only one is minimal. Here, we have illustrated the subregion $AB$ with $\alpha = \pi/6$, where two of the geodesics are degenerate. This is the case in which the HRRT surface probes deepest into the bulk, leaving a shadow region in the center. Nevertheless, the holographic slice spans the entire spatial slice depicted.

## Conical AdS

We first consider conical $AdS_3$ to illustrate that the holographic slice probes regions inside entanglement shadows. In order to obtain conical $AdS_3$, we start with the $AdS_3$ metric

$$ds^2 = -\left(1 + \frac{r^2}{L^2}\right)dt^2 + \left(1 + \frac{r^2}{L^2}\right)^{-1} dr^2 + r^2 d\theta^2, \tag{4.6}$$

where $L$ is the AdS length scale. We then perform a $\mathbb{Z}_n$ quotient, so that the angular coordinate $\theta$ has periodicity $2\pi/n$. Locally, this spacetime is identical to $AdS_3$, and solves the Einstein equations for a negative cosmological constant away from $r = 0$. However, there is a conical defect at $r = 0$ introduced by the $\mathbb{Z}_n$ quotient.

HRRT surfaces in this spacetime simply correspond to minimal length geodesics anchored to subregions at the conformal boundary. As illustrated in Fig. 4.3, there are $n$ geodesics in the parent $AdS_3$ spacetime which are candidate extremal surfaces for a given subregion. However, generically only one of them is minimal and corresponds to the HRRT surface.

The geodesics in $AdS_3$ are described by the equation

$$\tan^2\theta = \frac{r^2\tan^2\alpha - L^2}{r^2 + L^2}, \tag{4.7}$$

where $\alpha$ is the half-opening angle of the subregion being considered. Since the angular coordinate $\theta$ has a periodicity of $2\pi/n$, the minimal length geodesic that probes deepest into the bulk is obtained when $\alpha = \pi/2n$. From Eq. (4.7), this gives a critical radius of [85]

$$r_{\text{crit}}(n) = L\cot\left(\frac{\pi}{2n}\right), \tag{4.8}$$

which takes a nonzero finite value for $n \neq 1$. Thus, the region $r < r_{\text{crit}}(n)$ is an entanglement shadow, which cannot be probed by HRRT surfaces anchored to the conformal boundary.

The holographic slice is constructed by finding infinitesimal HRRT surfaces starting from the (regularized) conformal boundary. Since the spacetime is locally $AdS_3$, the HRRT surfaces for small regions are identical to those in $AdS_3$. Because of the static and spherically symmetric nature of $AdS_3$, the renormalized leaves correspond to surfaces of constant $r$ and $t$. Now, since $r_{\text{crit}}(n)$ is not an extremal surface barrier, as can be seen from the existence of non-minimal extremal surfaces penetrating it, the holographic slice suffers no obstruction in crossing over to the entanglement shadow. This implies that the holographic slice is simply given by a constant time slice that covers all of the spatial region $r \in [0, \infty)$.

In general, holographic slices do not have any difficulty in going into entanglement shadow regions, since these shadows are not associated with extremal surface barriers which any extremal surfaces anchored to the outside cannot penetrate [62]. In fact, holographic slices also sweep entanglement shadows other than those in the centers of conical AdS, e.g. regions around a dense star [86].

## Black Holes

Consider a two-sided eternal $AdS_{d+1}$ Schwarzschild black hole. The metric is given by

$$ds^2 = -f(r)\,dt^2 + \frac{1}{f(r)}dr^2 + r^2 d\Omega_{d-1}^2, \tag{4.9}$$

where

$$f(r) = 1 + \frac{r^2}{L^2} - \left(\frac{r_+}{r}\right)^{d-2}\left(1 + \frac{r_+^2}{L^2}\right), \tag{4.10}$$

with $r_+$ being the horizon radius. As can be seen in Fig. 4.4, the two exterior regions have a timelike Killing vector. Thus, the HRRT surfaces anchored to subregions with support only on one boundary respect the Killing symmetry and lie on the constant $t$ slice connecting the respective boundary to the bifurcation surface. Subregions anchored on both boundaries could potentially lie on a different spatial slice if the HRRT surface is connected. However, since we are considering the holographic slice being built up using HRRT surfaces anchored to infinitesimal subregions, those anchored on both sides always stay disconnected.

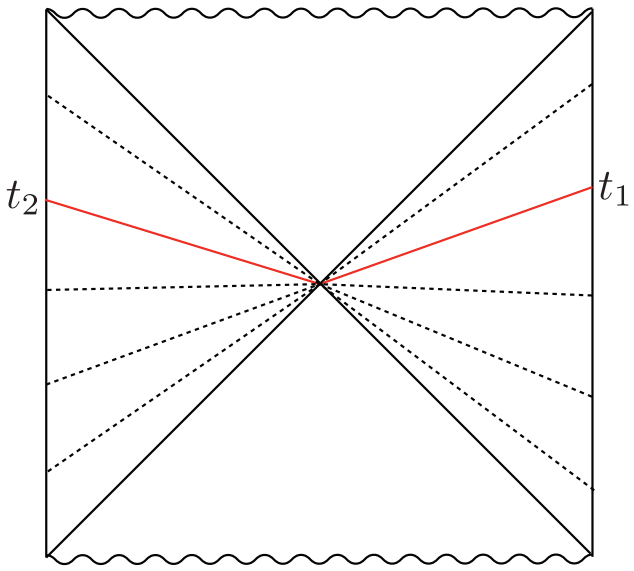


Figure 4.4: The exterior of a two-sided eternal AdS black hole can be foliated by static slices (black dotted lines). The holographic slice (red) connects the boundary time slices at $t = t_1$ on the right boundary and $t = t_2$ on the left boundary to the bifurcation surface along these static slices.

Thus, the holographic slice, as seen in Fig. 4.4, is the union of static slices in both exterior regions and terminates at the bifurcation surface. As shown in Ref. [34], the bifurcation surface itself is extremal and lies on a Killing horizon, and hence the process of renormalizing leaves must asymptote to this surface.

The phenomenon of a holographic screen being terminated at a nontrivial surface requires the existence of a bifurcation surface, which is absent in most physical situations. For example, consider an AdS-Vaidya metric where a black hole is formed from the collapse of a thin null shell of energy [88]. The metric in ingoing Eddington-Finkelstein coordinates is given by

$$ds^2 = -f(r,v)\,dv^2 + 2dv\,dr + r^2 d\Omega_{d-1}^2, \tag{4.11}$$

where

$$f(r,v) = 1 + \frac{r^2}{L^2} - \theta(v)\left(\frac{r_+}{r}\right)^{d-2}\left(1 + \frac{r_+^2}{L^2}\right), \tag{4.12}$$

with

$$\theta(v) = \begin{cases} 0 & \text{for } v < 0 \\ 1 & \text{for } v > 0. \end{cases} \tag{4.13}$$

The null shell lies at $v = 0$, and this spacetime is obtained simply by stitching together an AdS-Schwarzschild metric to the future of the shell and a pure AdS metric to the past. The composite global spacetime is time-dependent, but each of the building blocks admits

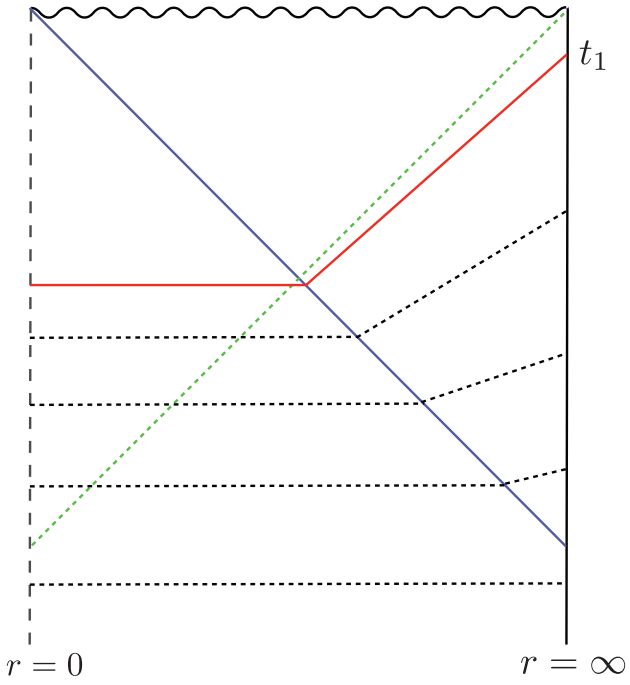


Figure 4.5: Penrose diagram of an AdS Vaidya spacetime formed from the collapse of a null shell (blue), resulting in the formation of an event horizon (green). Individual portions of the spacetime, the future and past of the null shell, are static. Thus, the holographic slice (red) can be constructed by stitching together a static slice in each portion.

a timelike Killing vector locally as shown in Fig. 4.5. As discussed earlier, since the HRRT surfaces relevant to the holographic slice are those of infinitesimal subregions, they only sense the local spacetime, which is static. This allows us to construct the holographic slice independently in each region. The static slices can then be stitched together to obtain the holographic slice as shown in Fig. 4.5.

An important feature here is that at late times, i.e. sufficiently after the black hole has stabilized, the holographic slice constructed from a leaf stays near the horizon for long time. Eventually, this flow terminates at $r = 0$. This behavior of holographic slices is, in fact, general in one-sided black holes; see Fig 4.6 for a schematic depiction.

Note that the picture of Fig 4.6 is obtained in the $G_{\mathrm{N}} \to 0$ limit. When $G_{\mathrm{N}} \neq 0$, renormalized leaves will hit the stretched horizon [63], where the semiclassical description of spacetime breaks down, before being subjected to the long flow near the horizon.

## FRW Spacetimes

We now discuss a nontrivial example in a time-dependent spacetime, away from the standard asymptotically AdS context. Consider a $(d+1)$-dimensional flat Friedmann-Robertson-

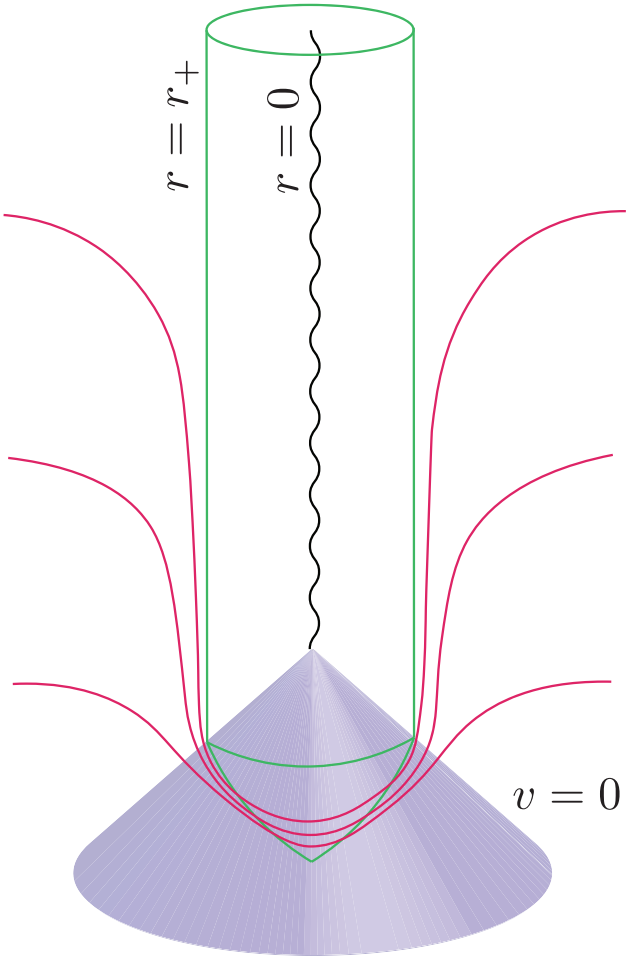


Figure 4.6: A schematic depiction of holographic slices for a spacetime with a collapse-formed black hole in ingoing Eddington-Finkelstein coordinates.

Walker (FRW) spacetime containing a single fluid component with equation of state parameter $w$

$$ds^2 = a(\eta)^2 \left(-d\eta^2 + dr^2 + r^2 d\Omega_{d-1}^2\right). \tag{4.14}$$

Here,

$$a(\eta) = c\,|\eta|^q, \tag{4.15}$$

where $c > 0$ is a constant, and

$$q = \frac{2}{d - 2 + dw}. \tag{4.16}$$

The discontinuity of $q$ at $w = (2-d)/d$ is an artifact of choosing conformal time, and physics is smooth across this value of $w$.

The spherically symmetric holographic screen is located at

$$r(\eta) = \frac{a(\eta)}{\frac{da}{d\eta}(\eta)} = \frac{\eta}{q}. \tag{4.17}$$

By spherical symmetry, the holographic slice must be a codimension-1 surface of the form $\eta = g(r)$, where each renormalized leaf is an $\mathbb{S}^{d-1}$. Consider a renormalized leaf at $\eta = \eta_*$ and $r = r_*$. Generalizing the results from Refs. [34, 119], HRRT surfaces anchored to a small spherical cap of half-opening angle $\gamma$ of the renormalized leaf are given by

$$\eta(\xi) = \eta_* + \frac{\dot{a}}{2a}\left(\xi_*^2 - \xi^2\right) + \ldots, \tag{4.18}$$

where $\xi = r\sin\theta$ and $\xi_* = r_*\sin\gamma$ with $\theta$ being the polar angle, and $a \equiv a(\eta_*)$ and $\dot{a} \equiv da/d\eta(\eta_*)$. We refer the reader to Appendix C.3 of Ref. [34] for more details.

The next renormalized leaf is generated by joining together the deepest point of each such HRRT surface. Suppose $\Delta\eta$ and $\Delta r$ represent the change in conformal time and radius from one renormalized leaf to the next. Then we have

$$\Delta\eta = \frac{\dot{a}}{2a}\xi_*^2 + \ldots, \tag{4.19}$$

$$\Delta r = -(r_* - r_*\cos\gamma), \tag{4.20}$$

so that

$$\frac{\Delta\eta}{\Delta r} = -\frac{\frac{\dot{a}}{2a}r_*^2\sin^2\gamma}{r_*(1-\cos\gamma)} = -\frac{\dot{a}}{a}r_*. \tag{4.21}$$

Taking the limit $\gamma \to 0$, we obtain a differential equation for the radial evolution of the holographic slice

$$\frac{d\eta}{dr} = -\frac{qr}{\eta}. \tag{4.22}$$

Integrating this equation gives us

$$\eta^2 + qr^2 = \eta_*^2 + qr_*^2 = \frac{1+q}{q}\eta_0^2, \tag{4.23}$$

where $\eta_0$ is the conformal time of the original non-renormalized leaf.

Let us highlight a few interesting features of this holographic slice. First, it spans the entire interior region of the holographic screen. Next, substituting $r = \eta/q$ into Eq. (4.22) tells us that the holographic slice starts out in the null direction from the leaf; see Eq. (4.17). This is because the $k$ direction locally has zero expansion there, as discussed in Section 4.3. As we move inward along the radial flow, however, the slope becomes flatter, and eventually the surface reaches the highest point given by

$$\eta(r=0) = \eta_0\sqrt{\frac{1+q}{q}}. \tag{4.24}$$

In Fig. 4.7 we have depicted holographic slices, given by Eq. (4.23), for several values of $w$ with $d = 3$.

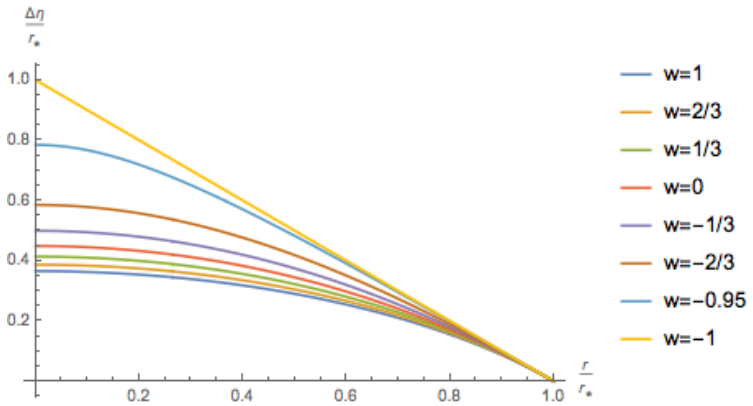


Figure 4.7: Holographic slices of $(3+1)$-dimensional flat FRW universes containing a single fluid component with equation of state parameter $w$.

## Asymptotically AdS and Flat Spacetimes

Here we discuss certain subtleties associated with holographic screens that lie on an asymptotic boundary. First, consider a $(d+1)$-dimensional asymptotically AdS spacetime, which can be expanded in a Fefferman-Graham series [138] near the boundary

$$ds^2 = \frac{L^2}{z^2}\{g_{ab}(x^a, z)dx^a dx^b + dz^2\}, \tag{4.25}$$

where $L$ is the AdS length scale, and

$$g_{ab}(x^a, z) = g^{(0)}_{ab}(x^a) + z^2 g^{(2)}_{ab}(x^a) + \dots. \tag{4.26}$$

Here, $g^{(0)}_{ab}$ represents the conformal boundary metric, and the subleading corrections represent deviations as one moves away from the boundary at $z = 0$.

In an asymptotically AdS spacetime, the holographic screen $H$ formally lies at spacelike infinity. In order to construct a holographic slice in such a situation, one needs to first consider a regularized screen $H'$ at $z = \epsilon$ and then take the limit $\epsilon \to 0$ after constructing the slice. Suppose that a leaf is given by a constant $t$ slice of $H'$, with $h_{ij}$ representing the induced metric on the leaf. The null normals are then given by

$$k_\mu = dz - dt + O(\epsilon^2), \tag{4.27}$$
$$l_\mu = -dz - dt + O(\epsilon^2), \tag{4.28}$$

where the $O(\epsilon^2)$ corrections arise due to deviations away from the boundary. The null

expansions are

$$\begin{aligned}\theta_k &= h^{ij}\Gamma^z_{ij} - h^{ij}\Gamma^t_{ij} \\ &= -\frac{\epsilon(d-1)}{L} + O(\epsilon^2), \end{aligned} \tag{4.29}$$

$$\begin{aligned}\theta_l &= -h^{ij}\Gamma^z_{ij} - h^{ij}\Gamma^t_{ij} \\ &= \frac{\epsilon(d-1)}{L} + O(\epsilon^2). \end{aligned} \tag{4.30}$$

Thus, we see that the expansion $\theta_k$ vanishes only in the limit $\epsilon \to 0$.

This implies that a leaf $\sigma'$ of a regularized screen $H'$ ($\epsilon \neq 0$) is, in fact, a renormalized leaf ($\theta_k \neq 0$), and thus the results in Section 4.3—that the holographic slice initially extends in the null direction and the leaf area remains constant—do not apply. In fact, the holographic slice extending from $\sigma'$ initially evolves inward along the $z$ direction up to corrections of $O(\epsilon)$, as can be seen from the fact that $\theta_k = -\theta_l$ up to $O(\epsilon)$. In the limit $\epsilon \to 0$, both $\theta_k$ and $\theta_l$ vanish simultaneously. This leads to a holographic screen at spacelike infinity in a formal sense.[7]

A similar situation arises in asymptotically flat spacetimes. A general asymptotically flat spacetime can be expanded in the Bondi-Sachs form [139, 140] as

$$\begin{aligned}ds^2 = &-\frac{V}{r}e^{2\beta}du^2 - 2e^{2\beta}dudr \\ &+ r^2 h_{AB}\big(dx^A - U^A du\big)\big(dx^B - U^B du\big), \end{aligned} \tag{4.31}$$

where each of the functions admits a large $r$ expansion with the following behavior:

$$V = r + O(1), \qquad \beta = O\left(\frac{1}{r^2}\right), \tag{4.32}$$

$$U^A = O\left(\frac{1}{r^2}\right), \qquad h_{AB} = O(1). \tag{4.33}$$

In order to construct a holographic slice, the holographic screen $H$ must be regularized to become a timelike surface $H'$ at $r = R$, where we can eventually take the limit $R \to \infty$. The null normals of a leaf on a constant time slice are

$$k_\mu = du, \tag{4.34}$$

$$l_\mu = -\frac{V}{r}du - 2dr, \tag{4.35}$$

[7]Strictly speaking, this does not satisfy the definition of the holographic screen in Section 4.3, which requires $\theta_l$ to be strictly positive.

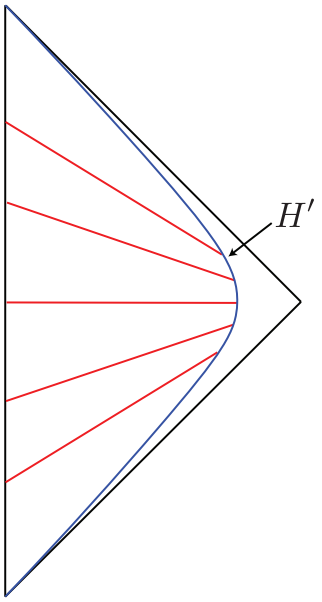


Figure 4.8: Penrose diagram of a Minkowski spacetime. The holographic slices (red) are anchored to the regularized holographic screen $H'$ (blue). As the limit $R \to \infty$ is taken, the holographic slices become complete Cauchy slices.

giving the null expansions near the boundary

$$\theta_k = -\frac{2}{R} + O\left(\frac{1}{R^2}\right), \tag{4.36}$$

$$\theta_l = \frac{2}{R} + O\left(\frac{1}{R^2}\right). \tag{4.37}$$

Thus, similar to the case of asymptotically AdS spacetimes, a leaf of a regularized holographic screen is a renormalized one, and both $\theta_k, \theta_l \to 0$ simultaneously as $R \to \infty$.

As a simple example, we illustrate the case of a Minkowski spacetime in Fig. 4.8. As the limit $R \to \infty$ is taken, the holographic slices become complete Cauchy hypersurfaces which are constant time slices anchored to spatial infinity. In the limit $t \to +\infty$ $(-\infty)$, future (past) null and timelike infinities are obtained as a holographic slice. In this situation, time evolution of the boundary theory from $t \to -\infty$ to $+\infty$ corresponds to an $S$-matrix description of the bulk.

## 4.5 Interpretation and Applications

We have introduced the geometric definition of the holographic slice and demonstrated some of its properties. But what does the slice correspond to in the boundary theory? What

questions can it help us address? The construction of the slice naturally lends itself to an interpretation of eliminating information at small scales, and hence can be well understood in the context of coarse-graining. Through this, we can think of the slice as an isometric tensor network. This provides us with a new way to think about holographic tensor networks and the bulk regions of spacetime that they encode.

Throughout this section we will be talking about various Hilbert spaces in which holographic states belong. To do so, we will be taking $G_{\mathrm{N}}$ to be finite but small. This is an appropriate approximation for classical spacetimes provided we only concern ourselves with length scales sufficiently larger than the Planck length.

## Coarse-Graining

We take the view that a boundary state, $|\psi(0)\rangle$, lives on the original leaf, $\Upsilon(0)$, i.e. it lives in an effective Hilbert space, $\mathcal{H}$, having a local product space structure with dimension $\log|\mathcal{H}| = \|\Upsilon(0)\|/4G_{\mathrm{N}}$. The HRRT prescription says that the emergent bulk geometry is intricately related to the entanglement of the boundary state. In particular, despite the fact that bulk information is delocalized in the boundary theory, a bulk region cannot be reconstructed if some boundary subregions are ignored. The size of the smallest subregion for this to occur gives us some idea of what scale of boundary physics this bulk region is encoded in. Using this intuition, we can then attempt to address what coarse-graining the boundary state corresponds to in the bulk.

At each step in the construction of the holographic slice, we eliminate the region of spacetime associated with a small length scale, $\delta$, of the boundary. In particular, this is the region of spacetime whose information is necessarily lost if we cannot resolve below length scale $\delta$. In this sense, we are coarse-graining over the scale $\delta$ and obtaining a new bulk region whose information has not been lost. Recursively doing this and sending $\delta$ to zero produces a continuum of bulk domains of dependence with unique boundaries sweeping out the holographic slice, $\Upsilon(\lambda)$. This is depicted in Fig. 4.9.

A consistency check for this interpretation is that the size of the effective Hilbert space should necessarily decrease as we coarse-grain over larger and larger scales. This is precisely the monotonicity property listed in Section 4.3: as one flows along the holographic slice, the area of the renormalized leaves decreases. This tells us that the size of the effective Hilbert space describing the bulk domain of dependence also decreases.

As the coarse-graining procedure progressively removes information at small scales, a corresponding removal of bulk information closest to the renormalized leaf occurs. Given this global removal of short range information, one should expect the entanglement between any region and its complement to correspondingly decrease. This is precisely the monotonicity of entanglement entropy property observed in Section 4.3. This is consistent with the interpretation that at each step we are removing short range entanglement.

Using the holographic slice, we can address the question of how much entanglement between a subregion and its complement is sourced by physics at different scales. By following the integral curves of $s$ for the subregion, we can stop at whatever scale we desire and use

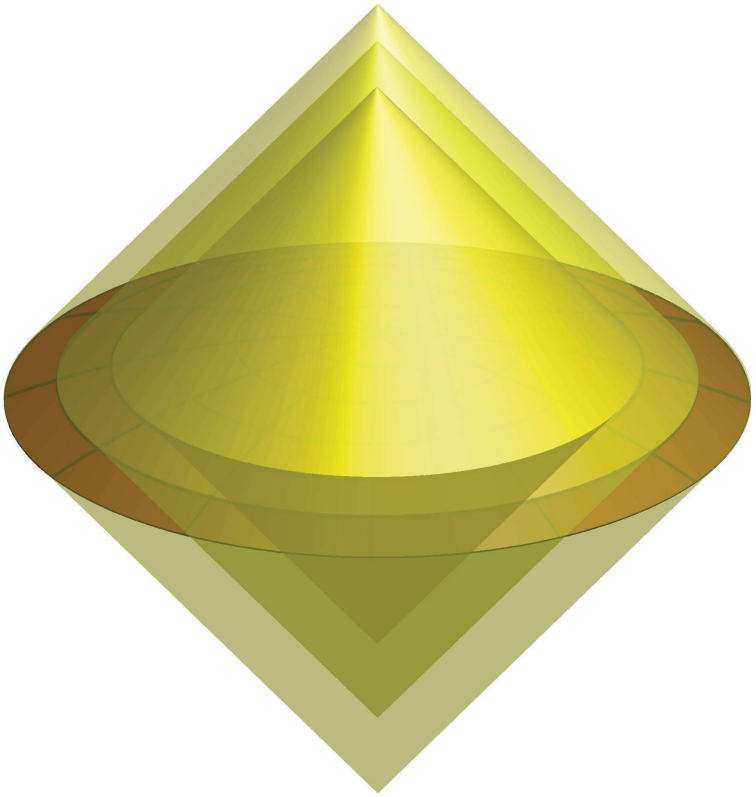

Figure 4.9: This depicts the holographic slice (maroon), and the successive domains of dependence encoded on each renormalized leaf.

the HRRT prescription on the renormalized leaf. This gives us the entanglement entropy sourced by physics at length scales larger than that associated with the renormalized leaf.

## Radial Evolution of States

We will now be more explicit in describing the framework for coarse-graining holographic states. Given a bulk region $D(\Upsilon(0))$, there exists a quantum state $|\psi(0)\rangle$ living in some fundamental holographic Hilbert space, $\mathcal{H}_{\text{UV}}$, in which the bulk information of $D(\Upsilon(0))$ is encoded via the HRRT prescription. This implies that $\mathcal{H}_{\text{UV}}$ has a locally factorizable structure. On the other hand, the area of $\Upsilon(0)$ provides an upper bound for the dimension of effective Hilbert space that $|\psi(0)\rangle$ lives in, which we call $\mathcal{H}_{\Upsilon(0)}$. That is, $|\psi(0)\rangle \in \mathcal{H}_{\Upsilon(0)} \subset \mathcal{H}_{\text{UV}}$. The dimension, $|\mathcal{H}_{\Upsilon(0)}|$, of the effective Hilbert space is defined as

$$\ln |\mathcal{H}_{\Upsilon(0)}| = \sum_i S_i = \frac{\|\Upsilon(0)\|}{4G_{\text{N}}}. \tag{4.38}$$

Here, $S_i$ represents the entanglement entropy of $|\psi(0)\rangle$ in an infinitesimally small subregion, $A_i$, of the holographic space $\Omega$ on which $\mathcal{H}_{\text{UV}}$ is defined. We sum over all of these small subregions such that $\Omega = \cup_i A_i$ and $A_i \cap A_j = \emptyset$ $(i \neq j)$. This reduces to calculating the area of $\Upsilon(0)$ because of the HRRT prescription. Namely, the size of the effective Hilbert space that $|\psi(0)\rangle$ lives in is determined by the entanglement between the fundamental degrees of freedom of $\mathcal{H}_{\text{UV}}$, and $\|\Upsilon(0)\|/4G_{\text{N}}$ is the thermodynamic entropy associated with this entanglement structure.

As one continuously coarse-grains $|\psi(0)\rangle$, information encoded in small scales is lost. Correspondingly, information of the bulk geometry that is stored in small scales is lost, and the dimension of the effective Hilbert space that the coarse-grained state lives in decreases. At a given scale of coarse-graining corresponding to $\lambda$, the new state, $|\psi(\lambda)\rangle$, lives in the same Hilbert space as the original leaf, $\mathcal{H}_{\text{UV}}$, but now in an effective subspace, $\mathcal{H}_{\Upsilon(\lambda)}$, with dimension given by $\ln|\mathcal{H}_{\Upsilon(\lambda)}| = \|\Upsilon(\lambda)\|/4G_{\text{N}}$. Additionally, $|\psi(\lambda)\rangle$ only contains information of $D(\Upsilon(\lambda))$, as we have explicitly lost the information necessary to reconstruct any part of $D(\Upsilon(0)) \setminus D(\Upsilon(\lambda))$.

Because all of the coarse-grained states live in the same Hilbert space, $\mathcal{H}_{\text{UV}}$, we can consider the coarse-graining procedure as a unitary operation that takes us from state to state, along the lines of the work of Ref. [141]. That is,

$$|\psi(\lambda)\rangle = U(\lambda, 0)|\psi(0)\rangle. \tag{4.39}$$

We can write $U(\lambda_1, \lambda_2)$ as

$$U(\lambda_1, \lambda_2) = P \exp\left[-i \int_{\lambda_2}^{\lambda_1} K(\lambda) d\lambda\right], \tag{4.40}$$

where $P$ represents path-ordering. $K(\lambda)$ is a Hermitian operator removing physical correlations between nearby subregions at the length scale, $l_\lambda$, associated to $\lambda$ on $\Omega$. Some appropriate measures of physical correlations would be the mutual information $(I(A, B))$, entanglement negativity $(N(A, B))$, or the entanglement of purification $(E(A, B))$ between neighboring small subregions of the leaf under consideration, $\Upsilon(\lambda)$. Note that as the boundary state becomes maximally entangled, all three of these measures will vanish. This also happens if the boundary state in consideration has no entanglement, i.e. is a product state.

Of the three measures, entanglement of purification already has a bulk description that naturally characterizes some measure of moving into the bulk. In particular, Refs. [40, 41] proposed that the entanglement of purification of two boundary subregions, $A$ and $B$, is calculated by the minimum cross section, $\zeta$, of a bipartition of the extremal surface anchored to $A \cup B$; see Fig. 4.10. Considering the case where $\partial A$ and $\partial B$ coincide at some point, and whose connected phase is the appropriate extremal surface, the entanglement of purification gives some measure of the depth of the extremal surface. In bulk dimensions higher than $2 + 1$, $\|\zeta\|$ will not be in units of length, but it is still related to the depth of the extremal surface. Thus it seems natural that $K(\lambda)$ is some (quasi-)local function, $F$, of physical

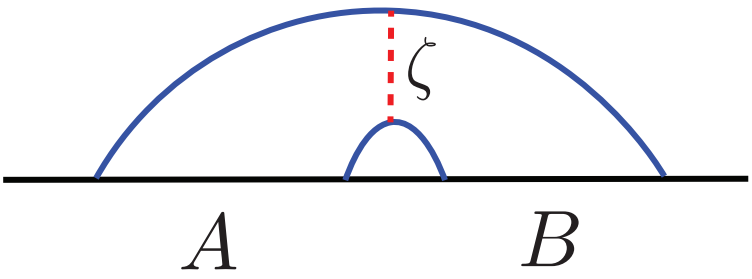


Figure 4.10: Let $A$ and $B$ two boundary subregions. The blue lines represent the HRRT surface of $A \cup B$ and $\zeta$ the minimal cross section. The entanglement of purification of $A$ and $B$ is given by $\|\zeta\|/4G_{\mathrm{N}}$. In the limit that $A$ and $B$ share a boundary point, $\zeta$ probes the depth of the extremal surface.

correlations, including but not necessarily limited to quantum entanglement, at the scale $l_\lambda$. For example, it may be related to the entanglement of purification:

$$K(\lambda) \sim \int d^{d-1}\mathbf{x}\, F\big(E_\lambda(\mathbf{x})\big), \tag{4.41}$$

where $\mathbf{x}$ are the coordinates of $\Omega$. Here, $E_\lambda(\mathbf{x})$ is the "density" of the entanglement of purification between the degrees of freedom in two neighboring regions on $\sigma(\lambda)$ around $\mathbf{x}$.

Alternately, the case of subregion coarse-graining as in Fig. 4.2 motivates the usage of results from Ref. [115], which can be used to map the state from $\sigma$ to $\sigma(\lambda)$. In AdS/CFT, modular evolution allows one to explicitly reconstruct bulk operators on the HRRT surface. With our assumption that the HRRT formula holds (with quantum corrections), a similar construction should be possible given complete knowledge of the boundary theory. $K(\lambda)$ may then be better understood as a convolution over modular evolutions with infinitesimal boundary subregions:

$$K(\lambda) \sim \int d^{d-1}\mathbf{x}\, F\big(\kappa_\lambda(\mathbf{x})\big), \tag{4.42}$$

where $\kappa_\lambda(\mathbf{x})$ is the modular Hamiltonian density on $\sigma(\lambda)$ at $\mathbf{x}$. It would be interesting to make the connection of $K(\lambda)$ to modular evolution clearer in the future.

The process of removing short range correlations continues until all correlations at the scale $l_\lambda$ have been removed, and hence no more bulk spacetime can be reconstructed. This can happen when the slice contracts to a point and no local product structure exists in the effective Hilbert space $\mathcal{H}_{\Upsilon(\lambda)}$. Note that in $\mathcal{H}_{\mathrm{UV}}$ this state corresponds to a product state, so that $S_i = 0$ for every subregion in $\mathcal{H}_{\mathrm{UV}}$. The other way in which all relevant correlations vanish is when the coarse-grained state becomes maximally entangled in $\mathcal{H}_{\Upsilon(\lambda)}$. In $\mathcal{H}_{\mathrm{UV}}$, this corresponds to a state which satisfies $S_A = \sum_{i \subset A} S_i$ for all subregions, $A$, of $\Omega$.

When the coarse-grained state becomes maximally entangled in $\mathcal{H}_{\Upsilon(\lambda)}$, $U(\lambda + d\lambda, \lambda)$ becomes the identity for Eq. (4.41) as $K(\lambda)$ becomes 0. Hence, the state remains invariant

under the coarse-graining operation. There are two ways for this to happen geometrically. One is if the slice approaches a bifurcation surface; then the extremal surfaces coincide with the renormalized leaf, hence preventing any further movement into the bulk. This is the case for eternal two-sided black holes. The second is if the slice approaches a null, non-expanding horizon and the state is identical along the horizon. This is the case in de Sitter space. This result is complementary to Theorem 1 of Ref. [34], which proves that if a boundary state is maximally entangled, it must either live on a bifurcation surface or a null, non-expanding horizon.

This may initially seem like a contradiction—that both the state becomes maximally entangled and that there are no more correlations to harvest. However, it is precisely because we are examining correlations at *small* scales that this occurs. A small boundary region is maximally entangled with the entire rest of the boundary, and hence the short range entanglement must vanish. One can quantify this by examining the entanglement negativity of bipartitions of small subregions on $\sigma(\lambda)$. As states become maximally entangled, the entanglement negativity vanishes for two small subregions. This places an upper bound on the real, distillable entanglement between these subregions. Hence, the true quantum entanglement at small scales vanishes as a state becomes maximally entangled. Correspondingly, the coarse-graining procedure halts. This is indeed what happens to the holographic slice.

The same can also be seen by considering the modular evolution, Eq. (4.42), of a maximally entangled subregion. In this case, the modular evolution is proportional to the identity operator, and hence the modular flow of the state is stationary. This corresponds to no movement into the bulk as expected by the properties of the holographic slice for maximally entangled states.

## Tensor Network Picture

In this language the relationship to tensor networks is very clear. The holographic slice arises as the continuous limit of a tensor network that takes a boundary state and disentangles below a certain scale, reducing the effective Hilbert space size. This is a slight generalization of continuous Multiscale Entanglement Renormalization Ansatz (cMERA) [122], which is restricted to hyperbolic geometries.

In general, we can consider a tensor network as a non-continuum modeling of the holographic slice, which isometrically embeds boundary states into spaces of lower effective dimension by removing short range correlations; see Fig. 4.11. In the ground state of AdS/CFT, this corresponds to an instance of Multiscale Entanglement Renormalization Ansatz (MERA) [142]. Each layer of the tensor network then lives on the corresponding renormalized leaf of the discrete version of $\Upsilon$. From this we see that the tensor network lives on this discrete version of the holographic slice. Because isometric tensor networks obey a form of HRRT, one may mistakenly conclude that the cut through the network computes the area of the corresponding surface in the bulk along the holographic slice. This is generally not the case; the maximin method tells us that this area provides only a lower bound on the entanglement. The entanglement calculated in this way instead corresponds to the area of

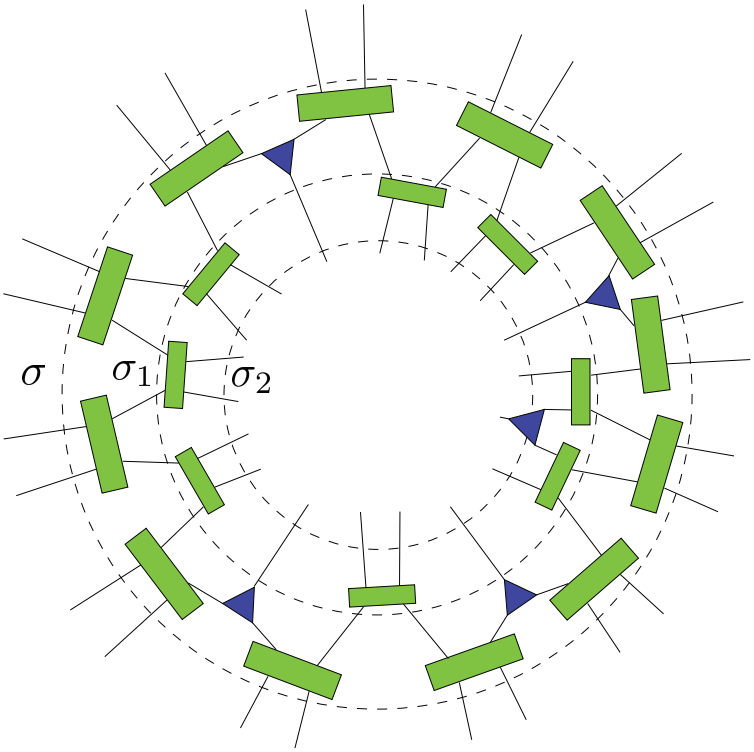


Figure 4.11: A tensor network for a non-hyperbolic geometry. The green rectangles correspond to disentanglers while the blue triangles are coarse-graining isometries. Each internal leg of the tensor network has the same bond dimension. We are imagining that $\sigma$ corresponds to a leaf of a holographic screen and each successive layer ($\sigma_1$ and $\sigma_2$) is a finite size coarse-graining step of the holographic slice. Through this interpretation, the tensor network lives on the holographic slice. However, the entanglement entropy calculated via the min-cut method in the network does not correspond to the distance of the cut along the holographic slice in the bulk. It corresponds to the HRRT surface in the appropriate domain of dependence. The locations of $\sigma_1$ and $\sigma_2$ in the bulk are found by convolving the HRRT surfaces for the small regions being disentangled and coarse-grained. The holographic slice is a continuous version of this tensor network.

the HRRT surface anchored to the appropriate subregion of a renormalized leaf. In other words, the tensor network should not be viewed as a discretization of the holographic slice, but rather as a set of boundary states dual to successively smaller domains of dependence.

In fact, this interpretation can be applied to any isometric tensor network, and we argue that this is the proper way to view tensor networks representing bulk spacetimes. That is, given a state represented by an isometric tensor network, one can find a set of states by pushing the boundary state through the tensors one layer at a time such that no two layers

have the same boundary legs.[8] These successive states are then dual to bulk domains of dependence that are successively contained in each other, and whose boundaries lie on (a discrete version of) the holographic slice.

### Time Evolution and Gauge Fixing

The preferred holographic slice of Section 4.3 provides us with a novel way to foliate spacetimes. By applying the holographic slice procedure to each boundary time slice, one foliates the bulk spacetime with holographic slices.

In order for this to provide a good gauge fixing, the holographic slices generated from different boundary time slices must not intersect. In spherically symmetric cases, these intersections do not occur. From the spherical symmetry of the spacetime, the renormalized leaves must also be spherical. Thus, if two holographic slices did intersect, they must intersect at a renormalized leaf. However, the evolution of the slice is unique from this leaf, and hence these two slices do not intersect. Furthermore, the reverse flow is also unique and hence the slices must exactly coincide. This prevents ambiguities in the gauge fixing of the bulk spacetime.

Outside of spherically symmetric cases, if $\mathrm{sgn}(K)$, the sign of the extrinsic curvature of the slice, is constant over the slice then no slices will intersect. By joining a slice with the past (future) portion of the holographic screen in the $K \geq 0$ ($\leq 0$) case, one can create a barrier for extremal surfaces anchored in the interior of the barrier. This implies that any slice constructed from a leaf cannot penetrate slices generated from leaves towards its future (past) if $K \geq 0$ ($\leq 0$).

As explained in Sections 4.3 and 4.4, the foliation generated by the holographic slices will not probe behind late-time horizons. Thus this foliation provides a gauge fixing of the region of spacetime exterior to black hole horizons. In this region, the foliation provides a covariant map from boundary time slices to bulk time slices.

## 4.6 Relationship to Renormalization

In this section, we discuss how our coarse-graining procedure is related to conventional renormalization, both in the context of standard quantum field theories and AdS/CFT.

### Analogy to Renormalization in Quantum Field Theories

We first draw an analogy between pulling in the boundary along the holographic slice and standard renormalization in quantum field theories. In particular, we liken the limitations of

[8] This picture can perhaps be used to show that the dynamical holographic entropy cone is contained within the holographic entropy cone [114]. By explicitly constructing the holographic slice tensor network that encodes a state of a time dependent geometry, we will have found a model that encodes the entropies in a way that ensures containment within the holographic entropy cone.

fixed order perturbation theory with the existence of reconstructable shadows. We begin by reviewing renormalization in quantum field theories phrased in a way to make the relationship clear.

Suppose one computes the amplitude of a process involving two widely separated mass scales $m$ and $E$ in fixed order perturbation theory. In terms of a renormalized coupling constant $g$, it is given generally in the form

$$\mathcal{M} = \sum_{n=0}^{\infty} c_n \left( \frac{g}{16\pi^2} \ln \frac{E}{m} \right)^n , \tag{4.43}$$

where $c_n$'s are of the same order. This implies that even if $g/16\pi^2$ is small, this perturbation theory breaks down when $\ln(E/m) \sim 16\pi^2/g$.

There is, however, a way to resum these logarithms—the renormalization group. Introducing the concept of running coupling constant, $g(\mu)$, defined at a sliding scale $\mu$, the amplitude of Eq. (4.43) can be written as

$$\mathcal{M} = \sum_{n=0}^{\infty} c_n \left( \frac{g(\mu)}{16\pi^2} \ln \frac{E}{\mu} \right)^n . \tag{4.44}$$

The process can now be calculated perturbatively as long as both $g(m)/16\pi^2$ and $g(E)/16\pi^2$ are small, where $g(m)$ and $g(E)$ are related by a continuous renormalization group evolution. In general, the range of validity of this renormalization group improved perturbation theory is larger than that of fixed order perturbation theory.

This phenomenon is analogous to the existence of shadows in the holographic reconstruction. If one tries to reconstruct the bulk in a "single shot" using HRRT surfaces anchored to the original leaf, then there can be regions in spacetime (shadows) that cannot be reconstructed. This, however, is not a fundamental limitation of the perturbative reconstruction of the bulk. As we have seen, we can reconstruct a portion of entanglement shadows by performing a reconstruction in multiple steps: first renormalizing the leaf and then using HRRT surfaces anchored to the renormalized leaf. By doing this renormalization with more steps, one can progressively probe deeper into shadow regions. Going to the continuum limit (the holographic slice), we find that we can describe physics in shadows without difficulty.

Even with the renormalization group improvement, the perturbative description of physics stops working when $g(\mu)$ hits a Landau pole or approaches a strongly coupled fixed point. This is analogous to the fact that the evolution of the holographic slice halts, $U(\lambda_1, \lambda_2) \propto \mathbb{1}$ in Eq. (4.40), once the renormalized leaf contracts to a point or approaches a horizon. Incidentally, this picture is consonant with the idea that describing the interior of a black hole would require "nonperturbative" physics.[9]

[9] In particular, an interior description may require changing the basis of multiple black hole microstates [143, 144], each of which can be viewed as having different background geometries corresponding to slightly different black hole masses [76, 78].

We stress that from the boundary point of view, renormalization of a leaf corresponds to coarse-graining of a state at a fixed time. A natural question is if there is an effective theory relating coarse-grained states at different times. We do not see a reason to doubt the existence of such a theory, at least for degrees of freedom sufficiently deep in the bulk. Since the coarse-graining depends on the state, however, the resulting description may well be applicable only within a given geometry, i.e. a selected semiclassical branch of the fundamental state in quantum gravity.

## Comparison to Holographic Renormalization in AdS/CFT

How is the holographic slice related to holographic renormalization in asymptotically AdS spacetimes? There has been extensive literature devoted to the latter subject. Here we will highlight the essential difference between our renormalization procedure and the perspective of Susskind and Witten [17].

If one kept $N^2$ (the number of field degrees of freedom) fixed per cutoff cell and applied the Susskind-Witten method of regularization deeper in the bulk, a local description of physics on the boundary would break down once $R \approx l_{\rm AdS}$. Here, $R$ and $l_{\rm AdS}$ are the radius of the cutoff surface and the AdS length scale, respectively. This is because the number of degrees of freedom within an $l_{\rm AdS}$-sized bulk region is of order $(l_{\rm AdS}/l_{\rm P})^{d-1}$, which is just $N^2$. Here, $l_{\rm P}$ is the Planck length in the bulk.

However, holography extends to sub-AdS scales, and the extremal surfaces anchored to a cutoff at $l_{\rm AdS}$ satisfy the appropriate properties to be interpreted as entanglement entropies [57, 56]. As emphasized throughout the text, the connection between entanglement and geometric quantities seems to extend beyond AdS/CFT [29, 27]. Because of this, we expect that there should be some way to renormalize the boundary state in such a way to preserve the HRRT prescription at all scales. This is, however, prohibited if we fix $N^2$ because already at an $l_{\rm AdS}$-sized region we lose the ability to talk about the entanglement of boundary subregions (as there is only one boundary cell).

Therefore, if one wants to preserve the ability to use the HRRT prescription, $N^2$ must change as the boundary is pulled in. Simply requiring that $N^2 \geq 1$ per cell will allow renormalization down to $l_{\rm P}$. This is easily seen by noticing that the number of cells for a boundary moved in to radius $R$ ($\leq l_{\rm AdS}$) is given by the total number of bulk degrees of freedom, $(R/l_{\rm P})^{d-1}$, divided by $N^2$. This implies that when $R = l_{\rm P}$ the number of cells is of order unity, and the holographic description must break down. In fact, the bulk description is expected to break down before this happens. Suppose that the gauge coupling, $g$, of the boundary theory stays constant. Then the requirement of a large 't Hooft coupling, $N^2 \geq 1/g^4 = (l_{\rm s}/l_{\rm P})^{d-1}$, implies that the bulk spacetime picture is invalidated when $R \lesssim l_{\rm s}$. Here, $l_{\rm s}$ is the string length. Assuming the existence of a renormalization scheme preserving the HRRT prescription implies that there exists a way to redistribute the original $N^2$ degrees of freedom spatially on a coarse-grained holographic space.

The construction of the holographic slice requires extremal surfaces to be anchored to renormalized leaves, so the renormalization procedure utilized must necessarily preserve the

ability to use the HRRT prescription. The holographic slice, therefore, must employ the special renormalization scheme described above.

## 4.7 Discussion

The holographic slice is defined using HRRT surfaces, and hence is inherently background dependent. This prohibits the use of the holographic slice as some way to analyze the coarse-grained behavior of complex quantum gravitational states with no clear bulk interpretation. In particular, if a state is given by a superposition of many different semiclassical geometries,

$$|\Psi\rangle = c_1|\psi_1\rangle + c_2|\psi_2\rangle + \cdots , \tag{4.45}$$

then the holographic slice prescription can be applied to each branch of the wavefunction, $|\psi_i\rangle$, independently. However, there is no well-defined slice for $|\Psi\rangle$. This is the same limitation one would face when considering the entanglement wedge of similar states. Despite this, for superpositions of states within the code subspace, the analyses of Refs. [32, 110] tell us the holographic slice construction is well defined.

Regardless, the holographic slice sheds light on the nature of bulk emergence. The construction of the slice harvests short range entanglement between small subregions, not in the form of entanglement entropy. It is precisely this that allows the slice to flow into the bulk and through entanglement shadows. This work emphasizes the idea that entanglement entropy as measured by von Neumann entropy is not sufficient to characterize the existence of a semiclassical bulk viewed from the boundary. Other measures of entanglement (negativity, entanglement of purification, etc.) may be more useful to analyze bulk emergence. This was explored extensively in Ref. [34].

The slice additionally provides a very natural interpretation for non-minimal extremal surfaces as the entanglement entropy for subregions of coarse-grained states. Because the coarse-graining procedure mixes up the boundary degrees of freedom while removing the short range information, the interpretation of non-minimal extremal surfaces in terms of purely UV boundary terms will necessarily be very complicated [85]. However, once coarse-graining occurs these complicated quantities manifest with a simple interpretation. This is also what is seen in the entanglement of purification calculations.

By assuming that the holographic states all live within the same infinite dimensional Hilbert space, $\mathcal{H}_{\text{UV}}$, we were able to discuss the mapping from a boundary state to a coarse-grained version of itself. This is what gave rise to the $K(\lambda)$ operator in Section 4.5. Alternatively, rather than use $\mathcal{H}_{\text{UV}}$ to discuss coarse-graining, one can use it to talk about time evolution in the boundary theory. One of the major hurdles in formulating theories for holographic screens is the fact that the area of the screens are non-constant. If one were to view this area as determining the size of the true Hilbert space the state lived in, then time evolution would require transitions between Hilbert spaces. However, by viewing the leaf area as a measure of the size of the effective subspace that the state lives in, we are free from this complication. In fact, modeling time evolution is similar to performing

the reverse of the coarse-graining operation. This introduces entanglement at shorter and shorter scales, which increases the effective subspace's size. Of course, time evolution must account for other complex dynamics, but simply increasing the screen area is no difficulty. This interpretation suggests that the area of holographic screens is a thermodynamic entropy measure, rather than a measure of the fundamental Hilbert space size.

Concluding, the holographic slice is a novel, covariantly defined geometric object. It encodes the bulk regions dual to successively coarse-grained states and we propose that the flow along the slice is governed by distillable correlations at the shortest scales. This may be related to the entanglement of purification of small regions or the modular evolution of such regions. Investigation of the explicit boundary flow along the slice seems to be the most promising avenue of future work. It may also be fruitful to study the mean curvature vector flow of codimension-2 convex surfaces in Lorentzian spacetimes, as characterizing solutions to this flow may provide insights into the coarse-graining operation.

# Part II

# Holographic Dictionary

# Chapter 5

# Comments on Holographic Entanglement Entropy in $TT$ Deformed CFTs

## 5.1 Introduction

Gauge-gravity duality, specifically AdS/CFT, is our best known example of a holographic description of quantum gravity [14]. The so-called GKPW dictionary [16, 15] relating bulk physics to boundary dynamics takes the form

$$Z_{\text{CFT}}[\gamma_{ij}] = e^{-I_{\text{bulk}}[g_{\mu\nu}]}, \tag{5.1}$$

where $\gamma_{ij}$ is the background metric of the space in which the boundary CFT lives, and $g_{\mu\nu}$ is the bulk metric. A particularly consequential holographic correspondence given by this duality is the Ryu-Takayanagi (RT) formula

$$S(A) = \min_{\partial\Gamma=\partial A}\left[\frac{\|\Gamma\|}{4G}\right], \tag{5.2}$$

which relates the entanglement entropy of a subregion $A$ of the boundary space to the area of the bulk extremal surface $\Gamma$ anchored to the entangling surface $\partial A$ [18, 19, 20]. Throughout, we will work to leading order in the bulk Newton's constant, $G$, and suppress all bulk fields aside from $g_{\mu\nu}$. Higher order effects are well understood in the context of AdS/CFT [21, 22].

Other holographic dualities with similar features have been proposed. In particular, the $TT$ deformation of 2-dimensional CFTs and its appropriate generalizations to higher dimensions have been argued to have holographic duals [145, 146, 147]. Of crucial importance to our discussion is that the proposed dictionary relating the boundary and bulk observables in these theories takes the same form as Eq. (5.1), except that now Dirichlet boundary conditions are imposed on a cutoff surface in the bulk.

The simple idea we would like to highlight is that Eq. (5.2) was derived in the context of AdS/CFT from Eq. (5.1) under rather tame assumptions [36]. The same argument, therefore, can be used to show that the RT formula holds for all dualities adopting dictionaries of the form of Eq. (5.1). This straightforward result is known in the community; however, careful consideration of it resolves subtleties involving counterterms when calculating entanglement entropy in $TT$ deformed theories.

We start by reviewing some aspects of entanglement entropy from a field theory perspective in Section 5.2. We then proceed to a calculation in the particular case of $TT$ deformed theories in Section 5.2. We discuss the general holographic argument for the RT formula in Section 5.3, which is followed by a sample calculation in cutoff AdS in Section 5.3. Along the way, we address some subtleties related to holographic renormalization. We conclude with a discussion about the consequences for holography in general spacetimes in Section 5.4.

Note that several calculations of entanglement entropy in $TT$ deformed theories have appeared recently [148, 149, 150, 151, 152, 153, 154]. Our goal is to emphasize the generality of the arguments leading to an agreement between boundary entanglement entropy and the RT formula and clarify some of the calculations performed in these works.

### Conventions

The background metric of the space in which the boundary field theory lives is denoted by $\gamma_{ij}$, while $h_{ij}$ refers to the bulk induced metric on the cutoff surface at $r = r_c$. These are related by $h_{ij} = r_c^2 \gamma_{ij}$.

## 5.2 Field Theory Calculation

### Preliminaries

Consider a $D$-dimensional CFT with action $I[\phi] = \int d^D x \sqrt{\gamma}\, \mathcal{L}[\phi]$. One can prepare a density matrix $\rho$ on a spatial slice $\Sigma$ using an appropriate Euclidean path integral. In order to compute the entanglement entropy $S(A)$ of a subregion $A$ of $\Sigma$, one can use the replica trick as follows:

$$\begin{aligned} S(A) &= \lim_{n\to 1} \frac{\log\left(Z^{(b)}\left[M_n\right]\right) - n \log\left(Z^{(b)}\left[M_1\right]\right)}{1-n} \\ &= \left(1 - n\frac{d}{dn}\right) \log\left(Z^{(b)}[M_n]\right)\Big|_{n\to 1}, \end{aligned} \tag{5.3}$$

where

$$Z^{(b)}[M] = \int D\phi\, \exp\left(-\int_M d^D x \sqrt{\gamma}\, \mathcal{L}[\phi]\right) \tag{5.4}$$

is the "bare" partition function computed by the path integral on a given manifold $M$. $M_1$ is the manifold used to compute $\mathrm{Tr}\,\rho$, while $M_n$ is an $n$-sheeted version of $M_1$ which is a

branched cover with a conical excess of angle $\Delta\phi = 2\pi(n-1)$ localized at the $(D-2)$-dimensional submanifold $\partial A$.

The bare partition function $Z^{(b)}[M]$ typically diverges and takes the form

$$\log\left(Z^{(b)}[M]\right) = c_1(\Lambda a)^D + c_2(\Lambda a)^{D-2} + \ldots, \tag{5.5}$$

where $\Lambda$ is a UV cutoff and $a$ is the length scale associated with the manifold $M$ [155]. What are the contributions of these divergences to entanglement entropy? These divergence can be expressed as local integrals of background quantities [156, 157, 158]. (In even dimensions, there is a logarithmic divergence which cannot be expressed in this manner.) This implies that their contributions cancel in Eq. (5.4) everywhere away from $\partial A$, since $M_n$ and $n$ copies of $M_1$ are identical manifolds except at $\partial A$. However, $M_n$ has extra divergent contributions coming from curvature invariants localized at $\partial A$. This leads to

$$S(A) = \sum_{k=1}^{\lfloor D/2\rfloor} a_k \Lambda^{D-2k} \int_{\partial A} d^{D-2}x\sqrt{H}\left[\mathcal{R}, \mathcal{K}^2\right]^{k-1}, \tag{5.6}$$

where $[\mathcal{R}, \mathcal{K}^2]^{k-1}$ represents all possible scalar intrinsic and extrinsic curvature invariants of $\partial A$ of mass dimension $2k-2$, with their coefficients collectively written as $a_k$, and $H_{ab}$ is the intrinsic metric of $\partial A$. Here, we have suppressed possible finite terms to focus on the leading divergences. This is the famous "area law" associated with entanglement entropy, which comes from the short distance correlations between $A$ and $\bar{A}$.

Since the above behavior is sensitive to the cutoff, one often considers a renormalized version of entropy. In particular, the divergences in Eq. (5.5) can be subtracted (except for logarithmic ones) by introducing a counterterm action $I_{\rm ct}$ which involves local integrals of curvature invariants:

$$I_{\rm ct} = \sum_{k=1}^{\lfloor D/2\rfloor+1} b_k \Lambda^{D-2k+2} \int_M d^D x\sqrt{\gamma}\,\mathcal{R}^{k-1}. \tag{5.7}$$

Here, $\mathcal{R}^{k-1}$ represents all possible scalar curvature invariants of $M$ that one can write down at mass dimension $2k-2$, and their coefficients $b_k$ can be tuned exactly to cancel the divergences. The renormalized entropy is then given by

$$S_{\rm ren}(A) = \lim_{n\to 1} \frac{\log\left(Z_{\rm ren}[M_n]\right) - n\log\left(Z_{\rm ren}[M_1]\right)}{1-n}, \tag{5.8}$$

where $Z_{\rm ren}$ is the renormalized partition function which is computed using the action with the counterterms in Eq. (5.7). This renormalized entropy is universal, i.e. UV regulator independent in the continuum limit, and has been discussed previously in the literature [158]. A closely related version of renormalized entropy was discussed in Ref. [157]. These two are not identical, but they both extract the appropriate universal behavior in the CFT limit by subtracting the power divergences.

## Entanglement Entropy in $TT$ Deformed Theories

We now specialize to the case of a $D$-dimensional CFT deformed by a particular composite operator $X_D$ of the stress tensor [147]. The presence of this deforming irrelevant operator breaks conformal invariance and gives rise to a QFT that is conjectured to be holographically dual to AdS with a finite cutoff radius, where Dirichlet boundary conditions are imposed.

We will focus on computing the partition function of this $TT$ deformed theory on the manifold $S^D$ of radius $R$:

$$\gamma_{ij} = R^2 d\Omega_D^2. \tag{5.9}$$

The theory is defined by the flow equation dictated by $X_D$, and using this we obtain

$$\langle T_i^i \rangle = -D\lambda \langle X_D \rangle, \tag{5.10}$$

where $\lambda$ is the deformation parameter. $T_{ij}$ is the renormalized stress tensor, whose trace vanishes up to conformal anomalies in the CFT limit $\lambda \to 0$. The bare stress tensor $T_{ij}^{(b)}$ is related to the renormalized one[1] as

$$\langle T_{ij}^{(b)} \rangle = \langle T_{ij} \rangle - C_{ij}, \tag{5.11}$$

where $C_{ij}$ represent various terms involving the background metric $\gamma_{ij}$ that arise from variation of the counterterm action, which in the CFT limit is given by Eq. (5.7). For finite $\lambda$, the cutoff of the theory is provided by the deformation itself, so that $\Lambda$ is replaced by—or identified with—$\lambda^{-1/D}$ in Eqs. (5.5 – 5.7).

Since $S^D$ is a maximally symmetric space, the one point function of the stress tensor takes the form

$$\langle T_{ij} \rangle = \omega_D(R)\ \gamma_{ij}, \tag{5.12}$$

$$\langle T_{ij}^{(b)} \rangle = \omega_D^{(b)}(R)\ \gamma_{ij}. \tag{5.13}$$

Using the flow equation, one can solve for $\omega_D(R)$ and $\omega_D^{(b)}(R)$ as has been done in Ref. [153], yielding

$$\begin{aligned} \omega_D(R) = &- \frac{D-1}{2D\lambda}\sqrt{1+\frac{L_D^2}{R^2}} + \frac{D-1}{2D\lambda} \\ &+ \sum_{k=1}^{\lfloor (D-1)/2 \rfloor} \frac{f_{k,D}}{\lambda}\left(\frac{L_D}{R}\right)^{2k}, \end{aligned} \tag{5.14}$$

$$\omega_D^{(b)}(R) = - \frac{D-1}{2D\lambda}\sqrt{1+\frac{L_D^2}{R^2}}, \tag{5.15}$$

[1]The bare stress tensor is related to the Brown-York stress tensor [159], while the renormalized stress tensor is related to the Balasubramanian-Kraus stress tensor [160] by a factor of $r_c^{d-2}$.

where $L_D^2 = 2D(D-2)\alpha_D \lambda^{2/D}$ with $\alpha_D$ being quantities related to the central charges of the field theory, and $f_{k,D}$ are dimension dependent constants. (Note that $\alpha_D \propto 1/(D-2)$, so that $L_2 \neq 0$.) We stress that while $\omega_D(R)$ has been represented schematically, the expression for $\omega_D^{(b)}(R)$ is exact. The explicit expressions for $\omega_D(R)$ can be found in Ref. [153].

Now using these results, we can compute the bare partition function as

$$\frac{d}{dR}\log Z_{S^D}^{(b)} = -\frac{1}{R}\int_{S^D} d^D x\sqrt{\gamma}\,\langle T_i^{i(b)}\rangle, \tag{5.16}$$

obtaining

$$\begin{aligned}\log Z_{S^D}^{(b)} &= -D\Omega_D \int_0^R dR\;\omega_D^{(b)}(R)\,R^{D-1} \\ &= \frac{\Omega_D L_D R^{D-1}}{2\lambda}\,{}_2F_1\left[-\frac{1}{2},\frac{D-1}{2};\frac{D+1}{2};-\frac{R^2}{L_D^2}\right],\end{aligned} \tag{5.17}$$

where $\Omega_D$ is the volume of a unit $S^D$. The entanglement entropy of a subregion $A$ which is a hemisphere of the spatial $S^{D-1}$ can then be computed by a simple trick described in Ref. [149]:

$$\begin{aligned}S(A) &= \left(1 - n\frac{d}{dn}\right)\log\left(Z^{(b)}[S_n^D]\right)\Big|_{n\to 1} \\ &= \left(1 - \frac{R}{D}\frac{d}{dR}\right)\log Z_{S^D}^{(b)}.\end{aligned} \tag{5.18}$$

This gives us the answer

$$S(A) = \frac{\pi\Omega_{D-2}L_D R^{D-1}}{D(D-1)\lambda}\,{}_2F_1\left[\frac{1}{2},\frac{D-1}{2};\frac{D+1}{2};-\frac{R^2}{L_D^2}\right]. \tag{5.19}$$

We can also compute the renormalized entanglement entropy in multiple different ways, e.g. using Eq. (5.8), which results in a universal answer in the CFT limit [158]. Alternately, one can use the version employed in Ref. [157]. For finite $\lambda$ these two versions give different answers, which explains the discrepancy in Ref. [154] between the field theory calculation and the renormalized entropy.

We, however, emphasize that the $TT$ deformation provides a particular physical regulator for the entropy, so one need not focus their attention on the renormalized entropy. This regularization has a simple interpretation in field theory, which also has a geometric bulk interpretation. Specifically, on the field theory side one only includes the energy levels below the shock singularity, above which the energies take complex values. The existence of this regularization naturally leads us to consider the bare entanglement entropy in Eq. (5.19), which captures all the information about correlations between $A$ and $\bar{A}$.

## 5.3 Bulk Calculation

### Holographic Duality

Using the holographic dictionary in Eq. (5.1), the entanglement entropy $S(A)$ of a boundary subregion $A$ can be calculated as

$$S(A) = \lim_{n\to 1} \frac{I_{\text{bulk}}[B_n] - nI_{\text{bulk}}[B_1]}{n-1}, \tag{5.20}$$

where $B_n$ and $B_1$ are the saddle point bulk solutions dual to the boundary conditions dictated by the field theory path integral on $M_n$ and $M_1$, respectively [36]. Notably, the action $I_{\text{bulk}}$ dual to the bare partition function is the usual Einstein-Hilbert action supplemented by the Gibbons-Hawking-York boundary term. Assuming that the solution $B_n$ preserves the $\mathbb{Z}_n$ symmetry of the boundary, Ref. [36] showed that the contribution to the above expression is localized to the extremal surface $\Gamma$, resulting in the RT formula

$$S(A) = \min_{\partial\Gamma=\partial A} \left[\frac{\|\Gamma\|}{4G}\right]. \tag{5.21}$$

Our simple observation is that this proof carries through unmodified as long as one is computing the bare partition function. The $TT$ theory must then obey the RT formula by construction.

Counterterms added to the boundary action are well understood to correspond to boundary terms added to the bulk action [160, 161]. Per the discussion in Section 5.2, these terms give rise to extra contributions to $S(A)$ localized to the entangling surface $\partial A$. The saddle point solutions are not modified by the inclusion of these terms, which are pure functionals of the induced metric $h_{ij}$. This implies that the renormalized entropy can be calculated holographically as

$$S_{\text{ren}}(A) = \min_{\partial\Gamma=\partial A} \left[\frac{\|\Gamma\|}{4G}\right] + \tilde{S}(\partial A), \tag{5.22}$$

where the form of $\tilde{S}(\partial A)$ is discussed in Ref. [158].

### RT Formula in Cutoff AdS

As a simple check, we now compare the result of the RT formula to the entanglement entropy obtained in Section 5.2. On the bulk side, we need to compute the minimal surface $\Gamma$ anchored to the entangling surface $\partial A$ on the cutoff surface at $r = r_c$, on which the induced metric is given by

$$h_{ij} = r_c^2 R^2 d\Omega_D^2 \equiv r_0^2 d\Omega_D^2. \tag{5.23}$$

This calculation was performed in Ref. [154] and the answer obtained is

$$S(A) = \frac{r_0^{D-1}\Omega_{D-2}}{4G(D-1)}\,{}_2F_1\left[\frac{1}{2}, \frac{D-1}{2}; \frac{D+1}{2}; -\frac{r_0^2}{l^2}\right], \tag{5.24}$$

where $l$ is the AdS radius. By using the holographic identifications

$$\lambda = \frac{4\pi G l}{D r_c^D}, \tag{5.25}$$

$$l^2 = 2D(D-2)\alpha_D \lambda^{2/D} r_c^2 = L_D^2 r_c^2, \tag{5.26}$$

we find that this is identical to Eq. (5.19).

## 5.4 Discussion

### Holographic Dictionary

As emphasized throughout, if there exists a holographic duality between Einstein gravity in the bulk and a quantum field theory on the boundary such that the two are related by Eq. (5.1), then the RT formula will hold. This is true independent of the details of the bulk spacetime and the boundary field theory. Indeed, we have shown that the $TT$ deformed CFT provides an explicit example of the validity of the Lewkowycz-Maldacena (LM) proof beyond AdS/CFT at the conformal boundary.[2] In fact, all the results based only on this dictionary element will hold in any such duality, at least in a perturbative expansion in $G$. Two salient examples include the prescription for calculating refined Rényi entropies presented in Ref. [163] and generalizations of the RT formula in higher curvature gravity [164]. Though the robustness of the LM proof is far from unknown, we hope that highlighting this feature helps solidify the relationship between entanglement entropy and geometry in general spacetimes.

### Holographic Renormalization and Counterterms

In CFT calculations, one often considers only renormalized quantities because these are universally well-defined and survive the continuum limit. However, entanglement entropy is not one of these quantities. Nevertheless, since the $TT$ operator implements a particular physical cutoff which has a simple geometric dual, it is sensible to consider bare quantities. In particular, $TT$ deformations with different background geometries would implement different regularizations, leading to different entanglement entropies. On the bulk side, this manifests as different choices of the cutoff surface. This provides a better understanding of the UV-IR correspondence.

[2] An important assumption is the $\mathbb{Z}_n$ symmetry in the bulk. It is plausible that the argument holds after relaxing this assumption; See, e.g., Ref. [162].

The handling of counterterms is the only additional subtlety encountered when calculating entanglement entropy in $TT$ deformed CFTs. For finite deformations, all quantities are automatically regulated and hence the previous distinction between finite and divergent terms becomes muddled. We aimed to clarify the conceptual aspects of these terms and how they are related with the holographic result.

The fundamental idea is that the dictionary relation

$$Z_{\rm CFT}[\gamma_{ij}] = e^{-I_{\rm bulk}[g_{\mu\nu}]} \tag{5.27}$$

is precisely between the *bare* CFT on the boundary and Einstein-Hilbert gravity (plus the necessary Gibbons-Hawking-York term) in the bulk, both of which have divergent partition functions. This is the arena in which the RT formula was shown to hold. If one now chooses to introduce specific counterterms to renormalize the CFT stress tensor, then this will correspondingly alter the gravity side of the dictionary (specifically by adding terms localized to the boundary of the bulk). In particular, the addition of counterterms will alter the RT prescription to include terms beyond the standard area piece. This addition manifests as integrals of local geometric invariants at the entangling surface. In the CFT limit these are used to cancel power divergences, but with finite deformations one need not add a counterterm. Indeed, calculations including counterterms [149, 154] would necessarily miss the area law piece for $D > 2$, which is finite for finite deformations.

## Holography in General Spacetimes

The explicit verification of the RT formula beyond AdS/CFT at the conformal boundary of AdS provides a strong footing for the surface-state correspondence [57] and related constructions to understand holography in general spacetimes via entanglement entropy [56, 31, 32, 34, 35]. In previous work, the RT formula was used as an assumption to investigate properties of a hypothetical boundary theory and self consistency checks provided confidence in that assumption. Now, the evidence that a duality in the form of Eq. (5.1) exists beyond basic AdS/CFT, and the RT formula along with it, suggests that a duality may indeed exist for general spacetimes and bolsters our confidence in previous work.

The results of $TT$ deformations provide a particularly promising avenue to investigate flat space holography, since they hold down to scales below the AdS radius $l$. This contrasts with the conventional UV-IR correspondence, which would result in a single matrix-like theory describing an AdS volume [17]. It suggests that there is a way to redistribute degrees of freedom on the boundary theory in a way that maintains local factorization, and the $TT$ deformation implements this. This is explicitly seen in the calculation of entanglement entropy in the fact that it does not face an obstruction when a volume law scaling is reached at $r_0 \approx l$. Volume law scaling of entanglement entropy suggests that the boundary theory for asymptotically flat space is non-local, as is expected from the $TT$ deformation. Corresponding behavior is seen in cosmological spacetimes [34], and investigating properties of highly deformed CFTs may shed light on these theories. Since the $TT$ operator naturally imple-

ments some sort of coarse graining, it would be interesting to relate this to the geometric coarse graining procedure developed in Ref. [35].

# Chapter 6

# Holographic Renyi Entropy from Quantum Error Correction

## 6.1 Introduction

While the quantum error-correction interpretation of AdS/CFT was discovered by trying to resolve certain paradoxes [26], it has exceeded its original purpose. Among other things, it has led to proofs of entanglement wedge reconstruction [24, 116] and a better understanding of the black hole interior [25, 165].

One remarkable result was an appreciation of the Ryu-Takayanagi (RT) formula [18, 19, 20] as a property of the code [27]. The RT formula computes the von Neumann entropy $S(\rho_A) \equiv -\mathrm{tr}\rho_A \log \rho_A$ of a subregion $A$ of a holographic CFT via the area $\mathcal{A}$ of an extremal surface in the AdS dual:

$$S(\rho) = \frac{\mathcal{A}}{4G_N} + S_{\text{bulk}} \tag{6.1}$$

where $S_{\text{bulk}}$ is the entropy of the matter in the bulk subregion dual to $A$ [21]. While the area term is in general $\mathcal{O}(1/G_N)$, $S_{\text{bulk}}$ is in general $\mathcal{O}(1)$ and is the quantum (or "FLM") correction to RT [21].

The RT formula naturally appears when one computes the von Neumann entropy of an encoded state in a quantum error-correcting code. We demonstrate this now in the context of the type of code we will be using throughout: an operator-algebra quantum error-correcting (OQEC) code with complementary recovery. These appear to be the best codes to model AdS/CFT [27], and we will explain their details in Section 6.2. For now, it suffices to say that we consider a finite-dimensional Hilbert space $\mathcal{H} = \mathcal{H}_A \otimes \mathcal{H}_{\bar{A}}$, and a Hilbert space $\mathcal{H}_{\text{code}} \subseteq \mathcal{H}$. Furthermore, these Hilbert spaces have the following decompositions

$$\mathcal{H}_A = \oplus_\alpha (\mathcal{H}_{A_1^\alpha} \otimes \mathcal{H}_{A_2^\alpha}) \oplus \mathcal{H}_{A_3} \ , \tag{6.2}$$

$$\mathcal{H}_{\text{code}} = \oplus_\alpha (\mathcal{H}_{a_\alpha} \otimes \mathcal{H}_{\bar{a}_\alpha}) \ , \tag{6.3}$$

with $\dim \mathcal{H}_{A_1^\alpha} = \dim \mathcal{H}_{a_\alpha}$. In these codes, a "logical" density matrix $\rho$ acting on $\mathcal{H}_{\text{code}}$ is encoded in a "physical" density matrix acting on $\mathcal{H}$. Moreover, we say that $A$ encodes $a$ if there exists a unitary operation $U_A$ on $\mathcal{H}_A$ such that

$$\widetilde{\rho}_A = U_A \left(\oplus_\alpha (p_\alpha \rho_\alpha \otimes \chi_\alpha)\right) U_A^\dagger \ , \tag{6.4}$$

and the density matrices $\rho_\alpha$ act on $\mathcal{H}_{A_1^\alpha}$ and correspond to the state $\rho_{a_\alpha}$ that we wished to encode in $\widetilde{\rho}_A$. I.e. $\rho_\alpha$ acts on $\mathcal{H}_{A_1^\alpha}$ in the same way that $\rho_{a_\alpha}$ does on $\mathcal{H}_{a_\alpha}$. The density matrices $\chi_\alpha$ act on $\mathcal{H}_{A_2^\alpha}$ and correspond to the extra degrees of freedom that help encode. The von Neumann entropy is

$$S(\widetilde{\rho}_A) = \text{tr}\left(\widetilde{\rho}_A \mathcal{L}_A\right) - \sum_\alpha p_\alpha \log p_\alpha + \sum_\alpha p_\alpha S(\rho_\alpha) \tag{6.5}$$

where the "area operator" is defined as

$$\mathcal{L}_A \equiv \oplus_\alpha S(\chi_\alpha) \mathbb{1}_{a_\alpha \bar{a}_\alpha} \ . \tag{6.6}$$

Compare this to Eq. (6.1). The first term on the RHS of both are the expectation value of linear operators evaluated in the state of interest. The other terms are naturally the algebraic von Neumann entropy of the logical state [27]. This is the basic connection between RT and quantum error-correcting codes.

In AdS/CFT, there is a natural generalization of the RT formula that we now describe. The von Neumann entropy $S(\rho)$ has a well-known generalization called the Renyi entropies, $S_n(\rho) \equiv \frac{1}{1-n} \log \text{tr} \rho^n$. While the Renyi entropy equals the von Neumann entropy for $n = 1$, it is widely believed that the Renyi entropy does not satisfy anything qualitatively similar to the RT formula for $n \neq 1$ [163, 110]. However, a related quantity called the refined Renyi entropy

$$\widetilde{S}_n(\rho) \equiv n^2 \partial_n \left( \frac{n-1}{n} S_n(\rho) \right) \tag{6.7}$$

also reduces to the von Neumann entropy for $n = 1$ but in fact does satisfy a generalized version of the RT formula [163]. One computes $\widetilde{S}_n(\rho_A)$ holographically via the so-called "cosmic brane prescription," which works roughly as follows. Into the state $\rho_A$, insert an extremal codimension-2 cosmic brane in AdS homologous to the boundary region $A$, and let this brane have tension $T_n = \frac{n-1}{4nG_N}$. The refined Renyi entropy is related to the area of this brane:

$$\widetilde{S}_n(\rho_A) = \frac{\mathcal{A}_{\text{brane}}}{4G_N} + \widetilde{S}_{n,\text{bulk}} \ , \tag{6.8}$$

where $\widetilde{S}_{n,\text{bulk}}$ is the refined Renyi entropy of matter fields in the bulk region dual to $A$. We describe this prescription in detail in Section 6.4. As one might expect, the cosmic brane

prescription limits to the RT formula as $n \to 1$, because in that limit the tension vanishes and the cosmic brane reduces to an extremal surface.

Because the cosmic brane prescription generalizes RT, it behooves us to investigate whether the connection between RT and quantum error-correcting codes can be generalized to the cosmic brane prescription. Let us formulate this question more precisely. Does the refined Renyi entropy of $\widetilde{\rho}_A$ from Eq. (6.4) satisfy some formula like

$$\widetilde{S}_n(\widetilde{\rho}_A) \stackrel{?}{=} \mathrm{tr}(\widetilde{\rho}_{\mathrm{brane},A}\mathcal{L}_A) + \widetilde{S}_{n,\mathrm{logical}} \ , \tag{6.9}$$

for some state $\widetilde{\rho}_{\mathrm{brane},A}$, where $\widetilde{S}_{n,\mathrm{logical}}$ represents the refined Renyi entropy of the logical state? If $\widetilde{\rho}_A$ indeed satisfies such a formula, what determines the state $\widetilde{\rho}_{\mathrm{brane},A}$, and why does this state manifest in AdS/CFT as inserting a brane with a particular tension into $\widetilde{\rho}_A$?

Our main result is to answer these questions. In short, yes: one can derive the cosmic brane prescription within the formalism of OQEC, and we do this in Section 6.4. Notably, this derivation requires that the AdS/CFT code has certain special properties, which we now explain by discussing refined Renyi entropy in general OQEC codes.

For a general OQEC code, the refined Renyi entropy of $\widetilde{\rho}_A$ from Eq. (6.4) is

$$\widetilde{S}_n(\widetilde{\rho}_A) = \sum_\alpha p_\alpha^{(n)} \widetilde{S}_n(\chi_\alpha) + \widetilde{S}_{n,\mathrm{logical}} \ , \tag{6.10}$$

where

$$p_\alpha^{(n)} = \mathrm{tr}\left(P_\alpha \frac{\widetilde{\rho}_A^n}{\mathrm{tr}(\widetilde{\rho}_A^n)}\right) \tag{6.11}$$

and $P_\alpha = \sum_i |\alpha, i\rangle\langle\alpha, i|$ is a projector onto a particular value of $\alpha$. While this equation bears some resemblance to Eq. (6.9), they do not match in general.

Indeed, there are two aspects of the code that need to be true for Eq. (6.9) to hold. First, it must be the case that

$$\sum_\alpha p_\alpha^{(n)} \widetilde{S}_n(\chi_\alpha) = \mathrm{tr}\left(\widetilde{\rho}_A^{(n)} \mathcal{L}_A\right) \tag{6.12}$$

for some state $\widetilde{\rho}_A^{(n)}$ in the code subspace. We show that this is true if and only if $\chi_\alpha$ is maximally mixed. Second, when interpreted in the context of the AdS/CFT code, $\widetilde{\rho}_A^{(n)}$ needs to manifest as the state $\widetilde{\rho}_A$ with an inserted cosmic brane of exactly the right tension. One of our primary focuses is to demonstrate that CFT states with geometric duals indeed admit such an interpretation, as long as $\chi_\alpha$ is maximally mixed. Formulating this argument requires that we carefully interpret Eq. (6.4) in gravity. For example, we must understand that each $\alpha$-block corresponds to a particular geometry so that we can interpret some $\alpha$-blocks as geometries with cosmic branes. We must also understand that CFT states with geometric duals have non-vanishing support $p_\alpha$ on $\alpha$-blocks corresponding to many different classical geometries. This way, $\widetilde{\rho}_A^{(n)}$ can have its support predominantly on a different classical

geometry than $\widetilde{\rho}_A$ does. We provide these interpretations in Section 6.3, and we explicitly show how they manifest as a cosmic brane prescription within quantum error-correction in Section 6.4.

Also in Section 6.4, we emphasize the fact that a maximally-mixed $\chi_\alpha$ for each $\alpha$ implies both properties needed for a code to match the cosmic brane prescription. This leads us to conclude that $\chi_\alpha$ is maximally-mixed in AdS/CFT. This has a number of interesting implications, such as an improved definition of the area operator

$$\mathcal{L}_A = \oplus_\alpha \log \dim(\chi_\alpha) \mathbb{1}_{a_\alpha \bar{a}_\alpha} \ . \tag{6.13}$$

In Section 6.5, we discuss the implications of these results for tensor network models of AdS/CFT. While tensor networks tend to nicely satisfy the RT formula [72, 28, 29], historically they have struggled to have a non-flat spectrum of Renyi entropies. Our results suggest that there is a natural way to construct a holographic tensor network that not only has the correct Renyi entropy spectrum, but also computes the Renyi entropies via a method qualitatively similar to the cosmic brane prescription.

Finally, in Section 6.6 we conclude with a discussion of implications, future directions and related work. Note that this paper was released jointly with [166] where similar ideas are discussed.

## 6.2 Operator-algebra Quantum Error Correction

We start by reviewing the framework of operator-algebra quantum error correction (OQEC) as discussed in [27]. Consider a finite dimensional "physical" Hilbert space $\mathcal{H} = \mathcal{H}_A \otimes \mathcal{H}_{\bar{A}}$ and a "logical" code subspace $\mathcal{H}_{\text{code}} \subseteq \mathcal{H}$.[1] In the context of holography, one can think of $\mathcal{H}$ as the boundary Hilbert space and $\mathcal{H}_{\text{code}}$ as the Hilbert space of the bulk effective field theory (EFT).

Let $\mathcal{L}(\mathcal{H}_{\text{code}})$ be the algebra of all operators acting on $\mathcal{H}_{\text{code}}$ and $M \subseteq \mathcal{L}(\mathcal{H}_{\text{code}})$ be a subalgebra. In particular, we require that $M$ be a von Neumann algebra, i.e. it is closed under addition, multiplication, hermitian conjugation and contains all scalar multiples of the identity operator.

Any von Neumann algebra has an associated decomposition of the Hilbert space given by

$$\mathcal{H}_{\text{code}} = \oplus_\alpha \left( \mathcal{H}_{a_\alpha} \otimes \mathcal{H}_{\bar{a}_\alpha} \right) \ , \tag{6.14}$$

such that the operators in the von Neumann algebra are the set of $\alpha$ block diagonal operators that only act non-trivially on the $\mathcal{H}_{a_\alpha}$ factor within each block. Namely, they are of the form

$$\widetilde{O}_M = \oplus_\alpha \left( \widetilde{O}_{a_\alpha} \otimes \mathbb{1}_{\bar{a}_\alpha} \right) \ , \tag{6.15}$$

[1] More generally the physical Hilbert space need not factorize, e.g. if the boundary theory has gauge constraints. We expect the qualitative features of our result to be unchanged in that case.

where from now onward, we use the "tilde" to denote objects that naturally act on the code subspace.[2] The commutant of $M$, denoted $M'$, is defined by the set of operators that commute with all the operators in $M$. The operators in $M'$ are then similarly of the form

$$\widetilde{O}_{M'} = \oplus_\alpha \left( \mathbb{1}_{a_\alpha} \otimes \widetilde{O}_{\bar{a}_\alpha} \right) \ . \tag{6.16}$$

The center $Z_M$ consists of operators that belong to both $M$ and $M'$ take the form

$$\widetilde{O}_{M'} = \oplus_\alpha \left( \lambda_\alpha \mathbb{1}_{a_\alpha} \otimes \mathbb{1}_{\bar{a}_\alpha} \right) \ , \tag{6.17}$$

where $\lambda_\alpha$ could in general be different for each $\alpha$ block.

The OQEC code is then defined by requiring that for any state in the code subspace, the operators in the von Neumann algebra $M$ are robust against erasure of the subfactor $\mathcal{H}_{\bar{A}}$ of the physical Hilbert space. Equivalently, we require that all the operators in $M$ can be represented as physical operators acting non-trivially only on $\mathcal{H}_A$. In addition, by taking inspiration from AdS/CFT, we restrict to OQEC codes with complementary recovery, i.e. where operators in $M'$ are robust against erasure of $A$. Thus, we require that for all $|\widetilde{\psi}\rangle \in \mathcal{H}_{\text{code}}$, $\widetilde{O}_M \in M$ and $\widetilde{O}_{M'} \in M'$, there exists $O_A \in \mathcal{L}(\mathcal{H}_A)$ and $O_{\bar{A}} \in \mathcal{L}(\mathcal{H}_{\bar{A}})$ such that

$$\widetilde{O}_M |\widetilde{\psi}\rangle = O_A |\widetilde{\psi}\rangle \tag{6.18}$$

$$\widetilde{O}_M^\dagger |\widetilde{\psi}\rangle = O_A^\dagger |\widetilde{\psi}\rangle \tag{6.19}$$

$$\widetilde{O}_{M'} |\widetilde{\psi}\rangle = O_{\bar{A}} |\widetilde{\psi}\rangle \tag{6.20}$$

$$\widetilde{O}_{M'}^\dagger |\widetilde{\psi}\rangle = O_{\bar{A}}^\dagger |\widetilde{\psi}\rangle \tag{6.21}$$

Let us pause for a moment to make connections with holography. Suppose $A$ is a boundary subregion and $\gamma(A)$ is the bulk codimension 2 extremal surface of minimal area anchored to $\partial A$, i.e. the RT surface of $A$.[20, 60]. The entanglement wedge $\text{EW}(A)$ is defined as the bulk domain of dependence of any bulk spacelike surface $\Sigma$ such that $\partial\Sigma = A \cup \gamma(A)$ [128, 61, 167]. Given a pure boundary state, $\gamma(A) = \gamma(\bar{A})$ and thus, $\text{EW}(A) \cup \text{EW}(\bar{A})$ includes a complete Cauchy slice in the bulk.[3] Interpreting $M$ and $M'$ as the algebra of operators in $\text{EW}(A)$ and $\text{EW}(\bar{A})$ respectively, it is clear that Eq. (6.18) is the statement of entanglement wedge reconstruction [24, 115]. In holography, the surface $\gamma(A)$ is fixed irrespective of the state of bulk quantum fields at leading order in $G_N$. In fact even at first subleading order in $G_N$, one could calculate $S(A)$ by keeping $\gamma(A)$ fixed and including bulk entropy corrections at $\mathcal{O}(1)$ [21]. At higher orders in $G_N$, one has to take into account the quantum extremal surface prescription for $\gamma(A)$ wherein the surface can move depending on the bulk state [22, 168]. In general there would be a "no man's land" region in the bulk that cannot be reconstructed state-independently by either $A$ or $\bar{A}$. Thus, the OQEC code with complementary recovery

[2]The only exception to this is the notation for the refined Renyi entropy $\widetilde{S}_n$.

[3]If the boundary state is mixed, e.g. a thermal state, one could purify it, e.g. to a thermofield double [69].

only works as a toy model of holography when computing entanglement entropy to $\mathcal{O}(1)$ and hence, all our results hold only to this order.

As shown in [27], one can equivalently find unitaries $U_A$ and $U_{\bar{A}}$ such that

$$|\widetilde{\alpha, i\, j}\rangle = U_A\, U_{\bar{A}} \left( |\alpha, i\rangle_{A_1^\alpha} |\alpha, j\rangle_{\bar{A}_1^\alpha} |\chi_\alpha\rangle_{A_2^\alpha\, \bar{A}_2^\alpha} \right) \ , \tag{6.22}$$

where $|\widetilde{\alpha, i\, j}\rangle \equiv |\widetilde{\alpha, i}\rangle \otimes |\widetilde{\alpha, j}\rangle$ is a complete orthonormal basis for the code subspace. Here, the Hilbert space $\mathcal{H}_A$ has been decomposed as $\mathcal{H}_A = \oplus_\alpha \left( \mathcal{H}_{A_1^\alpha} \otimes \mathcal{H}_{A_2^\alpha} \right) \oplus \mathcal{H}_{A_3^\alpha}$ where $\dim(\mathcal{H}_{A_1^\alpha}) = \dim(\mathcal{H}_{a_\alpha})$. A similar decomposition has been applied to $\mathcal{H}_{\bar{A}}$.

This allows us to write a general density matrix $\widetilde{\rho}$ in the code subspace as

$$\widetilde{\rho} = U_A\, U_{\bar{A}} \left( \oplus_\alpha\, p_\alpha\, \rho_{A_1^\alpha \bar{A}_1^\alpha} \otimes |\chi_\alpha\rangle\langle\chi_\alpha|_{A_2^\alpha \bar{A}_2^\alpha} \right) U_{\bar{A}}^\dagger\, U_A^\dagger \ , \tag{6.23}$$

where we choose the normalizations such that $\mathrm{tr}_{A\bar{A}}(\widetilde{\rho}) = \mathrm{tr}_{A_1^\alpha \bar{A}_1^\alpha}(\rho_{A_1^\alpha \bar{A}_1^\alpha}) = \sum_\alpha p_\alpha = 1$. Restricting to subregion $A$, we obtain

$$\widetilde{\rho}_A = U_A \left( \oplus_\alpha\, p_\alpha\, \rho_\alpha \otimes \chi_\alpha \right) U_A^\dagger \ , \tag{6.24}$$

where we have relaxed the notation by using $\rho_\alpha = \mathrm{tr}_{\bar{A}_1^\alpha} \left( \rho_{A_1^\alpha \bar{A}_1^\alpha} \right)$ and $\chi_\alpha = \mathrm{tr}_{\bar{A}_2^\alpha} \left( |\chi_\alpha\rangle\langle\chi_\alpha|_{A_2^\alpha \bar{A}_2^\alpha} \right)$.

Using this it is straightforward to compute the von Neumann entropy of $\widetilde{\rho}_A$ and show that it satisfies a Ryu-Takayanagi formula, i.e.

$$S(\widetilde{\rho}_A) = \mathrm{tr}(\widetilde{\rho}\, \mathcal{L}_A) + S(\widetilde{\rho}, M) \ , \tag{6.25}$$

where $\mathcal{L}_A$ is the area operator,[4] an operator in the center of $M$ defined by

$$\mathcal{L}_A \equiv \oplus_\alpha\, S(\chi_\alpha) \mathbb{1}_{a_\alpha\, \bar{a}_\alpha} \ . \tag{6.26}$$

In a gravitational theory with the Einstein-Hilbert action, the area operator is given by

$$\mathcal{L}_A = \frac{\mathcal{A}(\gamma(A))}{4G_N} \ . \tag{6.27}$$

The second term in Eq. (6.25) is the algebraic entropy defined by

$$S(\widetilde{\rho}, M) \equiv -\sum_\alpha p_\alpha \log p_\alpha + \sum_\alpha p_\alpha S(\widetilde{\rho}_{a_\alpha}) \ . \tag{6.28}$$

[4]Note that the important feature of $\mathcal{L}_A$ is that it is localized to the RT surface $\gamma(A)$. For theories of higher derivative gravity, it would naturally correspond to the Dong entropy [164]

## 6.3 Interpretation of OQEC

In order to understand our result in Section 6.4, it will be crucial to interpret each piece of the state in Eq. (6.24) in holography. The unitary $U_A$ is simply a unitary operation that "encodes" the logical state $\rho_\alpha$ by mixing it with the redundant degrees of freedom $\chi_\alpha$. We ignore this piece and focus directly on the bulk reduced density matrix

$$\rho_a = \oplus_\alpha p_\alpha \, \rho_\alpha \otimes \chi_\alpha \ , \tag{6.29}$$

where one should think of the bulk subregion $a$ as EW($A$). We interpret these pieces by first reviewing lattice gauge theory, which has a similar block decomposition and was argued in [169] to have a similar interpretation. We then proceed by analogy for the case of gravity.

### Lattice Gauge Theory

Understanding the structure of the reduced density matrix in a gauge theory requires dealing with the novel feature that the Hilbert space doesn't factorize across a spatial partition due to gauge constraints [170, 171, 172, 169]. This can be easily visualized in lattice gauge theory, where the gauge field lives on the links of the graph, whereas other fields that transform under the gauge symmetry live on the nodes. These links are necessarily cut when partitioning the vertices to extract the reduced density matrix for a bulk subregion $a$. A prescription to compute $\rho_a$ was given in [170, 173] and has several consistency checks backing it [174, 175]. In order to find the reduced density matrix $\rho_a$, the prescription is to define an extended Hilbert space by first adding extra degrees of freedom at the entangling surface which are not required to satisfy a gauge constraint (see Fig. 6.1). These extra degrees of freedom allow the extended Hilbert space to factorize. The physical states that satisfy the gauge constraint form a subspace of this extended Hilbert space.

As shown in [170, 172], the requirement that physical states commute with the action of gauge transformations implies that the reduced density matrix must take the form

$$\rho_a = \oplus_R \, p(R) \, \rho(R) \otimes \frac{\mathbb{1}_R}{\dim R} \ , \tag{6.30}$$

where the direct sum is over all the different irreducible representations of the entangling surface symmetry group. Comparing this to Eq. (6.29), the state has a similar form with the restriction that $\chi_\alpha = \frac{\mathbb{1}}{\dim \chi_\alpha}$. This $\chi_\alpha$ can be interpreted as the maximally mixed state of the extra degrees of freedom that were added inside the entangling region.

The block-diagonal structure of Eq. (6.30) comes from the following. The representations $R$ determine all the local gauge invariant observables, e.g. the Casimir operator, and are thus distinguishable within the region $a$. Hence, the reduced density matrix is in a classical mixture of these superselection sectors with probability distribution $p(R)$.

It is worth commenting here on one aspect of the connection to gravity. When the bulk is treated semiclassically, one might interpret Eq. (6.29) as the gravitational equivalent of Eq. (6.30) [169, 176]. Diffeomorphisms then play the role of the gauge symmetry, and $\chi_\alpha$ represents degrees of freedom added across the boundary to enable factorization [169].

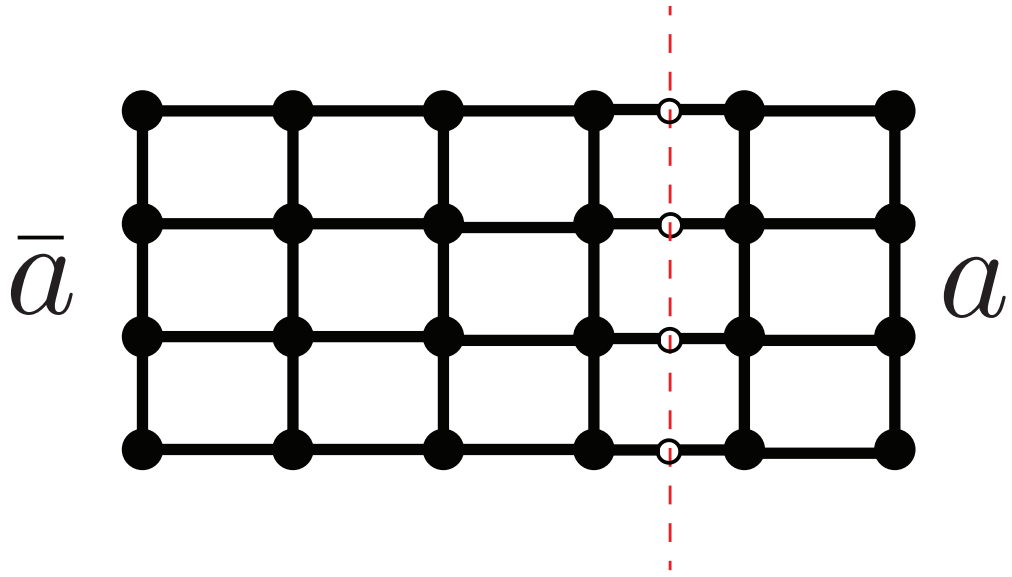


Figure 6.1: Decomposing a lattice gauge theory into subregions $a$ and $\bar{a}$ requires the introduction of extra degrees of freedom (denoted as white dots) at the entangling surface (denoted by a dashed red line).

## Gravity

Armed with the previous discussion, we now interpret each piece of Eq. (6.29) in gravity, occasionally drawing an analogy to Eq. (6.30).

### $\alpha$-blocks

Recall that the $\alpha$-blocks were defined by first choosing a von Neumann algebra $M$ and then finding the natural associated block decomposition of the Hilbert space. The algebra $M$ has a non-trivial center $Z_M$ since the gauge constraints from diffeomorphism invariance inhibit the low energy bulk Hilbert space from factorizing. Then, the simplest physical interpretation of the $\alpha$-blocks is as eigenspaces of the operators in the center $Z_M$. In holography, these include various gauge invariant observables localized to the RT surface, and in particular the area operator $\mathcal{L}_A$ from Eq. (6.26) is one such operator [169].[5] Hence the states in a given $\alpha$-block can be thought of as area eigenstates with the same value of the area operator.

Of course, we do not require infinite precision when comparing eigenvalues. Since we compute entropies accurately up to $\mathcal{O}(1)$, we consider two states to be in the same $\alpha$-block if

[5]In the presence of other gauge constraints, e.g. U(1) gauge fields in the bulk, there would in general be more center observables, e.g. the electric flux. The $\alpha$-blocks would then be labelled by the values of all such observables. We expect the observables related to non-gravitational constraints to leave the $\alpha$-block structure unchanged at leading order in $G_N$, though this is not important for our analysis.

and only if they have the same eigenvalue of $\mathcal{L}_A$ at $\mathcal{O}(1)$. That said, it is sometimes useful to acknowledge that states with the same eigenvalue at $\mathcal{O}(1/G_N)$ share a classical background geometry.[6] For example, empty AdS with a small field excitation might be in a different $\alpha$-block than vacuum AdS because the $\mathcal{A}/4G_N$ differs at $\mathcal{O}(1)$. But the two states still share the same classical background: empty AdS.

Note that our code subspace is relatively large: we include an $\alpha$-block for every geometry with $\mathcal{A}/4G_N$ different at $\mathcal{O}(1)$. Indeed, we identify the code subspace as the entire Hilbert space of bulk EFT. This is important for our results in Section 6.4, and so we emphasize that we are explicitly assuming this. We think it is likely to be well-grounded based on an extension of [110]; the analysis in that paper motivates the inclusion of different classical background geometries in the code subspace when working at $\mathcal{O}(1/G_N)$. Once that is established, it is easier to define a code subspace on top of each classical background. Perhaps an argument along these lines justifies including many classically different geometries in the same code subspace, even when working to $\mathcal{O}(1)$.

We are primarily interested in bulk states that are smooth geometries. In the $G_N \to 0$ limit, smooth geometries become area eigenstates, and hence have support exclusively on $\alpha$-blocks with one particular value of $\mathcal{A}/4G_N$ at leading order. When $G_N$ is finite, overlap with other blocks is best computed using the Euclidean path integral [74]. This formalism makes it clear that two classically different geometries have $e^{-\mathcal{O}(1/G_N)}$ overlap. We will go into more depth when we discuss $p_\alpha$ below.

We assume that non-perturbative corrections do not ruin the exactly block-diagonal structure of Eq. (6.29). As we will see in Section 6.4, this suffices to derive a prescription resembling the AdS/CFT calculation. It is unclear whether this is well-justified, but one argument for it is the following. We work exclusively in the context of semi-classical gravity, and semi-classical gravity states are non-perturbatively gauge invariant [74]. Gauge invariance demands the direct sum structure exactly. I.e., non-perturbatively small off block-diagonal terms might break non-perturbative gauge invariance. Again, this argument is intended heuristically, not as a proof. For our purposes, we simply assume that the off-diagonal terms are exactly zero.

### State $\rho_\alpha$

This physical understanding of $\alpha$-blocks lends itself to an easy interpretation of $\rho_\alpha$. The state $\rho_\alpha$ is the state of the bulk matter fields when restricted to the subspace of the bulk Hilbert space with a definite value of $\mathcal{A}/4G_N$ to $\mathcal{O}(1)$. From Eq. (6.26), we see that the definite value of $\mathcal{A}/4G_N$ is $S(\chi_\alpha)$.

[6] Strictly speaking, they need only have the same minimal extremal surface area, but need not be the same geometry. We expect that generically no two different geometries have exactly the same minimal extremal surface area given fixed boundary conditions at infinity. If they do, it would not greatly affect our results.

**State $\chi_\alpha$**

Since the bulk EFT degrees of freedom are captured by the $\rho_\alpha$ state, the $\chi_\alpha$ state must correspond to the high energy, quantum gravity degrees of freedom that were integrated out to define the semiclassical gravity EFT.

This is nicely consistent with the fact that the area operator $\mathcal{L}_A$ measures the entropy of these degrees of freedom. In semiclassical gravity, the generalized entropy of a subregion is defined as

$$S_{\text{gen}} = \frac{\mathcal{A}}{4G_N} + S_{\text{matter}} \ , \tag{6.31}$$

where $S_{\text{matter}}$ is the von Neumann entropy of the bulk matter fields. While $S_{\text{gen}}$ is defined purely in semiclassical gravity, it is widely believed that it corresponds to the von Neumann entropy of all the degrees of freedom in the "full" quantum gravity theory. The entropy of the quantum gravity degrees of freedom that were integrated out shows up as the area term in $S_{\text{gen}}$. Comparing with Eq. (6.25), we see that the entropy $S(\widetilde{\rho}_A)$ is interpreted in exactly this way: the part $S(\rho_\alpha)$ is the bulk matter entropy, and $S(\chi_\alpha)$ can be interpreted as the area.

One can gain further insight into the degrees of freedom described by $\chi_\alpha$ by drawing an analogy to lattice gauge theory. By comparing Eq. (6.29) and Eq. (6.30), one sees that the $\chi_\alpha$ degrees of freedom seem analogous to the surface symmetry degrees of freedom, which are in the state $\frac{\mathbb{1}_R}{\dim R}$. This was pointed out in [169, 176], in which they argue that because semi-classical gravity is a gauge theory, this should be understood as more than an analogy. One should expect that the $\chi_\alpha$ can be interpreted as playing the role of surface symmetry degrees of freedom for the diffeomorphism group.

This interpretation would come with an interesting implication. Because gauge invariance imposes that surface symmetry degrees of freedom are in the singlet state, it would have to be the case that $\chi_\alpha = \frac{\mathbb{1}_\alpha}{\dim \chi_\alpha}$. Confirming that $\chi_\alpha$ is indeed in this state in the AdS/CFT code will be one of our main results in Section 6.4.

**Distribution $p_\alpha$**

How would we compute $p_\alpha$ within the CFT? We could first prepare the state $\widetilde{\rho}_A$ with the Euclidean path integral. Then, based on Eq. (6.24), project onto block $\alpha$ – which has area eigenvalue $S(\chi_\alpha)$ – and take the trace to isolate $p_\alpha$.

The analogous procedure in the bulk first prepares a bulk density matrix with the Euclidean path integral. We define the bulk density matrix as follows. Let $(g_-, \phi_-)$ and $(g_+, \phi_+)$ correspond to two classical metric and matter field configurations at Euclidean time $\tau = 0$. The density matrix $\rho[g_-, \phi_-; g_+, \phi_+]$ is a functional of these two configurations defined by the path integral:

$$\rho[g_-, \phi_-; g_+, \phi_+] = \frac{1}{Z} \int_{\substack{g', \phi'|_\infty = \mathcal{J} \\ (g_-, \phi_-; g_+, \phi_+)}} Dg' D\phi' \, e^{-I_{\text{bulk}}[g', \phi']} \ , \tag{6.32}$$

where the notation $(g_-, \phi_-; g_+, \phi_+)$ is taken to enforce the following two boundary conditions, one on the integration over Euclidean time from $(-\infty, 0)$, and the other over $(0, \infty)$:

$$\tau \in (-\infty, 0): \qquad g(\tau = 0) = g_- \ , \quad \phi(\tau = 0) = \phi_- \quad , \tag{6.33}$$

$$\tau \in (0, +\infty): \qquad g(\tau = 0) = g_+ \ , \quad \phi(\tau = 0) = \phi_+ \quad . \tag{6.34}$$

The other boundary conditions on the path integral come from the AdS asymptotics: $g', \phi'|_\infty$, must be consistent with boundary conditions at infinity set by the boundary sources $\mathcal{J}$. With this bulk density matrix, one then defines the reduced density matrix $\rho_a$ by tracing out the complement of $a$, which is $\bar{a} \equiv \mathrm{EW}(\bar{A})$. This tracing is done by first identifying $g_- = g_+$ and $\phi_- = \phi_+$ in the region being traced out, then integrating over all metric and matter configurations in that region.

To obtain $p_\alpha$, we wish to project onto states in that $\alpha$-block and then take the trace. This is performed by tracing out $a$ from $\rho_a$ while including an extra boundary condition in the path integral that the RT area operator takes on definite value $S(\chi_\alpha)$.

All of these bulk path integral computations can be lumped into one step: we compute $p_\alpha$ by performing the entire Euclidean path integral subject to the boundary condition that the $\mathcal{A}/4G_N$ of $\gamma(A)$ takes on definite value $S(\chi_\alpha)$:[7]

$$p_\alpha = \frac{1}{Z} \int_{\substack{\mathcal{L}_A = S(\chi_\alpha) \\ g', \phi'|_\infty = \mathcal{J}}} Dg' \, D\phi' \, e^{-I_{\mathrm{bulk}}[g', \phi']} \ . \tag{6.35}$$

The leading order contribution to $p_\alpha$ can be computed with the saddle-point approximation:

$$p_\alpha \approx \left. \frac{e^{-I_{\mathrm{bulk}}[g_\alpha, \phi_\alpha]}}{Z} \right|_{g_\alpha, \phi_\alpha|_\infty = \mathcal{J}} \ . \tag{6.36}$$

We have denoted the saddle-point metric and field configuration for each $\alpha$ as $g_\alpha, \phi_\alpha$. We later schematically shorten this to $p_\alpha = e^{-I_{\mathrm{bulk}}[\alpha]}/Z|_{b.c.}$, for boundary conditions "b.c." Higher order corrections can be computed from a perturbative expansion of the path integral. We will pay special attention to the leading order piece in Section 6.4, because it will play the most important role in connecting to the cosmic brane prescription [163] for computing the refined Renyi entropy. Indeed, given a set of boundary conditions at infinity, we will interpret some $\alpha$-blocks as geometries with cosmic branes[8], and we will see that computing the refined Renyi entropy is exactly like computing the von Neumann entropy of a state with support predominantly in one of these cosmic brane $\alpha$-blocks.

What we have said here is so important to our main point that we emphasize it again now. A general CFT state $\widetilde{\rho}$ has non-vanishing support on many $\alpha$, not just the blocks that correspond to its dominant geometric dual. This support is computable, and is schematically $p_\alpha = e^{-I_{\mathrm{bulk}}[\alpha]}/Z$. Therefore, the boundary reduced density matrix $\widetilde{\rho}_A$ will in general be a mixture of states on different $\alpha$-blocks. We will use these facts when arguing that the cosmic brane prescription for computing refined Renyi entropy [163] is derivable from within OQEC.

[7] The path integration must also respect the boundary conditions at infinity.

[8] Equivalently, we interpret them as geometries with conical deficits.

## 6.4 Cosmic Brane Prescription in OQEC

Having established the framework, we now use the formalism of OQEC to compute the refined Renyi entropy defined as

$$\widetilde{S}_n(\widetilde{\rho}_A) \equiv n^2 \partial_n \left( \frac{n-1}{n} S_n(\widetilde{\rho}_A) \right) \ , \tag{6.37}$$

where $S_n(\widetilde{\rho}_A) \equiv \frac{1}{1-n} \log \mathrm{tr} \widetilde{\rho}_A^n$ is the Renyi entropy of subregion $A$. In [163, 168] it was shown that in AdS/CFT, the refined Renyi entropy of a boundary subregion $A$ is given by

$$\widetilde{S}_n(A) = \frac{\mathcal{A}}{4G_N} + \widetilde{S}_n^{\text{bulk}}(a) \ , \tag{6.38}$$

where $\mathcal{A}$ is the area of a brane with tension $T_n = \frac{n-1}{4nG_N}$ and extremal area. The region $a$ is the entanglement wedge of $A$. Our main result in this section will be to derive this prescription from the formalism of quantum error correction. By doing so we uncover an improved understanding of the high energy degrees of freedom in quantum gravity, as well as a more refined definition of the area operator.

### Quantum Error Correction calculation

The refined Renyi entropy of a general density matrix $\rho$ can be shown to satisfy

$$\widetilde{S}_n(\rho) = S(\rho^{(n)}) = -\ \mathrm{tr} \left( \rho^{(n)} \log \rho^{(n)} \right) \ , \tag{6.39}$$

$$\rho^{(n)} \equiv \frac{\rho^n}{\mathrm{tr}(\rho^n)} \ . \tag{6.40}$$

We now use this to compute the refined Renyi entropy of a reduced density matrix in OQEC. Consider an arbitrary state $\widetilde{\rho}$. From Eq. (6.24), we read off the reduced density matrix of subregion $A$ as

$$\widetilde{\rho}_A = U_A \left( \oplus_\alpha p_\alpha \, \rho_\alpha \otimes \chi_\alpha \right) U_A^\dagger \ . \tag{6.41}$$

Plugging this into Eq. (6.40) defines the state

$$\widetilde{\rho}_A^{(n)} = U_A \left( \oplus_\alpha p_\alpha^{(n)} \, \frac{\rho_\alpha^n}{\mathrm{tr}(\rho_\alpha^n)} \otimes \frac{\chi_\alpha^n}{\mathrm{tr}(\chi_\alpha^n)} \right) U_A^\dagger \ . \tag{6.42}$$

where

$$p_\alpha^{(n)} \equiv \frac{p_\alpha^n \mathrm{tr}(\chi_\alpha^n) \mathrm{tr}(\rho_\alpha^n)}{\sum_{\alpha'} p_{\alpha'}^n \mathrm{tr}(\chi_{\alpha'}^n) \mathrm{tr}(\rho_{\alpha'}^n)} = \frac{p_\alpha^n \, e^{-(n-1)S_n(\chi_\alpha) - (n-1)S_n(\rho_\alpha)}}{Z^{(n)}} \tag{6.43}$$

represents a normalized probability distribution that depends on $n$. Using this in Eq. (6.39) leads us to a crucial ingredient of our main result:

$$\widetilde{S}_n(\widetilde{\rho}_A) = \sum_\alpha p_\alpha^{(n)} \widetilde{S}_n(\chi_\alpha) - \sum_\alpha p_\alpha^{(n)} \log p_\alpha^{(n)} + \sum_\alpha p_\alpha^{(n)} \widetilde{S}_n(\rho_\alpha) \ . \tag{6.44}$$

It is illuminating to note the following connection to the Ryu-Takayanagi formula. In the special case where $\chi_\alpha$ is maximally mixed[9], one can write

$$\widetilde{S}_n(\widetilde{\rho}_A) = \mathrm{tr}\widetilde{\rho}_A^{(n)} \mathcal{L}_A - \sum_\alpha p_\alpha^{(n)} \log p_\alpha^{(n)} + \sum_\alpha p_\alpha^{(n)} S\left(\rho_\alpha^{(n)}\right) \ . \tag{6.45}$$

Written this way, $\widetilde{S}_n(\widetilde{\rho}_A)$ equals the expectation value of the area operator $\mathcal{L}_A$ plus the algebraic von Neumann entropy of the logical degrees of freedom, all evaluated in a state $\widetilde{\rho}_A^{(n)}$ that belongs to the code subspace.

Notably, to write Eq. (6.44) in the form Eq. (6.45) for arbitrary states $\widetilde{\rho}_A$ in the code subspace, the identification

$$\sum_\alpha p_\alpha^{(n)} \widetilde{S}_n(\chi_\alpha) = \mathrm{tr}\widetilde{\rho}_A^{(n)} \mathcal{L}_A \tag{6.46}$$

must hold term by term, because one could choose states with support on a single $\alpha$-block. This is equivalent to having $\widetilde{S}_n(\chi_\alpha) = S(\chi_\alpha)$ for all $\alpha$-blocks, and we show in Appendix A.8 that, for this, it is both necessary and sufficient that $\chi_\alpha$ be maximally mixed. Moreover, a maximally mixed $\chi_\alpha$ has another important implication. In the next subsection we shall argue that it is a necessary and sufficient condition for the gravitational interpretation of $\widetilde{\rho}_A^{(n)}$ to be a geometry containing a brane with the precise $n$-dependent tension required to match the cosmic brane prescription in [163].

## Connection to gravity

**Review of holographic refined Renyi entropy:** We start by carefully reviewing the cosmic brane prescription of [163]. One considers a CFT state $\widetilde{\rho}$ that can be prepared by the Euclidean path integral. The bulk dual of the reduced density matrix $\rho_A$ is given by the Hartle-Hawking wavefunction [177], which has the saddle-point approximation

$$\rho_A[g_-, \phi_-; g_+, \phi_+] = \left.\frac{e^{-I_{\mathrm{bulk}}[g,\phi]}}{Z}\right|_{\substack{g,\phi|_\infty = \mathcal{J} \\ (g_-,\phi_-;g_+,\phi_+)}} \ , \tag{6.47}$$

where $g, \phi$ are the saddle point field configurations given the boundary conditions at Euclidean time $\tau = 0$, $(g_-, \phi_-; g_+, \phi_+)$. Moreover, the AdS asymptotics $g, \phi|_\infty$ must be consistent with boundary conditions $\mathcal{J}$ at infinity that define the state $\widetilde{\rho}$.

[9] More generally it is given by a normalized projector, which can be thought of as being maximally mixed over the subspace on which it has support.

The cosmic brane prescription computes the refined Renyi entropy $\widetilde{S}_n(\widetilde{\rho}_A)$ in two steps. First, consider the bulk reduced density matrix

$$\rho_{\text{brane,A}}[g_-, \phi_-; g_+, \phi_+] = \left. \frac{e^{-nI_{\text{bulk}}[g,\phi]-(n-1)\frac{\mathcal{A}[g]}{4G_N}}}{Z} \right|_{\substack{g,\phi|_\infty=\mathcal{J} \\ (g_-,\phi_-;g_+,\phi_+)}} . \tag{6.48}$$

The action is $n$ times the sum of the bulk action $I_{\text{bulk}}$ and the area $\mathcal{A}$ of a brane with tension $T_n = \frac{n-1}{4nG_N}$ anchored to the boundary of region $A$. We refer to this as a "brane state," because of its bulk interpretation as $\rho$ with an inserted cosmic brane.

Second, in this brane state compute the expectation value of the area operator $\hat{\mathcal{A}}/4G_N$:

$$\widetilde{S}_n(\widetilde{\rho}_A) = \frac{\text{tr}\left(\rho_{\text{brane},A}\hat{\mathcal{A}}\right)}{4G_N} . \tag{6.49}$$

This computes the refined Renyi entropy to $\mathcal{O}(1/G_N)$. The $\mathcal{O}(1)$ part is computed by including the $\mathcal{O}(1)$ contribution of the area operator and adding the refined Renyi entropy of the entanglement wedge [163, 168].

Let us forestall a possible confusion. It is often said that the refined Renyi entropy equals the area of the extremal cosmic brane, and rightly so. Yet, the prescription above was to evaluate the area operator in the brane state. The area operator corresponds to the area of the *tensionless* extremal surface, so it's not obvious a priori why it should also correspond to the area of the brane with tension. In fact, in these brane states, the tensionless extremal surface coincides with the brane. Indeed, the branes satisfy the very strong condition that their extrinsic curvature tensor vanishes everywhere.[10] (Note, in the limit $n \to 1$ only the trace of the extrinsic curvature remains vanishing.)

This concludes the cosmic brane prescription for computing the refined Renyi entropy.

**Branes in quantum error-correction:** We now argue that this prescription is simply Eq. (6.45) combined with three special features of gravity. This is our main result.

The first special feature is the geometric interpretation of $\alpha$-blocks. As we discussed at length in Section 6.3, each $\alpha$ in $\widetilde{\rho}_A$ corresponds to states of definite area eigenvalue. We are interested in CFT states with smooth geometric bulk duals. Such states have support on many $\alpha$-blocks, and different distributions $p_\alpha$ correspond to different smooth geometries. Of course, one does not expect all possible distributions to correspond to some smooth geometry – after all, an equal mixture of two different classical geometries is likely not itself a smooth geometry. The point is that certain mixtures, such as those prepared by the Euclidean path integral, correspond to smooth geometries. This is crucial for deriving the cosmic brane prescription in OQEC, because immediately below, we will interpret a particular distribution $p_\alpha^{(n)}$ as defining a "brane geometry".

[10] We thank Aitor Lewkowycz for helping us understand this.

The second special feature is the type of support $p_\alpha$ has on many $\alpha$-blocks for smooth geometries. As we described in Section 6.3, $p_\alpha$ can be computed by performing the Euclidean path integral subject to the constraint that the area takes on the appropriate value. The leading order in $G_N$ part of $p_\alpha$ is given by the saddle-point approximation, and should be understood as a weight assigned to the classical geometry with that value of the area. Hence we can write the $p_\alpha$ of the state $\widetilde{\rho}_A$ as

$$p_\alpha = \left.\frac{e^{-I_{\text{bulk}}[\alpha]}}{Z}\right|_{b.c.} . \tag{6.50}$$

Here, the AdS asymptotics are required to match the boundary conditions (b.c.) that define the state $\widetilde{\rho}$. With this $p_\alpha$ in hand, plug Eq. (6.50) into Eq. (6.43) to obtain the distribution over $\alpha$-blocks of the state $\widetilde{\rho}_A^{(n)}$:

$$p_\alpha^{(n)} = \left.\frac{e^{-nI_{\text{bulk}}[\alpha]-(n-1)S_n(\chi_\alpha)-(n-1)S_n(\rho_\alpha)}}{Z^{(n)}}\right|_{b.c.} . \tag{6.51}$$

Note the boundary conditions are the same as those for $p_\alpha$. This is remarkably similar to Eq. (6.48), and includes the known quantum correction to the action from the matter Renyi entropy [168]. Indeed, if it were the case that $S_n(\chi_\alpha) = S(\chi_\alpha)$ for all $\alpha$, then $p_\alpha^{(n)}$ would look exactly like $p_\alpha$ but with the action shifted by the area operator:[11]

$$I_{\text{bulk}}[\alpha] \to nI_{\text{bulk}}[\alpha] + (n-1)\text{tr}(P_\alpha \widetilde{\rho}_A P_\alpha \mathcal{L}_A) . \tag{6.52}$$

where $P_\alpha = \sum_i |\alpha, i\rangle\langle\alpha, i|$ is a projector onto the particular $\alpha$-block we are looking at. Compare this to the AdS/CFT calculation of refined Renyi entropy. The action defining the brane state Eq. (6.48) is shifted in exactly this way relative to the state whose refined Renyi entropy we're computing, Eq. (6.47). This strongly suggests that indeed $S_n(\chi_\alpha) = S(\chi_\alpha)$ for all $\alpha$ and $n$ in the AdS/CFT code.

We already saw separate evidence for this. In order to write Eq. (6.44) in the form Eq. (6.45), it is necessary that $\chi_\alpha$ is maximally mixed. So, the same condition that allows us to relate the refined Renyi entropy to the expectation value of the area operator in a state $\widetilde{\rho}_A^{(n)}$ also guarantees that $\widetilde{\rho}_A^{(n)}$ has an interpretation as the "brane state" Eq. (6.48)!

This is strong evidence that in the AdS/CFT code, $\chi_\alpha$ is indeed maximally mixed. We label this the third special feature of gravity. With this conclusion, we have completed the argument that Eq. (6.45) is the cosmic brane prescription.

It is worth pausing to emphasize where the brane came from, from the point of view of the code. I.e., we now emphasize how one can look at the state $\widetilde{\rho}_A^{(n)}$ and determine that it equals $\widetilde{\rho}_A$ with a brane inserted into the action. The original sum over $\alpha$ in Eq. (6.41) included states of every possible geometry, including geometries with conical deficits. Morally, the reweighting $p_\alpha \to p_\alpha^{(n)}$ enhanced the contribution from the conical deficit geometries relative

[11] We have dropped $S_n(\rho_\alpha)$ for simplicity, but its presence only increases the resemblance.

to the others, exactly like inserting a brane. It does this via the factor $e^{-(n-1)\mathrm{tr}(P_\alpha \widetilde{\rho}_A P_\alpha \mathcal{L}_A)}$ in Eq. (6.43) – where we have used our conclusion that $S_n(\chi_\alpha) = S(\chi_\alpha)$ to write this in terms of the area operator like in Eq. (6.52). That factor suppresses geometries with large eigenvalues of the area operator in exactly the same way that inserting $e^{-(n-1)\mathcal{A}/4G_N}$ does when inserted into the bulk action.

Notably, the fact that $\chi_\alpha$ is maximally mixed has a number of interesting implications. For instance, it gives us an improved form of the area operator. Instead of Eq. (6.26), the AdS/CFT code's area operator is

$$\mathcal{L}_A = \oplus_\alpha \log \dim(\chi_\alpha) \mathbb{1}_{a_\alpha \bar{a}_\alpha} \ , \tag{6.53}$$

where $\dim(\chi_\alpha)$ is the dimension of the subspace on which $\chi_\alpha$ has support. This strengthens the argument that $\chi_\alpha$ corresponds to the surface symmetry degrees of freedom in lattice gauge theory. We discuss this more in Section 6.6.

Another implication is that states restricted to a single $\alpha$-block have flat Renyi spectra at leading order in $G_N$. In order for a holographic CFT state to have a non-flat spectrum, it must have support on many $\alpha$-blocks. In other words, the well-known $n$-dependence of $S_n$ and $\widetilde{S}_n$ for CFTs evidently comes entirely from the $n$-dependent support on $\alpha$-blocks, given by Eq. (6.43). This suggests an interesting fix to the notorious inability of tensor networks to have the correct Renyi spectrum [28, 29, 75, 173]. We explore this in detail in Section 6.5.

## 6.5 Tensor Networks

Holographic tensor networks have modeled certain aspects of AdS/CFT remarkably well [28, 29, 75, 173]. Yet, a common mismatch between these models and AdS/CFT has been the flatness of the tensor networks' Renyi spectrum. This flatness is in part a result of the maximal entanglement of the bonds. Hence some proposals for correcting the spectrum involve modifying the entanglement of the bonds to be less than maximal, often thermal, to match the expected Rindler entanglement across a spatial divide in quantum field theory [29].

It was proposed in [110] that since the code subspace can be enlarged to include very different background geometries, one might consider a direct sum of tensor networks with different graph structures as a natural toy model for holography. We now discuss how our results in Section 6.4 suggest that this approach of defining a "super tensor network" (STN) with a Hilbert space that is a direct sum of the Hilbert space of many dissimilar constituent tensor networks resolves the Renyi spectrum mismatch.

The key ingredient is the following. Instead of considering a tensor network to be a smooth geometry, tensor networks should be thought of as a single $\alpha$-block! I.e., one should think of states on a single tensor network as states with support on a single $\alpha$-block in the code subspace described in Section 6.2. Indeed, tensor networks are natural area eigenstates, because the "area" equals the product of the number of bonds cut and the bond dimension, which is independent of the state.

Moreover, considering tensor networks to be $\alpha$-blocks makes the maximal bond entanglement in tensor networks a feature for matching AdS/CFT's Renyi spectrum, instead of a bug. If a tensor network's bonds are maximally entangled, the degrees of freedom defining the area operator are maximally mixed (i.e. the state on the bonds cut by the minimal surface is maximally mixed). In Section 6.4, we called these degrees of freedom $\chi_\alpha$, and indeed we found that for a given $\alpha$, $\chi_\alpha$ is maximally mixed. Thus, there are strong reasons to treat tensor networks as area eigenstates (i.e. $\alpha$-blocks) and to model smooth geometries as coherent superpositions of tensor networks with different graph structures. The particular sorts of superpositions that correspond to smooth geometries are discussed in Section 6.3.

In fact, tensor networks are even more constraining than a single $\alpha$-block since they are eigenstates of the area operator for arbitrary subregions of the boundary. In AdS/CFT, it is not precisely clear how one would simultaneously project onto eigenstates of the area operators for different subregions. RT surfaces anchored to different subregions could cross, and in fact in the time-dependent generalization of RT [20], generically it wouldn't be possible to constrain all extremal surfaces to lie on the same Cauchy slice. Since tensor networks represent a coarse grained picture of the bulk with each tensor roughly corresponding to a single AdS volume, it might be possible to impose all the constraints simultaneously. Since tensor networks manage to perform this simultaneous projection, understanding them better may lead to an improved understanding of holography. It is also interesting to note that time evolution of tensor networks is not well understood. This potentially stems from the fact that they model eigenstates of the area operator at a given time and thus, very quickly evolve into states that are not geometric. It would be interesting to explore this further.

To summarise, a single tensor network with maximal bond entanglement is a good toy model for gravitational states with definite value of the area operator. The code subspace of AdS/CFT is nicely represented by a direct sum over these different tensor networks. The tensor network in [75] approximately takes this form since there is very small overlap between different networks and thus, any given state is roughly consistent with the direct sum structure. Our results imply that not only will the STN have a non-flat spectrum, but computing Renyi entropies will be qualitatively similar to the AdS/CFT prescription involving an extremal brane. One should also compare our results to those of [178]. They obtained the correct Renyi entropies in the case of $AdS_3$ by using the specific form of the gravitational action. We have taken inspiration from the result of [163] and instead considered the refined Renyi entropies, which seem to be a more natural quantity in holography.

## 6.6 Discussion

Inspired by the AdS/CFT result that $\widetilde{S}_n$ equals the area of an extremal cosmic brane, we showed that a similar, more general prescription holds for any operator-algebra quantum error correcting code. This helps better our understanding of the emergent bulk in terms of error correction.

For a code to satisfy the cosmic brane prescription, the redundant, quantum gravity

degrees of freedom split by the entangling surface must be maximally entangled. Somehow this fact is encoded in the gravitational path integral, because that was the only input into proving the brane prescription in AdS/CFT. It would be interesting to see a direct way of proving this within gravity.

We now proceed to discuss some interesting implications of our work and some potential future directions that would be interesting to pursue.

## Edge Modes and Lattice Gauge Theory

As we reviewed in Section 6.3, the reduced density matrix in a lattice gauge theory must take the form

$$\rho_A = \oplus_R \, p(R) \, \rho(R) \otimes \frac{\mathbb{1}_R}{\dim R} \ , \tag{6.54}$$

where the direct sum is over all the different representations of the entangling surface symmetry group. This strongly resembles states in the OQEC formalism, namely Eq. (6.24), given our conclusion from Section 6.4 that $\chi_\alpha = \frac{\mathbb{1}}{\dim \chi_\alpha}$.

There have been various arguments in favour of understanding the bulk as an emergent gauge theory [179]. The above picture then suggests that the area term in the Ryu Takayanagi formula could be analogous to the $\log \dim R$ term that arises in lattice gauge theory [176]. In order for this story to hold true, an important restriction as we saw above was that the state $\chi_\alpha$ be maximally mixed. However, we arrived at this from the independent consideration of requiring that the OQEC code satisfy the Dong prescription. Thus, this puts the emergent gravity proposal on a stronger footing.

In order to understand how the Ryu Takayanagi formula arises more precisely, one would have to study the representations of the surface symmetry group in the context of gravity. The results of [169, 180] motivate that the entropy from the $\chi_\alpha$ degrees of freedom must scale with the area. The real test would be to obtain the correct prefactor. The results in [181, 182, 183] might help provide a statistical interpretation to understand the edge mode counting in the case of a restricted class of codimension 2 surfaces.

## Holography in General Spacetimes

Holography beyond AdS/CFT has been quite elusive as yet. In fact, the AdS/CFT dictionary at length scales shorter than $l_{AdS}$ hasn't been completely understood and has been conjectured to involve the $N^2$ matrix degrees of freedom of the boundary theory in an important way. Various attempts at understanding holography more generally include [31, 32, 34, 35, 184, 185, 186, 187]. In each of these cases, there have been attempts to find some form of a Ryu Takayanagi (RT) formula [56, 185, 57]. To be precise, extremal surfaces anchored to subregions of the proposed boundary theory exist, and satisfy the expected holographic inequalities. However, it is not clear whether the area of such extremal surfaces really computes the entanglement entropy of some boundary theory.

As [24, 27] showed, if the RT formula is indeed computing the entropy of a boundary subregion, it automatically implies the existence of an error correcting code with subregion duality. Since our results have demonstrated that any such holographic duality must satisfy Dong's prescription for the Renyi entropy, it should be an additional feature of any of the above proposals in order for them to be consistent.

Another interesting direction to understand sub-AdS locality, while staying within the realm of AdS/CFT, is the $T\bar{T}$ deformation [145]. The $T\bar{T}$ deformation is an irrelevant deformation to the boundary CFT that has been conjectured to be dual to AdS with a Dirichlet boundary at finite radius. Interestingly, in [149], both the Ryu Takayanagi formula and the Dong prescription were shown to work precisely for a very symmetric setup of the $T\bar{T}$ deformation. This strongly motivates that one might in fact have a similar error correcting code with subregion duality even without referring to a conformal boundary.

## Properties of refined Renyi entropy

Entanglement entropies are known to satisfy various inequalities such as subadditivity and strong subadditivity. Despite the fact that their linear algebra proofs are quite involved, the holographic proofs are remarkably simple [81, 60]. The geometric dual and the minimization involved in the RT formula easily allow one to prove these inequalities. In fact, a large set of non-trivial inequalities satisfied by holographic states can be proven [114, 188].

Both Renyi and refined Renyi entropies are not in general subadditive, even though certain interesting classes of states [189] have been shown to satisfy such inequalities. In the holographic context, since the refined Renyi entropies are also obtained by following a minimization procedure on a dual geometry, one might be led to believe that similar proofs could be used to prove inequalities for the refined Renyi entropies. These could then be used to constrain the class of holographic states, i.e. a holographic refined Renyi entropy cone.[12]

However, there are subtleties in proving such inequalities due to the back-reaction from the cosmic brane. When considering refined Renyi entropies of two disjoint regions $A$ and $B$, one would in general have to consider different geometries for computing $\widetilde{S}_n(A)$, $\widetilde{S}_n(B)$ and $\widetilde{S}_n(A \cup B)$. It's possible that the OQEC formalism provides a useful, alternative way to prove such inequalities.

More generally, understanding properties of the refined Renyi entropy is interesting future work. The refined Renyi entropies seem to be a more natural generalization of von Neumann entropy in holography than the Renyi entropies. They can be computed by a quantity localized to a codimension 2 surface, while the Renyi entropies in general involve a non-local integral, even at leading order in $G_N$. It would be interesting to find quantum information theoretic uses for the refined Renyi entropy, perhaps stemming from Eq. (6.39). For example, if the von Neumann entropy of $\rho$ is too difficult to compute experimentally, one could instead compute the $n$-th refined Renyi entropy of $\sigma$, provided $\rho = \sigma^n/\mathrm{tr}(\sigma^n)$.

[12] We thank Ning Bao for discussions about this.

## Error Correction and Holography

Our analysis involved computing a quantity within the quantum error correction framework and comparing it with results from AdS/CFT. This helped us learn about novel aspects of both error correcting codes and AdS/CFT. Thus, it seems like a fruitful direction to analyze other known holographic results within the framework of error correction in order to refine our understanding of the emergent bulk. As we have seen, many results in AdS/CFT, such as the RT formula and the Dong prescription, are simple "kinematic" results from OQEC. We have also seen that AdS/CFT puts constraints on the type of OQEC that relates the boundary to the bulk. It seems plausible that there is much mileage to be gained from simply exploiting the OQEC framework without needing to reference the dynamics of the boundary theory.

A small caveat to keep in mind is that all our results were obtained by working with a finite dimensional Hilbert space. Interesting effects might arise from considering infinite dimensional Hilbert spaces. For example, [110] found that the Renyi entropies are discontinuous around $n = 1$ when taking the large $N$ limit. This is also true for the refined Renyi entropies that we have analyzed. Some features of infinite dimensional Hilbert spaces could be modeled by using the framework of approximate error correction [25].[13] Understanding the nuances of the large $N$ limit is an interesting direction that we leave for future work.

[13] We thank Patrick Hayden for a discussion about this.

# Chapter 7

# Entanglement Wedge Cross Sections Require Tripartite Entanglement

## 7.1 Introduction

We better understand quantum gravity every time we learn quantum information theoretic properties of holographic CFT states. This is the spirit of the "Geometry from Entanglement" slogan [190, 191], and it has been borne out in numerous discoveries. At the heart of these quantum information properties is the entanglement structure of the holographic CFT state. Know the structure explicitly, and you can in principle compute whatever quantum information property you want.

Hence it has been of great interest to probe this structure in any way tractable. Perhaps the most famous probe is a region's von Neumann entropy, whose bulk dual is simply the area divided by $4G_N$ of the minimal-area codimension-2 surface anchored to the boundary of the region [19, 18]. This is the Ryu-Takayanagi (RT) formula. It is well-known that the RT formula places strong constraints on the entanglement structure of the CFT state [114].

That said, the von Neumann entropy is a rather coarse measure of entanglement. It works well to quantify entanglement in a bipartite pure state, but doesn't capture all the information about entanglement structure for bipartite mixed states or multipartite states. Hence there is much less known about the multipartite structure of entanglement in holography, owing both to the fact that there have been fewer probes of it and that it is much harder to quantify (although there has been limited progress [192]).

It was in this context that a particularly powerful conjecture, which we call the "Mostly-Bipartite Conjecture" (MBC), was made by Cui et al. in [39]. We state this conjecture in detail now, as we understand it.

**Mostly-Bipartite Conjecture of [39]:** *Consider a state of a holographic CFT with a gravitational dual well-described by semiclassical gravity. Let $c \sim \frac{1}{G_N}$ represent its central charge. Given CFT subregions A,B, and C with Hilbert spaces that each admit the decom-*

*position $H_X = H_{X_1} \otimes H_{X_2} \otimes H_{X_3}$, the quantum state is "close" to the form*

$$|\psi\rangle_{ABC} = U_A\, U_B\, U_C |\psi_1\rangle_{A_1\, B_1} |\psi_2\rangle_{A_2\, C_1} |\psi_3\rangle_{B_2\, C_2} |\widetilde{\psi}\rangle_{A_3\, B_3\, C_3} \tag{7.1}$$

*in the $G_N \to 0$ limit, where we demand that $|\widetilde{\psi}\rangle_{A_3\, B_3\, C_3}$ is 'small' in the sense that its entropies are subleading in $G_N$,*

$$S(A_3), S(B_3), S(C_3) \sim \mathcal{O}(1) \ , \tag{7.2}$$

*while*

$$S(A_1) = S(B_1) \approx \frac{I(A:B)}{2} \ , \tag{7.3}$$

$$S(A_2) = S(C_1) \approx \frac{I(A:C)}{2} \ , \tag{7.4}$$

$$S(B_2) = S(C_2) \approx \frac{I(B:C)}{2} \ , \tag{7.5}$$

*where the "$\approx$" symbol means at $\mathcal{O}(\frac{1}{G_N})$, and the mutual information is defined as $I(A:B) \equiv S(A) + S(B) - S(AB)$.*

We will refer to this conjectured state (7.1) as the "MBC state" from now on. We place quotes around "close" because it is not specified in what sense the states should be close. As we discuss in detail below, we will take this to mean close in natural distance measures usually applied to quantum states.

The motivation for this conjecture comes from the bit threads paradigm, in which Cui et al. found that an optimal bit thread configuration with the above bipartite structure exists. Moreover, this simple entanglement structure is realized by random stabilizer tensor networks (RSTNs), which are simple toy models of holography in which the RT formula is satisfied [29, 193].

Our goal is to argue that this entanglement structure is inconsistent with two other conjectured properties of AdS/CFT. Both of these other conjectures relate the so-called "minimal entanglement wedge cross section" $EW(A:B)$, of any two CFT subregions $A$ and $B$, to information theoretic quantities of the CFT. We review these quantities in detail later, though see Fig. 7.1 for a quick visual. In the paper [42], the authors conjectured that $EW(A:B)$ equals one half a quantity called the reflected entropy, $S_R(A:B)$. The evidence for this conjecture is very strong, and we review it later. In the papers [40, 41], the authors conjectured that $EW(A:B)$ equals a quantity called the entanglement of purification, $E_P(A:B)$. There is also good evidence for this conjecture [194, 195, 196]. We shall refer to these as the $S_R$ and $E_P$ conjectures respectively.

Both $S_R$ and $E_P$ are more sensitive probes of multipartite entanglement than the von Neumann entropy is. It is this fact that places the $S_R$ and $E_P$ conjectures in tension with the MBC. Notably, our argument only works if either the $S_R$ or $E_P$ conjecture is true. This is because directly computing $S_R$ and $E_P$ is difficult, so we use their respective conjectures to compute them using the bulk.

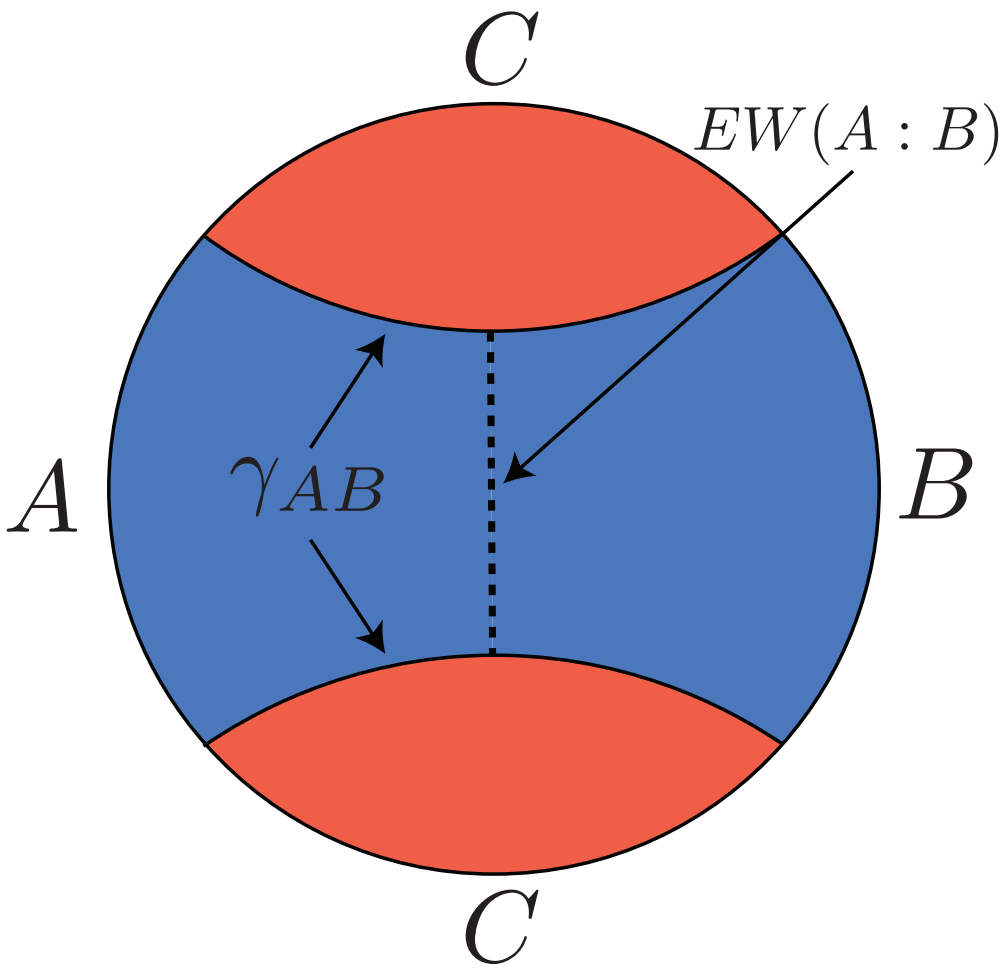


Figure 7.1: The entanglement wedge of boundary subregion $AB$ is shaded blue, while the complementary entanglement wedge, corresponding to boundary subregion $C$, is shaded red. The RT surface is $\gamma_{AB}$ (solid line), and the minimal cross section of the entanglement wedge is $EW(A:B)$ (dashed line).

## The Argument

In detail, our argument proceeds in two steps. First, we compute the reflected entropy and entanglement of purification of the state (7.1) and find that $S_R$ equals the mutual information – and $E_P$ half the mutual information – at leading order, $\mathcal{O}(\frac{1}{G_N})$. This is *not* true of holographic states, if either the $S_R$ or $E_P$ conjecture is correct. It is known that $2EW(A:B) - I(A:B)$ can be non-zero at $\mathcal{O}(\frac{1}{G_N})$, which implies $S_R - I$ and $2E_P - I$ should be non-zero at leading order as well. Therefore the MBC is in tension with the $S_R$ and $E_P$ conjectures.

That said, it is not obvious that this tension persists under small corrections to the MBC

state. Indeed, it is conceivable that some sort of small correction to (7.1) could affect its $S_R$ and $E_P$ at $\mathcal{O}(\frac{1}{G_N})$ while *not* affecting other quantities, such as its von Neumann entropy, at that order. In that case, there would be no tension between these conjectures, because at any finite $G_N$ the state would be of the MBC form up to subleading corrections and also have the correct $S_R$ and $E_P$. Something like this is true for Renyi entropies, where exponentially small changes to a state can affect the Renyi entropy at $\mathcal{O}(\frac{1}{G_N})$ but only change the von Neumann entropy an exponentially small amount.

The second step in our argument is to prove that $S_R$ and $E_P$ are not sensitive to such small changes in the state. More precisely, we prove that $S_R$ and $E_P$ satisfy a Fannes-like continuity inequality so that when the trace distance $\frac{1}{2}||\rho - \sigma||_1$ between $\rho$ and $\sigma$ is $\epsilon$, we have

$$|S_R(A:B)_\rho - S_R(A:B)_\sigma| \leq C_1\sqrt{\epsilon}\log d\ , \tag{7.6}$$

$$|E_P(A:B)_\rho - E_P(A:B)_\sigma| \leq C_2\sqrt{\epsilon}\log d\ , \tag{7.7}$$

where $C_1, C_2$ are $\mathcal{O}(1)$ constants and $d$ is the dimension of $\rho$ and $\sigma$. Moreover, we argue that $\epsilon < \mathcal{O}(1)$ if $\rho$ is a holographic CFT state and $\sigma$ is a state of the form Eq. (7.1). (Otherwise, $\rho$ would not take the MBC state form when $G_N \to 0$.) So, even though $\log d \sim \mathcal{O}(\frac{1}{G_N})$, the $S_R$ and $E_P$ of $\rho$ is not different from that of $\sigma$ at $\mathcal{O}(\frac{1}{G_N})$. Therefore, small corrections to Eq. (7.1) that vanish as $G_N \to 0$ do not resolve the tension between these conjectures.

## Why trace distance?

Before proceeding, let us motivate why we use the trace distance to quantify small corrections. The trace distance is arguably the most natural distance measure between two quantum states. If two states are close in trace distance, then all observables computed using one will be close to those computed using the other, inlcuding the von Neumann entropy. Moreover, other distance measures (such as the fidelity) are quantitatively equivalent to trace distance. There are some quantities, like the relative entropy, that quantify the similarity of two states but are not technically distance measures. The relative entropy would work equally well for our purposes: if the relative entropy between two states is small, then their trace distance is small due to Pinsker's inequality.

That said, there are some senses in which two states can be "close" without being close in trace distance. For example, they can be "close" in the sense that some restricted class of observables has similar values. It is this sense in which, for instance, "random states" are close to "Perfect states." Perfect states are $2n$-partite states that are maximally entangled accross any bipartition, for $n$ integer [28]. We define a random state by acting a Haar random unitary on a fiducial $2n$-partite state. Such random states are "close" to Perfect in the sense that they are nearly maximally entangled accross any bipartition. However, they are generally far from Perfect in trace distance.[1]

[1]This can be seen from a simple counting argument: there are far fewer Perfect states than the total

We choose not to consider "closeness" in this weaker sense because it is arguably against the spirit of the conjecture. Indeed, that the von Neumann entropies of holographic CFT states match those of the MBC state was the *motivation* for the MBC. The conjecture itself, as we understand it, is that the states are therefore close in some distance measure. Inferring this stronger claim about the state from the weaker matching of entropies is what makes the conjecture so valuable.

### Organization

The paper is organized as follows. We define and analyze the $S_R$ and $E_P$ conjectures in Section 7.2 and 7.3 respectively. Also in Section 7.2, we discuss why RSTNs – which satisfy the RT formula – fail to satisfy the $S_R$ conjecture, which naively seems like a simple application of RT. We briefly touch on tensor networks in Section 7.3 as well. Finally, we conclude with some discussion and future directions in Section 7.4.

### Notation

We will use the notation $S_R(A:B)$, $E_P(A:B)$ and $I(A:B)$ to denote the reflected entropy, entanglement of purification and mutual information relevant for the partition of the state about subregions $A$ and $B$. However, in other situations where the partition is understood and we would like to make explicit the state in which these quantities are being evaluated, we shall use the notation $S_R(\rho_{AB})$, $E_P(\rho_{AB})$ and $I(\rho_{AB})$ interchangeably with the above notation.

## 7.2 $S_R$ Conjecture vs Bipartite Entanglement

### Background

We now define the reflected entropy $S_R(A:B)$. Consider a density matrix $\rho_{AB}$ on the Hilbert space $\mathcal{H} = \mathcal{H}_A \otimes \mathcal{H}_B$. One can define its "canonical purification" in a way analogous to the relationship between the thermal density matrix and the thermofield double state [42]. There exists a natural mapping between the space of linear operators acting on a $\mathcal{H}$ and the space of states on a doubled Hilbert space $\mathcal{H} \otimes \mathcal{H}' = \mathcal{H}_A \otimes \mathcal{H}_B \otimes \mathcal{H}_{A'} \otimes \mathcal{H}_{B'}$. This mapping is sometimes labelled the channel-state duality. The inner product on this doubled Hilbert space is defined by

$$\langle \rho | \sigma \rangle_{ABA'B'} = \mathrm{tr}_{AB}(\rho^\dagger \sigma) \ . \tag{7.8}$$

Thus, the operator $\sqrt{\rho_{AB}}$ can be mapped to a state $|\sqrt{\rho_{AB}}\rangle_{ABA'B'}$, which is named the canonical purification of $\rho_{AB}$ (and is also known as the GNS state). This state easily can

number of states. In the limit that the Hilbert space dimension goes to infinity, the average distance between any given state and the nearest Perfect state tends to zero.

be checked to reduce to the original density matrix $\rho_{AB}$ upon tracing out the subregions $A'$ and $B'$. Given the above setup, then

**Definition 2.1:** *The* reflected entropy $S_R(A:B)$ *is defined as*

$$S_R(A:B) = S(AA')_{\sqrt{\rho_{AB}}} = S(BB')_{\sqrt{\rho_{AB}}} \ , \tag{7.9}$$

*where* $S(AA')_{\sqrt{\rho_{AB}}}$ *is the von Neumann entropy of the reduced density matrix on the subregion* $AA'$ *in the state* $|\sqrt{\rho_{AB}}\rangle$.

In [42], it was conjectured that in AdS/CFT,

$$2EW(A:B) = S_R(A:B) \ , \tag{7.10}$$

where $EW(A:B)$ is the area of the "entanglement wedge cross-section," i.e. the minimal-area surface that divides the entanglement wedge of $AB$ into two halves, one homologous to $A$ and the other to $B$. This conjecture is intuitive: the reduced density matrix of $AB$ is unchanged, and $A'B'$ has the same reduced density matrix. One can solve the equations of motion inwards from this data local to the boundary to conclude that a viable bulk solution is the one that is simply two copies of the $AB$ entanglement wedge glued together across the extremal surface that bounds it. (The subtleties of gluing across this extremal surface were discussed in [182].) Applying the RT formula to the $AA'$ region of this doubled bulk implies that $S(AA')_{\sqrt{\rho_{AB}}}$ equals the area of a minimal surface dividing $AA'$ from $BB'$. The symmetry between the entanglement wedges of $AB$ and $A'B'$ implies that this minimal surface has area $2EW$.[2].

## $S_R$ of the Bipartite Entangled State

We now compute the reflected entropy in the MBC state Eq. (7.1) and show that it approximately equals the mutual information,

$$S_R(A:B) \approx I(A:B) \ . \tag{7.11}$$

This, we will argue, is incompatible with AdS/CFT. Two properties of the reflected entropy will be useful to us. First, it is an additive quantity under tensor products:

$$S_R(\rho_1 \otimes \rho_2) = S_R(\rho_1) + S_R(\rho_2) \ . \tag{7.12}$$

This is because the canonical purification of a tensor product density matrix $\rho_1 \otimes \rho_2$ is given by the tensor product state $|\sqrt{\rho_1}\rangle \otimes |\sqrt{\rho_2}\rangle$. Second, the reflected entropy is invariant under unitaries local to $A$ or $B$, since this is equivalent to local unitaries on $A$, $A'$, $B$ and $B'$ in the purified state. Hence the reflected entropy of the MBC state is the same as for the state

$$U_A^\dagger U_B^\dagger \rho_{AB} U_A U_B = \rho_{A_1 B_1} \otimes \rho_{A_2} \otimes \rho_{B_2} \otimes \rho_{A_3 B_3} \ , \tag{7.13}$$

[2]Evidence for the conjecture in a time-dependent situation was provided in [197, 198]

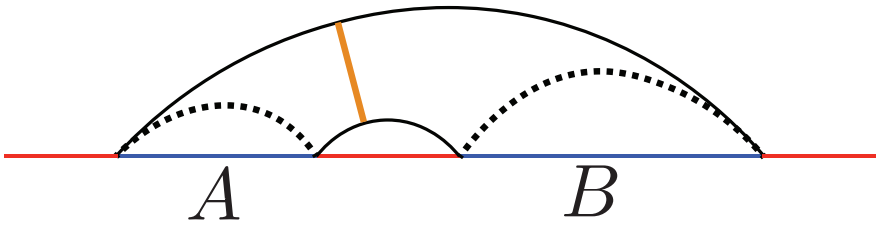


Figure 7.2: Subregion $AB$ at the threshold of a mutual information phase transition. There are two competing RT surfaces, denoted by solid and dashed black lines. The area of the dashed lines is equal to the area of the solid lines. $EW(A:B)$ before the transition is denoted by a solid orange line, while it vanishes after the transition.

where e.g. $\rho_{A_2} = \mathrm{tr}_{C_1}|\psi_2\rangle\langle\psi_2|_{A_2C_1}$. Thus, the calculation of $S_R$ splits into an individual calculation for each factor. First consider $\rho_{A_1B_1} = |\psi_1\rangle\langle\psi_1|_{A_1B_1}$. The canonical purification is simply a product state of two copies of $|\psi_1\rangle$, and therefore

$$S_R(\rho_{A_1B_1}) = 2S(\rho_{A_1}) = I(A_1:B_1)_{\rho_{A_1B_1}} \approx I(\rho_{AB}) \ . \tag{7.14}$$

Because the state $\rho_{A_2}$ only has support on $A$, its canonical purification is given by an entangled state shared between $A$ and $A'$ while $B$ and $B'$ remain trivial. The same argument can be applied to $\rho_{B_2}$ as well. Therefore their reflected entropies vanish,

$$S_R(\rho_{A_2}) = 0 \quad \text{and} \quad S_R(\rho_{B_2}) = 0 \ . \tag{7.15}$$

Although we have not specified any details of the state $|\tilde{\psi}\rangle_{A_3B_3C_3}$, we can use the general inequality

$$S_R(\rho_{A_3B_3}) \leq 2\ \min\{S(\rho_{A_3}), S(\rho_{B_3})\} = O(1) \tag{7.16}$$

to put an upper bound on the contribution to $S_R$ from $\rho_{A_3B_3}$. It is a positive $\mathcal{O}(1)$ number, at most. Putting everything together, we find that the reflected entropy equals

$$\begin{aligned} S_R(\rho_{AB}) &= S_R(\rho_{A_1B_1}) + S_R(\rho_{A_2}) + S_R(\rho_{B_2}) + S_R(\rho_{A_3B_3}) \\ &= I(\rho_{AB}) + O(1) \ . \end{aligned} \tag{7.17}$$

Hence in the $G_N \to 0$ limit, $S_R(A:B) = I(A:B)$ for the MBC state.

### AdS/CFT conflict

We now argue that this is in conflict with $S_R(A:B) = 2EW(A:B)$ in AdS/CFT. The idea is that $EW(A:B)$ can be larger than $I(A:B)$ at $\mathcal{O}(\frac{1}{G_N})$. This is true in many generic cases, but we now provide a sharp example in which this is especially clear, from [199].

Consider the setup in Fig. 7.2. As one varies the distance between subregions $A$ and $B$ of a fixed size, one encounters a phase transition in the RT surfaces. At the phase transition, both $I(A:B)$ and $EW(A:B)$ vanish. However, at slightly shorter separations the two are quite different. While the mutual information continuously shrinks to zero as the separation is increased, the cross-section remains $\mathcal{O}(\frac{1}{G_N})$ until exactly at the phase transition, where it discontinuously jumps to zero. Therefore, given $S_R(A:B) = 2EW(A:B)$, we must conclude that the MBC state is incompatible with AdS/CFT.

## Small Corrections

So far, we have not ruled out that the $S_R$ conjecture is consistent with the MBC state *with small corrections.* One might imagine that the reflected entropy, being non-linear in the state, could receive large corrections from terms that are subleading in $G_N$ to those in Eq. (7.1).[3] Then there would be no tension between the $S_R$ conjecture and MBC: For any finite $G_N$, the holographic CFT state could take the form of the MBC state up to subleading terms, but its reflected entropy could be different at $\mathcal{O}(\frac{1}{G_N})$. For comparison, this is how Renyi entropies work. Renyi entropies are also non-linear in the state, and can change at $\mathcal{O}(\frac{1}{G_N})$ under non-perturbatively small changes to the state.

We quantify corrections to the state in terms of the natural distance measure, trace distance, defined as

$$T(\rho,\sigma) = \frac{1}{2}||\rho-\sigma||_1 \ , \tag{7.18}$$

where $\rho$, $\sigma$ are two density matrices, and $||A||_1 = \mathrm{tr}(\sqrt{A^\dagger A})$ is the Schatten 1-norm or $L_1$ norm. It can take values $T(\rho,\sigma)\in[0,1]$, and when the trace distance is close to 0 then all observables are are close between the states. If the trace distance is exactly zero, then the two states are identically equal. If two states admit a $G_N$ expansion, like $\rho = \rho_0 + G_N\rho_1 + \mathcal{O}(G_N^2)$, then the trace distance between them does as well:

$$T(\rho,\sigma) = T_0(\rho,\sigma) + G_N T_1(\rho,\sigma) + \mathcal{O}(G_N^2) \ . \tag{7.19}$$

We say that two states are the same at leading order if $T_0 = 0$, i.e. $T(\rho,\sigma)\sim\mathcal{O}(G_N)$.[4] For our purposes, we could equally-well use other distance measures between states, such as the fidelity, or similarity measures like the relative entropy.

We interpret the MBC as the statement the trace distance vanishes at leading order in $G_N$ between a holographic CFT state $\rho$ and some state $\sigma$ of the form Eq. (7.1). This is for two reasons. First, as stated above, so that $\rho$ and $\sigma$ become the same in the $G_N\to 0$ limit. Second, because this would give a satisfactory reason for the von Neumann entropies to match at leading order (even at finite $G_N$). (After all, this was essentially the motivation

[3] We would like to thank Matt Headrick for discussions related to this.

[4] In fact, for the purpose of our analysis $T(\rho,\sigma)\sim\mathcal{O}(G_N^a)$ with any $a>0$ works.

for the conjecture in the first place!) This is due to Fannes inequality [200], which states

$$|S(\rho) - S(\sigma)| \leq 2T(\rho,\sigma)\log d - 2T(\rho,\sigma)\log(2T(\rho,\sigma)) \ , \tag{7.20}$$

where $d$ is the dimension of $\rho$ and $\sigma$. For holographic CFTs, $\log d \sim \mathcal{O}(\frac{1}{G_N})$, and thus if $T(\rho,\sigma) \lesssim \mathcal{O}(G_N)$, the von Neumann entropies will be guaranteed to match at $\mathcal{O}(\frac{1}{G_N})$.

So, we are interested in whether the reflected entropy can differ at $\mathcal{O}(\frac{1}{G_N})$ between the MBC state $\sigma$ and a holographic CFT state $\rho$ that differs from it only at $\mathcal{O}(G_N)$ and higher,

$$T(\rho,\sigma) \sim \mathcal{O}(G_N) \ . \tag{7.21}$$

We now prove this is, in fact, not possible; the reflected entropy satisfies a continuity inequality similar to Fannes inequality for the von Neumann entropy.

**Theorem 2** (Continuity of the Reflected Entropy)**.** Given two density matrices $\rho_{AB}$ and $\sigma_{AB}$ defined on a Hilbert space $\mathcal{H} = \mathcal{H}_A \otimes \mathcal{H}_B$ of dimension $d = d_A\, d_B$, such that $T_{AB} = T(\rho_{AB}, \sigma_{AB}) \leq \epsilon$, then

$$|S_R(\rho_{AB}) - S_R(\sigma_{AB})| \leq 4\sqrt{2T_{AB}}\log(\min\{d_A, d_B\}) - 2\sqrt{2T_{AB}}\log(T_{AB})$$

for $\epsilon \leq \frac{1}{8e^2}$.

*Proof.* In order to prove the above statement, we first consider the fidelity between the respective purified states $|\sqrt{\rho_{AB}}\rangle_{ABA'B'}$ and $|\sqrt{\sigma_{AB}}\rangle_{ABA'B'}$, which is given by

$$F_{ABA'B'} = |\,\langle\sqrt{\rho_{AB}}|\sqrt{\sigma_{AB}}\rangle\,| \ . \tag{7.22}$$

The inner product on the canonically purified states can equivalently be computed using the original density matrices by using Eq. (7.8),

$$\langle\sqrt{\rho_{AB}}|\sqrt{\sigma_{AB}}\rangle = \mathrm{tr}(\sqrt{\rho_{AB}}\sqrt{\sigma_{AB}}) \tag{7.23}$$

$$= Q_{1/2}(\rho_{AB}, \sigma_{AB}), \tag{7.24}$$

where $Q_{1/2}(\rho_{AB}, \sigma_{AB})$ is defined by the above equation and is the non-commutative generalization of the Bhattacharya coefficient.[5] Now we can use the inequality [201]

$$Q_{1/2}(\rho_{AB}, \sigma_{AB}) \geq 1 - T_{AB} \tag{7.25}$$

$$\implies F_{ABA'B'} = Q_{1/2}(\rho_{AB}, \sigma_{AB}) \geq 1 - T_{AB} \ . \tag{7.26}$$

This is essentially equivalent to the well known Powers-Stormer inequality. Upon tracing out $B$ and $B'$, the fidelity monotonically increases giving us

$$F_{AA'} \geq F_{ABA'B'} \geq 1 - T_{AB} \ . \tag{7.27}$$

[5]Note that $Q_{1/2}$ is a real quantity, which can be proven using cyclicity of trace and the fact that density matrices are Hermitian.

Now, we can use another well-known inequality relating fidelity to trace distance [201], giving us

$$T(\rho_{AA'}, \sigma_{AA'}) \leq \sqrt{1 - F^2_{AA'}} \leq \sqrt{2T_{AB}} \ , \tag{7.28}$$

where e.g., $\rho_{AA'}$ is the density matrix obtained by tracing out $BB'$ from the purified state $|\sqrt{\rho_{AB}}\rangle$. The second inequality in Eq. (7.28) follows from Eq. (7.27). Thus, starting from $\rho$ and $\sigma$ being $\epsilon$-close in trace distance on subregion $AB$, we have shown that their canonical purifications are $\sqrt{\epsilon}$-close in trace distance on subregion $AA'$. Finally, we use Fannes inequality [200] to show that

$$\begin{aligned} |S_R(A:B)_\rho - S_R(A:B)_\sigma| &= |S(\rho_{AA'}) - S(\sigma_{AA'})| \\ &\leq 2T_{AA'} \log(d_{AA'}) - 2T_{AA'} \log(2T_{AA'}) \\ &\leq 4\sqrt{2T_{AB}} \log(d_A) - 2\sqrt{2T_{AB}} \log(T_{AB}), \end{aligned} \tag{7.29}$$

where $T_{AA'} = T(\rho_{AA'}, \sigma_{AA'})$.[6] This inequality holds for $T_{AA'} \leq \frac{1}{2e}$, which is ensured by the bound $\epsilon \leq \frac{1}{8e^2}$. The entire analysis above was perfectly symmetric between $A$ and $B$, and from Eq. (7.9) we also have

$$|S_R(A:B)_\rho - S_R(A:B)_\sigma| \leq 4\sqrt{2T_{AB}} \log(d_B) - 2\sqrt{2T_{AB}} \log(T_{AB}). \tag{7.30}$$

Thus, combining Eq. (7.29) and Eq. (7.30), we get the strengthened inequality

$$|S_R(A:B)_\rho - S_R(A:B)_\sigma| \leq 4\sqrt{2T_{AB}} \log(\min\{d_A, d_B\}) - 2\sqrt{2T_{AB}} \log(T_{AB}) \ , \tag{7.31}$$

which proves Theorem 2. □

Note that it was crucial that we considered the *canonical* purification in order for e.g. $|S(\rho_{AA'}) - S(\sigma_{AA'})|$ to have such a bound. An arbitrary purification on $ABA'B'$ can be arbitrarily far in trace distance. For example, different Bell pairs purify a maximally mixed density matrix and have trace distance 1. The canonical purification ensures this redundancy in basis of purification doesn't play a role here.

We also emphasize that we have not found any examples where the inequality in Theorem (2) is saturated, despite the fact that it is easy to saturate all the individual inequalities required in proving it. Our preliminary numerical analysis suggests that $|S_R(\rho) - S_R(\sigma)| \sim O(\epsilon)$ in all the examples that we tested, instead of the $O(\sqrt{\epsilon})$ allowed by Theorem 2. This leaves open the possibility that a tighter bound exists. We haven't pursued a systematic numerical analysis of the above, but it would be interesting to probe this question in future.

[6] This result can be further tightened by using the Audenaart version of the inequality [202].

## Implication for AdS/CFT

Theorem 2 renders it impossible for two states $\rho_{AB}, \sigma_{AB}$ to have reflected entropy different at $\mathcal{O}(\frac{1}{G_N})$ unless $\sqrt{T_{AB}} \log d_{AB}$ is also $\mathcal{O}(\frac{1}{G_N})$. In a holographic CFT, $\log d_{AB} \sim \mathcal{O}(\frac{1}{G_N})$. So, the trace distance would need to be non-zero at leading order, $T_{AB} \sim \mathcal{O}(1)$.

However, this is not consistent with the MBC. Suppose $\sigma_{ABC}$ represents the density matrix corresponding to the MBC state, and $\rho_{ABC}$ represents the actual density matrix of a holographic CFT. As we argued above, the MBC requires they should be close in the sense that $T_{ABC} \equiv T(\rho_{ABC}, \sigma_{ABC}) \sim \mathcal{O}(G_N)$. Trace distances decrease under tracing out subregions, so $T_{AB} \leq T_{ABC} \sim \mathcal{O}(G_N)$. Therefore, $T_{AB}$ is too small for $\sigma$ and $\rho$ to have different reflected entropy at $\mathcal{O}(\frac{1}{G_N})$.

Said differently, Theorem 2 states that if $T_{ABC}$ is indeed $\mathcal{O}(G_N)$, then

$$|S_R(\rho_{AB}) - S_R(\sigma_{AB}))| = |2EW(A:B) - I(A:B)| \lesssim \mathcal{O}\left(\frac{1}{\sqrt{G_N}}\right) , \tag{7.32}$$

where we have used the $S_R$ conjecture in the equality and Theorem 2 in the inequality. This contradicts the fact that there exist examples in AdS/CFT where $|2EW(A:B) - I(A:B)| \sim \mathcal{O}(\frac{1}{G_N})$, e.g. the situation in Fig. 7.2. Thus, we see that even small corrections to the MBC state are incapable of making it compatible with the $S_R$ conjecture.

## Tensor Networks

We now resolve a conundrum that our results seem to create in tensor networks. Tensor networks have provided good toy models of holography, illustrating properties such as subregion duality and the RT formula. In particular, a network made of perfect tensors can be shown to satisfy the RT formula under certain reasonable assumptions [28]. Much more generally, it was shown that networks made from Haar random tensors also satisfy the RT formula [29].

It was also emphasized in [29] that Haar randomness was overkill, and the RT formula followed simply from choosing random tensors from a 2-design ensemble, i.e. one that agrees with the first two moments of the Haar measure. A particularly nice choice of 2-design ensemble is provided by stabilizer tensors of dimension $D = p^N$ in the limit of large $N$, where $p$ is a prime number. Such random stabilizer tensor networks (RSTN) were further studied in [193], where it was proven that their states always take the form

$$|\psi\rangle_{ABC} = U_A^\dagger U_B^\dagger U_C^\dagger |\phi^+\rangle_{A_1B_1}^{\otimes n_1} |\phi^+\rangle_{A_2C_1}^{\otimes n_2} |\phi^+\rangle_{B_2C_2}^{\otimes n_3} |\mathrm{GHZ}\rangle_{A_3B_3C_3}^{\otimes n_g} \tag{7.33}$$

where $|\phi^+\rangle$ denotes a $p$-dimensional Bell pair shared between the two parties, e.g.

$$|\phi^+\rangle_{A_1B_1} \equiv \frac{1}{\sqrt{p}} \sum_{i=0}^{p-1} |i\rangle_{A_1} |i\rangle_{B_1} , \tag{7.34}$$

and $|\text{GHZ}\rangle$ denotes a shared $p$-dimensional GHZ state,

$$|\text{GHZ}\rangle_{A_3B_3C_3} = \frac{1}{\sqrt{p}} \sum_{i=0}^{p-1} |i\rangle_{A_3} |i\rangle_{B_3} |i\rangle_{C_3} \ . \tag{7.35}$$

Neither of these states scale with $N$; they are elementary units of entanglement. The exponents, however, can indeed have $N$-dependence. That $N$-dependence was discovered in [193], where it was shown that in the large $N$ limit, $n_1$, $n_2$ and $n_3$ grow linearly with $N$, whereas $n_g$ remains $\mathcal{O}(1)$. Note that $N$ here is analogous to $\frac{1}{G_N}$ in AdS/CFT.

This is exactly an MBC state like that in Eq. (7.1). Our result in Section 7.2 shows that this is incompatible with the conjecture $S_R = 2EW$. This is startling at first: the $S_R$ conjecture was motivated by the RT formula, which RSTN satisfy. So, naively, we would expect RSTN to satisfy $S_R = 2EW$.

We now compute $S_R(A:B)$ in RSTN to explain why they, in fact, do not. The upshot will be that while the canonical purification of a state $\rho_{AB}$ is indeed given by a doubled version of its entanglement wedge (just like in AdS/CFT), the doubled entanglement wedge network does not itself satisfy RT in the naive way!

Consider the tensor network in Fig. 7.3. In order to restrict to $\rho_{AB}$, we can use the fact that there is an isometry from the boundary legs of subregion $C$ to the in-plane legs cut by the RT surface of subregion $AB$. This gives us an effective tensor network restricted to the entanglement wedge of $AB$. In order to compute the density matrix $\rho_{AB}$, we can glue together two copies of this tensor network as in Fig. 7.4. The density matrix $\rho_{AB}$ has a flat entanglement spectrum as can be seen from Eq. (7.33). Thus, it can be shown that the operator $\sqrt{\rho_{AB}}$, and hence the canonically purified state $|\sqrt{\rho_{AB}}\rangle_{ABA'B'}$ is represented by the same doubled tensor network TN' depicted in Fig. 7.4 up to normalization.

TN' geometrically resembles the bulk saddle geometry obtained in the holographic construction discussed in [42]. If TN' were to satisfy the RT formula, one would indeed be led to the claim that the entropy of subregion $AA'$ is computed by the minimal cross section in this effective tensor network. The RT surface in TN' is indeed just twice the original entanglement wedge cross section, and thus, we would have the conjectured result, $S_R(A:B) = 2EW(A:B)$.

However, this naive argument doesn't carry through because TN' has certain special properties that distinguish it from a completely random stabilizer tensor network. Importantly, the set of tensors used in Copy 2 in TN' are precisely correlated with the tensors in Copy 1. E.g., in Fig. 7.4, one can see $T_1^\dagger$ and $T_1$ placed at equivalent positions in either copy. The derivation of the RT formula depended on having completely uncorrelated tensors on both copies of the TN.

That this correlation spoils the RT formula is made manifest by the form of the state $|\psi\rangle_{ABC}$ in Eq. (7.33). After applying the local unitaries, which depend sensitively on the choice of tensors in the network, one gets a drastically simplified network as seen in Fig. 7.5. The canonical purification then takes a simple form, and computing $S(AA')$ in this simple

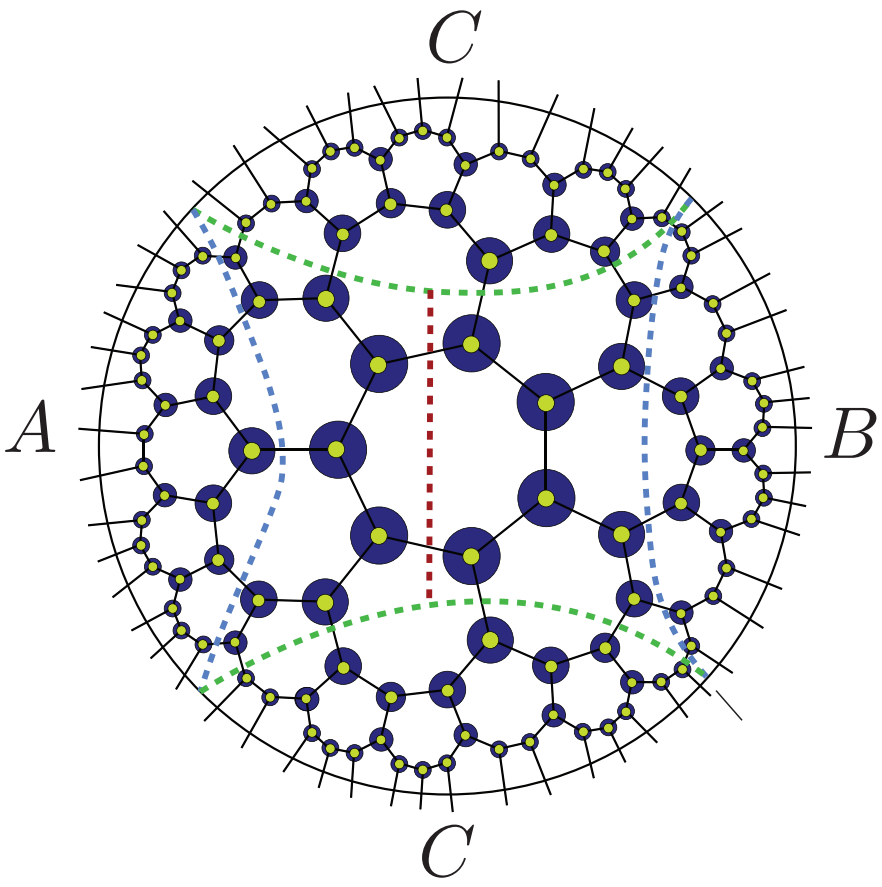


Figure 7.3: A random stabilizer tensor network with subregion $AB$ in the connected phase. The green dotted line represents the RT surface for subregion $AB$, while the yellow dotted lines represent the RT surface of $A$ and $B$ respectively. The red dotted line represents $EW(A:B)$.

network gives us

$$S_R(A:B) = 2n_1 \log p = I(A:B) \ . \tag{7.36}$$

We see that RSTN do not satisfy $S_R = 2EW$ because having correlated tensors precludes the application of the RT formula.

Indeed, the RT formula in the original RSTN only required the tensors be 2-designs. We expect that having the tensors agree with even higher moments of the Haar measure is sufficient for the network to continue to satisfy the RT formula, even when the network is built out of many copies of itself. If true, then the random tensor networks of [29] should satisfy the $S_R$ conjecture, and highly random tensors – rather than e.g. 2-designs – would be better models of holography. This is the subject of ongoing work [203].

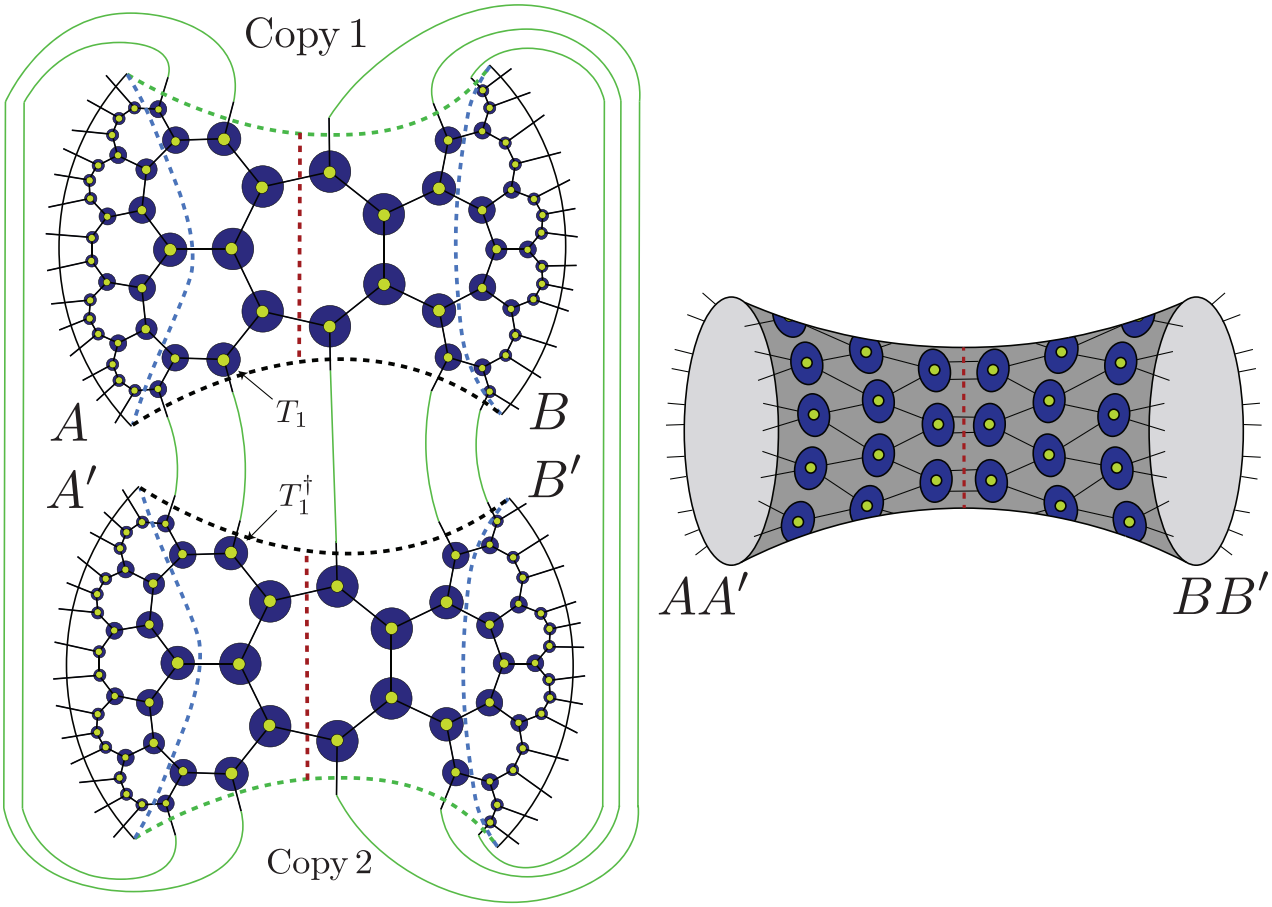


Figure 7.4: (Left): A reduced tensor network corresponding to the entanglement wedge of $AB$ is obtained by using the isometry from the boundary legs of subregion $C$ to the legs at the RT surface (denoted black and green dotted lines). Two copies of this RSTN glued as shown prepare the canonically purified state. We call this doubled network TN'.
(Right): Geometrically, this resembles the AdS/CFT construction discussed in [181, 182, 42]. If the RT formula holds, then $S_R(A:B) = 2EW(A:B)$.

## 7.3 $E_P$ Conjecture vs Bipartite Entanglement

There is a tension between the $E_P$ conjecture and the MBC that is qualitatively the same as that between the $S_R$ conjecture and the MBC. Given a density matrix $\rho_{AB}$, one can define its entanglement of purification as [204]

$$E_P(A:B) = \min_{|\psi\rangle} S(AA') \ , \tag{7.37}$$

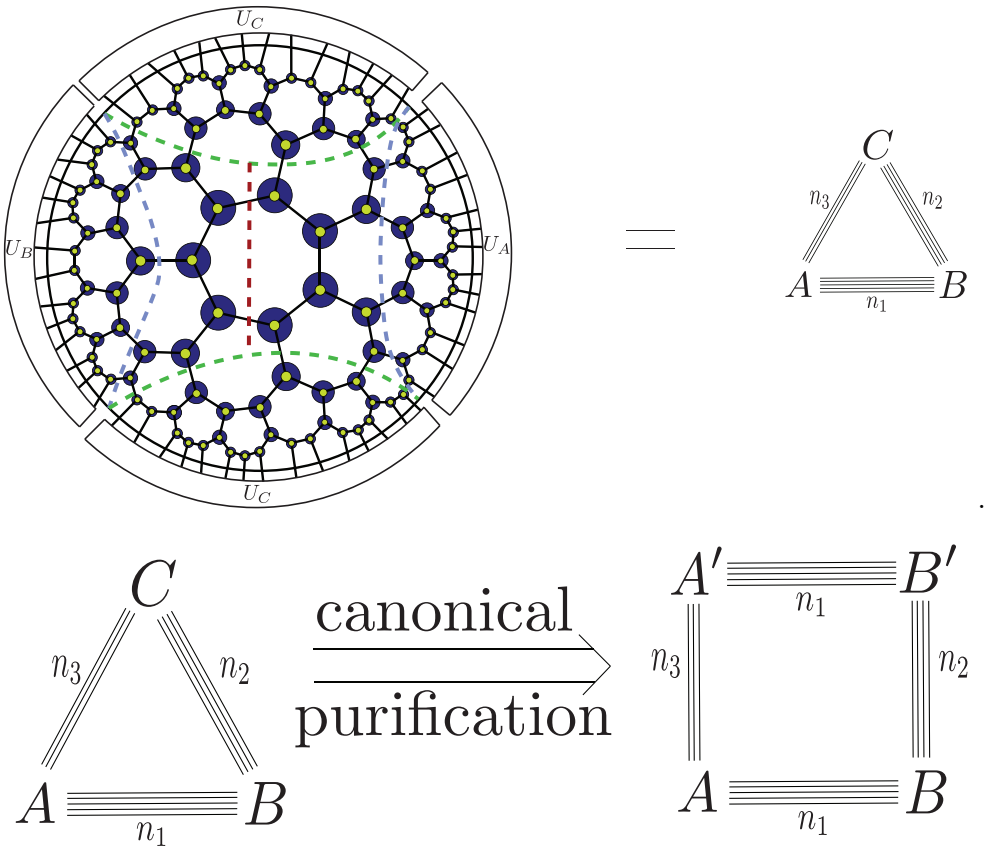


Figure 7.5: After applying local unitaries, the RSTN drastically simplifies to a combination of Bell pairs shared by the three parties. The Bell pairs then lead to a simple canonically purified state.

where the minimization is over all states $|\psi\rangle_{ABA'B'}$ that are pure and consistent with the reduced density matrix $\rho_{AB}$. In [40, 41], it was conjectured that in AdS/CFT

$$E_P(A:B) = EW(A:B). \tag{7.38}$$

This conjecture was motivated by the surface-state correspondence, wherein similar to tensor networks, a holographic state can be defined on any convex surface in the bulk [57, 35, 205, 206]. Further, since the minimization over all possible purifications is a computationally intractable problem, it was assumed that minimizing over geometric purifications was sufficient (for discussions of this point, see [207]). This conjecture, along with its multipartite generalizations, has received a lot of attention recently, although proofs or related computations have generally required various strong assumptions [208, 209, 210, 211, 196, 212, 194, 195, 213, 214, 215].

To argue that the $E_P$ conjecture is incompatible with the MBC, we review results that

are essentially known in the literature. This distinguishes this argument from the one in Section 7.2, which involved our Theorem 2 that was completely new.

In order to compute $E_P(A:B)$ in the MBC state, we first note that $E_P$ is a sub-additive quantity under tensor products [216]. In fact, additivity holds for pure states, $\rho_{AB} = |\psi\rangle_{AB}\langle\psi|_{AB}$, and completely decoupled states, $\rho_{AB} = \rho_A \otimes \rho_B$, but not in general [217]. Using this property, we find for the MBC state

$$E_P(\rho_{AB}) \leq E_P(\rho_{A_1\,B_1}) + E_P(\rho_{A_2}) + E_P(\rho_{B_2}) + E_P(\rho_{A_3\,B_3}). \tag{7.39}$$

The first term on the right hand side gives $E_P(\rho_{A_1B_1}) = S(\rho_{A_1}) = \frac{1}{2}I(A_1:B_1)$, because $\rho_{A_1B_1}$ is a pure state. The second and third terms involve only one of either $A$ or $B$ and thus give $E_P(\rho_{A_2}) = E_P(\rho_{B_2}) = 0$. The fourth term can be bounded using the known inequalities for $E_P$ to obtain

$$0 \leq E_P(\rho_{A_3\,B_3}) \leq 2\min\{S(\rho_{A_3}), S(\rho_{B_3})\}, \tag{7.40}$$

and thus, $E_P(\rho_{A_3\,B_3})$ is an $O(1)$ positive quantity. Putting these results together and using known inequalities, we find that

$$\frac{1}{2}I(A:B) \leq E_P(\rho_{AB}) \leq \frac{1}{2}I(A:B) + O(1). \tag{7.41}$$

Thus, for $G_N \to 0$, we obtain $E_P(A:B) \approx \frac{1}{2}I(A:B)$, where " $\approx$" denotes matching at $\mathcal{O}(\frac{1}{G_N})$. Similar to the result in Section 7.2, we find that the MBC state is incompatible with the $E_P$ conjecture.

## Small Corrections

One might again worry that small corrections to the MBC state might make it compatible with the $E_P$ conjecture. However, this too can be ruled out by the following theorem.

**Theorem 3** (Continuity of the Entanglement of Purification)**.** Given two density matrices $\rho_{AB}$ and $\sigma_{AB}$ defined on a Hilbert space $\mathcal{H} = \mathcal{H}_\mathcal{A} \otimes \mathcal{H}_\mathcal{B}$ of dimension $d = d_A\, d_B$, such that $T_{AB} = T(\rho_{AB}, \sigma_{AB}) \leq \epsilon$, then

$$|E_P(\rho_{AB}) - E_P(\sigma_{AB})| \leq 40\sqrt{T_{AB}}\log(d) - 4\sqrt{T_{AB}}\log(4\sqrt{T_{AB}})$$

for $\epsilon \leq \frac{1}{4e^2}$.

*Proof.* This proof essentially follows from Theorem 1 of [204], where it was shown that

$$|E_P(\rho_{AB}) - E_P(\sigma_{AB})| \leq 20D(\rho_{AB}, \sigma_{AB})\log(d) - D(\rho_{AB}, \sigma_{AB})\log(D(\rho_{AB}, \sigma_{AB})) \tag{7.42}$$

where $D(\rho_{AB}, \sigma_{AB}) = 2\sqrt{1 - F_{AB}}$ is the Bures distance. Using the inequality

$$1 - T_{AB} \leq F_{AB} \implies D(\rho_{AB}, \sigma_{AB}) \leq 2\sqrt{T_{AB}}, \tag{7.43}$$

we obtain the desired result. □

Using Theorem 3, we conclude that a slightly-corrected MBC state is still incompatible with the $E_P$ conjecture, by a similar argument to the one made in Section 7.2.

### Tensor Networks

$E_P$ is a difficult quantity to compute in general, and hence it is much harder to understand the tensor network story analogous to that in Section 7.2. However, in the case of RSTNs, the simplified network (obtained by applying local unitaries, as in Fig. 7.5) has an $E_P$ that can easily be calculated to give $\frac{1}{2}I(A:B)$ at leading order in $G_N$.

It is important to note that the $E_P$ conjecture was originally motivated by restricting to geometric purifications and computing the optimal RT surface anchored to the entanglement wedge. An important insight we gain here is that non-geometric tensor networks like the simplified network were crucial for the minimization in computing $E_P$, at least for RSTNs. It would be interesting to understand if this is more generally true [207].

## 7.4 Discussion

We have provided two pieces of evidence that suggest that holographic states require a large amount of tripartite entanglement: Having little tripartite entanglement is inconsistent with both the strongly-supported conjectures that $S_R = 2EW$ and $E_P = EW$. We now focus on some of the caveats, implications, and interesting future directions stemming from this work.

### Trace distance

We have demonstrated that holographic CFT states cannot be close in trace distance to the MBC state. It is still possible that they are "close" in another sense. Being close in trace distance is a strong criterion that ensures closeness in all observable quantities and is a standard measure of similarity of states in quantum information. If we allow weaker conditions of closeness on the state, such as closeness in a restricted class of observable quantities, it might be possible to make the MBC state consistent with the $S_R$ and $E_P$ conjectures. However, we do not see any evidence for other quantities that may be reproduced by assuming an MBC state, and in particular, measures of multipartite entanglement are in conflict with the conjectured state. It would be interesting to see if other weaker forms of closeness can lead to a version of the MBC that is both useful and compatible with the other two conjectures.

### Limitation on Tensor Networks

This analysis also illuminates limitations of tensor networks as toy models of holography. Since the von Neumann entropy is a reasonably coarse grained quantity, even 2-design tensor networks such as random stabilizer tensor networks were able to reproduce the RT formula. However, stabilizers are a very special class of tensors, and are generically far in trace distance from Haar random tensors (owing to the fact that there are many more Haar random tensors

than stabilizers). Hence, properties from any such tensor networks should be considered carefully, because they may not agree with actual holographic answers.

In fact, specific tensor network models have previously been used to model "mostly bipartite" entanglement that arises in certain regions of moduli space of multiboundary wormholes [218, 219]. It would be interesting to explore whether more refined tensor network models can capture the right form of multipartite entanglement employed by holographic states.

It is interesting to note that the tensor network in [220, 221] is close in trace distance to the holographic state, by construction. Certain classes of their tensor networks require the $E_P = EW$ conjecture, so it would be interesting to repeat the above analysis in their case.

## Entanglement measures

As we saw in our analysis in Section 7.2, the reflected entropy $S_R(A:B)$ is a much more fine-grained entanglement measure than individual entanglement entropies, for mixed density matrices. This quantity is very naturally motivated from holography and hasn't yet been studied in the quantum information literature. In this sense, it is similar to the refined Renyi entropies which is also a very natural quantity in holography, but hasn't been analyzed in quantum information [163, 38, 166, 222]. It would be interesting to understand its properties and generic behaviour in quantum systems.

There is, in fact, a zoo of quantities that measure multipartite entanglement and there is not a clear understanding of a canonically best choice. Owing to this fact, there have been many proposals in holography for such quantities including, among many others, the entanglement negativity and odd entropy [223, 224, 225, 199]. Similarly, higher party versions of the reflected entropy have also been proposed, motivated by AdS/CFT [226, 227, 228]. It would be interesting to understand each of these quantities in the context of holography, or even toy models such as tensor networks. If the program of understanding quantum gravity by understanding quantum information is to progress, it is crucial that we obtain a more refined understanding of multipartite entanglement measures.

## Applications for reflected entropy continuity

Our new bound in Theorem 2 has many interesting applications. For example, it might be useful in proving inequalities about $S_R$ that were conjectured in [42]. Indeed, those inequalities might be easier to prove for e.g. the fixed-area states defined in [38, 166]. Holographic CFT states are generally close in trace distance to one fixed-area state. So, bounds on the reflected entropy of one translate to bounds on the reflected entropy of the other. It would be interesting to find other uses for this theorem.

## GHZ isn't enough

While we have demonstrated that tripartite entanglement is necessary for the $S_R$ and $E_P$ conjectures, we have not emphasized what type of tripartite entanglement is required. In fact, GHZ entanglement – even a lot of it – does not help. One can show that GHZ entanglement also satisfies $S_R(A:B) = I(A:B)$. (Note that this problem is also not resolved by adding superselection sectors, similar to the $\alpha$ blocks in operator-algebra quantum error correction [27, 38, 166, 229]. These results strongly suggest that the "stabilizerness" of holographic states is very low, which will be discussed in upcoming work [230].[7])

Beyond this, there is little we can say. It is difficult to pinpoint what type of entanglement must be present, because there are many inequivalent forms of tripartite entanglement, and the classification is not well understood in general. In the case of three qubits, there are just two inequivalent forms of entanglement: GHZ and W [231]. For $A, B$ two of the three qubits in a W-state, $S_R(A:B) = 1.49\log 2$ while $I(A:B) = 0.92\log 2$, and therefore W-entanglement might be used to alleviate the gap between the MBC (and RSTNs) and holography. Similarly, numerical analyses suggest that $E_P(A:B) \neq \frac{1}{2}I(A:B)$ for such states [204, 217]. It would be interesting understand better the particular kind of tripartite entanglement that is crucial for holography.

[7] We thank Brian Swingle for discussions related to this.

# Chapter 8

# Islands for Reflected Entropy

## 8.1 Introduction

The black hole information paradox, in its various versions, has been a longstanding hurdle in our understanding of quantum gravity [1, 2, 232, 4, 5]. It was long believed that a UV complete description of the black hole evaporation process would be a necessary ingredient for resolving the paradox. However, significant progress has been made recently in resolving this issue within the realm of semiclassical gravity by invoking a new rule - the so called "islands formula" [44, 47, 46, 45, 48] [1].

The proposal to compute the fine-grained von Neumann entropy $S(A)$ of the subregion $A$ is given by

$$S(A) = S^{(\text{eff})}(A \cup \text{Is}(A)) + \frac{\text{Area}[\partial \text{Is}(A)]}{4G_N}, \tag{8.1}$$

where $S^{(\text{eff})}(A \cup \text{Is}(A))$ represents the von Neumann entropy computed in the effective semiclassical theory that includes contributions from possible *entanglement islands*, in the gravitating region, denoted $\text{Is}(A)$. In a general time-dependent situation, the location of the island is computed using a maximin procedure as we review in Section 8.2 [233]. This formula was first justified by considering holographic matter which itself has a bulk dual in [46], and then proved using the gravitational path integral in [45, 48]. An essential feature of the proof was the inclusion of new saddles in the path integral that are wormhole solutions connecting different replica manifolds. Importantly, entanglement islands can also be understood as a part of the *entanglement wedge* [128, 24, 116, 234], which is determined by Ryu-Takayanagi surface[18, 19, 20], within which bulk operators can be reconstructed by an observer sitting at the AdS boundary. For discussions on such reconstruction in the context of black hole information, see [45, 235, 236, 237].

In this paper we consider a bipartite correlation measure, the *reflected entropy* [42]. Given a reduced density matrix $\rho_{AB}$, one can canonically purify the state as $|\sqrt{\rho_{AB}}\rangle_{ABA'B'}$ in a

[1] For other related work, see [50] and references therein

doubled copy of the Hilbert space which includes subregions $A'$ and $B'$. This is the familiar procedure that one considers in going from the thermal density matrix to the thermofield double state [69]. Given this state, the reflected entropy is defined as

$$S_R(A:B) = S(AA'). \tag{8.2}$$

The reflected entropy serves as a measure of correlations between subregions $A$ and $B$, which includes both classical and quantum correlations [199, 225]. It satisfies various inequalities that make it consistent with this interpretation. This quantity, being a different measure of multipartite entanglement, often allows us to distinguish the fine structure of entanglement which the von Neumann entropy cannot capture [43]. Interestingly, it has a simple holographic dual, the "entanglement wedge cross section" which was originally proposed as a dual to the entanglement of purification, $E_P(A:B)$ [40, 41] [2].

In this paper, we propose an "islands formula" that captures reflected entropy in the presence of entanglement islands by relating it to the reflected entropy in the effective semi-classical theory. Concretely, the proposal is

$$S_R(A:B) = S_R^{(\text{eff})}(A \cup \text{Is}_R(A) : B \cup \text{Is}_R(B)) + \frac{\text{Area}[\partial \text{Is}_R(A) \cap \partial \text{Is}_R(B)]}{2G_N}, \tag{8.3}$$

where the *reflected entropy islands*, denoted $\text{Is}_R(A)$ and $\text{Is}_R(B)$, split the entanglement island $\text{Is}(AB)$ into two parts. We emphasize that these are in general different from the entanglement islands $\text{Is}(A)$ and $\text{Is}(B)$, and are also computed by a maximin procedure that we describe in Section 8.2.

This formula can be motivated by considering a $d$ dimensional BCFT dual to $d$ dimensional holographic matter, which itself has a $d+1$ dimensional bulk dual, i.e., the so called double holography scenario of [46]. In this case, we can simply use the entanglement wedge cross section to compute the reflected entropy. As seen in Fig. 8.1, the $d+1$ dimensional entanglement wedge cross section could reach the island, in which case there would be additional contributions from the perspective of the effective $d$ dimensional theory. This can be captured by the modified formula in Eq. (8.3).

In the remainder of this paper, we try to demonstrate how the proposed formula is applicable to much more general situations. In Section 8.2, we describe the proposed formula in Eq. (8.3) in detail, utilizing a maximin procedure to demonstrate that it indeed satisfies all the required properties of reflected entropy in a general time-dependent situation. In Section 8.3, we then provide a derivation of the above formula with a replica trick argument using the Euclidean gravitational path integral. We restrict to time-independent situations for convenience but the arguments are general enough that they can be extended to time-dependent cases. In Section 8.4, we then illustrate the use of the islands formula in various examples. This analysis sheds light on the structure of multipartite entanglement in the

[2] Note that $E_P(A:B)$ is a far harder quantity to compute away from Gaussian approximations [194, 213] and hence, it is difficult to prove statements about it. However, it is quite plausible that our modified formula for the reflected entropy $S_R(A:B)$ might extend to the case of $E_P(A:B)$. See [195, 199]

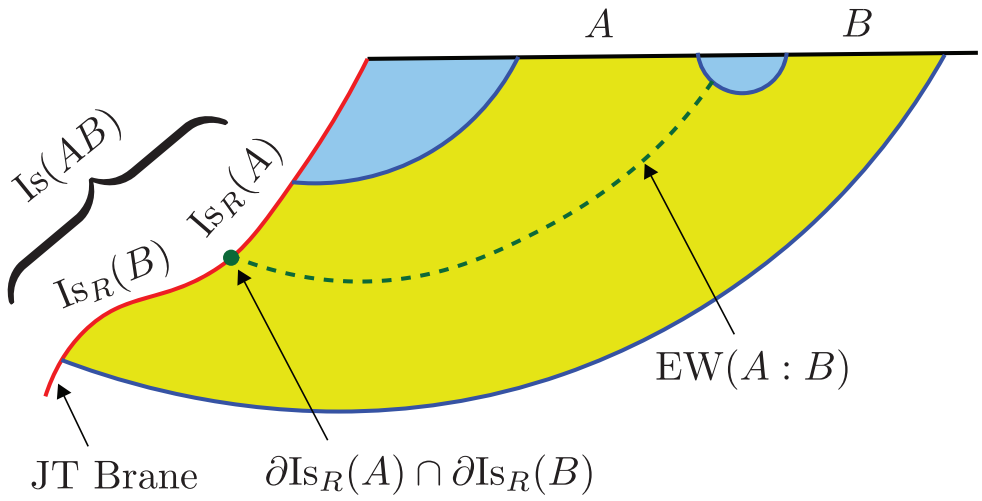


Figure 8.1: A $d$ dimensional BCFT has a $d$ dimensional effective description in terms of a gravitating brane coupled to flat space. In the presence of holographic matter, this effective theory itself has a $d+1$ dimensional bulk dual. The reflected entropy of the regions $A$ and $B$ in the BCFT can be computed using the entanglement wedge cross section $\mathrm{EW}(A:B)$ in the $d+1$ dimensional bulk dual. From the perspective of the effective $d$ dimensional theory, this leads to the islands formula of Eq. (8.3).

Hawking radiation, and demonstrates an interesting phase transition in the behaviour that isn't captured by the entanglement entropy. Finally, we discuss some implications of our analysis and interesting future directions in Section 8.5.

Note: This paper is being released in coordination with [238] which has some overlap with our work.

## 8.2 Islands Formula

### Proposal

In the presence of gravitating regions, the maximin formula for computing entanglement entropy is given by [233]

$$S(A) = \underset{\Sigma}{\mathrm{Max}}\underset{I\subset\Sigma}{\mathrm{Min}}\Big[S^{(\mathrm{eff})}(A\cup I) + \frac{\mathrm{Area}[\partial I]}{4G_N}\Big], \tag{8.4}$$

where one considers arbitrary Cauchy slices $\Sigma$ that include $A$ and finds the island $I$ on each $\Sigma$ that minimizes the hybrid entropy functional in Eq. (8.4) [3]. Then, we finally maximize over the choice of slice which results in an entanglement island that extremizes the hybrid entropy, which we shall denote as $\text{Is}(A)$.

In analogy with the holographic proposal in [42], we propose to use a similar procedure for computing the reflected entropy between regions $A$ and $B$. One first fixes the entanglement wedge of the region $AB$ by finding the relevant island $\text{Is}(AB)$. Then, we split it into two portions divided by a "minimal" entanglement wedge cross section on arbitrary Cauchy slices $\Sigma$ that contain $AB$ and $\text{Is}(AB)$. More precisely, we choose $I_A$ and $I_B$ such that $I_A \cup I_B = D(\text{Is}(AB)) \cap \Sigma$ where $D(\text{Is}(AB))$ is the causal domain of dependence of $\text{Is}(A)$. Finally one maximizes over the choice of slice to obtain

$$S_R(A:B) = \underset{\Sigma}{\text{Max}} \underset{I_A \cup I_B \subset \Sigma}{\text{Min}} \Big[ S_R^{(\text{eff})}(A \cup I_A : B \cup I_B) + \frac{\text{Area}[\partial I_A \cap \partial I_B]}{2G_N} \Big]. \tag{8.5}$$

It is useful to think of Eq. (8.5) as applying the usual islands formula, Eq. (8.4), in the state $|\sqrt{\rho_{AB}}\rangle$ [4]. In the non-gravitating regions, it is clear what this operation does, but it is much less clear how the gravitating regions change under this procedure. It has been proposed that one should glue a CPT conjugate copy of the geometry across the quantum extremal surface for the subregion $AB$ [181, 182, 42, 239]. The bulk state is chosen to be the canonical purification of the original bulk state. Applying Eq. (8.4) to this state leads us to Eq. (8.5). We conjecture that just like the entanglement islands formula, our reflected entropy islands formula works to all orders in $G_N$ perturbation theory [168]. There are various subtleties with graviton entanglement entropy that need to be resolved to make this concrete, but at the least we expect it to work to $\mathcal{O}(1)$, i.e., first subleading order.

## Consistency Checks

Having formulated our conjecture, we now show that our proposed formula satisfies the same properties as the reflected entropy $S_R(A:B)$. The entanglement of purification also satisfies a similar set of inequalities, and hence, the evidence provided in this section would suggest the same formula works for $E_P(A:B)$ as well. In fact, there are an additional set of inequalities relevant to $E_P(A:B)$ that our formula also satisfies as we show in Appendix A.9. These properties essentially follow from the definition in Eq. (8.5) and from the relative locations of entanglement islands, as dictated by the quantum focussing conjecture which we shall assume for this purpose [240].

In the following, we will use the notation $S(A,A')_\Sigma = S^{(\text{eff})}(AA') + \frac{\text{Area}[\partial A']}{4G_N}$ for the hybrid entropy on $\Sigma$ with $A'$ chosen as the candidate island before extremizing. Similarly, we define $S_R(A,A':B,B')_\Sigma = S_R^{(\text{eff})}(AA':BB') + \frac{\text{Area}[\partial(A' \cap B')]}{2G_N}$ for the reflected entropy, where the quantity is not yet extremized.

[3] In the presence of appropriate boundary conditions that allow for unitary evolution in the boundary, we can relax this condition to include only $\partial A$.

[4] We thank Thomas Faulkner for discussions about this.

**Properties**

- $S_R(A:B) \geq 0$

  This is obvious from the definition since both $S_R^{(\text{eff})}$ and Area are non-negative quantities.

- $S_R(A:B)$ is invariant upon acting with local unitaries on regions $A$ and $B$ respectively.

To show this, it is useful to think about the canonically purified state $|\sqrt{\rho_{AB}}\rangle$. In this state, the entanglement wedge of subregion $A$ must lie inside the entanglement wedge of $A \cup A^*$, where $A^*$ is the CPT conjugate subregion to $A$. This property, termed entanglement wedge nesting, has been proven in [233]. This implies that $D(\text{Is}(A)) \subset D(\text{Is}_R(A))$. A local unitary acting on subregion $A$ in the UV theory, acts as a local unitary on the region $A \cup \text{Is}(A)$ in the effective theory. Thus, the area of $\partial\text{Is}_R(A)$ and hence, $\partial\text{Is}_R(A) \cap \partial\text{Is}_R(B)$ cannot be affected. Further, the bulk state in the region $A \cup \text{Is}_R(A)$ is modified by a local unitary, and thus, $S_R^{(\text{eff})}$ remains invariant. The same argument above can be repeated for local unitaries acting on subregion $B$.

- $S_R(A:B) = 2S(A) = 2S(B)$ when $\rho_{AB}$ is pure.

Purity of $\rho_{AB}$ implies that $AB \cup \text{Is}(AB)$ is a complete Cauchy slice of the effective theory. In particular, the bulk effective field theory state on region $AB \cup \text{Is}(AB)$ is pure and hence, $S_R^{(\text{eff})}(A \cup I_A : B \cup I_B) = 2S(A \cup I_A) = 2S(B \cup I_B)$ for any choice of candidate reflected entropy islands $I_A$ and $I_B$. Further, purity implies that $I_A \cup I_B = \text{Is}(AB)$ spans the entire gravitating region, and $\partial(\text{Is}(A) \cup \text{Is}(B)) = \varnothing$. Thus, $\partial I_A = \partial I_B$ and using the islands formula in Eq. (8.5), we see that the optimization is identical to that in Eq. (8.4). Thus, $\text{Is}(A) = \text{Is}_R(A)$ and we find the above equality.

- $S_R(A:B) \leq 2\text{Min}(S(A),\ S(B))$.

Let $\Sigma_{A:B}$ denote the Cauchy slice on which the $S_R(A:B)$ optimization in Eq. (8.5) is maximized. Consider the subregion $A''$ of $\Sigma_{A:B}$ that minimizes $S(A, A'')_{\Sigma_{A:B}}$, i.e., the candidate minimal entanglement island on $\Sigma_{A:B}$. Now, since $A'' \subset \text{Is}(AB)$ using nesting, we can define $B'' = \text{Is}(AB) \setminus A''$ [60, 233]. Then, from the maximin procedure, we have

$$\begin{aligned} S_R(A:B) &\leq S_R(A, A'' : B, B'')_{\Sigma_{A:B}} && \text{(minimization)} \\ &\leq 2S(A, A'')_{\Sigma_{A:B}} && \text{(property of } S_R^{(\text{eff})}\text{)} \\ &\leq 2S(A) && \text{(maximization)}. \end{aligned}$$

A similar argument works for subregion $B$ and thus, we obtain the above inequality.

- $S_R(A:B) \geq I(A:B)$.

Consider the Cauchy slice $\Sigma$, on which each of $A \cup \text{Is}(A)$, $B \cup \text{Is}(B)$ and $AB \cup \text{Is}(AB)$ are extremal, which exists by the nesting arguments made in [60, 233]. $\Sigma \cap D(\text{ls}(AB))$, i.e., the island portion of the Cauchy slice, can be partitioned into $A'$ and $B'$, which minimizes $S_R(A, A' : B, B')_\Sigma$. In general, we have $\text{Is}(A) \cup \text{Is}(B) \subset A' \cup B'$. Then, from the maximin procedure, we obtain

$$\begin{aligned} I(A:B) &= S(A, \text{Is}(A))_\Sigma + S(B, \text{Is}(B))_\Sigma - S(AB, \text{Is}(AB))_\Sigma \\ &\leq S(A, A')_\Sigma + S(B, B')_\Sigma - S(AB, A'B')_\Sigma \\ &= I^{(\text{eff})}(AA' : BB') + \frac{\text{Area}[\partial A' \cap \partial B']}{2G_N} \\ &\leq S_R(AA' : BB')_\Sigma \leq S_R(A : B), \end{aligned}$$

where the second line follows from minimization and the last line follows from properties of $S_R^{(eff)}$ and maximization.

## 8.3 Path integral Argument

### Argument from Islands Formula

In this section, we give an argument for our proposed islands formula using the gravitational path integral. This argument is quite similar to that made in [42] with the added ingredient being the presence of entanglement islands in the bulk. We first describe the holographic dual of the canonically purified state $|\sqrt{\rho_{AB}}\rangle$. Using the islands formula for entanglement entropy in the dual spacetime then gives us our proposed islands formula. In what follows, we will use large central charge $c$ to ignore subtleties coming from gravitational fluctuations, however, it is quite plausible that these issues may be resolved without requiring large $c$ [168].

In order to understand the construction, we first consider the path integral that computes $Z_m = \text{tr}\, \rho_{AB}^m$ for even integer $m$. The path integral is evaluated on a manifold $\mathcal{M}_m$ which includes a non-gravitational portion $\mathcal{M}_m^{\text{fixed}}$ with fixed geometry, as well as gravitational regions with dynamical geometry denoted $\mathcal{M}_m^{\text{bulk}}$. In the gravitational region, we only specify asymptotic boundary conditions as fixed by $\mathcal{M}_m^{\text{fixed}}$ and integrate over all possible geometries consistent with them. Further, we use the saddle point approximation as $G_N \to 0$, and we expect a single geometry $\mathcal{M}_m^{\text{bulk}}$ to dominate the result. Thus, we obtain the replicated manifold $\mathcal{M}_m = \mathcal{M}_m^{\text{fixed}} \cup \mathcal{M}_m^{\text{bulk}}$

As shown in Fig. 8.2, we assume that the manifold $\mathcal{M}_m$ that dominates the path integral has a $\mathbb{Z}_m$ symmetry that cycles the individual replica copies in $\mathcal{M}_m^{\text{fixed}}$ and extends into $\mathcal{M}_m^{\text{bulk}}$. In order to construct the state $|\sqrt{\rho_{AB}}\rangle$, we need to analytically continue $Z_m$ in the parameter $m$. The prescription for analytic continuation is the one originally described in [36].

Using the $\mathbb{Z}_m$ symmetry, we consider an orbifold geometry $\tilde{\mathcal{M}}_m = \mathcal{M}_m/\mathbb{Z}_m$. $\tilde{\mathcal{M}}_m$ is a geometry with a conical defect with opening angle $2\pi/m$ that comes from the fixed point of

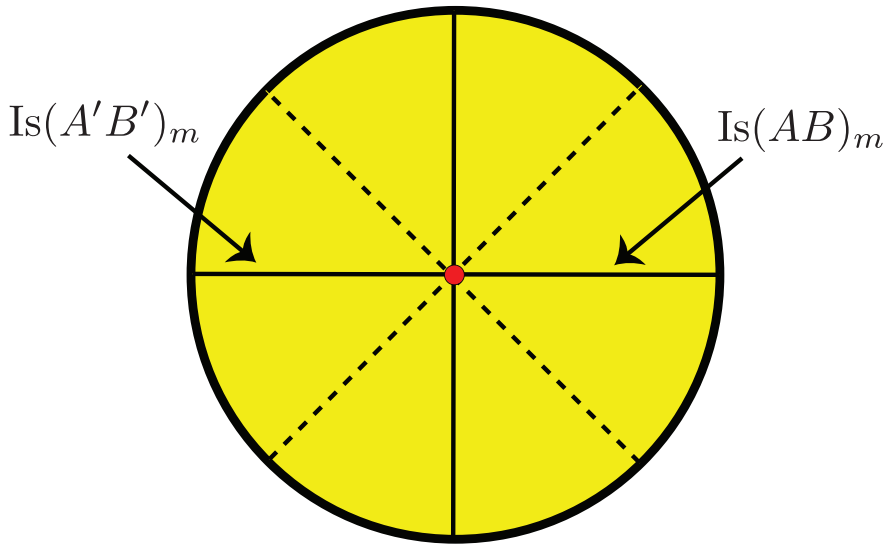


Figure 8.2: The gravitational region $\mathcal{M}_m^{\text{bulk}}$ (shaded yellow) of the manifold $\mathcal{M}_m$ that computes $Z_m$ for $m = 4$ is depicted here. In addition to a cyclic $\mathbb{Z}_m$ symmetry, we have a $\mathbb{Z}_2$ reflection symmetry which allows us to consider the bulk dual to the state $|\rho_{AB}^{m/2}\rangle$ by cutting open the path integral in half about the horizontal axis $\Sigma_m$. The Cauchy slice $\Sigma_m$ is made up of two pieces, that are denoted $\text{Is}(AB)_m$ and $\text{Is}(A'B')_m$, which become the entanglement islands of the respective regions in the limit $m \to 1$. The red dot denotes the fixed point of $\mathbb{Z}_m$ symmetry that becomes the quantum extremal surface as $m \to 1$. The dashed lines represent the complementary region to the island which has been traced out.

$\mathbb{Z}_m$ symmetry in $\mathcal{M}_m^{\text{bulk}}$. Simultaneously, the orbifold in the non-gravitational region induces twist operators at the entangling surface on the original manifold $\mathcal{M}_1^{\text{fixed}}$. Now for arbitrary $m$, one can simply define $\tilde{\mathcal{M}}_m^{\text{bulk}}$ by the bulk saddle with a conical defect of opening angle $2\pi/m$ that solves Einstein's equations everywhere else and asymptotically satisfies the correct boundary conditions prescribed by $\mathcal{M}_1^{\text{fixed}}$.

In addition, we assume that $\mathcal{M}_m$ has a $\mathbb{Z}_2$ symmetry owing to its time reversal invariance as seen in Fig. 8.2. This allows us to cut open the path integral at a $\mathbb{Z}_2$ symmetric Cauchy slice $\Sigma_m$ to construct the leading approximation to the bulk region corresponding to the fine-grained state $|\rho_{AB}^{m/2}\rangle$. $\Sigma_m$ then provides an initial data surface which can be evolved to find the entire Lorentzian spacetime. Having constructed the spacetime, we can now apply the entanglement islands formula, Eq. (8.1), for computing $S(AA')$, i.e., the reflected entropy, $S_R(A:B)$. Due to time reversal invariance, the quantum extremal surface lies on $\Sigma_m$ and gives an island-like contribution to the reflected entropy.

Finally, we can take the limit $m \to 1$, which gives us a spacetime as seen in Fig. 8.4 where $\Sigma_1$ is made up of two copies of the island region $\text{Is}(AB)$ glued together at the quantum extremal surface for the subregion $AB$, i.e., $\partial\text{Is}(AB)$. This is identical to the construction

proposed in [182] as the holographic dual of canonical purification. Importantly, the island appears as an additional closed universe portion of the bulk which is entangled with the region $AB \cup A'B'$. Now using the formula in Eq. (8.1) one obtains our proposed formula Eq. (8.3).[5]

## Heuristic Argument from Replica Trick

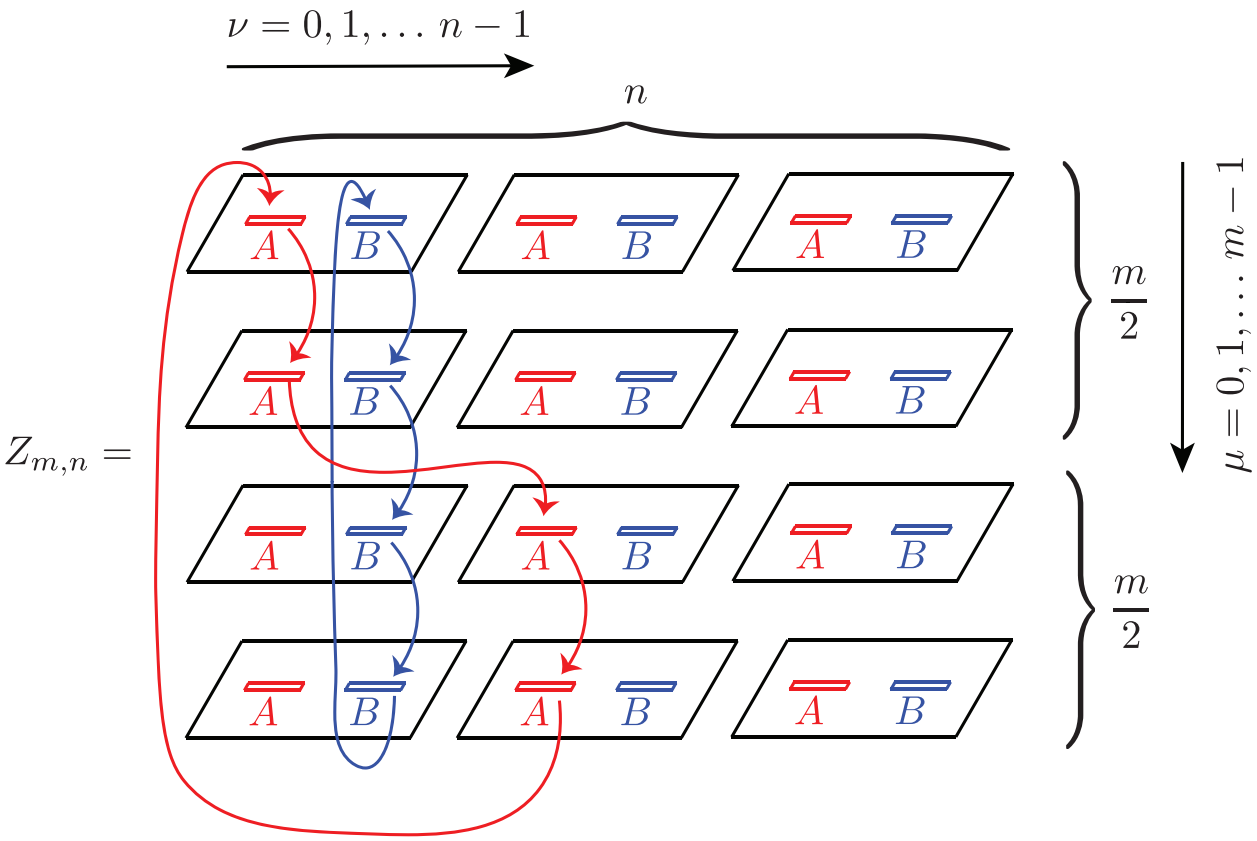


Figure 8.3: The manifold $\mathcal{M}_{m,n}$ involves gluing the subregions B cyclically in the vertical $\mu$ direction, whereas the subregions A are glued together cyclically in the vertical direction upto a cyclic twist, in the horizontal $\nu$ direction, at $\mu = 0, \frac{m}{2}$.

An alternate way to perform the calculation is to consider a more complicated replica

[5]Note that it was important that here we computed the entanglement entropy at arbitrary $m$ before continuing to $m = 1$. This specific order of limits was discussed in [42, 197] and seems to result in a sensible analytic continuation that commutes with the $G_N \to 0$ limit. Aspects of this analytic continuation will be discussed in [203].

trick [42]. In order to compute the reflected entropy, we can first compute

$$Z_{m,n} = \mathrm{tr}_{AA'}\left(\mathrm{tr}_{BB'}|\rho_{AB}^{m/2}\rangle\langle\rho_{AB}^{m/2}|\right)^n. \tag{8.6}$$

For integer $n$ and even integer $m$, we can compute $Z_{m,n}$ using a path integral on $mn$ copies of the system that are glued together as shown in Fig. 8.3.

We label the individual copies in terms of $(\mu,\nu) \in \mathbb{Z}_m \times \mathbb{Z}_n$. For each copy, we introduce cuts $A(\mu,\nu)^{\pm}$ and $B(\mu,\nu)^{\pm}$, where $\pm$ indicates the bra/ket portion of the reduced density matrix $\rho_{AB}$. $A(\mu,\nu)^+$ is then identified with $A(\mu,\nu)^-_{g_A}$ and $B(\mu,\nu)^+$ is identified with $B(\mu,\nu)^-_{g_B}$, where $g_A$ and $g_B$ refer to specific permutations that are illustrated in Fig. 8.3. To be precise, their actions are

$$g_A : (\mu,\nu) \to (\mu+1,\nu) \tag{8.7}$$
$$g_B : (\mu,\nu) \to (\mu+1,\nu+\delta_{\mu,m/2-1}-\delta_{\mu,m-1}) \tag{8.8}$$

The partition function $Z_{m,n}$ on the replicated manifold $\mathcal{M}_{m,n}$ can then be analytically continued to obtain the reflected entropy as

$$S_R(A:B) = -\lim_{m\to 1}\partial_n\left(\frac{\log\ Z_{m,n}}{n}\right)\Big|_{n=1}. \tag{8.9}$$

A convenient way to compute $Z_{mn}$ in a non-gravitational CFT is to use a permutation orbifold theory of $mn$ copies of the CFT, i.e., $\mathrm{CFT}^{\otimes mn}/S_{mn}$, where $S_{mn}$ is the permutation group on $mn$ elements. With this setup, the partition function $Z_{mn}$ can be computed as

$$Z_{mn} = \langle\Sigma_{g_A}\Sigma_{g_B}\rangle_{\mathrm{CFT}^{\otimes mn}/S_{mn}} \tag{8.10}$$

where $\Sigma_{g_A/g_B}$ represent twist operators that implement the gluing indicated in Fig. 8.3. $\Sigma_{g_A}$ and $\Sigma_{g_B}$ are operators with conformal dimensions proportional to $m-1$, we shall refer to these as Type-$m$ twist operators.

In this situation it is harder to perform an analytic continuation directly in the bulk, but it is useful to have a heuristic picture of the relevant physics. When coupled to gravitational regions, the Type-$m$ twist operators spontaneously create conical defects with opening angle $\frac{2\pi}{m}$ that we term Type-$m$ branes as seen in Fig. 8.4. These Type-$m$ branes demarcate the island region Is($AB$) associated as noted in [48]. Another useful operator to consider is $\Sigma_{g_A g_B^{-1}}$, the dominant operator exchanged between $\Sigma_{g_A}$ and $\Sigma_{g_B^{-1}}$. It has conformal dimension proportional to $n-1$ and we shall refer to it as a Type-$n$ twist operator. These induce Type-$n$ branes with opening angle $\frac{2\pi}{n}$, which land on the cross section of the island, and their contribution leads to our formula in Eq. (8.3). This discussion makes it clear that in order to avoid the branes backreacting on each other, we must consider the limit where $n \to 1$ first so that the Type-$n$ branes can be treated as probes.

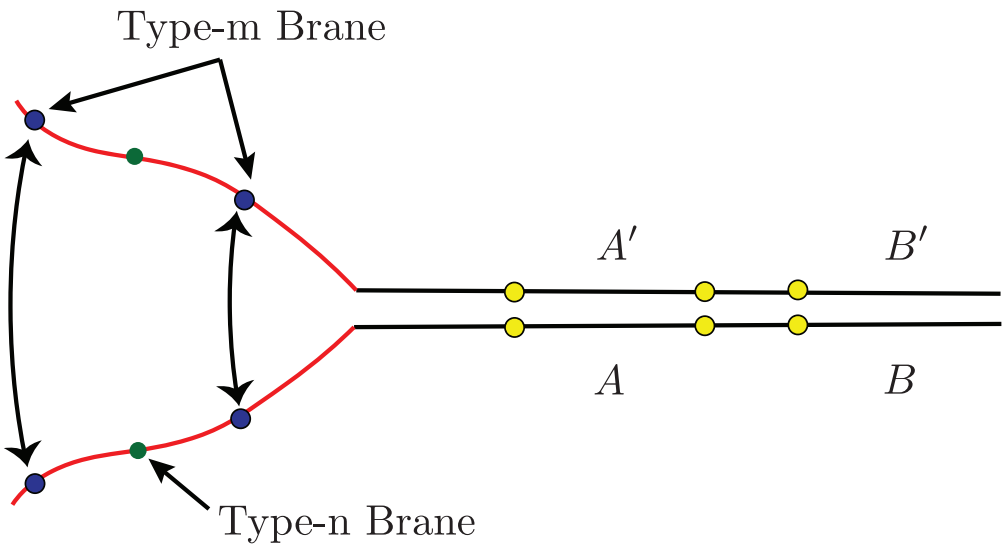


Figure 8.4: The time slice $\Sigma_m$ consists of a gravitating region (denoted red) where two copies of the island region Is$(AB)$ are glued together at $\partial$Is$(AB)$ (denoted purple). The non-gravitating region involves twist operators inserted at $\partial A$ and $\partial B$ (denoted yellow). The effect of these twist operators can be thought of as inducing two kinds of cosmic branes in the gravitating region, which we call Type-$m$ and Type-$n$ branes.

## 8.4 Phase transitions

In this section, we consider phase transitions of the reflected entropy in JT gravity coupled to a bath. In the gravitating $AdS_2$ region we have a $CFT_2$ eternally coupled to a $CFT_2$ in the Minkowski region, the latter of which serves as a "bath system". The full action of the theory is

$$I = \frac{1}{4\pi}\int d^2x\sqrt{-g}[\phi R + 2(\phi - \phi_0)] + I_{\text{CFT}} \tag{8.11}$$

where we follow the conventions of [49] in which $4G_N = 1$. Here $\phi_0$ is the extremal value of the dilaton $\phi$. We will consider two classes of examples, where the gravity theory is in equilibrium with the bath system, at either zero or finite temperature.

### Vacuum $AdS_2$

Here, we consider a vacuum $AdS_2$ solution glued to a half Minkowski space as seen in Fig. 8.5. This can be thought of as the zero temperature limit of an eternal black hole. The metric

and dilaton profile in the $AdS_2$ region are

$$ds^2 = -4\frac{dx^+dx^-}{(x^- - x^+)^2} \tag{8.12}$$

$$\phi(x) = \phi_0 + 2\frac{\phi_r}{x^- - x^+} \tag{8.13}$$

$$x^\pm = t \pm z,\ z \in (-\infty, 0] \tag{8.14}$$

In the flat space region the metric is the standard Minkowski metric,

$$ds^2 = -dt^2 + dz^2,\ z \in [0, \infty) \tag{8.15}$$

Given this setup, we will consider two different choices of subregions that will give us qualitatively different behaviour.

**Example 1**

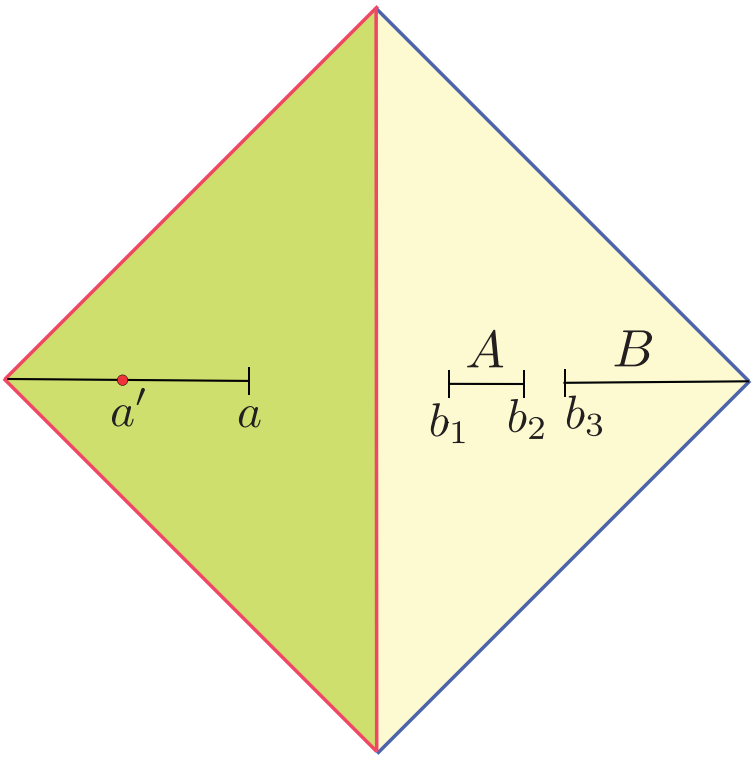


Figure 8.5: The Penrose diagram for the vacuum $AdS_2$ setup consisting of a finite subregion $A$ and a semi-infinite subregion $B$ in a half-Minkowski space (bath) eternally coupled to a gravitating region with the correspond island $a$ and cross-section $a'$.

The first example we consider involves two intervals in the bath region, $[b_1, b_2]$ and $[b_3, \infty)$ where $b_3 > b_2$. Let $(-\infty, -a]$ denote the corresponding island in the $AdS_2$ region.

We now compute the reflected entropy $S_R(A:B)$ for this setup. The calculation will be similar to that of [49], while making use of the techniques in [42]. To start with, the effective reflected entropy, is obtained from the $n \to 1$ limit of [42]

$$S_n(\rho_{AB}^{m/2}) = \frac{1}{1-n} \log \frac{\langle \Sigma_{g_A} \Sigma_{g_B} \rangle}{\langle \Sigma_{g_m} \Sigma_{g_m} \rangle^n} \tag{8.16}$$

where the operator dimensions are

$$\Delta_{g_A} = \Delta_{g_B} = \frac{cn(m^2-1)}{24m} = n\Delta_m \tag{8.17}$$

We now point out a useful property of the reflected entropy under Weyl transformations. Consider a Weyl transformation $g \to \Omega^2 g$ of the metric. Then,

$$\langle \Sigma_{g_A} \Sigma_{g_B} \rangle \to \Omega_A^{\Delta_A} \Omega_B^{\Delta_B} \langle \Sigma_{g_A} \Sigma_{g_B} \rangle \tag{8.18}$$

$$\langle \Sigma_{g_m} \Sigma_{g_m} \rangle^n \to (\Omega_A \Omega_B)^{n\Delta_m} \langle \Sigma_{g_m} \Sigma_{g_m} \rangle^n \tag{8.19}$$

Hence the Weyl factors cancel out in Eq. (8.16) for coincident points in the numerator and denominator. In general, if there is no island then the reflected entropy will be entirely Weyl invariant. If there is an island with a cross-section then the twist insertion at the cross-section will have an additional Weyl factor. This simplifies the analysis, since we can simply do the entire calculation in flat space by an appropriate Weyl transformation of Eq. (8.12).

Let us first review the salient aspects of computing $S_n(\rho_{AB}^{m/2})$ for a $CFT_2$ in flat space as described in [42]. In this case the twist operator $\Sigma_g$ associated to an interval become two quasi-local twist operators $\sigma_g, \sigma_{g^{-1}}$ inserted at the endpoints of the interval. The dominant exchange between $\sigma_{g_A}$ and $\sigma_{g_B^{-1}}$ is a composite operator denoted $\sigma_{g_A g_B^{-1}}$ which has dimension

$$\Delta_{g_A g_B^{-1}} = \frac{c}{12n}(n^2-1) = 2\Delta_n \tag{8.20}$$

The OPE coefficient of the exchange is

$$C_{n,m} = (2m)^{-4\Delta_n} \tag{8.21}$$

We can now do the calculation for the present setup. Let $a'$ denote the cross-section of the island. We must evaluate

$$S_{n,m} = \frac{1}{1-n} \log \frac{\langle \sigma_{g_A}(b_1) \sigma_{g_A^{-1}}(a) \sigma_{g_A^{-1}}(b_2) \sigma_{g_B}(b_3) \sigma_{g_A g_B^{-1}}(a') \rangle_{mn}}{\langle \sigma_{g_m}(b_1) \sigma_{g_m^{-1}}(a) \sigma_{g_m^{-1}}(b_2) \sigma_{g_m}(b_3) \rangle_m^n} \tag{8.22}$$

Note that once we map the $AdS_2$ region to flat space, all Weyl factors will cancel out except the one associated with the cross-section $a'$.

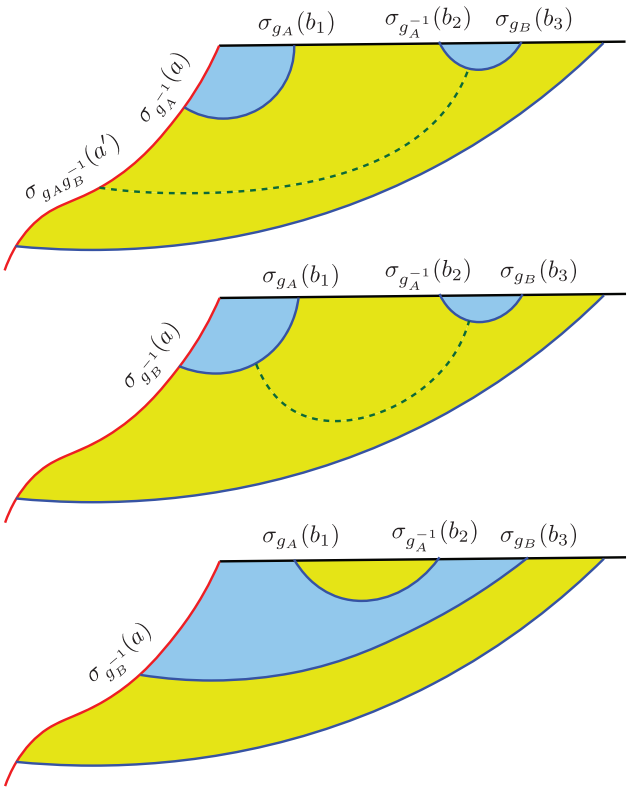


Figure 8.6: The three possible phases along with the associated contractions of twist operators. *Top*: connected phase of the entanglement island, with a non-trivial cross-section. *Middle*: connected phase of the entanglement island, with no cross-section. *Bottom:* disconnected phase of the entanglement island.

The contractions corresponding to the first phase are shown in Fig. 8.6. At this point we restrict to a large $c$ CFT, in which case the correlators factorize into their respective contractions [241], hence we get

$$\langle \sigma_{g_A}(b_1)\sigma_{g_A^{-1}}(a)\sigma_{g_A^{-1}}(b_2)\sigma_{g_B}(b_3)\sigma_{g_A g_B^{-1}}(a')\rangle_{mn} \tag{8.23}$$

$$= \langle \sigma_{g_A}(b_1)\sigma_{g_A^{-1}}(a)\rangle_{mn}\langle \sigma_{g_A^{-1}}(b_2)\sigma_{g_B}(b_3)\sigma_{g_A g_B^{-1}}(a')\rangle_{mn} \tag{8.24}$$

$$= \Omega^{2\Delta_n}(a')\frac{1}{(a+b_1)^{2n\Delta_m}}\frac{C_{n,m}}{(b_3-b_2)^{2n\Delta_m-2\Delta_n}(b_3+a')^{2\Delta_n}}\frac{1}{(b_2+a')^{2\Delta_n}} \tag{8.25}$$

Similarly,

$$\langle \sigma_{g_m}(b_1)\sigma_{g_m^{-1}}(a)\sigma_{g_m^{-1}}(b_2)\sigma_{g_m}(b_3)\rangle_m = \frac{1}{(a+b_1)^{2\Delta_m}}\frac{1}{(b_3-b_2)^{2\Delta_m}} \tag{8.26}$$

Putting this together, the reflected entropy of this phase is

$$S_R^{(1)} = \frac{c}{3}\left(\log(b_3+a') + \log(b_2+a') - \log 4a' - \log(b_3-b_2)\right) + 2\frac{\phi_r}{a'} + 2\phi_0 \tag{8.27}$$

The last term will be divergent in the limit $b_2 \to b_3$. However, we are only interested in extracting the phase transition in $S_R$. Therefore this divergence will not matter; as we will see below, the same divergent term appears in the reflected entropy of the other phase.

The location of $a'$ is then determined from the extremization

$$\frac{dS_R^{(1)}}{da'} = 0 \tag{8.28}$$

which yields the cubic equation

$$\frac{c}{3}\left(\frac{1}{b_3+a'} + \frac{1}{b_2+a'} - \frac{1}{a'}\right) - 2\frac{\phi_r}{(a')^2} = 0 \tag{8.29}$$

This is a cubic equation for $a'$ which can be solved in principle but is not quite illuminating. Instead we will consider the simplifying limit $b_2 \to b_3$. Then, Eq. (8.29) simplifies to the quadratic

$$(a')^2 - a'(b_3 + 6\frac{\phi_r}{c}) - 6\frac{\phi_r}{c}b_3 = 0 \tag{8.30}$$

whose solution is

$$2a' = b_3 + 6\frac{\phi_r}{c} + \sqrt{b_3^2 + 36\frac{\phi_r}{c}b_3 + 36\frac{\phi_r^2}{c^2}} \tag{8.31}$$

In order to analyze the phase transition, we also need the reflected entropy for the second non-trivial phase (see Fig. 8.6). This is the phase where there is no cross-section $a'$ so we just compute

$$S_R^{(2)} = \frac{1}{1-n}\log\frac{\langle\sigma_{g_B^{-1}}(a)\sigma_{g_A}(b_1)\sigma_{g_A^{-1}}(b_2)\sigma_{g_B}(b_3)\rangle_{mn}}{\langle\sigma_{g_m^{-1}}(a)\sigma_{g_m}(b_1)\sigma_{g_m^{-1}}(b_2)\sigma_{g_m}(b_3)\rangle_m^n} \tag{8.32}$$

This calculation is identical to the one done in [42], and the result is

$$S_R^{(2)} = \frac{2c}{3}\log\left(1 + \frac{\sqrt{1-x}}{\sqrt{x}}\right),\ x = \frac{(b_3-b_2)(b_1+a)}{(b_3-b_1)(b_2+a)} \tag{8.33}$$

In the limit $b_2 \to b_3$, the cross ratio $x \to 0$. Thus,

$$S_R^{(2)} \approx \frac{c}{3}\left(\log(b_3+a) + \log(b_3-b_1) - \log(b_1+a) - \log(b_3-b_2)\right) \tag{8.34}$$

As mentioned, we see that the same divergent term appears in both $S_R^{(1)}$ and $S_R^{(2)}$.

The expression for $a$ was obtained from the standard islands prescription in [49] and the result is

$$2a(b_1) = b_1 + 6\frac{\phi_r}{c} + \sqrt{b_1^2 + 36\frac{\phi_r}{c}b_1 + 36\frac{\phi_r^2}{c^2}} \tag{8.35}$$

which is valid for the connected phase of the entanglement island. Note that we have made the dependence $a(b_1)$ explicit since similar expressions will appear in other calculations too.

Lastly, we have the third phase in Fig. 8.6. This corresponds to the disconnected phase of the entanglement island, for which

$$S_R^{(3)} = 0 \tag{8.36}$$

For this phase, we simply have $a(b_3)$ instead of $a(b_1)$ in Eq. (8.35).

To summarize, the first two phases correspond to the case where the entanglement island of $AB$ is connected, whereas in the third phase the entanglement island of $AB$ is disconnected. The phase transition can then be analyzed in the following series of steps:

- Find the phase transition in the entanglement entropy, which corresponds to a transition in the entanglement island of $AB$
- Within each phase of the entanglement entropy, find the phase transition in the reflected entropy

To do this analysis analytically, we first work in the limit where $\phi_r/c \gg 1$. At leading order, for *both* phases, we then have

$$a \approx \frac{6\phi_r}{c} \tag{8.37}$$

Then at leading order the phase transition in the entanglement entropy occurs when

$$b_2 \approx \frac{b_1 + b_3}{2} \tag{8.38}$$

When $b_2$ is below this value we are in the disconnected phase, and when it is above this value we are in the connected phase. Note that in the limit $b_2 \to b_3$ we will always be in the connected phase.

In the simultaneous limits of large $\phi_r/c$ and $b_2 \to b_3$, we have

$$a' \approx 6\frac{\phi_r}{c} \tag{8.39}$$

We then see from Eqns. (8.27) and (8.34) that the following behavior holds:

$$S_R^{(1)} \sim \frac{c}{3}\log\frac{\phi_r}{c} + 2\phi_0 \tag{8.40}$$

$$S_R^{(2)} \sim \frac{c}{3}\log(b_3 - b_1) \tag{8.41}$$

Since $\phi_r/c \gg b_3, b_1$ is the largest scale in our parameter regime, we see that $S_R^{(1)} > S_R^{(2)}$ always. Thus, there is no phase transition within the connected entanglement island phase. Instead, we are always in the second phase in Fig. 8.6. Physically, the subsystem $A$ is too small to accommodate large bi-partite quantum entanglement with $B$, so that the entanglement island does not contribute to bi-partite correlation measures.

We now consider the opposite limit, $b_2 \to b_3 \gg \phi_r/c$. In this parameter regime, we have

$$a' \approx b_3 \tag{8.42}$$

$$a \approx b_1 \tag{8.43}$$

Consequently, the reflected entropies go like

$$S_R^{(1)} \sim \frac{c}{3}\log b_3 + 2\phi_0 \tag{8.44}$$

$$S_R^{(2)} \sim \frac{c}{3}\log b_3^2 \tag{8.45}$$

Thus we see that there is a phase transition when

$$b_3 \sim e^{6\phi_0/c} \tag{8.46}$$

This example demonstrates the fact that even the entanglement between subsystems in the Hawking radiation gets large modifications from gravity, provided that there is large entanglement.

In the next example, we consider a setup where one subsystem contains the black hole and the other is a subsystem in the bath.

**Example 2**

The second example we consider is of subregions that are adjacent intervals, $A := [0,\ b_1]$ and $B := [b_1,\ b_2]$. $A$ now contains QM system which is dual to JT gravity. We compute the reflected entropy as a function of $b_1$ holding $b_2$ fixed. We first describe the phase transition qualitatively as can be well understood in terms of the double holography picture seen in Fig. 8.7. We then plot the behaviour quantitatively in Fig. 8.8.

As found in [49], the subregion $A$ always includes an entanglement island and its von Neumann entropy is given by

$$S(A) = S_{\text{gen}}(b_1) := \phi_0 + \frac{\phi_r}{a} + \frac{c}{6}\log\frac{(a(b_1)+b_1)^2}{a(b_1)\epsilon}, \tag{8.47}$$

where $[-a(b_1), 0]$ is the corresponding island where $a(b_1)$ is given by Eq. (8.35). In various limits, it is approximately given by

$$a(b_1) \approx \begin{cases} \frac{6\phi_r}{c} & \text{if } b_1 \ll \frac{\phi_r}{c} \\ b_1 & \text{if } b_1 \gg \frac{\phi_r}{c} \end{cases}. \tag{8.48}$$

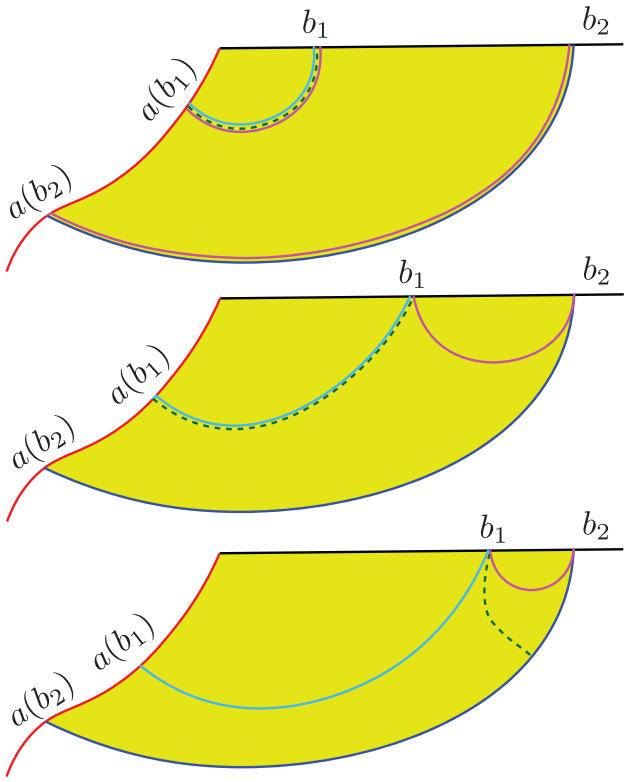


Figure 8.7: As we vary $b_1$ we see three possible phases based on the behaviour of the various surfaces in the double holography picture, RT surface of $A$ (light blue), RT surface of $B$ (pink) and the entanglement wedge cross section (green dashed line).

For the subregion $B$, it was shown in [49] that it contains an island for small $b_1$ only if $b_2 > \frac{\phi_r}{c}\exp(12\phi_0/c)$. We consider fixed but large $b_2$ such that $B$ can have an entanglement island.

For small $b_1$, it is preferable for $B$ to have an entanglement island leading to

$$S(B) = S_{\text{gen}}(b_1) + S_{\text{gen}}(b_2) \tag{8.49}$$

$$I(A:B) = 2S_{\text{gen}}(b_1) = 2S(A). \tag{8.50}$$

For large $b_1$, $B$ does not have an entanglement island, and we instead have

$$S(B) = \frac{c}{3}\log\frac{b_2 - b_1}{\epsilon}. \tag{8.51}$$

Thus, in this limit we obtain

$$I(A:B) = S_{\text{gen}}(b_1) + \frac{c}{3}\log\frac{b_2 - b_1}{\epsilon} - S_{\text{gen}}(b_2). \tag{8.52}$$

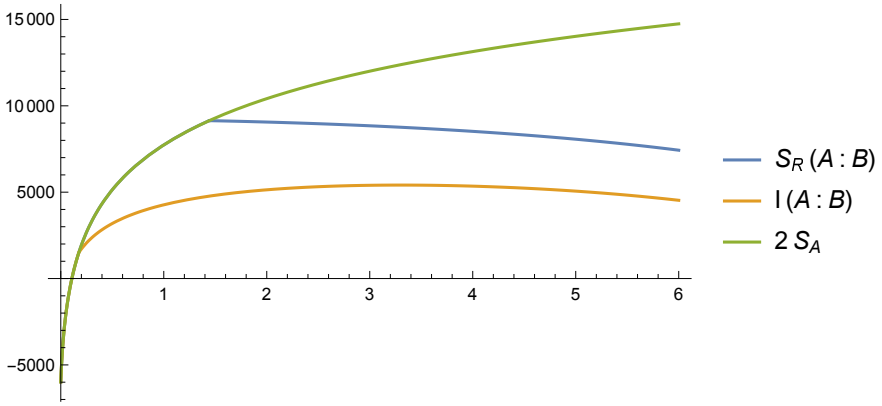


Figure 8.8: We plot the behaviour of $2S(A)$, $S_R(A:B)$ and $I(A:B)$ as a function of $b_1$, for $b_2 = 10$, $\phi_0 = 1000$. $\phi_r = 100$, and $c = 12000$. The phase transition of $S_R$ is in accord with Eq.(8.55).

In order to compute the reflected entropy, we can now include various reflected entropy islands as dictated by our proposed formula, Eq. (8.5). For small $b_1$, there is a non-trivial splitting of the entanglement island as seen in Fig. 8.7. This calculation can be done using the techniques employed in the previous section. In the end, the extremization to obtain the reflected entropy island ends up being identical to that in the entanglement island calculation. Hence, we obtain

$$S_R(A:B) = 2S_{\text{gen}}(b_1) = 2S(A). \tag{8.53}$$

At large $b_1$, there is no non-trivial reflected entropy island i.e. the entire island belongs to $A$. Again using techniques similar to the ones used in the previous example, we obtain

$$S_R(A:B) = \frac{c}{3}\log\frac{2(a(b_2)+b_1)(b_2-b_1)}{(a(b_2)+b_2)\epsilon}, \tag{8.54}$$

where $a(b_2)$ is the location of the island for $B$. The phase transition between these two phases of the reflected entropy occurs at

$$e^{\frac{6\phi_0}{c}} \approx \frac{(b_2+b_1)(b_2-b_1)}{4b_1b_2}. \tag{8.55}$$

We plot this behaviour quantitatively in Fig. 8.8.

## Eternal Black Hole

Having considered the vacuum $AdS_2$ example, we now come to the example of a two-sided eternal black hole glued to two halves of Minkowski space, one on each side. The full $CFT_2$ is in the Hartle-Hawking state, as considered in [49]. See Fig. 8.9 for the Penrose diagram

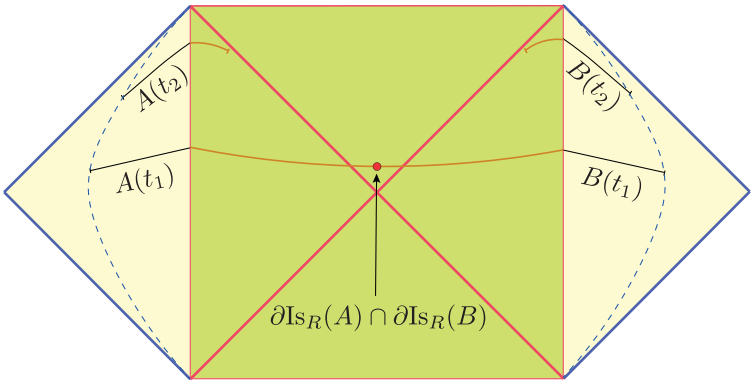


Figure 8.9: The eternal black hole coupled to a bath CFT in Minkowski space is considered with subregions $A$ and $B$ at different times. At early times, the subregion $AB$ has an entire Cauchy slice of the gravity region as its entanglement island (denoted orange). The computation of $S_R(A:B)$ then includes an area contribution from the boundary of the reflected entropy island (denoted red). At late times, the entanglement island is disconnected and $S_R(A:B)=0$.

of the setup. The metric and dilaton profile for each black hole exterior and respective bath are

$$ds^2 = -\frac{4\pi^2}{\beta^2}\frac{dy^+dy^-}{\sinh^2\frac{\pi}{\beta}(y^- - y^+)} \tag{8.56}$$

$$\phi = \phi_0 + \frac{2\pi\phi_r}{\beta}\frac{1}{\tanh\frac{\pi}{\beta}(y^- - y^+)} \tag{8.57}$$

where the $(y^+, y^-)$ coordinates are related to the $(x^+, x^-)$ coordinates via

$$x^\pm = \tanh\frac{\pi y^\pm}{\beta} \tag{8.58}$$

The calculation will proceed similarly to that of the previous section. Namely, we do a Weyl transformation to map the black hole geometry to flat space and apply standard $\mathrm{CFT}_2$ techniques to calculate the reflected entropy in the presence of an island. As before, we work in the large $c$ limit throughout, so that we can factorize correlators into their contractions.

At $t=0$ we consider an interval $[-b,0]$ in the left Minkowski region and an interval $[0,b]$ in the right Minkowski region. In this symmetric setup, the corresponding "island" in the black hole spacetime will be the entire bulk slice, with a cross-section $a'$ splitting it, see Fig. 8.9. This is the early time phase. Just as in [49] we then move both endpoints of the bath intervals forward in time, which introduces time-dependence into the setup. The resulting reflected entropy will therefore be a function of time. At late times there will be phase transition to a disconnected phase depicted in Fig. 8.9.

The rule as prescribed in our formula, Eq. 8.5, is to first find the phase transition in the entanglement entropy. Given the entanglement island, we can then find the phase transitions in the reflected entropy for subregions which all share the same island. In the present case the phase transition occurs entirely at the level of the entanglement entropy. In other words, the phase transition in $S_R(A:B)$ is completely dictated by the entanglement entropy phase transition.

The entanglement entropy $S(AB)$ grows linearly with time similar to the calculation in [242], and eventually has a phase transition as demonstrated in [49]. Note that our setup is simply the complement of the setup in [49]. Hence the entanglement entropy phase transition happens at the same time, given by

$$t \sim \frac{\beta S_{\text{BH}}}{c} \tag{8.59}$$

where $S_{\text{BH}} = 2(\phi_0 + 2\pi\phi_r/\beta)$ is the black hole entropy. This is therefore also the time at which the reflected entropy phase transition happens.

In order to compute the reflected entropy for the early time phase, we need to convert to global coordinates that cover the entire spacetime. Let $y_L^{\pm}$ denote the coordinates covering the left exterior and bath, and similarly for $y_R^{\pm}$. Then

$$w^{\pm} = \pm e^{\pm\frac{2\pi y_R^{\pm}}{\beta}},\ w^{\pm} = \mp e^{\mp\frac{2\pi y_L^{\pm}}{\beta}} \tag{8.60}$$

defines a global coordinate chart $(w^+, w^-)$ in which the metric simply reduces to that of Minkowski space. Let $w_1^{\pm}$ denote $a'$, $w_2^{\pm}$ denote the endpoint of the left bath interval, and $w_3^{\pm}$ denote the endpoint of the right bath interval. Moreover, recall the relations

$$y_L^{\pm} = t \mp z,\ y_R^{\pm} = t \pm z \tag{8.61}$$

where $z$ denotes the spatial coordinate. Lastly, by symmetry we have that $w_1^+ = w_1^- := \delta$. We can now compute the *effective* reflected entropy for this phase, which is given by

$$S_R^{(\text{eff})} = -\lim_{n\to 1}\partial_n\left[\frac{c}{12}\frac{(n-\frac{1}{n})}{n}\log\frac{\varepsilon^2(1+w_1^+w_1^-)^2}{4\left(\frac{w_{12}^+w_{12}^-w_{13}^+w_{13}^-}{w_{23}^+w_{23}^-}\right)} + \frac{1}{n}\log C_n^2\right] \tag{8.62}$$

$$= \frac{c}{3}\log 2 + \frac{c}{6}\log\varepsilon^2\frac{e^{4\pi b/\beta}(e^{2\pi t/\beta}-\delta e^{-2\pi b/\beta})^2(\delta e^{-2\pi b/\beta}+e^{-2\pi t/\beta})^2}{(1+\delta^2)\cosh^2 2\pi t/\beta} \tag{8.63}$$

where $\varepsilon$ is the UV cutoff. The reflected entropy of this phase is therefore

$$S_R^{(1)} = \text{ext}_\delta\left(S_R^{(\text{eff})} + 2\left(\phi_0 + \frac{2\pi\phi_r}{\beta}\frac{1-\delta^2}{1+\delta^2}\right)\right) \tag{8.64}$$

In the limit $b \to \infty$, the solution to

$$\frac{dS_R^{(1)}}{d\delta} = 0 \tag{8.65}$$

is simply $\delta \to 0$ which is a consequence of the symmetry in the setup.

Thus, the final expression for the reflected entropy of the non-trivial phase in this limit is

$$S_R^{(1)} = 2(\phi_0 + \frac{2\pi\phi_r}{\beta}) + \frac{c}{3}\log 2 - \frac{c}{6}\log\frac{\cosh^2 2\pi t/\beta}{\varepsilon^2 e^{4\pi b/\beta}} \tag{8.66}$$

Thus, we see that at early times the reflected entropy decreases linearly just like the mutual information [48]. On the other hand, the reflected entropy for the late time phase clearly vanishes,

$$S_R^{(2)} = 0. \tag{8.67}$$

Since the transition is completely dictated by the entanglement entropy phase transition, generically there is a discontinuous jump in $S_R(A:B)$ from a non-zero value to zero when the transition occurs. This is analogous to the situation in the phase transition for two intervals in pure AdS [199, 43].

## 8.5 Discussion

### Generalizations

In this work, we have proposed a formula in Eq. (8.3) that generalizes the holographic conjecture for reflected entropy to situations where the entanglement wedge includes an island. There have also been holographic proposals for other measures of bipartite correlation such as entanglement negativity, odd entropy and entanglement wedge mutual information[243, 244, 223, 245, 224, 199]. Similarly, multipartite versions of the reflected entropy and entanglement of purification have also been proposed previously [211, 227, 226]. Although we have focused on the reflected entropy in this paper, the generalization essentially can be understood as applying the usual holographic formula after including the island in the entanglement wedge. Hence, all the proposals discussed above can also be generalized in a similar manner to include island contributions. We expect such generalizations will help understanding the entanglement structure of Hawking radiation, while it is also important to understand physical implications of those correlation measures.

### Interpretation of Results

We now attempt to interpret some of the results we have obtained in Section 8.4. The reflected entropy is known to be a correlation measure that includes contributions from both classical and quantum correlations [42, 199, 225, 246]. However, there isn't a general understanding of the precise kind of correlations quantified by the reflected entropy, and also no general classification of multipartite entanglement. Hence, we will use suggestive examples that exhibit features similar to those found in Section 8.4.

The interesting features of the examples in Section 8.4, especially the behaviour found in Fig. 8.8, can be understood from the interplay between the reflected entropy $S_R(A:B)$, and its upper and lower bounds given by

$$\min\{2S(A), 2S(B)\} \geq S_R(A:B) \geq I(A:B). \tag{8.68}$$

In certain regions of parameter space, we see saturation of the upper and lower bounds and we can take this as a guiding principle to indicate the structure of entanglement of the states. We will demonstrate these features in two examples and conjecture that this is indicative of the general correlations quantified by $S_R(A:B)$.

### Qubit example

The first example comprises a three party qubit state, where the multipartite entanglement structure is quite well understood [247, 248]. The simplest form of entanglement is Bell pair like bipartite entanglement between any two of the parties, e.g.,

$$|\text{Bell}\rangle = \frac{1}{\sqrt{2}}(|00\rangle + |11\rangle) \otimes |0\rangle. \tag{8.69}$$

Genuine tripartite entangled states can be classified into two categories represented by the GHZ state and W state given by

$$|\text{GHZ}\rangle = \frac{1}{\sqrt{2}}(|000\rangle + |111\rangle) \tag{8.70}$$

$$|\text{W}\rangle = \frac{1}{\sqrt{3}}(|001\rangle + |010\rangle + |100\rangle) \tag{8.71}$$

Heuristically the difference between these two kinds of states is that any two parties are only classically correlated in the GHZ state, whereas they have genuine quantum correlation in a W state.

A simple computation tells us that the Bell state saturates both upper and lower bounds in Eq. (8.68). Similarly, the GHZ state saturates only the lower bound whereas the W state saturates neither. This gives us a heuristic picture that non-saturation of the upper bound is related to the existence of tripartite entanglement, whereas non-saturation of the lower bound is related to the existence of quantum correlation [6].

Given this discussion, we can discuss the structure of entanglement found in Fig. 8.8. Clearly, the region before the first phase transition corresponds to Bell pair like entanglement as seen from saturation of both bounds. So we now focus on the region after the first phase transition where the upper bound is saturated but the lower bound is not. A simple model

[6] Note that the Bell state has to be treated carefully in a limiting procedure since it saturates both bounds.

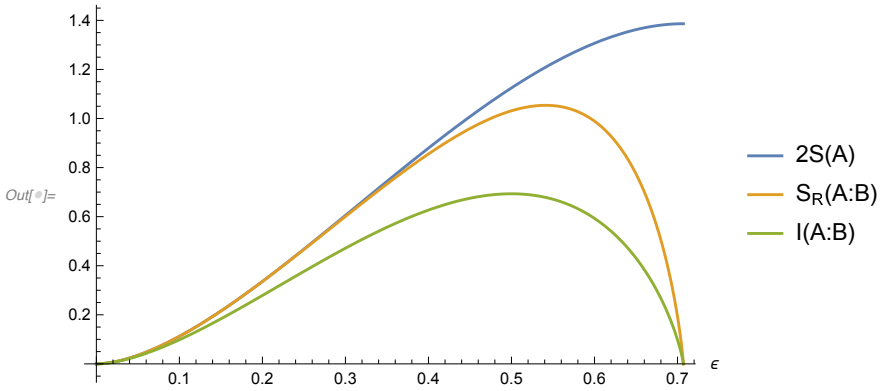


Figure 8.10: The reflected entropy for the state $|W_\epsilon\rangle$ as a function of $\epsilon$ is compared to its upper and lower bounds. We see that it has qualitative features similar to that found in Section 8.4.

that captures this feature is a state that can be thought of as a W-like perturbation to a product state which we denote as $|W_\epsilon\rangle$,

$$|W_\epsilon\rangle = \epsilon|100\rangle + \epsilon|001\rangle + \sqrt{1-2\epsilon^2}|010\rangle. \tag{8.72}$$

In Fig. 8.10, we plot the three relevant quantities of this state discussed in Eq. (8.68) and it can easily be seen that for a significant neighbourhood near $\epsilon = 0$, the state saturates the upper bound while staying far away from the lower bound. More precisely, we find that perturbatively around $\epsilon = 0$, we have

$$|S_R(A:B) - I(A:B)| = O(\epsilon^2) \tag{8.73}$$

$$|S_R(A:B) - 2S(A)| = O(\epsilon^4 \log(\epsilon)) \tag{8.74}$$

This hints at the fact that $S_R(A:B)$ is in fact more sensitive to the existence of quantum correlations than it is to the existence of tripartite entanglement of the $|W\rangle$ type. The importance of W-type tripartite entanglement for holographic states was emphasized in [43]. Going beyond qubit systems, it is unclear what exactly we mean by W-type entanglement since the multipartite entanglement classification becomes much more complicated [249, 248]. In the context of reflected entropy, what we really mean is states that are far from saturating the lower bound in Eq. (8.68). In the context of qubits, we can numerically test that this non-saturation is maximized by a state close to the $|W\rangle$ state.

### Random tensor example

Having provided a specific example, we now provide a much more general example that is likely to be relevant to holography. In the past few years, it has been understood that there are deep connections between random matrix theory and gravity [29, 250, 251, 252, 45]. In

particular, the entanglement structure of holographic states is well approximated by random tensor networks [29].

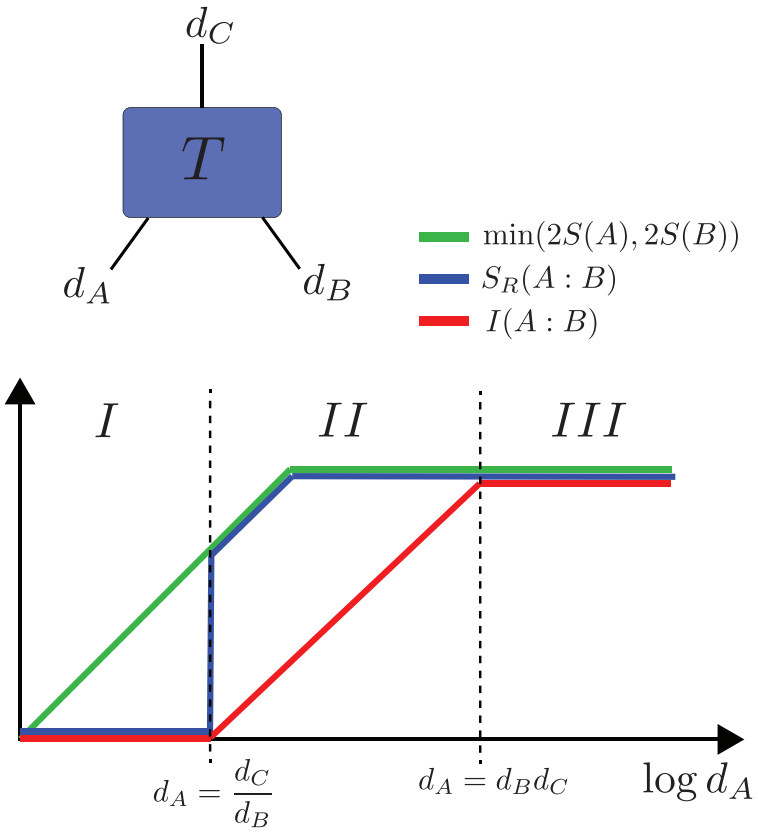


Figure 8.11: A tripartite state comprising a single random tensor $T$ with legs of bond dimensions $d_A$, $d_B$ and $d_C$. We sketch the reflected entropy $S_R(A:B)$ and its upper and lower bounds as a function of the bond dimension $d_A$ while holding $d_B$ and $d_C$ fixed.

Motivated by this, we consider the example of a random tripartite state generated by a single random tensor as shown in Fig. 8.11. This state is characterized by the dimensions of the individual parties denoted $d_A$, $d_B$ and $d_C$. This can be thought of as a discrete model of a multiboundary wormhole with three asymptotic boundaries where the bond dimensions are a measure of the area of the mouths of the wormhole [192, 218, 253]. This example will be discussed in much more detail in [203], but here we use the basic result to emphasize a connection to the results obtained in Section 8.4. Essentially, the results described below arise from using the holographic proposals for computing entropy and reflected entropy.

We consider the phase diagram as we hold $d_B$ and $d_C$ fixed such that $d_B^2 \geq d_C \geq d_B$, and vary $d_A$. The large $d$ behaviour of the relevant quantities in this state is sketched in Fig. 8.11 and demonstrates essentially three phases. Phase I corresponds to the state being dominated by Bell pairs shared separately between $AC$ and $BC$. Similarly, Phase III corresponds to the

state being dominated by Bell pairs shared between $AC$ and $AB$. Phase II has the interesting feature which is analogous to the $|W_\epsilon\rangle$ state discussed in the qubit example where the upper bound is saturated at leading order while the lower bound is far from being saturated. We can clearly see that this example reproduces precisely the behaviour found in Fig. 8.8. It would be interesting to use this simple model and probe other correlation measures to make this connection tighter.

# Chapter 9

# Gravity Dual of Connes Coycle Flow

## 9.1 Introduction

The AdS/CFT duality [14, 15, 16] has led to tremendous progress in the study of quantum gravity. However, our understanding of the holographic dictionary remains limited. In recent years, quantum error correction was found to play an important role in the emergence of a gravitating ("bulk") spacetime from the boundary theory [26, 27, 25]. The study of modular operators led to the result that the boundary relative entropy in a region $A$ equals the bulk relative entropy in its entanglement wedge EW($A$) [23]. The combination of these insights was used to derive subregion duality: bulk operators in EW($A$) can in principle be reconstructed from operators in the subregion $A$ [24].

The relation between bulk modular flow in EW($A$) and boundary modular flow in $A$ has been used to explicitly reconstruct bulk operators both directly [115, 254], and indirectly via the Petz recovery map and its variants [116, 255, 45]. Thus, modular flow has shed light on the emergence of the bulk spacetime from entanglement properties of the boundary theory.

Modular flow has also played an important role in proving various properties of quantum field theory (QFT), such as the averaged null energy condition (ANEC) and quantum null energy condition (QNEC) [256, 257]. Tomita-Takesaki theory, the study of modular flow in algebraic QFT, puts constraints on correlation functions that are otherwise hard to prove directly [258].

Recently, an alternate proof of the QNEC was found using techniques from Tomita-Takesaki theory [259]. The key ingredient was Connes cocyle (CC) flow. Given a subregion $A$ and global pure state $\psi$, Connes cocycle flow acts with a certain combination of modular operators to generate a sequence of well-defined global states $\psi_s$. In the limit $s \to \infty$, these states saturate Wall's "ant conjecture" [260] on the minimum amount of energy in the complementary region $A'$. This proves the ant conjecture, which, in turn, implies the QNEC.

CC flow also arises from a fascinating interplay between quantum gravity, quantum information, and QFT. Recently, the classical black hole coarse-graining construction of Engelhardt and Wall [181] was conjecturally extended to the semiclassical level [239]. In the

non-gravitational limit, this conjecture requires the existence of flat space QFT states with properties identical to the $s \to \infty$ limit of CC flowed states. This is somewhat reminiscent of how the QNEC was first discovered as the nongravitational limit of the quantum focusing conjecture [261]. Clearly, CC flow plays an important role in the connection between QFT and gravity. Our goal in this paper is to investigate this connection at a deeper level within the setting of AdS/CFT.

In Section 9.2, we define CC flow and discuss some of its properties. If $\partial A$ lies on a null plane in Minkowski space, operator expectation values and subregion entropies within the region $A$ remain the same, whereas those in $A'$ transform analogously to a boost [259]. Further, CC flowed states $\psi_s$ exhibit a characteristic stress tensor shock at the cut $\partial A$, controlled by the derivative of the von Neumann entropy of the region $A$ in the state $\psi$ under shape deformations of $\partial A$ [239].

As is familiar from other examples in holography, bulk duals of complicated boundary objects are often much simpler [18, 262]. Motivated by the known properties of CC flow, we define a bulk construction in Section 9.3, which we call the "kink transform." This is a one-parameter transformation of the initial data of the bulk spacetime dual to the original boundary state $\psi$. We consider a Cauchy surface $\Sigma$ that contains the Ryu-Takayanagi surface $\mathcal{R}$ of the subregion $A$. The kink transform acts as the identity except at $\mathcal{R}$, where an $s$-dependent shock is added to the extrinsic curvature of $\Sigma$. We show that this is equivalent to a one-sided boost of $\Sigma$ in the normal bundle to $\mathcal{R}$. We prove that the new initial data satisfies the gravitational constraint equations, thus demonstrating that the kink transform defines a valid bulk spacetime $\mathcal{M}_s$. We show that $\mathcal{M}_s$ is independent of the choice of $\Sigma$.

We propose that $\mathcal{M}_s$ is the holographic dual to the CC-flowed state $\psi_s$, if the boundary cut $\partial A$ is (conformally) a flat plane in Minkowski space.

In Section 9.4, we provide evidence for this proposal. The kink transform separately preserves the entanglement wedges of $A$ and $A'$, but it glues them together with a relative boost by rapidity $2\pi s$. This implies the one-sided expectation values and subregion entropies of the CC flowed state $\psi_s$ are correctly reproduced when they are computed holographically in the bulk spacetime $\mathcal{M}_s$. We then perform a more nontrivial check of this proposal. By computing the boundary stress tensor holographically in $\mathcal{M}_s$, we reproduce the stress tensor shock at $\partial A$ in the CC-flowed state $\psi_s$.

Having provided evidence for kink transform/CC flow duality, we use the duality to make a novel prediction for CC flow in Section 9.5. The kink transform fully determines all independent components of the shock at $\partial A$ in terms of shape derivatives of the entanglement entropy. Strictly, our results only apply only to the CC flow of a holographic CFT across a planar cut. However, their universal form suggests that they will hold for general QFTs under CC flow. Moreover, the shocks we find agree with properties required to exist in quantum states under the coarse-graining proposal of Ref. [263]. Thus, our new results may also hold for CC flow across general cuts of a null plane.

In Section 9.6, we discuss the relation of our construction to earlier work on the role of modular flow in AdS/CFT [167, 23, 264]. The result of Jafferis *et al.* (JLMS) [23] has conventionally been understood as a relation that holds for a small code subspace of bulk

states on a fixed background spacetime. However, results from quantum error correction suggest that this code subspace could be made much larger to include different background geometries [27, 38, 166, 229]. Our proposal then follows from such an extended version of the JLMS result which includes non-perturbatively different background geometries. Equipped with this understanding, we can distinguish our proposal from the closely related bulk duals of one-sided modular flowed states [167, 264]. We provide additional evidence for our proposal based on two sided correlation functions of heavy operators, and we discuss generalizations and applications of the proposed kink transform/CC flow duality.

In Appendix A.10 we derive the null limit of the kink transform, and show that it generates a Weyl shock, which provides intuition for how the kink transform modifies gravitational observables.

## 9.2 Connes Cocycle Flow

In this section, we review Connes cocycle flow and its salient properties; for more details see [259, 239]. We then reformulate Connes cocycle flow in as a simpler map to a state defined on a "precursor" slice. This will prove useful in later sections.

### Definition and General Properties

Consider a quantum field theory on Minkowski space $\mathbb{R}^{d-1,1}$ in standard Cartesian coordinates $(t, x, y_1, \ldots, y_{d-2})$. Consider a Cauchy surface $\mathcal{C}$ that is the disjoint union of the open regions $A_0, A_0'$ and their shared boundary $\partial A_0$. Let $\mathcal{A}_0, \mathcal{A}_0'$ denote the associated algebras of operators. Let $|\psi\rangle$ be a cyclic and separating state on $\mathcal{C}$, and denote by $|\Omega\rangle$ the global vacuum (the assumption of cyclic and separating could be relaxed for $|\psi\rangle$, at the cost of complicating the discussion below). The Tomita operator is defined by

$$S_{\psi|\Omega;\mathcal{A}_0}\alpha|\psi\rangle = \alpha^\dagger|\Omega\rangle, \forall\alpha \in \mathcal{A}_0 \ . \tag{9.1}$$

The relative modular operator is defined as

$$\Delta_{\psi|\Omega} \equiv S^\dagger_{\psi|\Omega;\mathcal{A}_0} S_{\psi|\Omega;\mathcal{A}_0} \ , \tag{9.2}$$

and the vacuum modular operator is

$$\Delta_\Omega \equiv \Delta_{\Omega|\Omega} \ . \tag{9.3}$$

Note that we do not include the subscript $\mathcal{A}_0$ on $\Delta$; instead, for modular operators, we indicate whether they were constructed from $\mathcal{A}_0$ or $\mathcal{A}_0'$ by writing $\Delta$ or $\Delta'$.

Connes cocycle (CC) flow of $|\psi\rangle$ generates a one parameter family of states $|\psi_s\rangle$, $s \in \mathbb{R}$, defined by

$$|\psi_s\rangle = (\Delta'_\Omega)^{is}(\Delta'_{\Omega|\psi})^{-is}|\psi\rangle \ . \tag{9.4}$$

Thus far the definitions have been purely algebraic. In order to elucidate the intuition behind CC flow, let us write out the modular operators in terms of the left and right density operators, $\rho^{\psi}_{A_0} = \mathrm{Tr}_{A_0'}|\psi\rangle\langle\psi|$ and $\rho^{\psi}_{A_0'} = \mathrm{Tr}_{A_0}|\psi\rangle\langle\psi|$:[1]

$$\Delta_{\psi|\Omega} = \rho^{\Omega}_{A_0} \otimes (\rho^{\psi}_{A_0'})^{-1} \ . \tag{9.5}$$

One finds that the CC operator acts only in $\mathcal{A}_0'$:

$$(\Delta'_{\Omega})^{is}(\Delta'_{\Omega|\psi})^{-is} = (\rho^{\Omega}_{A_0'})^{is}(\rho^{\psi}_{A_0'})^{-is} \in \mathcal{A}_0' \ . \tag{9.6}$$

It follows that the reduced state on the right algebra satisfies

$$\rho^{\psi_s}_{A_0} = \rho^{\psi}_{A_0} \ . \tag{9.7}$$

Therefore, expectation values of observables $\mathcal{O} \in \mathcal{A}_0$ remain invariant under CC flow. These heuristic arguments would be valid only for finite-dimensional Hilbert spaces [265]; but Eq. (9.6) can be derived rigorously [259].

It can also be shown that $(\Delta'_{\psi|\Omega})^{is}\Delta^{is}_{\Omega|\psi} = 1$. Hence for operators $\mathcal{O}' \in \mathcal{A}_0'$, one finds that CC flow acts as $\Delta^{is}_{\Omega}$ inside of expectation values:

$$\begin{aligned}
\langle\psi_s|\mathcal{O}'|\psi_s\rangle &= \mathrm{Tr}_{\mathcal{A}_0'}\left[\rho^{\psi}_{A_0'}(\Delta^{-is}_{\psi|\Omega}\Delta^{is}_{\Omega})\mathcal{O}'(\Delta^{-is}_{\Omega}\Delta^{is}_{\psi|\Omega})\right] \ , \\
&= \mathrm{Tr}_{\mathcal{A}_0'}\left(\rho^{\psi}_{A_0'}(\rho^{\Omega}_{A_0'})^{-is}\mathcal{O}'(\rho^{\Omega}_{A_0'})^{is}\right) \qquad (9.8) \\
&= \mathrm{Tr}\left[|\psi\rangle\langle\psi|\Delta^{is}_{\Omega}(\mathbf{1}\otimes\mathcal{O}')\Delta^{-is}_{\Omega}\right] \ , \qquad (9.9)
\end{aligned}$$

where we have used the cyclicity of the trace.

To summarize, expectation values of one-sided operators transform as follows:

$$\langle\psi_s|\mathcal{O}|\psi_s\rangle = \langle\psi|\mathcal{O}|\psi\rangle \ , \tag{9.10}$$

$$\langle\psi_s|\mathcal{O}'|\psi_s\rangle = \langle\psi|\Delta^{is}_{\Omega}\mathcal{O}'\Delta^{-is}_{\Omega}|\psi\rangle \ . \tag{9.11}$$

There is no simple description of two-sided correlators in $|\psi_s\rangle$ such as $\langle\psi_s|\mathcal{O}\mathcal{O}'|\psi_s\rangle$; we discuss such objects in Section 9.6.

## CC Flow from Cuts on a Null Plane

Let us now specialize to the case where $\partial A_0$ corresponds to a cut $v = V_0(y)$ of the Rindler horizon $u = 0$. We have introduced null coordinates $u = t - x$ and $v = t + x$ and denoted the transverse coordinates collectively by $y$. It can be shown that the modular operator $\Delta^{is}_{\Omega}$

[1] We follow the conventions in [265] where complement operators are written to the right of the tensor product.

acts locally on each null generator $y$ of $u = 0$ as a boost about the cut $V_0(y)$ [266]. More explicitly, one can define the *full* vacuum modular Hamiltonian $\widehat{K}_{V_0}$ by

$$\widehat{K}_{V_0} = -\log \Delta_{\Omega;\mathcal{A}_{V_0}} \ . \tag{9.12}$$

We can write the full modular Hamiltonian as

$$\widehat{K}_{V_0} = K_{V_0} \otimes \mathbf{1}' - \mathbf{1} \otimes K'_{V_0} \ . \tag{9.13}$$

Let $\Delta$ denote vacuum subtraction, $\Delta\langle\mathcal{O}\rangle = \langle\mathcal{O}\rangle_\psi - \langle\mathcal{O}\rangle_\Omega$. Then, for arbitrary cuts of the Rindler horizon, we have [266]

$$\Delta\langle K'_{V_0}\rangle = -2\pi \int dy \int_{-\infty}^{V_0} dv[v - V_0(y)]\langle T_{vv}\rangle_\psi \ , \tag{9.14}$$

and similarly for $K_{V_0}$. Thus $K'_{V_0}$ is simply the boost generator about the cut $V_0(y)$ in the left Rindler wedge. That is, it generates a $y$-dependent dilation,

$$v \to V_0(y) + [v - V_0(y)]e^{2\pi s} \ . \tag{9.15}$$

This allows us to evaluate Eq. (9.11) explicitly for local operators at $u = 0$. For example, the CC flow of the stress tensor is

$$\langle\psi_s|T_{vv}|\psi_s\rangle|_{v<V_0} = e^{-4\pi s}\langle\psi|T_{vv}\left(V_0 + e^{-2\pi s}(v - V_0)\right)|\psi\rangle|_{v<V_0} \ , \tag{9.16}$$

and similarly for the other components of $T_{\mu\nu}$. There is a slight caveat here since $\Delta_\Omega^{is}$ only acts as a boost strictly at $u = 0$. This would be sufficient for free theories, where $T_{vv}$ can be defined through null quantization on the Rindler horizon with a smearing that only needs support on $u = 0$ [113]. More generally, $T_{\mu\nu}$ must be smeared in an open neighborhood of $u = 0$. However, if $V_0(y)$ is a perturbation of a flat cut then one can show that inside correlation functions $\Delta_\Omega^{is}$ approximately acts as a boost with subleading errors that vanish as $u \to 0$, to all orders in the perturbation [257, 267]. In the non-perturbative case, evidence comes from the fact that classically the vector field on the Rindler horizon which generates boosts about $V_0(y)$ can be extended to an approximate Killing vector field in a neighborhood of the horizon [268, 269]. Therefore we expect Eq. (9.16) to hold on the null surface even after smearing.

Now consider a second cut $V(y)$ of the Rindler horizon which lies entirely below $V_0(y)$, so $V < V_0$ for all $y$. The cut defines a surface $\partial A_V$ that splits a Cauchy surface $\mathcal{C}_V = A'_V \cup \partial A_V \cup A_V$; we take $A'_V$ to be the "left" side ($v < V$), with operator algebra $\mathcal{A}'_V$. The Araki definition of relative entropy is [265]

$$S'_{\rm rel}(\psi|\Omega; V) = -\langle\psi|\log \Delta_{\psi|\Omega;\mathcal{A}'_V}|\psi\rangle \ . \tag{9.17}$$

It has the following transformation properties [259]:

$$S_{\rm rel}(\psi_s|\Omega;V) = S_{\rm rel}(\psi|\Omega;V_0+e^{-2\pi s}(V-V_0)) \ , \tag{9.18}$$

$$\frac{\delta S_{\rm rel}(\psi_s|\Omega;V)}{\delta V} = e^{-2\pi s}\frac{\delta S_{\rm rel}(\psi|\Omega;V_0+e^{-2\pi s}(V-V_0))}{\delta V} \ . \tag{9.19}$$

Moreover, the "left" von Neumann entropy is defined as

$$S'(\psi,V) = -{\rm tr}_{A'_V}\rho^{\psi}_{A'_V}\log\rho^{\psi}_{A'_V} \ . \tag{9.20}$$

With these definitions in hand, one can decompose the relative entropy as

$$S'_{\rm rel}(\psi|\Omega;V) = \Delta\langle K'_V\rangle - \Delta S'(V) \ . \tag{9.21}$$

At this point we drop the explicit vacuum subtractions, as we will only be interested in shape derivatives of the vacuum subtracted quantities, which automatically annihilate the vacuum expectation values. In particular, one can directly compute shape derivatives of $K'_V$:

$$\frac{\delta\langle K'_V\rangle_\psi}{\delta V}\Big|_{V_0} = 2\pi\int_{-\infty}^{V_0}dv\ \langle T_{vv}\rangle_\psi \ . \tag{9.22}$$

Hence the transformations of both $K'_V$ and its derivative simply follow from Eq. (9.16).

Combining Eq. (9.18) and Eq. (9.14), as well as Eq. (9.19) and Eq. (9.22), we see that $S'(\psi,V)$ and its derivative transform as

$$S'(\psi_s,V) = S'(\psi,V_0+e^{-2\pi s}(V-V_0)) \ , \tag{9.23}$$

$$\frac{\delta S'}{\delta V}\Big|_{\psi_s,V} = e^{-2\pi s}\frac{\delta S'}{\delta V}\Big|_{\psi,V_0+e^{-2\pi s}(V-V_0)} \ . \tag{9.24}$$

The respective properties of the complement entropy follow from purity.

## Stress Tensor Shock at the Cut

CC flow generates a stress tensor shock at the cut $V_0$, proportional to the jump in the variation of the one-sided von Neumann entropy under deformations, at the cut [239]. To see this, let us start with the sum rule derived in [259] for null variations of relative entropy:[2]

$$2\pi(P_s - e^{-2\pi s}P_0) = (e^{-2\pi s}-1)\frac{\delta S'_{\rm rel}(\psi|\Omega;V)}{\delta V}\Big|_{V_0} \ , \tag{9.25}$$

where

$$P \equiv \int_{-\infty}^{\infty}dv\ T_{vv} \tag{9.26}$$

[2]For type I algebras, one can derive the analogous sum rule from simpler arguments [11].

is the averaged null energy operator at $u = 0$, and $P_s \equiv \langle\psi_s|P|\psi_s\rangle$, so in particular $P_0 \equiv \langle\psi|P|\psi\rangle$. (There is one such operator for every generator, *i.e.*, for every $y$.)

Inserting Eq. (9.21) and Eq. (9.22) into Eq. (9.25), and making use of Eq. (9.16), we see that there must exist a shock at $v = V_0(y)$:

$$\langle\psi_s|T_{vv}|\psi_s\rangle = (1 - e^{-2\pi s})\frac{1}{2\pi}\frac{\delta S'}{\delta V}\Big|_{V_0}\delta(v - V_0) + o(\delta) \ . \tag{9.27}$$

Here $o(\delta)$ designates the finite (non-distributional) terms. These are determined by Eq. (9.16), and by its trivial counterpart in the $v > V_0$ region.

This $s$-dependent shock is a detailed characteristic of the CC flowed state. As such, reproducing it through the holographic dictionary will be the key test of our proposal of the bulk dual of CC flow (see Section 9.4).

## Flat Cuts and the Precursor Slice

For the remainder of the paper we further specialize to flat cuts of the Rindler horizon, so that $\partial A_0$ corresponds to $u = v = 0$. We therefore set $V_0 = 0$ in what follows. We take $\mathcal{C}$ to be the Cauchy surface $t = 0$, so that $A_0$ ($t = 0$, $x > 0$) and $A_0'$ ($t = 0$, $x < 0$) are partial Cauchy surfaces for the right and left Rindler wedges.

In this case $\Delta_\Omega^{is}$ is a global boost by rapidity $s$ about $\partial A_0$ [270]. Thus, it has a simple geometric action not only on the null plane $u = 0$, but everywhere. CC flow transforms observables in $\mathcal{A}_0'$ by $\Delta_\Omega^{is}$ and leaves invariant those in $\mathcal{A}_0$. For a flat cut, this action can be represented as a geometric boost in the entire left Rindler wedge. This allows us to characterize the CC flowed state $|\psi(s)\rangle$ on $\mathcal{C}$ very simply in terms of a different state on a different Cauchy surface which we call the "precursor slice". This description will motivate the formulation of our bulk construction in Section 9.3.

By Eq. (9.11), the CC flowed state on the slice $\mathcal{C}$,

$$|\psi_s(\mathcal{C})\rangle = (\Delta_\Omega')^{is}(\Delta_{\Omega|\psi}')^{-is}|\psi(\mathcal{C})\rangle \ , \tag{9.28}$$

satisfies

$$\langle\psi_s(\mathcal{C})|\mathcal{O}_A|\psi_s(\mathcal{C})\rangle = \langle\psi(\mathcal{C})|\mathcal{O}_A|\psi(\mathcal{C})\rangle \ , \tag{9.29}$$

$$\langle\psi_s(\mathcal{C})|\Delta_\Omega^{-is}\mathcal{O}_{A'}\Delta_\Omega^{is}|\psi_s(\mathcal{C})\rangle = \langle\psi(\mathcal{C})|\mathcal{O}_{A'}|\psi(\mathcal{C})\rangle \ , \tag{9.30}$$

where $\mathcal{O}_A$ and $\mathcal{O}_{A'}$ denote an arbitrary collection of local operators that act on spacelike half-slices $A$ and $A'$ of $\mathcal{C}$ respectively.[3] In the second equality above, we used the fact that $\Delta_\Omega^{is}$ acts as a global boost to move it to the other side of the equality, compared to Eq. (9.11).

[3]More precisely, one would have to smear the operator in a codimension 0 neighborhood of points on the slices.

We work in the Schrödinger picture where the argument $\mathcal{C}$ should be interpreted as the time variable. The fact that $\Delta_\Omega^{is}$ acts as a boost around $\partial A_0$ motivates us to consider the time slice

$$\mathcal{C}_s = A'_s \cup \partial A_0 \cup A_0 \ , \tag{9.31}$$

where

$$A'_s = \{t = (\tanh 2\pi s)x, \ x < 0\} \ . \tag{9.32}$$

By Eqs. (9.29) and (9.30), each side of the CC-flowed state $|\psi_s(\mathcal{C}_s)\rangle$ is simply related to the left and right restrictions of the original state on the original slice:

$$\langle\psi_s(\mathcal{C}_s)|\mathcal{O}_A|\psi_s(\mathcal{C}_s)\rangle = \langle\psi(\mathcal{C})|\mathcal{O}_A|\psi(\mathcal{C})\rangle \ , \tag{9.33}$$

$$\langle\psi_s(\mathcal{C}_s)|\mathcal{O}_{A'_s}|\psi_s(\mathcal{C}_s)\rangle = \langle\psi(\mathcal{C})|\mathcal{O}_{A'}|\psi(\mathcal{C})\rangle \ . \tag{9.34}$$

In the second equation, $\mathcal{O}_{A'_s}$ denotes local operators on $A'_s$ which are analogous to $\mathcal{O}_{A'}$ on $A'$. More precisely, because the intrinsic metric of $A'$ and $A'_s$ are the same, there exists a natural map between local operators on $A'$ and $A'_s$.

In words, Eqs. (9.33) and (9.34) say that correlation functions in each half of $\mathcal{C}$ in the state $|\psi(\mathcal{C})\rangle$ are equal to the analogous correlation functions on each half of $\mathcal{C}_s$ in the state $|\psi_s(\mathcal{C}_s)\rangle$. This justifies calling $\mathcal{C}_s$ the precursor slice since the CC flowed state on $\mathcal{C}$ arises from it by time evolution.

We find it instructive to repeat this point in the less rigorous language of density operators. In the density operator form of CC flow,

$$|\psi_s(\mathcal{C})\rangle = (\rho^\Omega_{A'_0})^{is}(\rho^\psi_{A'_0})^{-is}|\psi(\mathcal{C})\rangle \ , \tag{9.35}$$

it is evident that the action of $(\rho^\Omega_{A'_0})^{is}$ can be absorbed into a change of time slice $\mathcal{C} \to \mathcal{C}_s$:

$$|\psi_s(\mathcal{C}_s)\rangle = (\rho^\psi_{A'_0})^{-is}|\psi(\mathcal{C})\rangle \ . \tag{9.36}$$

Tracing out each side of $\partial A_0$ implies

$$\rho^{\psi_s}_{A_0} = \rho^\psi_{A_0} \ , \tag{9.37}$$

$$\rho^{\psi_s}_{A'_s} = \rho^\psi_{A'_0} \ . \tag{9.38}$$

The first equality is trivial and was already discussed in Eq. (9.7). The second equality follows because $(\rho^\psi_{A'_0})^{is}$ commutes with $(\rho^\psi_{A'_0})$. This is the density operator version of Eqs. (9.33) and (9.34).

Eq. (9.36) should be contrasted with the one-sided modular-flowed state $|\phi(\mathcal{C})\rangle = (\rho^\psi_{A'_0})^{-is}|\psi(\mathcal{C})\rangle$. The latter state would live on the original slice $\mathcal{C}$, but it is not well-defined since it would have infinite energy at the entangling surface.

It will be useful to define new coordinates adapted to the precursor slice $\mathcal{C}_s$. Let

$$\tilde{v} = v\,\Theta(v) + e^{-2\pi s}\,v\,(1 - \Theta(v)) \ , \tag{9.39}$$

$$\tilde{u} = e^{2\pi s}u\,\Theta(u) + \ u\,(1 - \Theta(u)) \ , \tag{9.40}$$

where $\Theta(.)$ is the Heaviside step function. Let $\tilde{t} = \frac{1}{2}(\tilde{v} + \tilde{u})$ and $\tilde{x} = \frac{1}{2}(\tilde{v} - \tilde{u})$. In these coordinates, the Minkowski metric takes the form

$$ds^2 = \left[\Theta(\tilde{t}+\tilde{x}) + e^{2\pi s}(1-\Theta(\tilde{t}+\tilde{x}))\right]\left[e^{-2\pi s}\Theta(\tilde{t}-\tilde{x}) + (1-\Theta(\tilde{t}-\tilde{x}))\right](-d\tilde{t}^2 + d\tilde{x}^2) + d^{d-2}y \ , \tag{9.41}$$

and the precursor slice corresponds to $\tilde{t} = 0$.

In these "tilde" coordinates, the stress tensor shock of Eq. (9.27) takes the form[4]

$$\langle\psi_s|T_{\tilde{v}\tilde{v}}|\psi_s\rangle = \frac{1}{2\pi}\left(\frac{\partial v}{\partial \tilde{v}}\right)^2 (1-e^{-2\pi s})\frac{\delta S}{\delta V}\Big|_{V=0}\delta(v) + o(\delta) \ . \tag{9.42}$$

Recall that the entropy variation is evaluated in the state $|\psi\rangle$. By Eq. (9.24),

$$\frac{\delta S}{\delta V}\Big|_{\psi} = \frac{\delta S}{\delta \widetilde{V}}\Big|_{\psi_s} \ , \tag{9.43}$$

where $\widetilde{V}(y)$ is a cut of the Rindler horizon in the $\tilde{v}$ coordinates. Thus we may instead evaluate the entropy variation in the state $|\psi_s\rangle$ on the precursor slice. This will be convenient when matching the bulk and boundary.

The Jacobian in Eq. (9.42) has a step function in it, as will the Jacobian coming from $\delta(v)$. A step function multiplying a delta function is well-defined if one averages the left and right derivatives:

$$\left(\frac{\partial v}{\partial \tilde{v}}\right)^2 \delta(v) = \frac{1}{2}\left(\frac{\partial v}{\partial \tilde{v}}\Big|_{0^-} + \frac{\partial v}{\partial \tilde{v}}\Big|_{0^+}\right)\delta(\tilde{v}) \ . \tag{9.44}$$

Thus Eq. (9.42) becomes

$$\langle\psi_s|T_{\tilde{v}\tilde{v}}(\tilde{v})|\psi_s\rangle = \frac{1}{2\pi}\sinh(2\pi s)\frac{\delta S}{\delta \widetilde{V}}\Big|_{\psi_s,\widetilde{V}=0}\delta(\tilde{v}) + o(\delta). \tag{9.45}$$

Since we are dealing with a flat cut, the symmetry $s \leftrightarrow -s, v \leftrightarrow u$ implies that CC flow also generates a $T_{uu}$ shock in the state $|\psi_s\rangle$ at $u = v = 0$:

$$\langle\psi_s|T_{\tilde{u}\tilde{u}}|\psi_s\rangle = \frac{1}{2\pi}\sinh(2\pi s)\frac{\delta S}{\delta \widetilde{U}}\Big|_{\psi_s,\widetilde{V}=0}\delta(\tilde{u}) + o(\delta) \ . \tag{9.46}$$

(Note that $\delta/\delta V$ goes to $-\delta/\delta U$.) The linear combination

$$\langle\psi_s|T_{\tilde{t}\tilde{x}}(\tilde{t},\tilde{x})|\psi_s\rangle = \frac{1}{2\pi}\sinh(2\pi s)\frac{\delta S}{\delta \widetilde{X}}\Big|_{\psi_s,\widetilde{X}=0}\delta(\tilde{x}) + \langle\psi|T_{tx}(t=\tilde{t},x=\tilde{x})|\psi\rangle \ . \tag{9.47}$$

will be useful in Section 9.4. The last term was obtained from Eqs. (9.37) and (9.38); it makes the finite piece explicit. Note that these equations are valid in the entire left and right wedges, not just on $\mathcal{C}_s$.

[4]We remind the reader that $o(\delta)$ refers to any finite (non-distributional) terms.

## 9.3 Kink Transform

In this section, we introduce a novel geometric transformation called the kink transform. The construction is motivated by thinking about what the bulk dual of the boundary CC flow would be in the context of AdS/CFT. As we discussed in Section 9.2, CC flow boosts observables in $D(A')$ and leaves observables in $D(A)$ unchanged. Subregion duality in AdS/CFT then implies that the bulk dual of the state $|\psi_s\rangle$ has to have the property that the entanglement wedges of $D(A)$ and $D(A')$ will be diffeomorphic to those of the state $|\psi\rangle$, but are glued together with a "one-sided boost" at the HRT surface. In a general geometry, a boost Killing symmetry need not exist. The kink transform appropriately generalizes the notion of a one-sided boost to any extremal surface.

In Section 9.3, we formulate the kink transform. In Section 9.3, we describe a different but equivalent formulation of the kink transform and show that the kink transform results in the same new spacetime, regardless of which Cauchy surface containing the extremal surface is used for the construction. In Section 9.4, we will describe the duality between the bulk kink transform and the boundary CC flow in AdS/CFT and provide evidence for it.

### Formulation

Consider a $d+1$ dimensional spacetime $\mathcal{M}$ with metric $g_{\mu\nu}$ satisfying the Einstein field equations. (We will discuss higher curvature gravity in Section 9.6.) Let $\Sigma$ be a Cauchy surface of $\mathcal{M}$ that contains an extremal surface $\mathcal{R}$ of codimension 1 in $\Sigma$. (That is, the expansion of both sets of null geodesics orthogonal to $\mathcal{R}$ vanishes.)

Initial data on $\Sigma$ consist of [271] the intrinsic metric $(h_\Sigma)_{ab}$ and the extrinsic curvature,

$$(K_\Sigma)_{ab} = P_a^\mu P_b^\nu \nabla_{(\mu} t_{\nu)} \ . \tag{9.48}$$

Here $P_a^\mu$ is the projector from $\mathcal{M}$ onto $\Sigma$, and $t^\mu$ is the unit norm timelike vector field orthogonal to $\Sigma$. Indices $a, b, \ldots$ are reserved for directions tangent to $\Sigma$. For matter fields, initial data consist of the fields and normal derivatives, for example $\phi(w^a)$ and $[t^\mu \nabla_\mu \phi](w^a)$, where $\phi$ is a scalar field and $w^a$ are coordinates on $\Sigma$.

By the Einstein equations, the initial data on $\Sigma$ must satisfy the following constraints:

$$r_\Sigma + K_\Sigma^2 - (K_\Sigma)_{ab}(K_\Sigma)^{ab} = 16\pi G\, T_{\mu\nu} t^\mu t^\nu \ , \tag{9.49}$$

$$D^a (K_\Sigma)_{ab} - D_b K_\Sigma = 8\pi G\, T_{b\nu} t^\nu \ , \tag{9.50}$$

where $D_a = P_a^\mu \nabla_\mu$ is the covariant derivative that $\Sigma$ inherits from $(\mathcal{M}, g_{\mu\nu})$; $r_\Sigma$ is the Ricci scalar intrinsic to $\Sigma$; and $K_\Sigma$ is the trace of the extrinsic curvature: $K_\Sigma = (h_\Sigma)^{ab}(K_\Sigma)_{ab}$.

Let $\Sigma$ be a Cauchy slice of $\mathcal{M}$ containing $\mathcal{R}$ and smooth in a neighborhood of $\mathcal{R}$. The kink transform is then a map of the initial data on $\Sigma$ to a new initial data set, parametrized by a real number $s$ analogous to boost rapidity. The transform acts as the identity on all data except for the extrinsic curvature, which is modified only at the location of the extremal

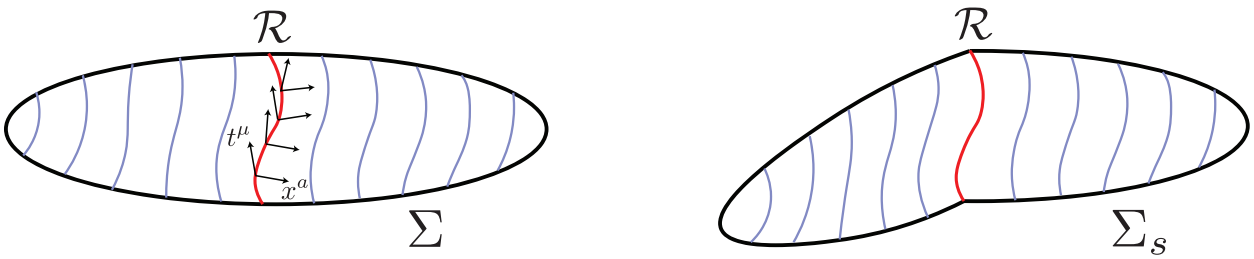


Figure 9.1: Kink transform. Left: a Cauchy surface $\Sigma$ of the original bulk $\mathcal{M}$. An extremal surface $\mathcal{R}$ is shown in red. The orthonormal vector fields $t^a$ and $x^a$ span the normal bundle to $\mathcal{R}$; $x^a$ is tangent to $\Sigma$. Right: The kink transformed Cauchy surface $\Sigma_s$. As an initial data set, $\Sigma_s$ differs from $\Sigma$ only in the extrinsic curvature at $\mathcal{R}$ through Eq. (9.51). Equivalently, the kink transform is a relative boost in the normal bundle to $\mathcal{R}$, Eq. (9.68).

surface $\mathcal{R}$, as follows:

$$(K_\Sigma)_{ab} \to (K_{\Sigma_s})_{ab} = (K_\Sigma)_{ab} - \sinh(2\pi s)\; x_a x_b\; \delta(\mathcal{R}) \; . \tag{9.51}$$

Here $x^a$ is a unit norm vector field orthogonal to $\mathcal{R}$ and tangent to $\Sigma$, and we define

$$\delta(\mathcal{R}) \equiv \delta(x) \; , \tag{9.52}$$

where $x$ is the Gaussian normal coordinate to $\mathcal{R}$ in $\Sigma$ ($\partial_x = x^a$). Thus, the only change in the initial data is in the component of the extrinsic curvature normal to $\mathcal{R}$. An equivalent transformation exists for initial choices of $\Sigma$ that are not smooth around $\mathcal{R}$ though the transformation rule will be more complicated than Eq. (9.51). We will discuss this later in the section.

Let $\Sigma_s$ be a time slice with this new initial data, as in Fig. 9.1, and let $\mathcal{M}_s$ be the Cauchy development of $\Sigma_s$. That is, $\mathcal{M}_s$ is the new spacetime resulting from the evolution of the kink-transformed initial data. Since the intrinsic metric of $\Sigma_s$ and $\Sigma$ are the same, they can be identified as $d$-manifolds with metric; the subscript $s$ merely reminds us of the different extrinsic data they carry. In particular the surface $\mathcal{R}$ can be so identified; thus $\mathcal{R}_s$ has the same intrinsic metric as $\mathcal{R}$. It also trivially has identical extrinsic data with respect to $\Sigma_s$. In fact, we will find below that like $\mathcal{R}$ in $\mathcal{M}$, $\mathcal{R}_s$ is an extremal surface in $\mathcal{M}_s$. However, the trace-free part of the extrinsic curvature of $\mathcal{R}_s$ in $\mathcal{M}_s$ may have discontinuities.

We will now show that the constraint equations hold on $\Sigma_s$; that is, the kink transform generates valid initial data. This need only be verified at $\mathcal{R}$ since the transform acts as the identity elsewhere. Here we will make essential use of the extremality of $\mathcal{R}$ in $\mathcal{M}$, which we express as follows.

The extrinsic curvature of $\mathcal{R}$ with respect to $\mathcal{M}$ has two independent components. Often

these are chosen to be the two orthogonal null directions, but we find it useful to consider

$$(B^{(t)}_{\mathcal{R}})_{ij} = P^\mu_i P^\nu_j \nabla_{(\mu} t_{\nu)} \ , \tag{9.53}$$

$$(B^{(x)}_{\mathcal{R}})_{ij} = P^\mu_i P^\nu_j \nabla_{(\mu} x_{\nu)} \ . \tag{9.54}$$

Here $i, j$ represent directions tangent to $\mathcal{R}$, and $P^\mu_i$ is the projector from $\mathcal{M}$ to $\mathcal{R}$. Extremality of $\mathcal{R}$ in $\mathcal{M}$ is the statement that the trace of each extrinsic curvature component vanishes:

$$B^{(t)}_{\mathcal{R}} = (\gamma_{\mathcal{R}})^{ij}(B^{(t)}_{\mathcal{R}})_{ij} = 0 \ , \tag{9.55}$$

$$B^{(x)}_{\mathcal{R}} = (\gamma_{\mathcal{R}})^{ij}(B^{(x)}_{\mathcal{R}})_{ij} = 0 \ , \tag{9.56}$$

where $(\gamma_{\mathcal{R}})_{ij} = P^a_i P^b_j (h_\Sigma)_{ab}$ is the intrinsic metric on $\mathcal{R}$.

Orthogonality of $t^\mu$ and $x^\mu$ implies that $P^\mu_i = P^a_i P^\mu_a$, and hence

$$(B^{(t)}_{\mathcal{R}})_{ij} = P^a_i P^b_j (K_\Sigma)_{ab} \ . \tag{9.57}$$

Since $x^a$ is the unit norm orthogonal vector field at $\mathcal{R}$, the trace of $(K_\Sigma)_{ab}$ at $\mathcal{R}$ can be written as:

$$K_\Sigma|_{\mathcal{R}} = x^a x^b (K_\Sigma)_{ab} + (\gamma_{\mathcal{R}})^{ij}(B^{(t)}_{\mathcal{R}})_{ij} = x^a x^b (K_\Sigma)_{ab} \ . \tag{9.58}$$

A little algebra then implies

$$(K_{\Sigma_s})^2 - (K_{\Sigma_s})_{ab}(K_{\Sigma_s})^{ab} = (K_\Sigma)^2 - (K_\Sigma)_{ab}(K_\Sigma)^{ab} \ . \tag{9.59}$$

Moreover, we have $r_\Sigma = r_{\Sigma_s}$ since the two initial data slices have the same intrinsic metric. Thus Eq. (9.49) implies that the kink-transformed slice satisfies the scalar constraint equation:

$$r_{\Sigma_s} + (K_{\Sigma_s})^2 - (K_{\Sigma_s})_{ab}(K_{\Sigma_s})^{ab} = 16\pi G T_{\mu\nu} t^\mu t^\nu \ . \tag{9.60}$$

To check the vector constraint Eq. (9.50), we separately consider the two cases of $b = x$ and $b = i$ where $i, j$ represent directions tangent to $\mathcal{R}$:

$$\begin{aligned} D_a(K_{\Sigma_s})^a_x - D_x K_{\Sigma_s} &= D_a(K_\Sigma)^a_x - D_x K_\Sigma + B^{(x)}_{\mathcal{R}} \sinh(2\pi s)\delta(x) \\ &= D_a(K_\Sigma)^a_x - D_x K_\Sigma = 8\pi G\, T_{x\nu} t^\nu \ , \end{aligned} \tag{9.61}$$

$$D_a(K_{\Sigma_s})^a_i - D_i K_{\Sigma_s} = D_a(K_\Sigma)^a_i - D_i K_\Sigma = 8\pi G\, T_{i\nu} t^\nu \ , \tag{9.62}$$

where the second line of the first equation follows from the extremality of $\mathcal{R}$.

We conclude that the kink transform is a valid modification to the initial data. For both constraints to be satisfied after the kink, it was essential that $\mathcal{R}$ is an extremal surface. Thus

the kink transform is only well-defined across an extremal surface. Note also that $\mathcal{R}_s \subset \Sigma_s$ is an extremal surface in $\mathcal{M}_s$. By Eq. (9.57),

$$(B^{(t)}_{\mathcal{R}_s})_{ij} = P^a_i P^b_j \, (K_{\Sigma_s})_{ab}|_{\mathcal{R}_s} = (B^{(t)}_{\mathcal{R}})_{ij} \implies B^{(t)}_{\mathcal{R}_s} = 0 \ . \tag{9.63}$$

In the second equality we used Eq. (9.51) as well as the fact that all relevant quantities are intrinsic to $\Sigma_s$, so $\mathcal{R}_s$ can be identified with $\mathcal{R}$. Moreover,

$$(B^{(x)}_{\mathcal{R}_s})_{ij} = (B^{(x)}_{\mathcal{R}})_{ij} \implies B^{(x)}_{\mathcal{R}_s} = 0 \ , \tag{9.64}$$

since this quantity depends only on the intrinsic metrics of $\Sigma$ and $\Sigma_s$, which are identical.

## Properties

We will now establish important properties and an equivalent formulation of the kink transform.

Let us write $\Sigma$ as the disjoint union

$$\Sigma = a' \cup \mathcal{R} \cup a \ . \tag{9.65}$$

The spacetime $\mathcal{M}$ contains $D(a)$ and $D(a')$ where $D(.)$ denotes the domain of dependence. The kink transformed slice $\Sigma_s$ contains regions $a$ and $a'$ with identical initial data, so $\mathcal{M}_s$ also contains $D(a)$ and $D(a')$. Because $\Sigma_s$ has different extrinsic curvature at $\mathcal{R}$, the two domains of dependence will be glued to each other differently in $\mathcal{M}_s$, so the full spacetime will differ from $\mathcal{M}$ in the future and past of $\mathcal{R}$. This is depicted in Fig. 9.2.

We will now derive an alternative formulation of the kink transform as a one-sided local Lorentz boost at $\mathcal{R}$. The unit vector field $t^\mu_{\Sigma_s}$ normal to $\Sigma_s$ is discontinuous at $\mathcal{R}$ due to the kink. Let

$$(t^\mu_{\Sigma_s})_R = \lim_{x \to 0^+} t^\mu_{\Sigma_s} \ , \tag{9.66}$$

$$(t^\mu_{\Sigma_s})_L = \lim_{x \to 0^-} t^\mu_{\Sigma_s} \tag{9.67}$$

be the left and right limits to $\mathcal{R}$. The metric of $\mathcal{M}_s$ is continuous since it arises from valid initial data on $\Sigma_s$. Therefore, the normal bundle of 1+1 dimensional normal spacetimes to points in $\mathcal{R}$ is well-defined. The above vector fields $(t^\mu_{\Sigma_s})_R$ and $(t^\mu_{\Sigma_s})_L$ belong to this normal bundle. Therefore at each point on $\mathcal{R}$, the two vectors can only differ by a Lorentz boost acting in 1+1 dimensional Minkowski space. The kink transform, Eq. (9.51), implies:

$$(t^\mu_{\Sigma_s})_R = (\Lambda_{2\pi s})^\mu_\nu (t^\nu_{\Sigma_s})_L \ , \tag{9.68}$$

where $(\Lambda_{2\pi s})^\mu_\nu$ is a Lorentz boost of rapidity $2\pi s$. In this sense, the kink transform resembles a local boost around $\mathcal{R}$. Alternatively, we can view Eq. (9.68) as the definition of the kink transform. This definition can be applied to Cauchy slices that are not smooth around $\mathcal{R}$, but it reduces to Eq. (9.51) in the smooth case.

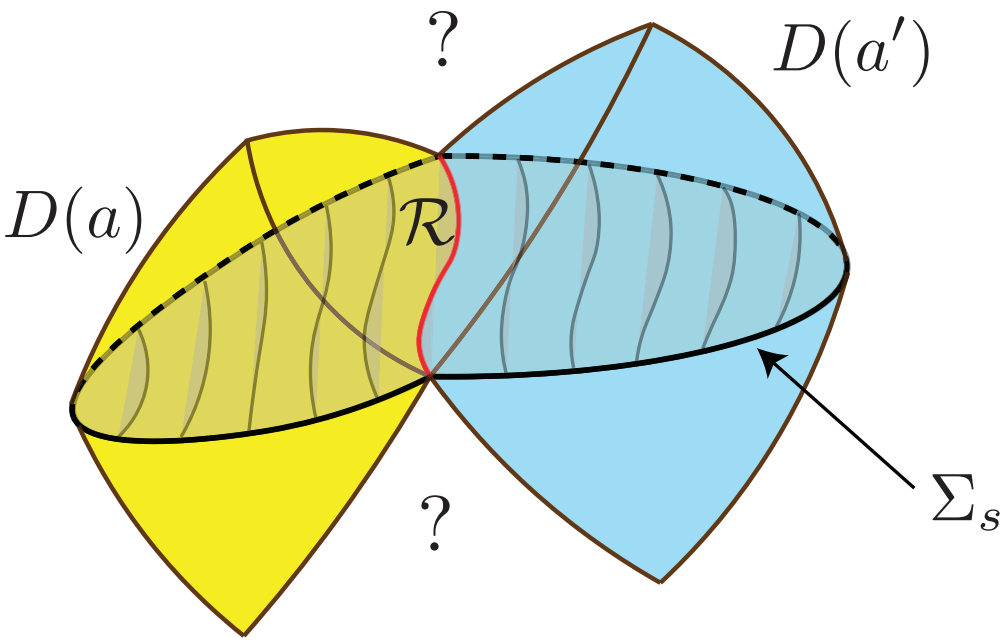


Figure 9.2: The kink-transformed spacetime $\mathcal{M}_s$ is generated by the Cauchy evolution of the kinked slice $\Sigma_s$. This reproduces the left and right entanglement wedges $D(a)$ and $D(a')$ of the original spacetime $\mathcal{M}$. The future and past of the extremal surface $\mathcal{R}$ are in general not related to the original spacetime.

This observation applies equally to any other vector field $\xi^\mu$ in the normal bundle to $\mathcal{R}$, if $\xi^\mu$ has a smooth extension into $D(a')$ and $D(a)$ in $\mathcal{M}$. The norm of $\xi^\mu$ and its inner products with $(t^\mu_{\Sigma_s})_L$ and $(t^\mu_{\Sigma_s})_R$ are unchanged by the kink transform. Hence, in $\mathcal{M}_s$, the left and right limits of $\xi^\mu$ to $\mathcal{R}$ will satisfy

$$\xi^\mu_R = (\Lambda_{2\pi s})^\mu_\nu \xi^\nu_L \ . \tag{9.69}$$

Now let $\Xi \supset \mathcal{R}$ be another Cauchy slice of $D(\Sigma)$. Since $\Xi$ contains $\mathcal{R}$, its timelike normal vector field $\xi^\mu$ (at $\mathcal{R}$) lies in the normal bundle to $\mathcal{R}$. We have shown that Eq. (9.68) is equivalent to the kink transform of $\Sigma$; that Eq. (9.69) is equivalent to the kink transform of $\Xi$; and that Eq. (9.68) is equivalent to Eq. (9.69). Hence the kink transform of $\Sigma$ is equivalent to the kink transform of $\Xi$. In other words, the spacetime resulting from a kink transform about $\mathcal{R}$ does not depend on which Cauchy surface containing $\mathcal{R}$ we apply the kink transform to.

The kink transform (with $s \neq 0$) always generates physically inequivalent initial data. However $\mathcal{M}_s$ need not differ from $\mathcal{M}$. They will be the same if and only if $\Sigma_s$ is an initial data set in $\mathcal{M}$. There is an interesting special case where this holds for all values of $s$. Namely, suppose $\mathcal{M}$ has a Killing vector field that reduces to a boost in the normal bundle to $\mathcal{R}$.

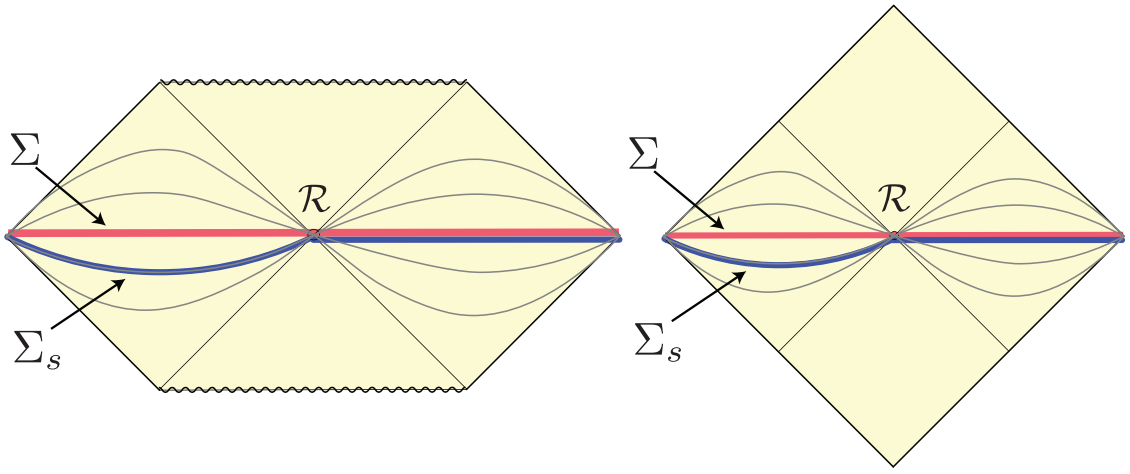


Figure 9.3: Straight slices $\Sigma$ (red) in a maximally extended Schwarzschild (left) and Rindler (right) spacetime get mapped to kinked slices $\Sigma_s$ (blue) under the kink transform about $\mathcal{R}$.

Then $\Sigma_s \subset \mathcal{M}$ (as a full initial data set), for all $s$. For example, the kink transform maps straight to kinked slices in the Rindler or maximally extended Schwarzschild spacetimes (see Fig. 9.3).

We can also consider the kink transform of matter fields on a fixed background spacetime with the above symmetry. Geometrically, $\mathcal{M} = \mathcal{M}_s$ for all $s$, but the matter fields will differ in $\mathcal{M}_s$ by a one-sided action of the Killing vector field. For example, let $\mathcal{M}$ be Minkowski space, with two balls at rest at $x = \pm 1$, $y = z = 0$ (see Fig. 9.4); and let $\mathcal{R}$ given by $x = t = 0$. In the spacetime $\mathcal{M}_s$ obtained by a kink transform, the two balls will approach with velocity $\tanh 2\pi s$ and so will collide. The right and left Rindler wedge, $D(a)$ and $D(a')$, are separately preserved; the collision happens in the past or future of $\mathcal{R}$.

## 9.4 Bulk Kink Transform = Boundary CC Flow

In this section, we will argue that the kink transform is the bulk dual of boundary CC flow. We will show that the kink transform satisfies two nontrivial necessary conditions. First, in Section 9.4, we show that the left and right bulk region are the subregion duals to the left and right boundary region, respectively. In Section 9.4 we show that the bulk kink transform leads to precisely the stress tensor shock at the boundary generated by boundary CC flow, Eq. (9.47). (In Section 9.5 we will show that the kink transform predicts additional shocks in the CC flowed state, which have not been derived previously purely from QFT methods.)

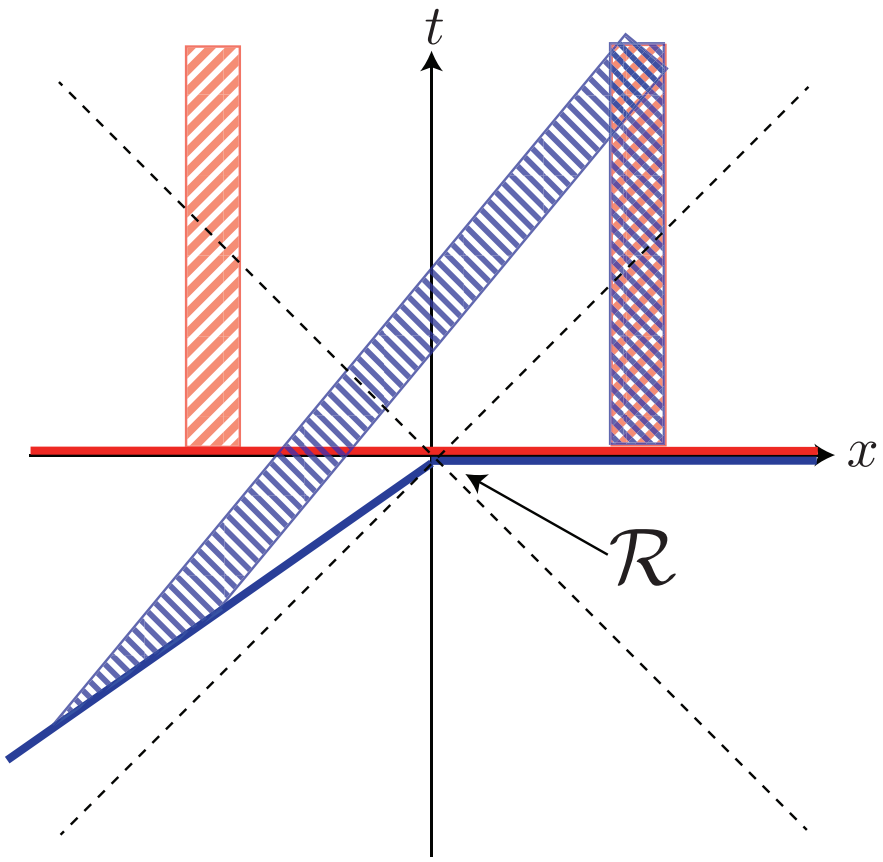


Figure 9.4: On a fixed background with boost symmetry, the kink transform changes the initial data of the matter fields. In this example, $\mathcal{M}$ is Minkowski space with two balls relatively at rest (red).The kink transform is still Minkowski space, but the balls collide in the future of $\mathcal{R}$ (blue).

## Matching Left and Right Reduced States

The entanglement wedge of a boundary region $A$ in a (pure or mixed) state $\rho_A$,

$$\mathrm{EW}(\rho_A) = D[a(\rho_A)] \tag{9.70}$$

is the domain of dependence of a bulk achronal region $a$ satisfying the following properties [18, 20, 21, 22]:

1. The topological boundary of $a$ (in the unphysical spacetime that includes the conformal boundary of AdS) is given by $\partial a = A \cup \mathcal{R}$.

2. $S_{\mathrm{gen}}(a)$ is stationary under small deformations of $\mathcal{R}$.

3. Among all regions that satisfy the previous criteria, $\mathrm{EW}(\rho_A)$ is the one with the smallest $S_{\mathrm{gen}}(a)$.

We neglect end-of-the-world branes in this discussion [272, 273]. The generalized entropy is given by

$$S_{\mathrm{gen}} = \frac{\mathrm{Area}(\mathcal{R})}{4G\hbar} + S(a) + \dots \ , \tag{9.71}$$

where $S(a)$ is the von Neumann entropy of the region $a$ and the dots indicate subleading geometric terms. The entanglement wedge is also referred to as the Wheeler-DeWitt patch of $A$.

There is significant evidence [24, 25] that $\mathrm{EW}(\rho_A)$ represents the entire bulk dual to the boundary region $A$. That is, all bulk operators in $\mathrm{EW}(\rho_A)$ have a representation in the algebra of operators $\mathcal{A}$ associated with $A$; and all simple correlation functions in $A$ can be computed from the bulk. In other words, the entanglement wedge appears to be the answer [22] to the question [127, 274, 128, 275] of "subregion duality." A bulk surface $\mathcal{R}$ is called quantum extremal (with respect to $A$ in the state $\rho$) if it satisfies the first two criteria, and quantum RT if it satisfies all three. When the von Neumann entropy term in Eq. (9.71) is neglected, $\mathcal{R}$ is called an extremal or RT surface, respectively. This will be the case everywhere in this paper except in Section 9.6.

We now specialize to the setting in which CC flow was considered in Section 9.2. Recall that the pure boundary state $|\psi(\mathcal{C})\rangle$ is given on a boundary slice $\mathcal{C}$ corresponding to $t = 0$ in standard Minkowski coordinates; and that we regard $\mathcal{C}$ as the disjoint union of the left region $A_0'$ ($x < 0$), with reduced state $\rho^{\psi}_{A_0}$; the cut $\partial A_0$ ($x = 0$); and the right region $A_0$ ($x > 0$), with reduced state $\rho^{\psi}_{A_0'}$. Let $a_0'$ and $a_0$ be arbitrary Cauchy surfaces of the associated entanglement wedges $\mathrm{EW}(\rho^{\psi}_{A_0'})$ and $\mathrm{EW}(\rho^{\psi}_{A_0})$.

The entanglement wedges of non-overlapping regions are always disjoint, so

$$\mathrm{EW}(\rho^{\psi}_{A_0'}) \cap \mathrm{EW}(\rho^{\psi}_{A_0}) = \varnothing \ . \tag{9.72}$$

For the bipartition of a pure boundary state $\psi$, entanglement wedge complementarity holds:

$$a[|\psi(\mathcal{C})\rangle] = a_0' \cup \mathcal{R} \cup a_0 \ , \tag{9.73}$$

where $a[|\psi(\mathcal{C})\rangle]$ is a Cauchy surface of $\mathrm{EW}(|\psi(\mathcal{C})\rangle)$. In particular, the left and right entanglement wedge share the same HRT surface $\mathcal{R}$.

Crucially, the classical initial data on $a[|\psi(\mathcal{C})\rangle]$ is almost completely determined by the data on $a_0'$ and $a_0$; however the data on $\mathcal{R}$ are not contained in $a_0'$ nor in $a_0$. In the semiclassical regime, the quantum state on $a[|\psi(\mathcal{C})\rangle]$ also includes global information (through its entanglement structure) that neither subregion contains on its own. Hence in general

$$\mathrm{EW}(|\psi(\mathcal{C})\rangle) = D\left[\mathrm{EW}(\rho^{\psi}_{A_0'}) \cup \mathcal{R} \cup \mathrm{EW}(\rho^{\psi}_{A_0})\right] \tag{9.74}$$

is a proper superset of $\mathrm{EW}(\rho^{\psi}_{A'_0}) \cup \mathrm{EW}(\rho^{\psi}_{A_0})$ that also includes some of the past and future of $\mathcal{R}$.

Now consider the CC-flowed state on the precursor slice $|\psi_s(\mathcal{C}_s)\rangle$. By Eqs. (9.37) and (9.38), we have

$$\mathrm{EW}(\rho^{\psi_s}_{A'_s}) = \mathrm{EW}(\rho^{\psi}_{A'_0}) = D(a'_0) \ , \tag{9.75}$$

$$\mathrm{EW}(\rho^{\psi_s}_{A_0}) = \mathrm{EW}(\rho^{\psi}_{A_0}) = D(a_0) \ , \tag{9.76}$$

Since $|\psi_s\rangle$ is again a pure state, $\mathrm{EW}[|\psi_s(\mathcal{C}_s)\rangle] = D\left(a[|\psi_s(\mathcal{C}_s)\rangle]\right)$ where

$$a[|\psi_s(\mathcal{C}_s)\rangle] = a'_0 \cup \mathcal{R} \cup a_0 \ . \tag{9.77}$$

We see that this initial data slice has the same intrinsic geometry as that of the original bulk dual. Indeed, by the remarks following Eq. (9.73), the full classical initial data for the bulk dual to $|\psi_s\rangle$ will be identical on $a'_0 \cup a_0$ and can only differ from the initial data for the original bulk at $\mathcal{R}$.

We pause here to note that a kink transform of $a[|\psi(\mathcal{C})\rangle]$ centered on $\mathcal{R}$ satisfies this necessary condition and hence becomes a candidate for $a[|\psi_s(\mathcal{C}_s)\rangle]$. However, this does not yet constrain the value of $s$. In order to go further, we would now like to show that a kink transform of $a[|\psi(\mathcal{C})\rangle]$ with parameter $s$ yields a bulk slice whose boundary is geometrically the precursor slice $\mathcal{C}_s$.

The bulk metric takes the asymptotic form [276]:[5]

$$ds^2 = \frac{1}{z^2}\left[dz^2 + \eta_{AB}dx^A dx^B + O(z^d)\right] \ , \tag{9.78}$$

where $\eta_{AB}$ is the metric of Minkowski space. Consider a stationary bulk surface $\mathcal{R}$ anchored on the boundary cut $u = v = 0$. At leading order, $\mathcal{R}$ will reside at $u = v = 0$ in the asymptotic bulk, in the above metric [262]. (The first subleading term, which appears at order $z^d$, will be crucial in our derivation of the boundary stress tensor shock in Section 9.4.)

Let $\Sigma$ be a bulk surface that contains $\mathcal{R}$ and satisfies $t = 0 + O(z^d)$ in the metric of Eq. (9.78). Since the initial data on each side of $\mathcal{R}$ are separately preserved (see Section 9.3), Eq. (9.68) dictates that the kink transform $\Sigma_s$ of $\Sigma$ satisfies $t = 0$ $(x > 0)$ and $t = x \tanh 2\pi s$ $(x < 0)$, again up to corrections of order $z^d$. The corrections all vanish at $z = 0$, where $\Sigma$ is bounded by $\mathcal{C}$ and $\Sigma_s$ is bounded by $\mathcal{C}_s$ (see Eq. (9.32)). Recall also that the kink transform is slice-independent. Thus we have established that the kink transform of any Cauchy surface $a[|\psi(\mathcal{C})\rangle]$, by $s$ along $\mathcal{R}$, yields a Cauchy surface bounded by the precursor slice $\mathcal{C}_s$.

The above arguments establish that

$$\mathrm{EW}[|\psi_s(\mathcal{C}_s)\rangle] = D\left(a[|\psi_s(\mathcal{C}_s)\rangle]\right) \ , \tag{9.79}$$

where $a[|\psi_s(\mathcal{C}_s)\rangle]$ is given by Eq. (9.77). In words, the bulk dual of the CC-flowed boundary state is the Cauchy development of the kink-transform of a Cauchy slice containing the HRT

[5] We set $\ell_{\mathrm{AdS}} = 1$.

surface $\mathcal{R}$. Note that the classical initial data on this Cauchy surface is fully determined by the initial data on $a_0'$ and $a_0$ inherited from the bulk dual of $|\psi(\mathcal{C})\rangle$, combined with the distributional geometric initial data consisting of the extrinsic curvature shock at $\mathcal{R}$. The full spacetime geometry will differ from EW$[|\psi(\mathcal{C})\rangle]$ because of the different gluing at $\mathcal{R}$.

## Matching Bulk and Boundary Shocks

In Section 9.3, we gave a prescription for generating bulk geometries in AdS by inserting a kink on the Cauchy surface, at the HRT surface. With the standard holographic dictionary, the resulting geometry manifestly yields the correct behavior of one-sided boundary observables under CC flow. This was shown in the previous subsection.

Another characteristic aspect of the CC flowed state $|\psi_s\rangle$ is the presence of a stress tensor shock at the cut (Section 9.2), proportional to shape derivatives of the von Neumann entropy; see Eq. (9.47). We will now verify that this shock is reproduced by the kink transform in the bulk, upon applying the AdS/CFT dictionary. Notably, the shock is not localized to either wedge. Verifying kink/CC duality for this observable furnishes an independent, nontrivial check of our proposal.

We will now keep the first subleading term in the Fefferman-Graham expansion of the asymptotic bulk metric [276, 262]:

$$ds^2 = \frac{1}{z^2}\left(dz^2 + g_{AB}(x,z)dx^A dx^B\right) \ , \tag{9.80}$$

$$g_{AB}(x,z) = \eta_{AB} + z^d \frac{16\pi G}{d}\langle T_{AB}\rangle + o(z^d) \ , \tag{9.81}$$

where indices $A, B, \ldots$ correspond to directions along $z =$ const. surfaces.

The location of the RT surface $\mathcal{R}$ in the bulk can be described by a collection of $(d-1)$ embedding functions

$$X^\mu(y,z) = (z, X^A(y,z)) \ , \tag{9.82}$$

where $(y,z)$ are intrinsic coordinates on $\mathcal{R}$. The expansion in $z$ takes the simple form

$$X^A(y,z)) = z^d X^A_{(d)} + o(z^d) \ , \tag{9.83}$$

because the boundary anchor is the flat cut $u = v = 0$ of the Rindler horizon [262]. Stationarity of $\mathcal{R}$ can be shown to imply [262]

$$X^A_{(d)} = -\frac{4G}{d}\left.\frac{\delta S}{\delta X^A}\right|_{\mathcal{R}} \ . \tag{9.84}$$

We consider a bulk Cauchy slice $\Sigma \supset \mathcal{R}$ for which $\partial\Sigma$ corresponds to the $t = 0$ slice on the boundary. Since the subleading terms in Eqs. (9.81) and (9.83) start at $z^d$, we are free to choose $\Sigma$ so that it is given by

$$t = z^d \varsigma(x) + o(z^d) \ , \tag{9.85}$$

Recall that the vector fields $t^\mu$ and $x^\mu$ are defined to be orthogonal to $\mathcal{R}$, and respectively orthogonal and tangent to $\Sigma_s$. In FG coordinates one finds:

$$t^A = z\left(t^A_{(0)} + z^d t^A_{(d)} + o(z^d)\right) \ , \tag{9.86}$$

$$x^A = z\left(x^A_{(0)} + z^d x^A_{(d)} + o(z^d)\right) \ , \tag{9.87}$$

$$t^z = z\left(z^{d-1} t^z_{(d-1)} + o(z^{d-1})\right) \ , \tag{9.88}$$

$$x^z = z\left(z^{d-1} x^z_{(d-1)} + o(z^{d-1})\right) \ . . \tag{9.89}$$

The overall factor of $z$ is due to normalization. Note that $t^\mu_{(0)}$ is a coordinate vector field but in general, $t^\mu$ is not. Individual coordinate components of vectors and tensors are defined by contractions with $t^\mu_{(0)}$ and $x^\mu_{(0)}$ respectively, for example $t^t \equiv t_\mu t^\mu_{(0)}$.

We now consider a contraction of the extrinsic curvature tensor on $\Sigma$,

$$(K_\Sigma)_{ab} x^b = P^\mu_a x^\nu \nabla_{(\mu} t_{\nu)} \ . \tag{9.90}$$

We would like to further project the $a$ index onto the $z$ direction. Deep in the bulk the $z$ direction does not lie entirely in $\Sigma$. However, note that $g_{\mu z} t^\mu \to 0$ in the limit $z \to 0$ due to Eq. (9.88). Therefore, at leading order in $z$, the $z$ direction does lie entirely in $\Sigma$; moreover, $P^\mu_z \to \delta^\mu_z$ as $z \to 0$. We will only be interested in evaluating Eq. (9.90) at leading order in $z$ so we may freely set $a = z$, which yields:[6]

$$(K_\Sigma)_{z\nu} x^\nu - x^\nu \partial_{(z} t_{\nu)} = x^\nu t_\gamma \, \Gamma^\gamma_{\nu z} \tag{9.91}$$

$$= z^2 \Gamma_{txz} + z x^t \Gamma_{ttz} + z t^x \Gamma_{xxz} + x^z t^z \Gamma_{zzz} + o(z^{d-1}) \tag{9.92}$$

$$= \frac{(d-2)}{2} z^{d-1} \frac{16\pi G}{d} \langle T_{tx} \rangle - z^{-3} t^z x^z - z^{d-1}(t^x_{(d)} - x^t_{(d)}) + o(z^{d-1}) \ . \tag{9.93}$$

The condition $x_\mu t^\mu = 0$ implies that

$$z^{d-1} \frac{16\pi G}{d} \langle T_{tx} \rangle + z^{-3} x^z t^z + z^{d-1}(t^x_{(d)} - x^t_{(d)}) + o(z^{d-1}) = 0 \ . \tag{9.94}$$

Hence we find

$$(K_\Sigma)_{z\nu} x^\nu - x^\nu \partial_{(z} t_{\nu)} = z^{d-1} \, 8\pi G \, \langle T_{tx} \rangle + o(z^{d-1}) \ . \tag{9.95}$$

We now apply the kink transform to $\Sigma$ (viewed as an initial data set). This yields a new initial data set on a slice $\Sigma_s$ in a new spacetime $\mathcal{M}_s$. We again expand in Fefferman-Graham coordinates:

$$ds^2 = \frac{1}{z^2}\left(dz^2 + \tilde{g}_{AB}(\tilde{x}, z) d\tilde{x}^A d\tilde{x}^B\right) \ , \tag{9.96}$$

$$\tilde{g}_{AB}(x, z) = \tilde{\eta}_{AB} + z^d \frac{16\pi G}{d} \langle \tilde{T}_{AB} \rangle + o(z^d) \ . \tag{9.97}$$

[6] In $d > 2$ the terms involving $x^z t^z$ will be higher order, by Eqs. (9.88) and (9.89), and need not be included. Since they cancel out either way, we include them here to avoid an explicit case distinction.

Here $\tilde{\eta}_{AB}$ is still Minkowski space; any change in the bulk geometry will be encoded in the subleading term.

The notation $\tilde{\eta}_{AB}$ indicates that we will be using the specific coordinates in which the metric of $d$-dimensional Minkowski space takes the nonstandard form given by Eq. (9.41). This has the advantage that the *coordinate* form of all vectors, tensors, and embedding equations in $D(a') \cup \mathcal{R} \cup D(a)$ will be unchanged by the kink transform, if we use standard Cartesian coordinates before the transform and the tilde coordinates afterwards.

For example, the invariance of the left and right bulk domains of dependence under the kink transform implies that $\Sigma_s$ is given by

$$\tilde{t} = z^d \varsigma(\tilde{x}) + o(z^d) \ , \tag{9.98}$$

with the *same* $\varsigma$ that appeared in Eq. (9.85). (In fact, this extends to at all orders in $z$.) As already shown in the previous subsection, $\partial\Sigma_s$ lies at $\tilde{t} = 0$, $z = 0$.

As another example, the coordinate components of the unit normal vector to $\Sigma_s$ in $\mathcal{M}_s$, $\tilde{t}^\mu$, will be the same as the components of the normal vector to $\Sigma$ in $\mathcal{M}$, $t^\mu$, and therefore

$$\partial_{(z} t_{\nu)}\big|_{\mathcal{M}} = \partial_{(z} \tilde{t}_{\nu)}\big|_{\mathcal{M}_s} \ . \tag{9.99}$$

Below we will use the convention that any quantity with a tilde is evaluated in $\mathcal{M}_s$, in the coordinates of Eq. (9.97). Any quantity without a tilde is evaluated in $\mathcal{M}$, in the coordinates of Eq. (9.81). The only exception is the extrinsic curvature tensor, where the corresponding distinction is indicated by the subscript $\Sigma_s$ or $\Sigma$, for consistency with Section 9.3.

We now consider the extrinsic curvature of $\Sigma_s$. A calculation analogous to the derivation of Eq. (9.95) implies

$$(K_{\Sigma_s})_{z\nu} \tilde{x}^\nu - \tilde{x}^\nu \partial_{(z} \tilde{t}_{\nu)} = z^{d-1}\, 8\pi G\, \langle \tilde{T}_{\tilde{t}\tilde{x}} \rangle + o(z^{d-1}) \ . \tag{9.100}$$

From Eqs. (9.95) and (9.99) we find

$$z^{d-1} \langle \tilde{T}_{\tilde{t}\tilde{x}} \rangle = z^{d-1} \langle T_{tx} \rangle + \frac{1}{8\pi G} \left[ (K_{\Sigma_s})_{z\nu} - (K_\Sigma)_{z\nu} \right] x^\nu + o(z^{d-1}) \ , \tag{9.101}$$

$$= z^{d-1} \langle T_{tx} \rangle - \frac{\sinh(2\pi s)}{8\pi G} \delta(\mathcal{R}) x_z + o(z^{d-1}) \ . \tag{9.102}$$

In the first equality, we used the fact that $x^\mu$ and $\tilde{x}^\mu$ can be identified as vector fields, and the extrinsic curvature tensors can be compared, in the submanifold $\Sigma = \Sigma_s$. The second equality follows from the definition of the kink transform, Eq. (9.51).

By Eq. (9.87), $\delta(\mathcal{R}) = \delta(z^{-1}\tilde{x}) = z\delta(\tilde{x})$. The condition $x_\mu \partial_z X^\mu = 0$ yields

$$x_z = -d\, z^{d-2} \widetilde{X}_{(d)} + o(z^{d-2}) \ , \tag{9.103}$$

where $\widetilde{X}_{(d)}$ is the $A = \tilde{x}$ component of $X^A_{(d)}$. Taking $z \to 0$ and using Eq. (9.84), we thus find

$$\langle \tilde{T}_{\tilde{t}\tilde{x}} \rangle = \langle T_{tx} \rangle + \frac{1}{2\pi} \sinh(2\pi s) \frac{\delta S}{\delta \widetilde{X}}\Big|_{\widetilde{X}=0} \delta(\tilde{x}) \ , \tag{9.104}$$

which agrees precisely with Eq. (9.47).

Note that this derivation applies to any boosted coordinate system $(\check{t}, \check{x})$ as well. Linear combinations of Eq. (9.104) with its boosted version reproduces both the $T_{\tilde{u}\tilde{u}}$ shock of Eq. (9.46) and the $T_{\tilde{v}\tilde{v}}$ shock of Eq. (9.45) holographically.

## 9.5 Predictions

Having found nontrivial evidence for kink transform/CC flow duality, we now change our viewpoint and assume the duality. In this section, we will derive a *novel* property of CC flow from the kink transform: a shock in the $\langle T_{xx} \rangle$ component of the stress tensor in the CC flowed state. We do not yet know of a way to derive this directly in the quantum field theory, so this result demonstrates the utility of the kink transform in extracting nontrivial properties of CC flow. We further argue that $\langle T_{xx} \rangle$ and $\langle T_{tx} \rangle$ constitute all of the independent, nonzero stress tensor shocks in the CC flowed state.

Our holographic derivation only depends on near boundary behavior, and the value of the shock takes a universal form similar to Eq. (9.104). Thus, we expect that the properties we find in holographic CC flow hold in non-holographic QFTs as well.

To derive the $\langle T_{xx} \rangle$ shock, we use the Gauss-Codazzi relation [277]

$$P_a^\mu P_b^\nu P_c^\alpha P_d^\beta R_{\mu\nu\alpha\beta} = K_{ac} K_{bd} - K_{bc} K_{ad} + r_{abcd} \ , \tag{9.105}$$

where $r_{abcd}$ is the intrinsic Riemann tensor of $\Sigma$. It is important to note that this relation is purely intrinsic to $\Sigma$. Since $\Sigma = \Sigma_s$ as submanifolds, we can not only evaluate Eq. (9.105) in both $\mathcal{M}$ and $\mathcal{M}_s$ but also meaningfully subtract the two. We emphasize that the following calculation is only nontrivial in $d > 2$ (in $d = 2$, the Gauss-Codazzi relation is trivial). We comment on $d = 2$ at the end.

First we evaluate Eq. (9.105) in $\mathcal{M}$. We will only be interested in evaluating it to leading order in $z$ in the Fefferman-Graham expansion. As argued in Section 9.4, when working at leading order we can freely set $a = c = z$. We then compute the following at leading order in $z$:

$$R_{zxzx} = K_{zz} K_{xx} - (K_{xz})^2 + r_{zxzx} \ . \tag{9.106}$$

We start by computing $K_{zz}$. First we note that $\Gamma^\alpha_{zz} t_\alpha = 0$ identically. Therefore,

$$K_{zz} = \partial_z t_z = 4G(d-2) z^{d-3} \frac{\delta S}{\delta T}\Big|_{\mathcal{R}} + o(z^{d-3}) \ . \tag{9.107}$$

We have made use of

$$t_z = 4G z^{d-2} \frac{\delta S}{\delta T}\Big|_{\mathcal{R}} + o(z^{d-2}) \ , \tag{9.108}$$

which follows from $t_\mu \partial_z X^\mu = 0$.

Next we compute

$$R_{zxzx} = \partial_x \Gamma^x_{zz} - \partial_z \Gamma^x_{xz} + \Gamma^x_{x\mu}\Gamma^\mu_{zz} - \Gamma^x_{z\mu}\Gamma^\mu_{xz} \ . \tag{9.109}$$

One finds

$$\partial_z \Gamma^x_{xz} = \frac{1}{2}(d-2)(d-1) z^{d-2} \frac{16\pi G}{d} \langle T_{xx} \rangle + o(z^{d-2}) \ , \tag{9.110}$$

$$\Gamma^x_{xz}\Gamma^z_{zz} = -\frac{1}{2}(d-2) z^{d-2} \frac{16\pi G}{d} \langle T_{xx} \rangle + o(z^{d-2}) \ , \tag{9.111}$$

with all other terms either subleading in $z$ or identically vanishing, and hence

$$R_{zxzx} = -8\pi G(d-2) z^{d-2} \langle T_{xx} \rangle + o(z^{d-2}) \ . \tag{9.112}$$

Putting all this together, we have

$$-8\pi G(d-2) z^{d-2} \langle T_{xx} \rangle = 4G z^{d-3} \frac{\delta S}{\delta \widetilde{T}}\Big|_{\mathcal{R}} K_{xx} - (K_{xz})^2 + r_{zxzx} + o(z^{d-2}) \ . \tag{9.113}$$

The analogous relation evaluated in $\mathcal{M}_s$ reads

$$-8\pi G(d-2) z^{d-2} \langle \tilde{T}_{\tilde{x}\tilde{x}} \rangle = 4G z^{d-3} \frac{\delta S}{\delta \widetilde{T}}\Big|_{\mathcal{R}} \tilde{K}_{\tilde{x}\tilde{x}} - (\tilde{K}_{\tilde{x}z})^2 + \tilde{r}_{z\tilde{x}z\tilde{x}} + o(z^{d-2}) \ , \tag{9.114}$$

where we have made use of Eq. (9.99) to set $K_{zz} = \tilde{K}_{zz}$. We can now subtract these two relations. First note that $\tilde{r}_{abcd} = r_{abcd}$ since it is purely intrinsic to $\Sigma$. Next, recall from the definition of the kink transform Eq. (9.51) that

$$\tilde{K}_{\tilde{x}\tilde{x}} - K_{xx} = -z \sinh(2\pi s) \delta(\tilde{x}) \ . \tag{9.115}$$

Lastly, it is easy to check that $K_{xz} \sim o(z^{d-2})$ hence its contribution to Eq. (9.113) is subleading, and similarly for Eq. (9.114). Thus, subtracting Eq. (9.114) from Eq. (9.113) yields

$$\langle \tilde{T}_{\tilde{x}\tilde{x}} \rangle - \langle T_{xx} \rangle = \frac{1}{2\pi} \sinh(2\pi s) \frac{\delta S}{\delta \widetilde{T}}\Big|_{\widetilde{X}=0} \delta(\tilde{x}) \ . \tag{9.116}$$

The above calculation only works in $d > 2$. In $d = 2$, since the boundary theory is a CFT, tracelessness of the boundary stress tensor further implies that $\langle T_{tx} \rangle$ is the *only* independent component of the stress tensor shock so there is no need for a calculation analogous to the one above. We expect that this argument is robust under relevant deformations of the CFT since the shock is highly localized and should universally depend only on the UV fixed point.

Together with the $\langle T_{tx} \rangle$ shock we reproduced in the previous section, and using Lorentz invariance of the boundary, this result determines the transformation of the the stress tensor

contracted with any pair of linear combinations of $t$ and $x$, such as $\langle T_{tt}\rangle$. This linear space contains all of the independent nonvanishing components of the shock. To see this, note that

$$x^\nu \left(\nabla_\nu \tilde{y}_\mu - \nabla_\nu y_\mu\right) = 0 \ , \tag{9.117}$$

$$y^\nu \left(\nabla_\nu \tilde{y}_\mu - \nabla_\nu y_\nu\right) = 0 \ , \tag{9.118}$$

$$y^\nu \left(\nabla_\nu \tilde{t}_\mu - \nabla_\nu t_\mu\right) = 0 \ , \tag{9.119}$$

where $y^\mu = P_i^\mu y^i$ for any vector field $y^i$ in the tangent bundle of $\mathcal{R}$. Eqs. (9.117) and (9.118) follow trivially from the fact that the prescription Eq. (9.69) only introduces a discontinuity in vector fields in the normal bundle of $\mathcal{R}$, while Eq. (9.119) simply follows from Eq. (9.51). Evaluating the $\mu = z$ components in the same way as in Section 9.4, we find,

$$\langle \tilde{T}_{\tilde{\mu}\tilde{y}}\rangle - \langle T_{\mu y}\rangle = 0 \ . \tag{9.120}$$

For $s \to \infty$, the shocks derived in the previous two sections agree with those found to be required for the existence of certain coarse grained bulk states in Ref. [239]. In that work, the cut was allowed to be a wiggly or flat cut of a bifurcate horizon such as a Rindler horizon, and the state could belong to any quantum field theory. Interpolation of these results suggests that the shocks we have derived here generalize to the case of CC flow for a wiggly cut of the Rindler horizon, in general QFTs with a conformal fixed point.

## 9.6 Discussion

### Relation to JLMS and One Sided Modular Flow

The bulk dual of one-sided modular flow [167, 264] resembles the kink transform. CC flow yields a well defined state, however, whereas a one sided modular flowed state is singular in QFT. Correspondingly, the kink transform defined here yields a smooth bulk solution whereas the version implicitly defined in Ref. [264] results in a singular spacetime (see also Ref. [259], footnote 4). We will now explain this in detail.

Consider a boundary region $A_0$ with reduced state $\rho_{A_0}$, dual to a semi-classical state $\rho_a$ in the bulk entanglement wedge $a$ associated to $A_0$ as seen in Fig. 9.5. We denote by $K_A = -\log \rho_A$ and $K_a = -\log \rho_a$ the boundary and bulk modular Hamiltonians, respectively. The JLMS result [23] states that

$$\hat{K}_{A_0} = \frac{\hat{A}[\mathcal{R}]}{4G} + \hat{K}_a \ , \tag{9.121}$$

where $\hat{A}[\mathcal{R}]$ is the area operator that formally evaluates the area of the quantum extremal surface $\mathcal{R}$ [22].

Suppose now that $A_0$ has a nonempty boundary $\partial A_0$. Then there is an interesting asymmetry in Eq. (9.121). The one-sided boundary modular operator appearing on the left

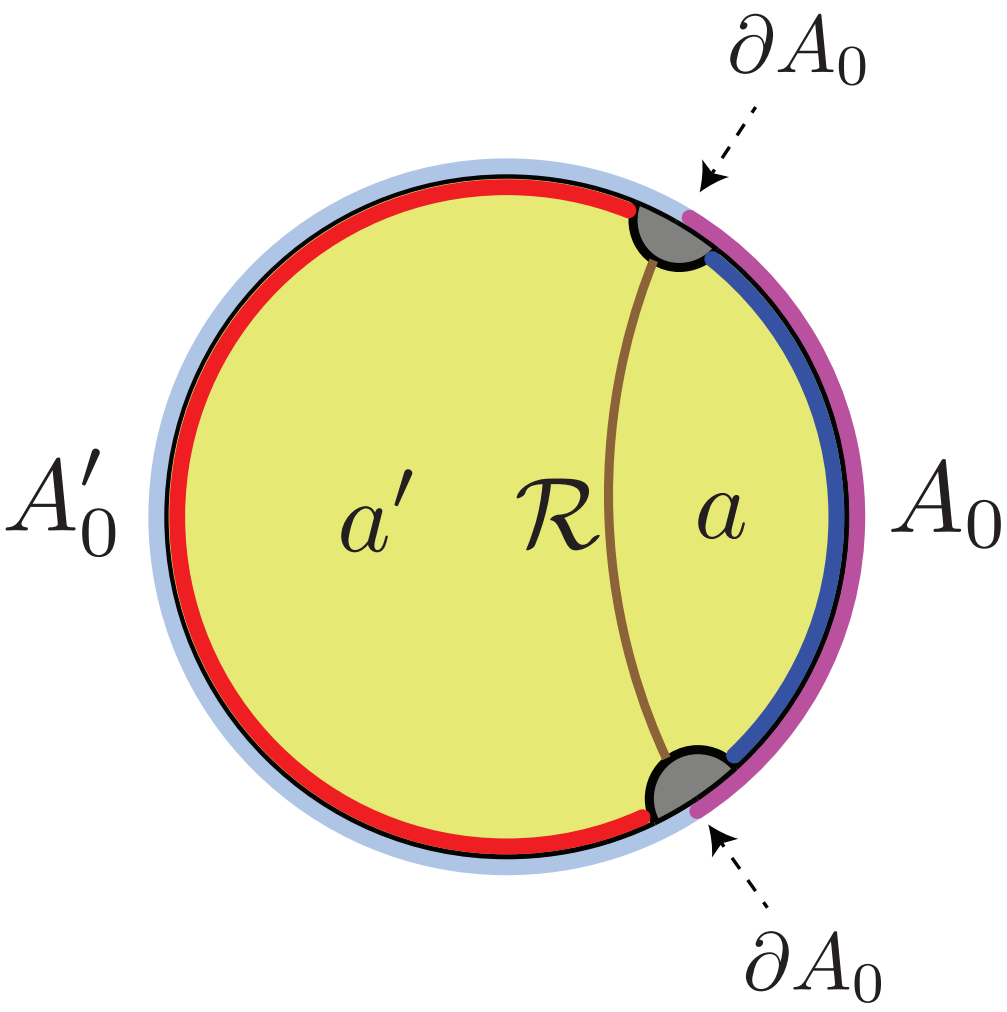


Figure 9.5: A boundary subregion $A_0$ (pink) has a quantum extremal surface denoted $\mathcal{R}$ (brown) and an entanglement wedge denoted $a$. The complementary region $A_0'$ (light blue) has the entanglement wedge $a'$. CC flow generates valid states, but one-sided modular flow is only defined with a UV cutoff. For example, one can consider regulated subregions $A^{(\epsilon)}$ (deep blue) and $A'^{(\epsilon)}$ (red). In the bulk, this amounts to excising an infrared region (gray) from the joint entanglement wedge (yellow).

hand side is well-defined only with a UV cutoff. On the other hand, at least the leading (area) term in the bulk modular operator on the right hand side has a well-defined action. Let us discuss each side in turn.

In Einstein gravity, the area operator $\hat{A}$ is the generator of one-sided boosts. To see this, let us restrict the gravitational phase space to the bulk region $D(\Sigma_\epsilon)$. There exists a (non-unique) vector field $\xi^a$ in $D(a') \cup \mathcal{R}$ such that $\xi^a$ generates an infinitesimal one-sided

boost at $\mathcal{R}$ [278, 279]. This boost can be quantified by a parameter $s$ in the normal bundle to $\mathcal{R}$, as described in Section 9.3. The area functional $A[\mathcal{R}]/4G$ is the Noether charge at $\mathcal{R}$ associated to $\xi^a$, given by the expectation value of the area operator in the semi-classical bulk state:

$$A[\mathcal{R}] = \langle \hat{A}[\mathcal{R}] \rangle \ . \tag{9.122}$$

Each point in the gravitational phase space can be specified by the metric in $D(a')$, the metric in $D(a)$, and the boost angle $s$ at $\mathcal{R}$ with which the two domains of dependence are glued together [264, 279, 280, 166]. The action of

$$\langle e^{2\pi i s \hat{A}[\mathcal{R}]/4G} \rangle \tag{9.123}$$

on points in the gravitational phase space is to simply shift the conjugate variable, *i.e.*, the relative boost angle between the left and right domains of dependence, by $s$. Note that the metrics in the left and right domains of dependence are unchanged since the area functional acts purely on the phase space data at $\mathcal{R}$. This is the classical analogue of the statement that the area operator is in the center of the algebras of the domains of dependence [27]. Comparing with Section 9.3, we see that this action is equivalent to the kink transform of $\Sigma_\epsilon$ about $\mathcal{R}$ by $s$. We stress that this action is well-defined even if $\mathcal{R}$ extends all the way out to the conformal boundary, *i.e.*, in the far ultra-violet from the boundary perspective.

We turn to the right hand side of Eq. (9.121), still assuming that $A_0$ has a nonempty boundary $\partial A$. Since the algebra of a QFT subregion $A_0$ is a Type-III$_1$ von Neumann algebra, the Hilbert space does not factorize across $\partial A_0$ [265]. A reduced density matrix $\rho_{A_0}$, and hence $\hat{K}_{A_0}$, do not exist. Physically, the action of $\hat{K}_{A_0}$ on a fixed boundary time slice would break the vacuum entanglement of arbitrarily short wavelength modes across $\partial A_0$; this would create infinite energy.

Therefore, any discussion of $\hat{K}_{A_0}$ requires introducing a UV regulator. Consider the regulated subregions $A_0^{(\epsilon)}$ and $A_0^{\prime(\epsilon)}$ shown in Fig. 9.5. The split property in algebraic QFT [265, 42] guarantees the existence of a (non-unique) Type-I von Neumann algebra $\mathcal{N}$ nested between the algebras of subregion $A_0^{(\epsilon)}$ and the complementary algebra of $A_0^{\prime(\epsilon)}$, *i.e.*,

$$\mathcal{A}_0^{(\epsilon)} \subset \mathcal{N} \subset \left(\mathcal{A}_0^{\prime(\epsilon)}\right)' \ . \tag{9.124}$$

With this prescription, one can define a regulated version of the reduced density matrix $\rho_A$ by using the Type-I factor $\mathcal{N}$ [281]. It has been suggested that there exists an $\mathcal{N}$ consistent with the geometric cutoff shown in Fig. 9.5 [40, 42]: the quantum extremal surface $\mathcal{R}$ in the bulk is regulated by a cutoff brane $B$ demarcating the entanglement wedge of the subregion $A_0^{(\epsilon)} \cup A_0^{\prime(\epsilon)}$. The regulated area operator $\hat{A}[\mathcal{R}]/4G$ is well defined once boundary conditions on $B$ are specified.

Let us now specialize to the case for which we have conjectured kink transform/CC-flow duality: the boundary slice $\mathcal{C} = A_0 \cup A_0'$ is a Cauchy surface of Minkowski space, and $\partial A_0$ is the flat cut $u = v = 0$ of the Rindler horizon. We have just argued that the kink transformation is generated by the area operator through Eq. (9.123). By Eq. (9.121), the

boundary dual of this action should be one-sided modular flow, not CC flow. By Eqs. (9.4) and (9.6), these are manifestly different operations. Indeed, unlike one-sided modular flow, Connes cocycle flow yields a well-defined boundary state for all $s$, without any UV divergence at the cut $\partial A_0$: $|\psi(\mathcal{C})\rangle \to |\psi_s(\mathcal{C})\rangle$.

In fact there is no contradiction. For both modular flow and CC flow on the boundary, a bulk-dual Cauchy surface $\Sigma_s$ is generated by the kink transform. The difference is in how $\Sigma_s$ is glued back to the boundary.

For modular flow, $\Sigma_s$ is glued back to the original slice $\mathcal{C}$. Generically, this would violate the asymptotically AdS boundary conditions, necessitating a regulator such as the excision of the grey asymptotic region in Fig. 9.5 and interpolation by a brane $B$. The boundary dual is an appropriately regulated modular flowed state with energy concentrated near the cut $\partial A_0$. This construction is possible even if $\partial A_0$ is not a flat plane, but the regulator is ambiguous and cannot be removed.[7]

For CC flow, $\Sigma_s$ is glued to the precursor slice $\mathcal{C}_s$ as discussed in Section 9.3. This yields $|\psi_s(\mathcal{C}_s)\rangle$. Time evolution on the boundary yields $|\psi_s(\mathcal{C})\rangle$, the CC-flowed state on the original slice $\mathcal{C}$.

On the boundary, we can use the one-sided modular operator in two ways. As a map between states on $\mathcal{C}$ [23, 115] it requires a UV regulator. As a map that takes a state on $\mathcal{C}$ to a state on the precursor slice $\mathcal{C}_s$, $|\psi(\mathcal{C})\rangle \to |\psi_s(\mathcal{C}_s)\rangle$, it is equivalent to CC flow on $\mathcal{C}$ by Eqs. (9.35) and (9.36). This is a more natural choice due to its UV-finiteness. But it is available only if the vacuum modular operator for cut $\partial A$ is geometric, so that the precursor slice is well-defined.

## Quantum Corrections

It is natural to include semiclassical bulk corrections to all orders in $G$ to our proposal. The natural guess would be to perform the kink transform operation about the quantum extremal surface along with a CC flow for the bulk state. In general, it is difficult to describe this procedure within EFT. In states far from the vacuum, the background spacetime changes under the kink transform, and it is unclear how to map states from one spacetime to another. However, we will find some evidence that suggests that the bulk operation relating the two states is a generalized version of CC flow in curved spacetime.

To see this, note that the quantum extremal surface $\mathcal{R}$ satisfies the equations

$$\mathcal{B}^{(t)}_{\mathcal{R}} + 4G\hbar \frac{\delta S}{\delta T} = 0 \ , \tag{9.125}$$

$$\mathcal{B}^{(x)}_{\mathcal{R}} + 4G\hbar \frac{\delta S}{\delta X} = 0 \ , \tag{9.126}$$

[7] There is evidence that a code subspace can be defined with an appropriate regulator such that one-sided modular flow keeps the state within the code subspace [166, 38, 229].

where $(\mathcal{B}^{(t)}_{\mathcal{R}})$ and $(\mathcal{B}^{(x)}_{\mathcal{R}})$ denote the trace of the extrinsic curvature (expansion) in the two normal directions to $\mathcal{R}$, *i.e.*, $t^\mu$ and $x^\mu$ respectively. Similarly $\frac{\delta S}{\delta T}$ and $\frac{\delta S}{\delta X}$ are the entropy variations in the $t^\mu$ and $x^\mu$ directions respectively.

The classical kink transform involves an extrinsic curvature shock at the classical RT surface. As shown in Section 9.3, extremality of the surface ensures that the constraint equations continue to be satisfied after the kink transform in this case. However, the quantum extremal surface has non-vanishing expansion, the constraint equations are not automatically satisfied when an extrinsic curvature shock is added at the quantum RT surface.

More precisely, the left hand side of the constraint equations on a slice $\Sigma$ are modified by the kink transform by

$$\Delta\left(r_\Sigma - (K_\Sigma)_{ab}(K_\Sigma)^{ab} + (K_\Sigma)^2\right) = 8G\hbar\,\sinh(2\pi s)\,\frac{\delta S}{\delta T}\,\delta(X)\ , \tag{9.127}$$

$$\Delta\left(D_a(K_\Sigma)^a_x - D_x K_\Sigma\right) = 4G\hbar\,\sinh\left(2\pi s\right)\,\frac{\delta S}{\delta X}\,\delta(X)\ , \tag{9.128}$$

$$\Delta\left(D_a(K_\Sigma)^a_i - D_i K_\Sigma\right) = 0\ , \tag{9.129}$$

where $\Delta$ represents the difference in the constraint equations between the original spacetime $\mathcal{M}$ and the kink transformed spacetime $\mathcal{M}_s$, and we have used Eqs. (9.125) and (9.51). These are essentially the analogs of Eqs. (9.60) and (9.61), and we have simplified the notation slightly.

For the constraint equations to be solved, the kink transform would have to generate the same change on the right hand side of the constraints. It would thus have to induce an additional stress tensor shock of the form

$$\Delta T_{TT} = \frac{1}{2\pi}\sinh(2\pi s)\,\frac{\delta S}{\delta T}\,\delta(X)\ , \tag{9.130}$$

$$\Delta T_{TX} = \frac{1}{2\pi}\sinh(2\pi s)\,\frac{\delta S}{\delta X}\,\delta(X)\ . \tag{9.131}$$

Formally, these conditions agree precisely with the properties of CC flow discussed in Section 9.2. Thus, we might expect a generalized bulk CC flow to result in shocks of precisely this form.

In fact, the existence of semiclassical states satisfying the above equations was conjectured in [239]; the fact that CC flow generates such states in the non-gravitational limit was interpreted as non-trivial evidence in support of the conjecture. Thus, we expect a kink transform at the quantum extremal surface with a suitable modification of the state to provide the bulk dual of CC flow to all orders in $G$.

At a more speculative level, we can also discuss the bulk dual of CC flow in certain special states called fixed area states, which serve as a natural basis for modular flow [38, 166, 229]. These are approximate eigenstates of the area operator and are therefore unlike smooth semiclassical states which are analogous to coherent states. The Lorentzian bulk dual of such states potentially involves superpositions over geometries [282].

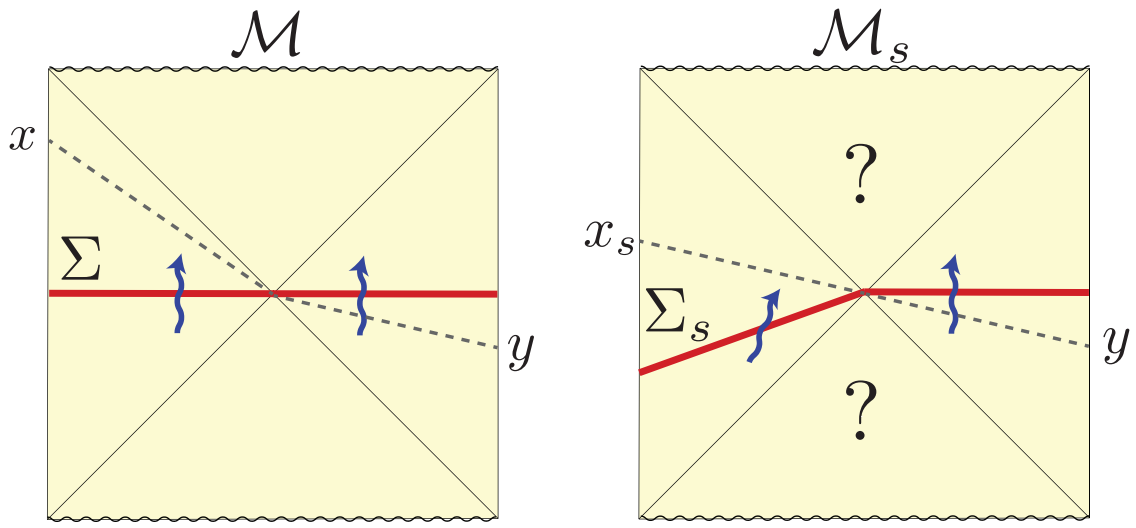


Figure 9.6: An arbitrary spacetime $\mathcal{M}$ with two asymptotic boundaries is transformed to a physically different spacetime $\mathcal{M}_s$ by performing a kink transform on the Cauchy slice $\Sigma$. A piecewise geodesic (dashed gray line) in $\mathcal{M}$ connecting $x$ and $y$ with boost angle $2\pi s$ at $\mathcal{R}$ becomes a geodesic between $x_s$ and $y$ in $\mathcal{M}_s$.

However, by construction, the reduced density matrix is maximally mixed at leading order in $G$. Thus, the state $|\psi\rangle$ is unaffected by one sided modular flow, and the only effect of CC flow is that we describe the state on a kinematically related slice $\mathcal{C}_s$. Thus, the dual description must be invariant under CC flow up to a diffeomorphism.

In such states, one could apply the semiclassical prescription using Eq. (9.121). As discussed above, the action of the area operators results in a diffeomorphism of the geometric description, if it exists. From Eq. 9.121, the remaining action of the boundary CC flow is to simply induce a bulk CC flow.

## Beyond Flat Cuts

Kink transform/CC flow duality can be generalized to other choices of boundary subsystems, so long as a precursor slice can be defined. The precursor slice is generated by acting on the original slice with the vacuum modular Hamiltonian; this is well-defined only if this action is geometric. In Section 9.2, we ensured this by taking the boundary to be Minkowski space and choosing a planar cut. Precursor slices also exist in any conformally related choice, such as a spherical cut.

But there are other settings where the vacuum modular Hamiltonian acts geometrically. This includes multiple asymptotically AdS boundaries where the boundary manifold has a time translation symmetry. For example, consider a two-sided black hole geometry $\mathcal{M}$ with a compact RT surface $\mathcal{R}$ as seen in Fig. 9.6. The boundary manifold is of the form

$\mathcal{C} \times \mathbb{R}$, where the first factor corresponds to the spatial geometry and the second corresponds to the time direction. The boundary Hilbert spaces factorizes; each boundary algebra is a Type-I factor. Thus, the version of CC flow defined in terms of density matrices in Eq. (9.6) becomes rigorous in this situation. A natural choice of vacuum state is the thermofield double [283, 69]. The reduced state on each side is thermal, $\rho_{A_0} \sim \exp(-\beta H)$. Thus the modular Hamiltonian is proportional to the ordinary Hamiltonian on each boundary. This generates time translations and so is geometric.

Now, in any such geometry $\mathcal{M}$ one can pick a Cauchy slice $\Sigma$ that ends on boundary time slices on both sides and contains $\mathcal{R}$. In obvious analogy with Section 9.3, we conjecture that the domain of dependence of the kink transformed slice $\Sigma_s$ in a modified geometry $\mathcal{M}_s$ is dual to the boundary state:

$$|\psi_s(\mathcal{C}_s)\rangle_{LR} = \rho_L^{-is} |\psi(\mathcal{C})\rangle_{LR} \ , \tag{9.132}$$

where we have used the notation of Eq. (9.36).

In such a situation, it is again manifest that the Wheeler-DeWitt patches dual to either side are preserved by arguments similar to those made in Section 9.4. However, since there is no portion of $\mathcal{R}$ that reaches the asymptotic boundary, there is no analog of the shock matching done in Section 9.4. Notably, since $\partial A = \varnothing$ in this case, there is no subtlety regarding boundary conditions for JLMS and thus, one-sided modular flow makes sense without any regulator. Thus, our construction is simply kinematically related to the construction in [264].

An interesting situation arises for wiggly cuts of the Rindler horizon, *i.e.*, $u = 0$ and $v = V(y)$. The modular Hamiltonian acts locally, but only when restricted to the null plane [266]. Its action becomes non-local when extended to the rest of the domain of dependence. The properties of CC flow described in Sections 9.2-9.2 all hold for this choice of cut. This constrains one-sided operator expectation values on the null plane, subregion entropies for cuts entirely to one side of $V(y)$, and even the $T_{vv}$ shock at the cut. Interestingly, all of them are matched by the kink transform, by the arguments given in Section 9.3. Even the expected stress tensor shock can still be derived, by taking a null limit of our derivation as described in Appendix A.10. One might then guess that the kink transform is also dual to CC flow for arbitrary wiggly cuts.

Even in the vacuum, however, the kink transform across a wiggly cut results in a boundary slice that cannot be embedded in Minkowski space, due to the absence of a boost symmetry that preserves the entangling surface. Thus, the kink transform would have to be modified to work for wiggly cuts. The transformation of boundary observables off the null plane is quite complicated for wiggly cut CC flow. Thus, we also expect that regions of the entanglement wedge probed by such observables should be drastically modified, unlike the case where the entangling surface is a flat Rindler cut.

However, the wiggly-cut boundary transformation remains simple for observables restricted to the null plane. Thus one could try to formulate a version of the kink transform on Cauchy slices anchored to the null plane on the boundary and the RT surface in the

bulk. Perhaps a non-trivial transformation of the entanglement wedge arises from the need to ensure that the kink transformed initial data be compatible with corner conditions at the junction where the slice meets the asymptotic boundary [284]. We leave this question to future work.

## Other Probes of CC Flow

In Section 9.4, we provided evidence for kink transform/CC flow duality. The preservation of the left and right entanglement wedges under the kink transform ensures that all one-sided correlation functions transform as required. It would be interesting to consider two sided correlation functions. However, these do not change universally and are difficult to compute in general. In the bulk, this is manifested by the fact that the future and past wedges do not change simply and need to be solved for.

However, because of the shared role of the kink transform, we can take advantage of the modular toolkit for one-sided modular flow [264]. Let $|\widetilde{\psi}_s\rangle = \rho_A^{-is}|\psi\rangle$ be a family of states generated by one-sided modular flow as discussed in Section 9.6. Then certain two sided correlation functions $\langle\widetilde{\psi}_s|O(x)\,O(y)|\widetilde{\psi}_s\rangle$ can be computed as follows.

Suppose $O(x)$ is an operator dual to a "heavy" bulk field with mass $m$ such that $1/\ell_{\text{AdS}} \ll m \ll 1/\ell_{\text{P}}, 1/\ell_{\text{s}}$. Correlation functions for such an operator can then be computed using the geodesic approximation,

$$\langle O(x)O(y)\rangle \approx \exp(-mL)\ , \tag{9.133}$$

where $L$ is the length of the bulk geodesic connecting boundary points $x$ and $y$. Now consider boundary points $x$ and $y$ such that there is a piecewise bulk geodesic of length $L(x,y)$ joining them in the spacetime dual to the state $|\psi\rangle$.

This kinked geodesic is required to pass through the RT surface of subregion $A$ with a specific boost angle $2\pi s$ as seen in Fig. 9.6. (This is a fine-tuned condition on the set of points $x, y$.) Since single sided modular flow behaves locally as a boost at the RT surface, it straightens out the kinked geodesic such that it is now a true geodesic in the spacetime dual to the state $|\widetilde{\psi}_s\rangle$. Thus, we have

$$\langle\widetilde{\psi}_s|O(x)\,O(y)|\widetilde{\psi}_s\rangle \approx \exp(-mL(x,y))\ . \tag{9.134}$$

As discussed in Section 9.2, the CC flowed state can equivalently be thought of as the single sided modular flowed state $|\widetilde{\psi}_s\rangle$ on a kinematically transformed slice $\mathcal{C}_s$. Thus, the above rules can still be used to compute two sided correlation functions in the CC flowed state $|\psi_s\rangle = u_s|\psi\rangle$ as

$$\langle\psi_s|O(x_s)O(y)|\psi_s\rangle \approx \exp(-mL(x,y))\ , \tag{9.135}$$

where $x_s$ is the point related to $x$ by the vacuum modular flow transformation.

We also note that the shock matching performed in Section 9.4 was a near boundary calculation. However, a bulk shock exists everywhere on the RT surface. One could solve for

the position of the RT surface to further subleading orders and relate the bulk shock to the boundary stress tensor. This would yield a sequence of relations that the stress tensor must satisfy in order to be dual to the kink transform. In general these relations may be highly theory-dependent, but it would be interesting to see if some follow directly from CC flow or make interesting universal predictions for CC flow in holographic theories.

## Higher Curvature Corrections

In Section 9.4, we argued that the bulk kink transform in a theory of Einstein gravity satisfies properties consistent with the boundary CC flow. However, this result is robust to the addition of higher curvature corrections in the bulk theory. The preservation of the two entanglement wedges, *i.e.*, Eq. (9.38), is a geometric fact that remains unchanged.[8]

Further, the matching of the stress tensor shock crucially depended on two ingredients. Firstly, Eq. (9.81), the holographic dictionary between the boundary stress tensor and the bulk metric perturbation and secondly, Eq. (9.84), the relation between the boundary entropy variation and the shape of the RT surface. Both of these relations are modified once higher curvature corrections are included [286, 287]. However, it follows generally from dimension counting arguments that

$$g_{ij}^{(d)} = \eta_1 \frac{16\pi G}{d} \langle T_{ij} \rangle \ , \tag{9.136}$$

$$X_{(d)}^{A} = -\eta_2 \frac{4G}{d} \left. \frac{\delta S}{\delta X^A} \right|_{\mathcal{R}} \ , \tag{9.137}$$

where $\eta_1$ and $\eta_2$ are constants that depend on the higher curvature couplings. Using the first law of entanglement, it can be shown that in fact $\eta_1 = \eta_2$ [286, 287]. Hence, the boundary stress tensor shock obtained from the kink transform is robust to higher curvature corrections.

## Holographic proof of QNEC

A recent proof of the QNEC from the ANEC [259] considers CC flow for a subregion $A$ on the null plane $u = 0$ with entangling surfaces $v = V_1(y)$ and $v = V_2(y)$ surrounding a given point $p$. From the transformation properties of the stress tensor under CC flow described in Section 9.2, $T_{vv} \to 0$ as $s \to \infty$. In addition, there are stress tensor shocks at $\partial A$, as described in Section 9.2, of weight $f(s) \frac{\delta S}{\delta V(y)} \Big|_{\psi, \partial A}$. In the limit $V_1(y) \to V_2(y)$, computing the ANEC in the CC flowed state, one obtains contributions from the stress tensor $T_{vv}(p)$ in subregion $A$, and a contribution proportional to $\frac{\delta^2 S}{\delta V(y_1) \delta V(y_2)} \Big|_{\psi, p}$ from the shocks. Positivity

[8] Here we assume that the initial value formulation of Einstein gravity can be perturbatively adjusted to include higher curvature corrections despite the fact that a non-perturbative classical analysis of higher curvature theories is often problematic due to the Ostrogradsky instability [285].

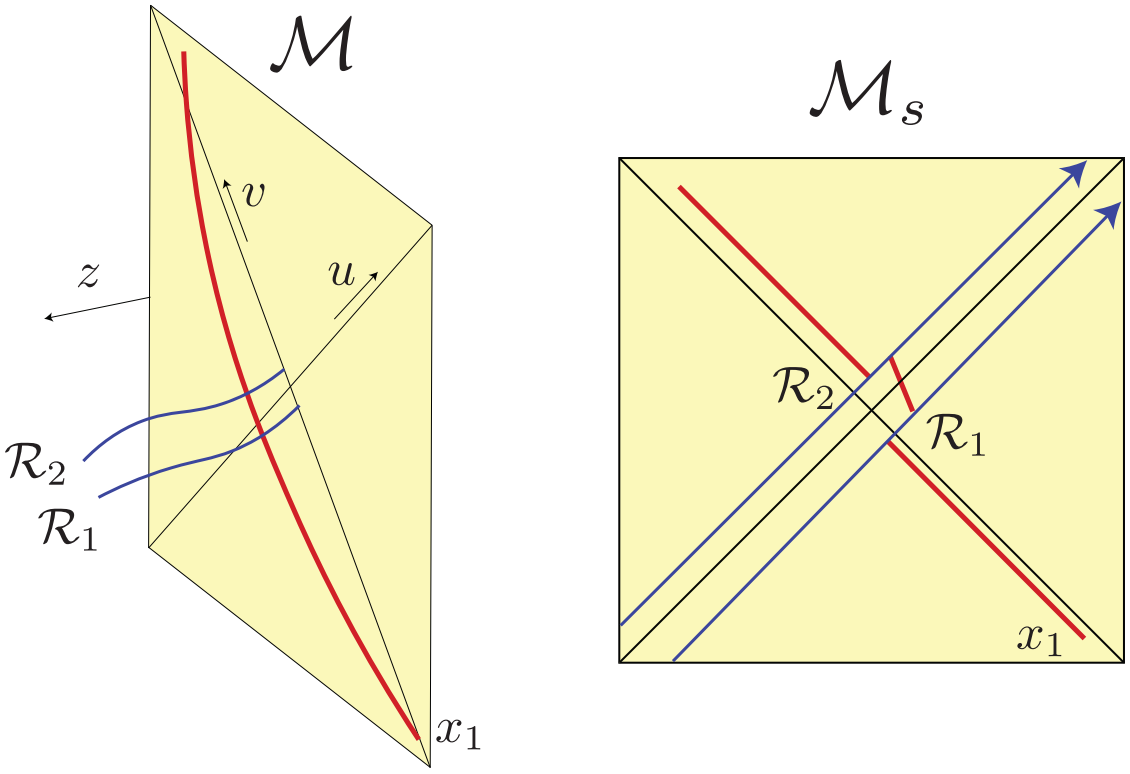


Figure 9.7: Holographic proofs. *Left:* Boundary causality is respected by the red curve that goes through the bulk in a spacetime $\mathcal{M}$; this is used in proving the ANEC. The RT surfaces $\mathcal{R}_1$ and $\mathcal{R}_2$ must be spacelike separated; this is used in proving the QNEC. *Right:* In the kink transformed spacetime $\mathcal{M}_s$ as $s \to \infty$, the QNEC follows from causality of the red curve, which only gets contributions from the Weyl shocks (blue) at $\mathcal{R}_1$ and $\mathcal{R}_2$, and the metric perturbation in the region between them.

of the averaged null energy in the CC flowed state then implies the QNEC in the original state.

Prior to the QFT proofs, both the ANEC and QNEC had been proved holographically [288, 262]. The guiding principle behind both of these proofs was the fact that consistency of the holographic duality requires bulk causality to respect boundary causality as we demonstrate in Fig. 9.7. In the case of the ANEC, one considers an infinitely long curve connecting points on past null infinity to future null infinity through the bulk and demands that it respect boundary causality [288]. In the proof of the QNEC, one requires that curves joining the RT surfaces of subregions $v < V_1(y)$ and $v > V_2(y)$, denoted $\mathcal{R}_1$ and $\mathcal{R}_2$, respect boundary causality [262, 257]. There are two contributions to the lightcone tilt of this bulk curve coming from the metric perturbation $h_{vv}$ in the near boundary geometry, and the shape of the RT surface $X^\mu(y, z)$. By the holographic dictionary, these contributions can be related

to the boundary stress tensor $T_{vv}$ and the entropy variations $\frac{\delta S}{\delta V}$ as discussed in Section 9.4.

Now performing the kink transform removes the contribution coming from the shape of the RT surface and puts it into a time advance/delay coming from shocks in the bulk Weyl tensor that we compute in Appendix A.10. Considering the extended curve from past to future null infinity, we see that whether or not it respects boundary causality is determined entirely by the region between the entangling surfaces $\mathcal{R}_1$ and $\mathcal{R}_2$ since the bulk solution approaches the vacuum everywhere else in the limit $s \to \infty$. Requiring causality of the ANEC curve then results in the QNEC, making the connection to the boundary proof manifest.

# Appendix A

# Appendix

## A.1 Reconstruction from a Single Leaf

In this appendix, we study what portion of the bulk can be reconstructed from a *single* leaf, i.e. by Eq. (2.21) with all $\Gamma$ on a single leaf. We refer to three types of spacetime regions discussed in Sections 2.4, 2.4, and 2.4 as non-shadow, reconstructable shadow, and non-reconstructable shadow regions, respectively.

Let us first consider a spacetime point $p$ in a non-shadow region. We show that generically a codimension-0 neighborhood of $p$ can be directly reconstructed from a single leaf $\sigma$. For this purpose, we consider a timelike geodesic, $p(\tau)$, that goes through $p$ at $\tau = 0$ and stays in the non-shadow region. We then introduce a map $f$ from the coordinates, $\Phi = (\phi_1, \cdots, \phi_{d-1})$, parameterizing $\sigma$ to $\tau$ as follows. For each $\Phi$, we consider a continuous family of HRT surfaces associated with subregions of $\sigma$ which are taken to enlarge naturally from the point specified by $\Phi$ toward its antipodal point. Generically, one of these HRT surfaces intersects with $p(\tau)$ at some $\tau$, which we take as the image of the map: $\tau = f(\Phi)$. Now, we can choose $\sigma$ so that $\max_\Phi f(\Phi) > 0$ and $\min_\Phi f(\Phi) < 0$. The set satisfying $f(\Phi) = 0$ is generally codimension-1

| | Single leaf | Multiple leaves |
|---|---|---|
| Non-shadow | codimension-0<br>(codimension-1 for $t \leftrightarrow -t$) | codimension-0 |
| Reconstructable shadow | none | codimension-0 |
| Non-reconstructable shadow | none | none |

Table A.1: The dimensions of bulk spacetime regions directly reconstructable from a single leaf (the left column) and multiple leaves (the right column). The entry "none" means that no region can be reconstructed.

in the space of $\Phi$, hence there are many such $\Phi$ which have an HRT surface passing through $p$. This tells us that $p$ can be reconstructed from this single leaf. In addition, continuity suggests that some interval of $p(\tau)$ is reconstructed from this leaf. Applying this argument for points outside of entanglement shadows tells us that a single leaf generally allows for the reconstruction of a codimension-0 region of the bulk.

Note that there is a case in which the above argument does not apply. Suppose the spacetime is time reflection symmetric with respect to $\sigma$, as in the case of a static system. Then all HRT surfaces anchored to $\sigma$ live on the same bulk hypersurface corresponding to the reflection symmetric point. This therefore allows for reconstructing only a codimension-1 region. The situation for reconstructing non-shadow regions from a single leaf is summarized in the upper-left entry of Table A.1.

We now prove that a single leaf cannot reconstruct any portion of an entanglement shadow. We will do so by contradiction. Suppose a point $p$ resides within an entanglement shadow but can be reconstructed by a single leaf, $\sigma$. Then there is a subregion of $\sigma$, $A$, such that $p$ lies on the boundary of the entanglement wedge of $A$. Now, suppose some subregion of $\sigma$, $B$, has nonzero overlap with $A$, i.e. $A \cap B$ is codimension-0 on the leaf. Then $\mathrm{EW}(A) \cap \mathrm{EW}(B)$ is codimension-0 in the bulk, and will not be sufficient to localize $p$. Therefore, there must be some subregion of $\sigma$, $C$, where $C \subseteq \bar{A}$ and the boundary of $\mathrm{EW}(C)$ intersects $p$. However, from entanglement wedge nesting, $\mathrm{EW}(C) \subseteq \mathrm{EW}(\bar{A})$, and thus it cannot be the case. Note that this is a result of subregion duality, which tells us that the only intersection of $\mathrm{EW}(A)$ and $\mathrm{EW}(\bar{A})$ is the HRT surface. This implies that multiple leaves are necessary to reconstruct bulk regions in entanglement shadows.

Table A.1 gives a summary of directly reconstructable bulk regions from boundary states.

## A.2 Reconstructability of Two-sided Black Holes and Complementarity

In the main part of the text, we have focused on spacetimes having a simply connected boundary. It is interesting to consider when this is not the case and examine which (if any) results persist. For definiteness, we here analyze the case of a two-sided eternal black hole in asymptotically AdS space. In this case, the holographic screen is the union of the two asymptotic boundaries at spacelike infinity. The boundary theory comprises two CFTs, $\mathrm{CFT}_L$ and $\mathrm{CFT}_R$, which are decoupled from each other. Hence, the Hamiltonian for the system is given by

$$H_{\text{total}} = H_L + H_R. \tag{A.1}$$

The times $t_L$ and $t_R$ associated respectively with $H_L$ and $H_R$ run in opposite directions along the two asymptotic boundaries.

Since the theories are decoupled, it might appear that one could evolve each of the theories independently—effectively foliating the holographic screen by two independent parameters, $(t_L, t_R)$. Per the construction outlined in Section 2.4, the directly reconstructable region

would then be the union of all points localized by intersecting entanglement wedges of HRRT surfaces individually anchored to "one" leaf, each of which is labeled by $(t_L, t_R)$. Here, "one" leaf corresponds to picking a connected, equal time slice of the left boundary and independently a connected, equal time slice of the right boundary. If this were the case, the reconstructable region would be most of the spacetime, including a macroscopic portion of the interior (aside from a region near the singularity with $r < r_+/2^{1/d}$, where $r_+$ is the horizon radius) [289].

However, a theory described by Hamiltonian dynamics should have a single time parameter. To make the holographic theory compatible with this, we postulate that there is a single parameter $t$ that foliates the multiple disconnected components of the holographic screen. From this assumption, there are multiple suitable foliations, and among them we must pick one—this corresponds to choosing a reference frame, a gauge for the holographic redundancy [55]. In the case of a two-sided black hole, this gives us a one parameter family of foliations corresponding to the freedom in choosing the relative time shift between $t_L$ and $t_R$ in the CFTs, even after choosing a natural foliation at each boundary.

In general, each of these individual foliations reconstruct a different region of the bulk spacetime. For example, adopting the usual thermofield double state construction [69] corresponds to choosing a reference frame

$$t_L = t_R = t, \tag{A.2}$$

in which the $t = 0$ slice in the bulk is the one passing through the bifurcation surface. Since time translation is a Killing symmetry in this spacetime, and the bifurcation surface is invariant under this translation, the HRRT surfaces for any time $t$ never enter the interior of the black hole. Connected HRRT surfaces always pass through the bifurcation surface in such a situation (unless the subregion has support on only one of the boundaries, in which case the HRRT surface stays in one side of the black hole). The reconstructable region in this reference frame, therefore, does *not* include the interior of the black hole.

However, one could alternatively consider a reference frame in which there is a relative shift in the two times

$$t_L = t + \Delta, \quad t_R = t. \tag{A.3}$$

In this case, the connected HRRT surfaces would not necessarily pass through the bifurcation surface and could probe regions of the interior, and hence parts of the interior will be reconstructable. We can interpret this foliation dependence of the reconstructable region as a version of complementarity [63]. In this light, the canonical thermofield double time foliation corresponds to an entirely exterior description of the black hole, while increasing $\Delta$ allows for more of the region behind the horizon to be reconstructed. An important point is that we should not consider leaves with different $\Delta$'s in a single description—they correspond to different descriptions in different reference frames. We also note that regardless of the foliation, we cannot reconstruct near the singularity because of the extremal surface barrier located at $r = r_+/2^{1/d}$. This suggests that in order to probe physics of the singularity we must use a different method.

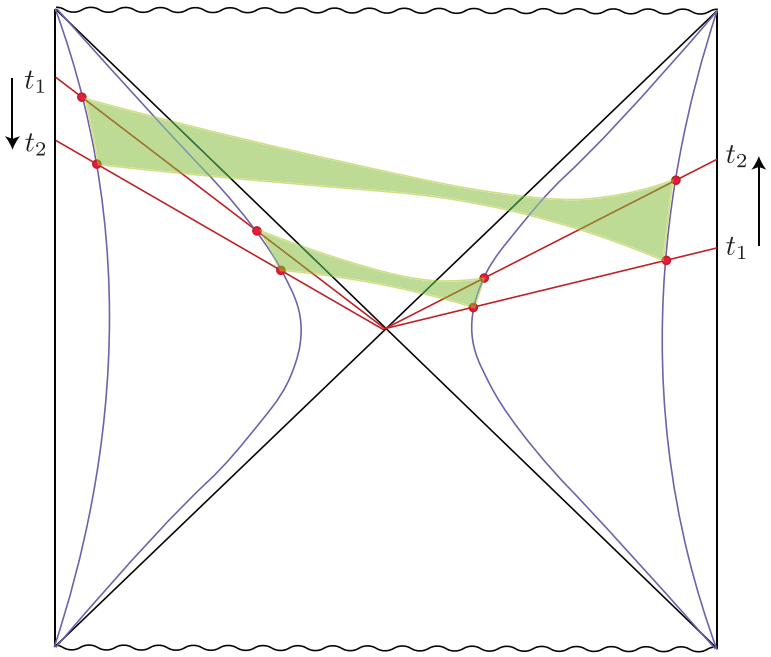


Figure A.1: The spacetime regions reconstructable using connected HRRT surfaces anchored to subregions with support on both asymptotic boundaries within the range $t \in [t_1, t_2]$ are depicted (green shaded regions) for two different values of black hole horizon radius $r_+$ in a two-sided eternal AdS black hole. The holographic screen (blue) in both cases is the cutoff surface $r = R$. Here, we superimpose the respective Penrose diagrams in the two cases to compare the amount of reconstructable spacetime volume available by allowing connected HRRT surfaces.

With this interpretation of bulk reconstruction, we would like to examine whether or not spacetime "disappears" as we approach maximal entropy. A priori, it seems that a macroscopic spacetime region would remain as we increase the black hole radius because some portion of the interior is reconstructable. However, this apparent contradiction is resolved by considering a finite coordinate time interval and examining the reconstructable volume as one increases the temperature.

Consider any foliation where the relative time shift between $t_L$ and $t_R$ has been fixed. In order to carry out the analysis analogous to Section 3.2, we fix an interval of coordinate time $\Delta t$ and fix the cutoff surface at $r = R$. Increasing the temperature of the black hole moves the horizon closer and closer to the cutoff surface, which can be represented in the Penrose diagram as in Fig. A.1. The allowed range of times is depicted by the constant time surfaces $t_1$ and $t_2$. As we take the limit $r_+ \to R$, which corresponds to taking the temperature of the black hole $T_{\mathrm{H}} \to \Lambda$ where $\Lambda$ is the cutoff in the boundary theory, the finite range of time collapses down to the bifurcation surface on both sides. Thus, the relative reconstructable

spacetime volume shrinks to zero.

We find that our claim persists despite the addition of a disconnected boundary region that allows for the reconstruction of spacetime behind a black hole horizon.

## A.3 Calculations for the Schwarzschild-AdS Spacetime

In this appendix, we provide explicit calculations of the spatial volume and HRRT surfaces of the Schwarzschild-AdS spacetime.

### Reconstructable volume

The Schwarzschild-AdS spacetime in $d+1$ dimensions is described by the metric

$$ds^2 = -\left(\frac{r^2}{l^2} + 1 - \frac{2\mu}{r^{d-2}}\right)dt^2 + \frac{dr^2}{\frac{r^2}{l^2} + 1 - \frac{2\mu}{r^{d-2}}} + r^2 d\Omega_{d-1}^2, \tag{A.4}$$

where $l$ is the AdS radius, and $\mu$ is related with the black hole horizon radius $r_+$ as

$$2\mu = \frac{r_+^d}{l^2}\left(1 + \frac{l^2}{r_+^2}\right). \tag{A.5}$$

The Hawking temperature of the black hole is given by

$$T_{\mathrm{H}} = \frac{dr_+^2 + (d-2)l^2}{4\pi r_+ l^2}. \tag{A.6}$$

Consider a large AdS black hole $r_+ \gg l$. In this limit,

$$2\mu = \frac{r_+^d}{l^2}, \qquad T_{\mathrm{H}} = \frac{dr_+}{4\pi l^2}, \tag{A.7}$$

and the metric is well approximated by

$$ds^2 = -\left(\frac{r^2}{l^2} - \frac{r_+^d}{l^2 r^{d-2}}\right)dt^2 + \frac{dr^2}{\frac{r^2}{l^2} - \frac{r_+^d}{l^2 r^{d-2}}} + r^2 d\Omega_{d-1}^2. \tag{A.8}$$

Let us now introduce an infrared cutoff $r \leq R$ and consider the spatial volume between the black hole horizon and the cutoff

$$\begin{aligned} V(r_+, R) &= A_{d-1}\int_{r_+}^{R} \frac{r^{d-1}}{\sqrt{\frac{r^2}{l^2} - \frac{r_+^d}{l^2 r^{d-2}}}}\, dr \\ &= \frac{2\pi^{d/2}}{\Gamma(d/2)}\, l\, r_+^{d-1}\int_1^{\frac{R}{r_+}} \frac{x^{d-2}}{\sqrt{1 - \frac{1}{x^d}}}\, dx, \end{aligned} \tag{A.9}$$

where $A_{d-1} = 2\pi^{d/2}/\Gamma(d/2)$ is the area of the $(d-1)$-dimensional unit sphere. Here, we have focused on the spatial volume because the system is static.

We normalize this volume by the volume of the region $r \leq R$ in empty AdS space

$$\begin{aligned} V(R) &= A_{d-1} \int_0^R \frac{r^{d-1}}{\sqrt{\frac{r^2}{l^2}+1}}\, dr \\ &= \frac{2\pi^{d/2}}{(d-1)\Gamma(d/2)}\, l\, R^{d-1}, \end{aligned} \tag{A.10}$$

where we have used $R \gg l$ in the second line. This gives us the quantity quoted in Eq. (3.1):

$$f\Big(\frac{r_+}{R}\Big) \equiv \frac{V(r_+, R)}{V(R)} = (d-1)\frac{r_+^{d-1}}{R^{d-1}} \int_1^{\frac{R}{r_+}} \frac{x^{d-2}}{\sqrt{1-\frac{1}{x^d}}}\, dx. \tag{A.11}$$

## HRRT surfaces

Consider a large black hole in asymptotically AdS space. The holographic theory is then a CFT. Suppose the temperature of the system $T$ is lower than the cutoff scale, $T < \Lambda$. Here we study the behavior of the von Neumann entropy of a spherical cap region $A$ on $r = R$ in this setup.

The region is specified by a half opening angle $\psi$

$$0 \leq \theta \leq \psi, \tag{A.12}$$

where $\theta$ is a polar angle parameterizing $S^{d-1}$ with constant $t$ and $r$. The HRRT surface $\gamma_A$ is then given by function $r(\theta)$, which is determined by minimizing the area functional:

$$\|\gamma_A\| = \min_{r(\theta)} \left[ A_{d-2} \int_0^\psi r^{d-2} \sin^{d-2}\theta \sqrt{r^2 + \frac{(\frac{dr}{d\theta})^2}{\frac{r^2}{l^2}+1-\frac{2\mu}{r^{d-2}}}}\, d\theta \right], \tag{A.13}$$

with the boundary condition

$$r(\psi) = R, \tag{A.14}$$

where $A_{d-2}$ is the area of the $(d-2)$-dimensional unit sphere, and $\mu$ is given by Eq. (A.4). Here and below, we assume $\psi \leq \pi/2$. For $\psi > \pi/2$, the entropy of $A$ is determined by $S(\psi) = S(\pi - \psi)$.

The surface $\gamma_A$ is well approximated to consist of two components: (i) a "cylindrical" piece with $\theta = \psi$, which is perpendicular to the cutoff surface $r = R$ and extends down to $r = r_0$ $(< R)$ and (ii) the "bottom lid" with $r = r_0$ and $0 \leq \theta \leq \psi$; see Fig. A.2. The area of the surface is then given by

$$\|\gamma_A\| = \min_{r_0} \left[ A_{d-2} \sin^{d-2}\psi \int_{r_0}^R \frac{r^{d-2}}{\sqrt{\frac{r^2}{l^2} - \frac{r_+^d}{l^2 r^{d-2}}}}\, dr + A_{d-2}\, r_0^{d-1} \int_0^\psi \sin^{d-2}\theta\, d\theta \right], \tag{A.15}$$

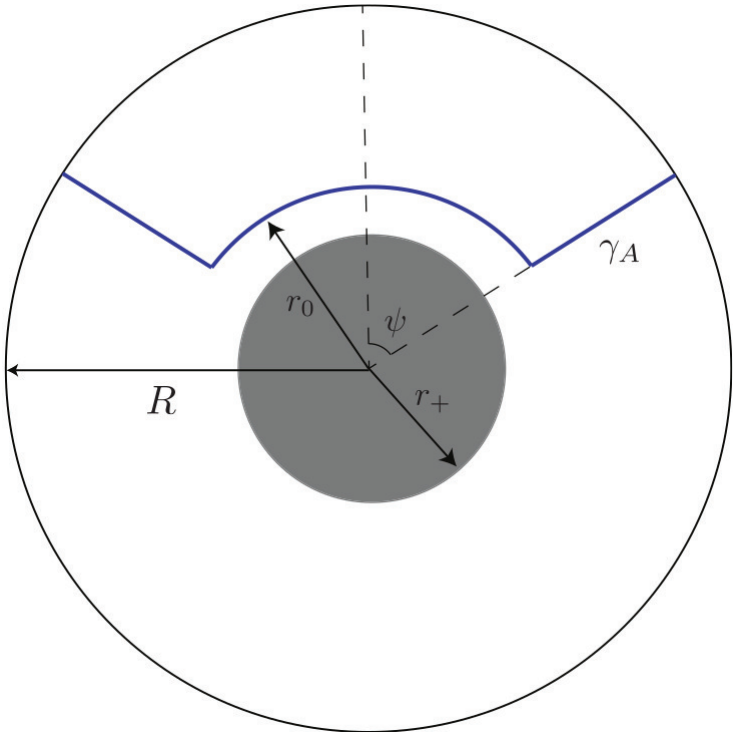


Figure A.2: The HRRT surface $\gamma_A$ in the Schwarzschild-AdS spacetime can be well approximated by consisting of two components: a "cylindrical" piece with $\theta = \psi$ and a "bottom lid" piece with $r = r_0$.

where $r_+$ is the horizon radius, and we have used the approximation that $r_+ \gg l$ and hence Eq. (A.7). The value of $r_0$ is determined by the minimization condition

$$\sqrt{r_0^2 - \frac{r_+^d}{r_0^{d-2}}} = \frac{\sin^{d-2}\psi}{(d-1)\int_0^\psi \sin^{d-2}\theta\, d\theta} l. \tag{A.16}$$

As discussed in Section 3.2, the cutoff at $r = R$ in our context simply means that the renormalization scale in the boundary theory is lowered; in particular, it does not mean that the theory is modified by actually terminating space there. The length in the boundary theory, therefore, is still measured in terms of the $d$-dimensional metric at infinity, $r = \infty$, with the conformal factor stripped off. The radius of the region $A$ is then given by

$$L = l\,\psi, \tag{A.17}$$

and not $R\psi$. Since the cutoff length is $1/\Lambda \approx l^2/R$, we should only consider the region $\psi \gtrsim l/R$.

The solution of Eq. (A.16) behaves as

$$\text{(i)} \quad r_0 = \frac{l}{\psi} \ (\gg r_+) \qquad \text{for } \frac{l}{R} < \psi \ll \frac{l}{r_+}, \tag{A.18}$$

$$\text{(ii)} \quad r_0 - r_+ = \frac{l^2}{d\psi^2 r_+} \ (\ll \frac{r_+}{d}) \quad \text{for } \frac{l}{r_+} \ll \psi \ll 1, \tag{A.19}$$

$$\text{(iii)} \quad r_0 - r_+ = O(1)\,\frac{l^2}{r_+} \qquad \text{for } \psi \approx O(1). \tag{A.20}$$

In the case of (i), $\|\gamma_A\|$ is dominated by the first term in Eq. (A.15), so that

$$\|\gamma_A\| = \frac{A_{d-2}}{d-2} l R^{d-2} \psi^{d-2}. \tag{A.21}$$

Here and below, we assume $d > 2$. We thus obtain an area law for the entropy

$$S_A = \frac{\|\gamma_A\|}{4 l_{\rm P}^{d-1}} \approx c A_{d-2} L^{d-2} \Lambda^{d-2}, \tag{A.22}$$

where $c \approx (l/l_{\rm P})^{d-1}$ is the central charge of the boundary CFT.

In the case of (ii), $\|\gamma_A\|$ is given by

$$\|\gamma_A\| = \frac{A_{d-2}}{d-2} l R^{d-2} \psi^{d-2} + \frac{A_{d-2}}{d-1} r_+^{d-1} \psi^{d-1}. \tag{A.23}$$

We find that the first (second) term is larger for

$$\psi < (>) \, \frac{d-1}{d-2} \frac{l R^{d-2}}{r_+^{d-1}}, \tag{A.24}$$

so that the entanglement entropy behaves as

$$S_A \approx \begin{cases} c A_{d-2} L^{d-2} \Lambda^{d-2} & \text{for } L \ll L_*, \\ c A_{d-2} \frac{r_+^{d-1} L^{d-1}}{l^{2d-2}} \approx c \left(\frac{T}{\Lambda}\right)^{d-1} A_{d-2} L^{d-1} \Lambda^{d-1} & \text{for } L \gg L_*, \end{cases} \tag{A.25}$$

where

$$L_* \approx \frac{l^2 R^{d-2}}{r_+^{d-1}} \approx \frac{\Lambda^{d-2}}{T^{d-1}}. \tag{A.26}$$

For $\psi \approx O(1)$, i.e. case (iii), we find

$$S_A \approx c \left(\frac{T}{\Lambda}\right)^{d-1} A_{d-2} L^{d-1} \Lambda^{d-1}. \tag{A.27}$$

Combining the results in all three cases gives the expression in Eqs. (3.17, 3.18).

## A.4 Calculations for the de Sitter Limit of FRW Universes

This appendix collects explicit calculations for entropies and HRRT surfaces in the de Sitter limit of FRW spacetimes.

### Entropies in the case of (2 + 1)-dimensional bulk

Here we see that for (2+1)-dimensional FRW spacetimes, the results of Ref. [31] immediately tell us that the entanglement entropy of an arbitrary (not necessarily connected) subregion $A$ is maximal in the de Sitter limit:

$$S_{A,w\to-1} = \frac{1}{4l_{\mathrm{P}}}\min\{\|A\|, \|\bar{A}\|\}. \tag{A.28}$$

Consider an FRW universe in $d$+1 dimensions dominated by a single ideal fluid component with the equation of state parameter $w = p/\rho$ ($|w| \leq 1$). From the analysis of Ref. [31], we know that the holographic entanglement entropy of a spherical cap region $A$ on a leaf—parameterized by the half opening angle $\psi$ as viewed from the center of the bulk—scales with the smaller of the volumes of $A$ and $\bar{A}$. The proportionality constant

$$Q_w(\psi) \equiv \frac{S(\psi)}{\frac{1}{4l_{\mathrm{P}}^{d-1}}\min\{\|A\|, \|\bar{A}\|\}}, \tag{A.29}$$

satisfies the properties

$$Q_w(\psi \to 0) \to 1, \qquad Q_{w\to-1}(\psi) \to 1, \tag{A.30}$$

$$\left.\frac{\partial Q_w(\psi)}{\partial\psi}\right|_{\psi=0} = 0, \qquad \left.\frac{\partial Q_w(\psi)}{\partial\psi}\right|_{\psi<\frac{\pi}{2}} \leq 0, \qquad \frac{\partial Q_w(\psi)}{\partial w} < 0. \tag{A.31}$$

(The original analysis was performed for (3 + 1)-dimensional FRW universes, but these properties persist in arbitrary spacetime dimensions.)

The second relation in Eq. (A.30) implies that in the de Sitter limit, $w \to -1$, the holographic entanglement entropy of a spherical cap region is maximal. Now, consider (2 + 1)-dimensional FRW universes, in which a leaf has only one spatial dimension. We consider a subregion on the leaf consisting of the union of two small intervals $A$ and $B$. Note that a similar setup is often discussed in AdS/CFT, where two possible extremal surfaces homologous to the subregion compete, so that a phase transition from the disconnected to connected HRRT surfaces occurs as the regions $A$ and $B$ are taken to be closer; see Fig. A.3. We want to understand what happens in the case of FRW spacetimes.

We denote the areas of two possible extremal surfaces by

$$\begin{aligned} E_{\mathrm{disconnected}}(AB) &= E(A) + E(B) \\ &= Q_w(A)\,\|A\| + Q_w(B)\,\|B\|, \end{aligned} \tag{A.32}$$

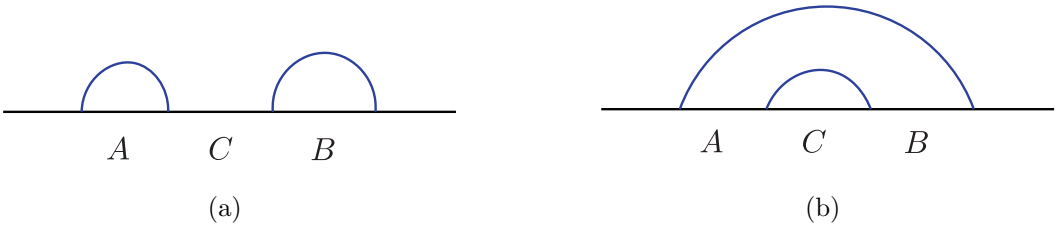


(a) (b)

Figure A.3: Two possible extremal surfaces anchored to the boundary of a subregion $AB$ on a leaf, given by the union of two disjoint intervals $A$ and $B$. The areas of the surfaces depicted in (a) and (b) are denoted by $E_{\text{disconnected}}(AB)$ and $E_{\text{connected}}(AB)$, respectively.

and

$$\begin{aligned} E_{\text{connected}}(AB) &= E(ABC) + E(C) \\ &= Q_w(ABC)\,\|ABC\| + Q_w(C)\,\|C\|, \end{aligned} \tag{A.33}$$

where $A$, $B$, and $C$ are defined in Fig. A.3. A phase transition can occur when

$$E_{\text{disconnected}}(AB) = E_{\text{connected}}(AB). \tag{A.34}$$

The condition of Eq. (A.34) can be satisfied for any $w$ away from the de Sitter limit because of the second relation in Eq. (A.31). Since a larger region has a greater volume but also has a smaller coefficient, it is possible for the two extremal surfaces to compete. However, in the de Sitter limit the requirement for a phase transition becomes

$$\|ABC\| + \|C\| = \|A\| + \|B\|, \tag{A.35}$$

which is clearly impossible because the left hand side is always greater. Since a general subregion of the leaf is a union of disconnected intervals, the above argument implies that the entanglement entropy is merely the sum of each interval's volume for sufficiently small regions. Extending the argument to large regions in which their complements matter, we can conclude that arbitrary subregions have maximal entanglement entropies in a $(2+1)$-dimensional de Sitter universe.

## Entropies in the $w \to -1$ limit of FRW spacetimes

The global spacetime structure in the case of a single fluid component with $w \neq -1$ is qualitatively different from the case discussed mainly in Section 3.2, i.e. the case in which a universe approaches de Sitter space at late times. Nevertheless, here we show that the holographic entanglement entropy of an arbitrary subregion on a leaf becomes maximal in the $w \to -1$ limit.

Let us consider an FRW universe filled with a single fluid component with the equation of state $w$. The scale factor is then given by

$$a(t) = c\, t^{\frac{2}{d(1+w)}}, \tag{A.36}$$

where $c > 0$ is a constant. We focus on a leaf $\sigma_*$ at time $t_*$ and the causal region $D_{\sigma_*}$ associated with it. Following Ref. [31], we perform $t_*$-dependent coordinate transformation on the FRW time and radial coordinates $t$ and $r$:

$$\eta = \frac{2}{d-2+dw}\left\{\left(\frac{t}{t_*}\right)^{\frac{d-2+dw}{d(1+w)}} - 1\right\}, \tag{A.37}$$

$$\rho = \frac{2}{d(1+w)} c\, t_*^{-\frac{d-2+dw}{d(1+w)}} r. \tag{A.38}$$

This converts the metric into the form

$$ds^2 = \left(\frac{\mathcal{A}_*}{A_{d-1}}\right)^{\frac{2}{d-1}} \left(\frac{d-2+dw}{2}\eta + 1\right)^{\frac{4}{d-2+dw}} \left(-d\eta^2 + d\rho^2 + \rho^2 d\Omega_{d-1}^2\right), \tag{A.39}$$

where $A_{d-1}$ is the area of the $(d-1)$-dimensional unit sphere, defined below Eq. (A.9), and $\mathcal{A}_*$ is the volume of the leaf $\sigma_*$

$$\mathcal{A}_* = \left(\frac{d(1+w)}{2}\right)^{d-1} A_{d-1}\, t_*^{d-1}. \tag{A.40}$$

In these coordinates, $D_{\sigma_*}$ is mapped into the region $\eta \in [-1, 1]$ and $\rho \in [0, 1-|\eta|]$.[1]

We can now take $w = -1 + \epsilon$ in Eq. (A.39) and expand it around $\epsilon = 0$. This gives

$$ds^2 = \left(\frac{\mathcal{A}_*}{A_{d-1}}\right)^{\frac{2}{d-1}} \left(\frac{1}{(1-\eta)^2} - d\frac{\eta + (1-\eta)\ln(1-\eta)}{(1-\eta)^3}\epsilon + \cdots\right)\left(-d\eta^2 + d\rho^2 + \rho^2 d\Omega_{d-1}^2\right). \tag{A.41}$$

The leading order term describes the causal region inside a leaf of volume $\mathcal{A}_*$ in de Sitter space with conformal coordinates. The time translational Killing symmetry in these coordinates is

$$\eta \to a\eta + 1 - a, \tag{A.42}$$

$$\rho \to a\rho. \tag{A.43}$$

The expansion in Eq. (A.41) is not valid when $\eta \lesssim 1-\epsilon$. However, this occurs only for a small subset of all the subregions on $\sigma_*$, which becomes measure zero when $\epsilon \to 0$. Continuity then tells us that the entanglement entropy $S_A$ of any subregion $A$ on $\sigma_*$ takes the same value as

[1] For $w \geq -1 + 4/d$, the region $D_{\sigma_*}$ hits the big bang singularity, so we need to restrict our attention to a portion of $D_{\sigma_*}$, e.g. $D^+_{\sigma_*} = \{p \in D_{\sigma_*} \mid t(p) \geq t_*\}$. This issue is not relevant to our discussion here.

that calculated in de Sitter space in the $\epsilon \to 0$ limit. However, we have already concluded from the argument in Section 3.2 that the entanglement entropies take the maximal form in de Sitter space, hence

$$S_A \underset{w\to -1}{\longrightarrow} \frac{1}{4l_{\rm P}^{d-1}} \min\{\|A\|, \|\bar{A}\|\}. \tag{A.44}$$

Note that the area of the leaf, $\mathcal{A}_*$, keeps growing indefinitely, so that $D_{\sigma_*}$ at each time $t_*$ is mapped to a different auxiliary de Sitter space. The ratio $Q_w(A) = S_A/(\min\{\|A\|, \|\bar{A}\|\}/4l_{\rm P}^{d-1})$, however, depends only on $w$ and not $t_*$.

## HRRT surfaces

Here we present two examples in which one can analytically see the convergence of the HRRT surfaces onto the future boundary of the causal region of a leaf in the de Sitter limit.

### The de Sitter limit of FRW universes in $2+1$ dimensions

As the first example, consider the de Sitter limit of FRW universes in $2+1$ dimensions

$$ds^2 = a^2(\eta)\,(-d\eta^2 + dx^2 + dy^2). \tag{A.45}$$

Here, $\eta \in (-\infty, 0)$ is the conformal time, and the scale factor is given by

$$a(\eta) = \frac{c}{\eta}, \tag{A.46}$$

where $c$ is a positive constant. In this case, we can obtain an analytic solution for HRRT surfaces, which are geodesics in $2+1$ dimensions.

In order to find a spacelike geodesic anchored to two points on the leaf, we can use the symmetry of the problem to rotate our axes so that the points lie at constant $y = y_0$. To find a geodesic, we need to extremize the distance functional

$$\mathcal{D} = \int d\eta\, \frac{c}{\eta}\sqrt{\dot{x}^2 - 1}, \tag{A.47}$$

where $\dot{x} = dx/d\eta$, and we have used the fact that the geodesic lies on the $y = y_0$ hypersurface. This functional has no explicit dependence on $x$, which means the existence of a quantity that is conserved along the geodesic

$$\frac{\partial \mathcal{D}}{\partial \dot{x}} = \frac{c\dot{x}}{\eta\sqrt{\dot{x}^2 - 1}} \equiv p_x. \tag{A.48}$$

Using this, we obtain a first-order ordinary differential equation

$$\frac{d\eta}{dx} = \sqrt{1 - \frac{c^2}{p_x^2\eta^2}}, \tag{A.49}$$

which can be easily solved to give the analytic expression for the geodesic

$$\begin{cases} \eta(x) &= -\sqrt{x^2 + \frac{c^2}{p_x^2}}, \\ y(x) &= y_0. \end{cases} \tag{A.50}$$

The holographic screen of FRW universes in the de Sitter limit lies on

$$\eta = -\sqrt{x^2 + y^2} \equiv -r. \tag{A.51}$$

Consider a leaf at $\eta = \eta_* = -r_*$ and a subregion on it specified by a half opening angle $\psi$ ($0 \leq \psi \leq \pi$). The end points of the HRRT surface are then at

$$(x, y) = (\mp\eta_* \sin\psi, -\eta_* \cos\psi). \tag{A.52}$$

This can be used to determine $p_x$ and $y_0$ in Eq. (A.50), giving the final expression for the geodesic

$$\begin{cases} \eta(x) &= -\sqrt{x^2 + y_0^2}, \\ y(x) &= y_0, \end{cases} \tag{A.53}$$

where $y_0 = -\eta_* \cos\psi$. By varying the angle $\psi$, the HRRT surfaces sweep a codimension-1 surface in the bulk, which is indeed the future boundary of the causal region of the leaf:

$$\eta = -r, \qquad 0 \leq r \leq r_* \, (= -\eta_*). \tag{A.54}$$

These surfaces are depicted in $x$-$y$-$\eta$ space in Fig. A.4. We can clearly see that all the HRRT surfaces are spacelike, except for that corresponding to $\psi = \pi/2$ which is null.

**Small spherical caps in FRW universes in $d+1$ dimensions**

Another example in which simple analytic expressions are obtained is the limit of small spherical cap regions, $\psi \ll 1$, on a leaf. Consider a flat FRW universe in $d+1$ dimensions

$$ds^2 = a(\eta)^2 \big(-d\eta^2 + dr^2 + r^2 d\Omega_{d-1}^2\big), \tag{A.55}$$

filled with a single fluid component with the equation of state $w$. We consider the leaf $\sigma_*$ at $\eta = \eta_*$, which is located at

$$r = \frac{a}{\dot{a}}. \tag{A.56}$$

The future boundary $F_*$ of the causal region $D_{\sigma_*}$ is then given by

$$F_* : \eta(r) = \eta_* + \frac{a}{\dot{a}} - r. \tag{A.57}$$

Here and below, the scale factor and its derivatives without an argument represent those at $\eta = \eta_*$:

$$a \equiv a(\eta_*), \qquad \dot{a} \equiv \left.\frac{da(\eta)}{d\eta}\right|_{\eta=\eta_*}, \qquad \ddot{a} \equiv \left.\frac{d^2 a(\eta)}{d\eta^2}\right|_{\eta=\eta_*}. \tag{A.58}$$

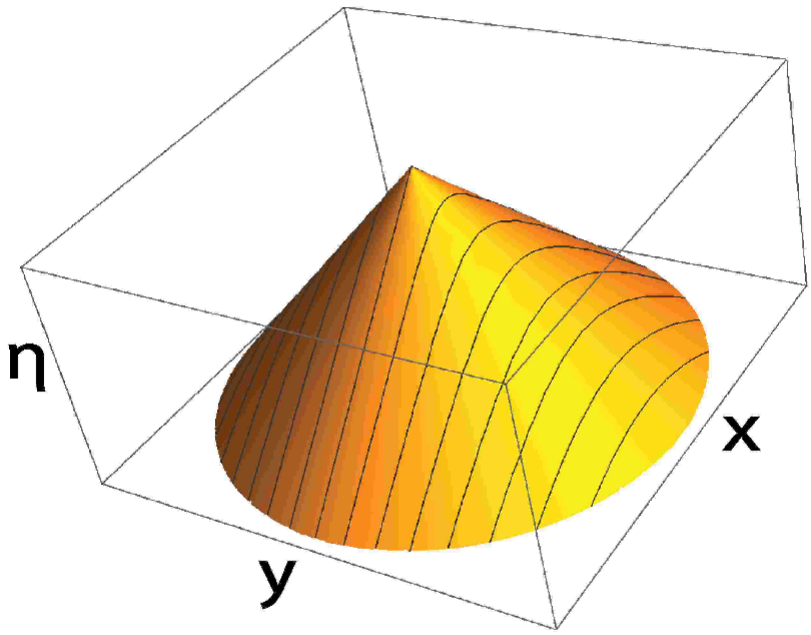


Figure A.4: HRRT surfaces anchored to subregions on a leaf in $(2+1)$-dimensional de Sitter space. They all lie on the future boundary of the causal region associated with the leaf.

We consider a spherical cap region $A$ on the leaf $\sigma_*$, specified by a half opening angle $\psi$

$$0 \leq \theta \leq \psi, \tag{A.59}$$

where $\theta$ is a polar angle parameterizing $S^{d-1}$ with constant $\eta$ and $r$. Following Ref. [31], we go to cylindrical coordinates:

$$\xi = r \sin\theta, \qquad z = r\cos\theta - \frac{a}{\dot{a}}\cos\psi. \tag{A.60}$$

In these coordinates, the null cone $F_*$ in Eq. (A.57) is given by

$$F_* : \eta(\xi) = \eta_* + \frac{a}{\dot{a}} - \sqrt{\xi^2 + \left(z + \frac{a}{\dot{a}}\cos\psi\right)^2}, \tag{A.61}$$

and the boundary of $A$, $\partial A$, is located at

$$\eta = \eta_*, \qquad \xi = \frac{a}{\dot{a}}\sin\psi \equiv \xi_*, \qquad z = 0. \tag{A.62}$$

The HRRT surface $\gamma_A$ anchored to $\partial A$ is on the $z = 0$ hypersurface [31]. We would like to compare this HRRT surface with the intersection of $F_*$ and $z = 0$:

$$l_A : \eta(\xi) = \eta_* + \frac{a}{\dot{a}} - \sqrt{\xi^2 + \frac{a}{\dot{a}}\cos\psi}, \tag{A.63}$$

see Fig. A.5. Using Eq. (A.62) and expanding in powers of $\psi \sim \xi/(a/\dot{a})$, this can be written as

$$l_A : \eta(\xi) = \eta_* + \frac{\dot{a}}{2a}(\xi_*^2 - \xi^2) + \frac{\dot{a}^3}{8a^3}(\xi_*^2 - \xi^2)^2 + \cdots . \tag{A.64}$$

For $\psi \ll 1$, the HRRT surface can be expressed in a power series form

$$\gamma_A : \eta(\xi) = \eta_* + \eta^{(2)}(\xi) + \eta^{(4)}(\xi) + \cdots , \tag{A.65}$$

where

$$\eta^{(2)}(\xi) = \frac{\dot{a}}{2a}(\xi_*^2 - \xi^2), \tag{A.66}$$

$$\begin{aligned}\eta^{(4)}(\xi) = &- \frac{\dot{a}}{8a^3(d+1)}(\xi_*^2 - \xi^2) \\ &\times \Big[\dot{a}^2\big\{(d+5)\xi_*^2 - (d-3)\xi^2\big\} - a\ddot{a}\big\{(d+3)\xi_*^2 - (d-1)\xi^2\big\}\Big].\end{aligned} \tag{A.67}$$

In the universe dominated by a single fluid component, the scale factor behaves as

$$a(\eta) \propto \eta^{\frac{2}{d-2+dw}}. \tag{A.68}$$

Plugging this into Eq. (A.67), we obtain

$$\eta^{(4)}(\xi) = \frac{\dot{a}^3}{16(d+1)a^3}(\xi_*^2 - \xi^2)\Big[\big\{2 - (1+3w)d - (1+w)d^2\big\}\xi_*^2 - \big\{2 + (3+w)d - (1+w)d^2\big\}\xi^2\Big]. \tag{A.69}$$

We find that for $w = -1$, the surface given by Eqs. (A.65, A.66, A.69) agree with $l_A$ in Eq. (A.64). Namely, the HRRT surface $\gamma_A$ is on the null cone $F_*$.

One can see how $\gamma_A$ approaches $F_*$ as $w \to -1$ by subtracting Eq. (A.65) from Eq. (A.64):

$$\begin{aligned}\eta^{l_A}(\xi) - \eta^{\gamma_A}(\xi) &= \frac{\dot{a}^3}{16a^3}\frac{d}{d+1}(1+w)(\xi_*^2 - \xi^2)\big\{(d+3)\xi_*^2 - (d-1)\xi^2\big\} \\ &\geq 0.\end{aligned} \tag{A.70}$$

The inequality is saturated only for $w = -1$ (except at the end points at $\xi = \xi_*$).

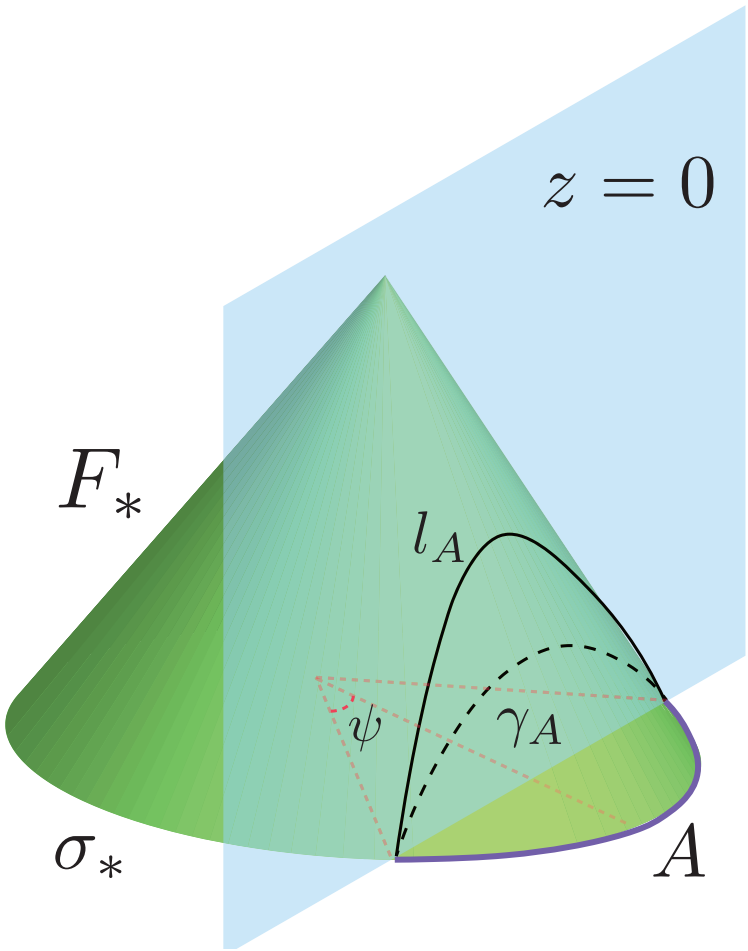


Figure A.5: The HRRT surface $\gamma_A$ for subregion $A$ of a leaf $\sigma_*$ specified by a half opening angle $\psi$ is on the $z = 0$ hypersurface. It approaches the surface $l_A$, the intersection of the null cone $F_*$ and the $z = 0$ hypersurface, in the de Sitter limit.

## A.5 Intersection of Domains of Dependence

**Lemma 1.** Let $\Sigma$ be a closed, achronal set and $D(\Sigma)$ be the domain of dependence of $\Sigma$. Let $p$ and $q$ be points in $D(\Sigma)$, and $\lambda$ a causal curve such that $\lambda(0) = p$ and $\lambda(1) = q$ where $p$ lies to the past of $q$. Then, all points $r = \lambda(t)$ for $t \in [0, 1]$ are contained in $D(\Sigma)$.

*Proof.* Suppose such a point $r$ does not belong to $D(\Sigma)$. Then, there must exist an inextendible causal curve $\lambda'$ that passes through $r$ and does not intersect $\Sigma$. Without loss of generality, assume that $r$ lies to the past of $\Sigma$. Consider a causal curve composed of $\lambda$ to the past of $r$ and $\lambda'$ to the future of $r$. This would then be an inextendible causal curve passing through $p$ but not intersecting $\Sigma$, implying that $p$ does not belong to $D(\Sigma)$, thus

contradicting the assumption. □

**Lemma 2.** Let $R$ be a closed set such that every causal curve connecting two points in $R$ lies entirely in $R$. Let $\Sigma$ be the future boundary of $R$ defined by points $p \in R$ such that $\exists$ a timelike curve $\lambda$ passing through $p$ that does not intersect $R$ anywhere in the future. Then,

1. $\Sigma$ is an achronal set.
2. $R \subseteq D(\Sigma)$.

*Proof.* We first show that $\Sigma$ is an achronal set. Suppose there exist two points $p$ and $q$ in $\Sigma$ that were timelike related. Without loss of generality, assume that $p$ lies to the past of $q$. Consider an open neighborhood of $p$ denoted by $U(p)$. Consider a point $r$ such that $r \in \{I_+(p) \cap U(p)\} \setminus R$. By continuity, $\exists$ a timelike curve $\lambda$ connecting $r$ to $q$. $\lambda$ can then be extended to pass through $p$ in the past. Thus, we have found a causal curve that connects points $p$ and $q$, both of which belong to $R$, and passes through $r \notin R$. This contradicts the assumption, and hence, $\Sigma$ must be an achronal set.

Now, we can show that $R \subseteq D(\Sigma)$. Consider a point $p$ such that $p \in R \setminus \Sigma$. Then, $I_+(p)$ must intersect $\Sigma$. To show this, suppose it were not true and consider a future causal curve $\lambda$ from $p$ which does not intersect $\Sigma$. The boundary point of $\lambda \cap R$ then also has a timelike curve through it which does not intersect $R$ anywhere in the future, and thus should be included in the set $\Sigma$. Therefore, $I_+(p)$ either intersects $\Sigma$ everywhere in the interior of $\Sigma$ or intersects some portion of the boundary of $\Sigma$. In the first case, all inextendible causal curves through $p$ necessarily pass through $\Sigma$, and hence $p \in D(\Sigma)$. In the second case, extend $\Sigma$ in a spacelike manner to an open neighborhood around $\Sigma$ where a point $q$ outside $\Sigma$ is timelike related to $p$. Causal curves from $p$ to $q$ would not intersect $\Sigma$ since $q$ is spacelike related to all points on $\Sigma$. Consider the intersection of this curve with $R$. It must have a boundary point which does not belong to $\Sigma$. This point would then have inextendible timelike curves through it that do not intersect $R$ in the future. This contradicts the assumption that this point was not in $\Sigma$. This implies that the second case is impossible. Hence, we have proved that $R \subseteq D(\Sigma)$. □

**Theorem 4.** Consider two codimension-1 spacelike subregions $\Sigma_1$ and $\Sigma_2$ that are compact. Let their domains of dependence be $D(\Sigma_1) = D_1$ and $D(\Sigma_2) = D_2$. Then $D = D_1 \cap D_2$ is the domain of dependence of the future boundary of $D$ denoted by $\Sigma$.

*Proof.* Consider any two points $p$ and $q$ that belong to $D$. Both $p$ and $q$ belong to $D_1$ and $D_2$. Using Lemma 1, we can conclude that all points on a causal curve joining $p$ and $q$ belong to both $D_1$ and $D_2$. Hence, any such point also belongs to $D$. Thus, $D$ satisfies the condition required for $R$ above in Lemma 2. Using Lemma 2 then tells us that $D \subseteq D(\Sigma)$.

Since $\Sigma$ is defined to be the future boundary of $D$, $\Sigma$ itself is necessarily contained in $D$. Now consider any $p \in D(\Sigma)$. Any causal curve $\lambda$ passing through $p$ intersects $\Sigma$ by definition. However, since $\Sigma \subseteq D$, all inextendible causal curves through $\Sigma$ necessarily intersect both

$\Sigma_1$ and $\Sigma_2$. Thus, all inextendible causal curves through $p$ also pass through both $\Sigma_1$ and $\Sigma_2$. This implies $D(\Sigma) \subseteq D$.

Combining the above two results, we have shown that $D = D(\Sigma)$. Namely, the intersection of two domains of dependence is also a domain of dependence. □

## A.6 Uniqueness of the Holographic Slice

Consider a codimension-2, closed, achronal surface $\sigma$ in an arbitrary $(d+1)$-dimensional spacetime $M$. Suppose $\sigma$ is a convex boundary. We assume that both $M$ and $\sigma$ are sufficiently smooth so that variations in the spacetime metric $g_{\mu\nu}$ and induced metric on $\sigma$, denoted by $h_{ij}$, occur on characteristic length scales $L$ and $L_\sigma$, respectively.

**Theorem 5.** Consider subregion $R$ of characteristic length $\delta \ll L, L_\sigma$ on $\sigma$. To leading order, the extremal surface anchored to $\partial R$ lives on the hypersurface generated by the vector $s = \theta_t t - \theta_z z$ normal to $\sigma$. Here, $t$ and $z$ are orthonormal timelike and spacelike vectors perpendicular to $\sigma$, and $\theta_t = h^{ij}K^t_{ij}$ and $\theta_z = h^{ij}K^z_{ij}$ where $K^t_{ij}$ and $K^z_{ij}$ are the extrinsic curvature tensors of $\sigma$ for $t$ and $z$, respectively. This property is independent of the shape of $R$.

*Proof.* Start from a point $p \in R$ and set up Riemann normal coordinates in the local neighborhood of $p$.

$$g_{\mu\nu}(x) = \eta_{\mu\nu} - \frac{1}{3}R_{\mu\rho\nu\sigma}x^\rho x^\sigma + O(x^3). \tag{A.71}$$

In these coordinates, we are considering a patch of size $\delta$ around the origin $p$ with $R_{\mu\rho\nu\sigma} \sim O(1/L^2)$. Equivalently, we could consider a conformally rescaled metric

$$x^\mu = \epsilon y^\mu, \tag{A.72}$$

$$ds^2 = \epsilon^2 g_{\mu\nu}(\epsilon y)\, dy^\mu dy^\nu, \tag{A.73}$$

$$\begin{aligned} d\tilde{s}^2 &= g_{\mu\nu}(\epsilon y)\, dy^\mu dy^\nu \\ &= \tilde{g}_{\mu\nu}(y)\, dy^\mu dy^\nu, \end{aligned} \tag{A.74}$$

where $\epsilon = \delta/L \ll 1$.

In this alternate way of viewing the problem, we have a patch of size $L$ with the metric varying on a larger length scale $L/\epsilon$. In these coordinates, each derivative of the conformal metric brings out an extra power of $\epsilon$; for example,

$$\frac{\partial^2}{\partial y^\rho \partial y^\sigma}\tilde{g}_{\mu\nu} = \epsilon^2 \frac{\partial^2}{\partial x^\rho \partial x^\sigma} g_{\mu\nu} \sim \frac{\epsilon^2}{L^2}. \tag{A.75}$$

The connection coefficients $\Gamma^{\mu}_{\rho\sigma}$ vanish at $p$ due to our choice of Riemann normal coordinates. This implies that for points in the neighborhood of $p$, we can Taylor expand to find

$$\Gamma^{\mu}_{\rho\sigma} \sim \frac{\epsilon^2}{L}, \tag{A.76}$$

$$R_{\mu\rho\nu\sigma} \sim \frac{\epsilon^2}{L^2}. \tag{A.77}$$

Note that these quantities are obtained using the rescaled metric $\tilde{g}_{\mu\nu}$ in the $y^{\mu}$ coordinates.

Since there is still a remaining $SO\,(d,1)$ symmetry that preserves the Riemann normal coordinate form of the metric, we can use these local Lorentz boosts and rotations to set $t$ and $z$ as the coordinates in the normal direction to $\sigma$ at $p$ while $y^i$ parameterize the tangential directions. This is a convenient choice to solve the extremal surface equation in a perturbation series order by order. The extremal surface equation is given by [20]

$$\tilde{g}^{\rho\sigma}\Big(\partial_\rho\partial_\sigma Y^{\mu} + \Gamma^{\mu}_{\lambda\eta}\partial_\rho Y^{\lambda}\partial_\sigma Y^{\eta} - \Gamma^{\lambda}_{\rho\sigma}\partial_\lambda Y^{\mu}\Big) = 0. \tag{A.78}$$

This is a set of $d+1$ equations for the embedding of the extremal surface $Y^{\mu}$, which are functions of $d-1$ independent coordinates. The equations in the tangential directions are trivially satisfied by taking the $d-1$ parameters to be $y^i$. This leaves only two equations in the normal directions to be solved.

From the discussion above, when restricted to the local patch of size $L$, we have

$$\tilde{g}^{\mu\nu} = \eta^{\mu\nu} + O(\epsilon^2), \tag{A.79}$$

$$\Gamma^{\mu}_{\rho\sigma} = O\bigg(\frac{\epsilon^2}{L}\bigg). \tag{A.80}$$

Assuming the extremal surface is smooth, derivatives of $Y^{\mu}$ typically bring down a power of $L_\sigma$. Thus,

$$\partial Y \sim O(1), \tag{A.81}$$

$$\partial^2 Y \sim O\bigg(\frac{1}{L_\sigma}\bigg). \tag{A.82}$$

Using this, at the leading order in $\epsilon$ and $\epsilon_\sigma = \delta/L_\sigma$, the extremal surface equations simply become

$$\delta^{ij}\partial_i\partial_j Y^{\mu} = 0, \tag{A.83}$$

where $\mu$ takes the $t$ and $z$ directions. We write these as

$$\nabla^2 t_{\rm E} = \nabla^2 z_{\rm E} = 0, \tag{A.84}$$

where $t_{\rm E}$ and $z_{\rm E}$ are functions of $y^i$.

Let $K^t_{ij}$, $K^z_{ij}$ denote the extrinsic curvature tensors for the $t$ and $z$ normals, respectively. Following the above scaling arguments, $K^t_{ij}$, $K^z_{ij} \sim \epsilon/L_\sigma$. Here, we have assumed that

$L_\sigma \lesssim L$, although this is not essential for the final result. Because $t$ and $z$ are normal to the leaf, the equations for the leaf, described by $t_{\rm L}(y^i)$ and $z_{\rm L}(y^i)$, can be Taylor expanded in the neighborhood $R$ as

$$t_{\rm L}(y^i) = -\frac{1}{2}K^t_{ij}y^iy^j + O\left(\frac{\epsilon^2 y^3}{L_\sigma^2}\right), \tag{A.85}$$

$$z_{\rm L}(y^i) = \frac{1}{2}K^z_{ij}y^iy^j + O\left(\frac{\epsilon^2 y^3}{L_\sigma^2}\right), \tag{A.86}$$

where the negative sign in the first line is due to the timelike signature of the $t$ normal. The boundary conditions for the extremal surface equation are

$$t_{\rm E}(\partial R) = t_{\rm L}(\partial R), \tag{A.87}$$

$$z_{\rm E}(\partial R) = z_{\rm L}(\partial R). \tag{A.88}$$

Now, consider $\delta t = t_{\rm E} - t_{\rm L}$ and $\delta z = z_{\rm E} - z_{\rm L}$. The extremal surface equations are then given by

$$\nabla^2\,\delta t = -\nabla^2 t_{\rm L} = \theta_t\left\{1 + O(\epsilon_\sigma)\right\}, \tag{A.89}$$

$$\nabla^2\,\delta z = -\nabla^2 z_{\rm L} = -\theta_z\left\{1 + O(\epsilon_\sigma)\right\}, \tag{A.90}$$

where $\theta_t = h^{ij}K^t_{ij}$ and $\theta_z = h^{ij}K^z_{ij}$. Note that $h_{ij} = \eta_{ij}$ at this order. The boundary conditions are given by

$$\delta t\,(\partial R) = \delta z\,(\partial R) = 0. \tag{A.91}$$

It is now clear that at leading order $\delta t/\theta_t$ and $-\delta z/\theta_z$ satisfy the same equation with the same boundary conditions. Thus,

$$\frac{\delta t}{\delta z} = -\frac{\theta_t}{\theta_z} + O(\epsilon_\sigma), \tag{A.92}$$

for all points on the extremal surface. Rewritten, the extremal surface lives on the hypersurface generated by $s = \theta_t t - \theta_z z$, orthogonal to $\sigma$.

This result is independent of the explicit shape of subregion $R$. □

Theorem 5 essentially brings us to the uniqueness of the holographic slice. The new surface, $\sigma'$, is generated by a convolution of the "deepest" points on each $\gamma(R)$. Considering balanced shapes such that the "deepest" point corresponds to $y^i = 0$, $\delta t/\delta z$ has the interpretation of the slope of the evolution vector $s$ from $p$ which takes it to the new leaf $\sigma'$. Slight imbalances in the shape would only affect the slope at subleading order in $\epsilon, \epsilon_\sigma$ and thus, the slope of $s$ is determined in a shape independent manner in the limit $\epsilon, \epsilon_\sigma \to 0$. In order to move to $\sigma'$, we must also specify the distance, $\delta\lambda(p)$, by which we move along $s$ at each step. If the size of $C(p)$ is homogeneous across $\sigma$, then $\delta\lambda(p)$ is independent of $p$ to leading order. Thus, the new leaf $\sigma'$ obtained at each stage is unique up to small error

terms. Following a similar procedure at each stage, e.g. by choosing random uncorrelated shapes of size $\delta'$ (found by mapping length $\delta$ to $\sigma'$ by $s$) for subregions $C'(p)$ at each point $p$, ensures that the error terms do not add up coherently. This implies that the holographic slice is obtained by following the integral curves of the evolution vector $s$ starting from each point $p \in \sigma$, and hence is unique.

**Corollary 2.** Construct a holographic slice such that $C^i(p)$ is homogeneous and uncorrelated with $C^j(p)$, $j \neq i$. Let the sizes of $C^i(p)$ be determined by mapping the characteristic length, $\delta$, of $C(p)$ on $\sigma$ to $\sigma^i$ by $s$. The continuum version (sending $\delta \to 0$) of all such slices are identical.

As an aside, there are certain interesting features that this analysis highlights. Consider a generic leaf of a holographic screen $\sigma$ and the future directed orthogonal null vectors $k$ and $l$ normalized as $k \cdot l = -2$. The $t$ and $z$ vectors are then given by

$$t = \frac{1}{2}(k + l), \qquad z = \frac{1}{2}(k - l). \tag{A.93}$$

From the linearity of extrinsic curvature, this leads to

$$\theta_t = \frac{1}{2}(\theta_k + \theta_l), \qquad \theta_z = \frac{1}{2}(\theta_k - \theta_l). \tag{A.94}$$

The evolution vector $s$ and its associated expansion $\theta_s$ are given by

$$s = \theta_t t - \theta_z z = \frac{1}{2}(\theta_k l + \theta_l k), \tag{A.95}$$

and

$$\theta_s = \theta_t^2 - \theta_z^2 = \theta_k \theta_l \leq 0, \tag{A.96}$$

respectively.

At the holographic screen, $\theta_k = 0$. This leads to

$$s \propto k, \qquad \theta_s = 0. \tag{A.97}$$

Namely, the initial evolution of the holographic slice from a non-renormalized leaf occurs in the $k$ direction with a non-expanding or contracting leaf area.

## A.7 Convexity of Renormalized Leaves

**Definition.** On a spacelike slice $\Sigma$, a compact set $S$ is defined to be convex if all the codimension-1 minimal surfaces $\gamma(A)$ anchored to a codimension-2 region $A \subset S$ are such that $\forall A$, $\gamma(A) \subset S$.

**Lemma 3.** $S$ is convex if and only if $K_\Sigma(\partial S) \leq 0$, where $K_\Sigma(\partial S)$ is the trace of the extrinsic curvature of $\partial S$ embedded in $\Sigma$ for the normal pointing inward.

*Proof.* This follows from the fact that if $K_\Sigma(\partial S) \leq 0$, $\partial S$ acts as a minimal surface barrier and hence, all the minimal surfaces must be contained within $S$. For the converse, suppose $K_\Sigma(\partial S) > 0$ somewhere on $\partial S$, then by considering small enough subregions anchored to this portion of $\partial S$, one can explicitly construct minimal surfaces that are outside $S$. □

**Definition.** In a spacetime $M$, a codimension-2 compact surface $\sigma$ is called a convex boundary if on every codimension-1 spacelike slice $\Sigma$ such that $\sigma \subset \Sigma$, the closure of the interior of $\sigma$ is a convex set.

**Theorem 6.** $\sigma$ is a convex boundary if and only if the null expansions in the inward direction, i.e. $\theta_k$ and $\theta_{-l}$, are both non-positive.

*Proof.* An inward normal $n$ on a spacelike slice $\Sigma$ is given by a linear superposition of $k$ and $l$, i.e. $n = \alpha k - \beta l$ with some $\alpha, \beta \geq 0$. If $\theta_k \leq 0$ and $\theta_l \geq 0$, then $K_\Sigma(\sigma) = \theta_n = \alpha\theta_k - \beta\theta_l \leq 0$ for all choices of $\alpha, \beta \geq 0$. Thus, from Lemma 3, $\sigma$ would be convex on all $\Sigma$ containing $\sigma$. For the converse, suppose $\theta_k > 0$. One can then choose $\Sigma$ such that $K_\Sigma(\sigma) > 0$ by taking $\beta \ll \alpha$. Thus, from Lemma 3, $\sigma$ would not be convex on $\Sigma$, and hence $\sigma$ would not be a convex boundary. The same argument applies if $\theta_l < 0$. □

**Fact.** A leaf of a holographic screen is a convex boundary. The boundary of any entanglement wedge is also a convex boundary.

**Theorem 7.** The intersection of the interior domains of dependence of two convex boundaries $\sigma_1$ and $\sigma_2$, represented by $D_1$ and $D_2$ is the interior domain of dependence of a convex boundary $\sigma'$.

*Proof.* As shown in Appendix A.5, $D' = D_1 \cap D_2$ is the interior domain of dependence of some $\sigma'$. We only need to show that $\sigma'$ is convex. In order to show this, we can consider two slices $\Sigma_1$ and $\Sigma_2$ passing through $\sigma_1$ and $\sigma_2$ such that they are identical in the interior of $\sigma'$ and are disjoint in the exterior of $\sigma'$. Let us denote the slice through the interior of $\sigma'$ to be $\Sigma'$. Now consider any codimension-2 region $A \subset \Sigma'$. Then, from the convexity of $\sigma_1$, the minimal surface $\gamma(A)$ is contained in the interior of $\sigma_1$ on $\Sigma_1$. Similarly, $\gamma(A)$ is contained in the interior of $\sigma_2$ on $\Sigma_2$. This is only possible if $\gamma(A)$ is contained in the interior of $\sigma'$ on $\Sigma'$. This is true for arbitrary $\Sigma'$ and hence, by definition, $\sigma'$ is a convex boundary. The maximin process can now be applied to $\sigma'$. □

**Corollary 3.** In a black hole spacetime or the case of a spacelike screen in an FRW spacetime, the coarse-graining procedure moves away from the singularity in the direction where the expansions $\theta_k$ and $\theta_l$ have opposite signs. At each step of coarse-graining, $\theta_k$ and $\theta_l$ in general have opposite signs.

## A.8 Flat Renyi Spectrum

Here we prove that if a density matrix $\rho$ satisfies the condition $\widetilde{S}_n(\rho) = S(\rho)$ for all $n$, it must be a normalized projector. We show this by first showing that this condition of having a flat refined Renyi entropy spectrum is equivalent to having a flat Renyi entropy spectrum.

From the definition of the refined Renyi entropy and the above condition, we have

$$\widetilde{S}_n(\rho) = n^2 \partial_n \left( \frac{n-1}{n} S_n(\rho) \right) \tag{A.98}$$

$$= S(\rho) \ . \tag{A.99}$$

We can integrate with respect to $n$ to obtain

$$\int_1^{n'} \frac{S(\rho)}{n^2} = \left[ \frac{n-1}{n} S_n(\rho) \right]_1^{n'} \tag{A.100}$$

$$\implies S(\rho) = S_{n'}(\rho) \ , \tag{A.101}$$

where this condition is true for arbitrary $n'$. Now we can use the fact that $\rho$ and $\rho^n$ can be simultaneously diagonalized to arrive at the identity

$$\partial_n S_n(\rho) = -\frac{1}{(1-n)^2} \sum_{i=1}^{\dim(\rho)} q_i \log \left( \frac{q_i}{p_i} \right) \ , \tag{A.102}$$

where $p_i$ are the eigenvalues of $\rho$ and $q_i = p_i^n / (\sum_{i=1}^{\dim(\rho)} p_i^n)$. If indeed Eq. (A.101) is true, then the LHS equals zero for all $n$. For the RHS to equal zero implies the relative entropy (Kullback-Leibler divergence) between probability distributions $q_i$ and $p_i$ vanishes. Using a standard result, we can conclude that the distributions are indeed identical. This gives us our desired result that

$$p_i = \left( \sum_{i=1}^{\text{rank}(\rho)} p_i^n \right)^{1/(n-1)} \tag{A.103}$$

$$= \frac{1}{\text{rank}(\rho)} \ , \tag{A.104}$$

where we have restricted to the non-zero elements only and used the normalization condition. Thus, in its diagonal basis $\rho$ takes the form

$$\rho = \frac{1}{\text{rank}(\rho)} \sum_{i=1}^{\text{rank}(\rho)} |i\rangle\langle i| \ , \tag{A.105}$$

namely, it is a normalized projector.

## A.9 Inequalities of Entanglement of Purification

The entanglement of purification satisfies an inequality analogous to extensiveness,

$$S_R(A:B) \leq S_R(A:BC), \tag{A.106}$$

the analogue of which we do not yet know for reflected entropy. Let us assume $S_R^{(\text{eff})}$ satisfies this inequality. Let us consider the Cauchy slice $\Sigma_{A:B}$ on which $S_R(A:B)$ is optimized. We can divide the region $D(ABC \cup \text{Is}(ABC))$ into regions $A''$, $B''$ and $C''$ which minimize $S_R(AA'':BB''CC'')_{\Sigma_{A:B}}$ on $\Sigma_{A:B}$. On the other hand, by entanglement wedge nesting we know that $D(AB \cup \text{Is}(AB)) \subset D(ABC \cup \text{Is}(ABC))$. Thus, we have $D(AB \cup \text{Is}(AB)) \cap \Sigma_{A:B} \subset D(ABC \cup \text{Is}(ABC)) \cap \Sigma_{A:B}$. Given this, we can define $A' = A'' \cap D(AB \cup \text{Is}(AB)) \cap \Sigma_{A:B}$, and $B' = (B'' \cup C'') \cap D(ABC \cup \text{Is}(ABC)) \cap \Sigma_{A:B}$. $A'$ and $B'$ now cover the region of $\Sigma_{A:B}$ inside $D(AB) \cup \text{Is}(AB)$ and can be considered as candidates for the optimization of $S_R(A:B)$. Using this, we have

$$\begin{aligned} S_R(A:B) \quad &\leq S_R(AA'':BB'')_{\Sigma_{A:B}} \leq S_R(AA'':BB''CC'')_{\Sigma_{A:B}} \\ &\leq S_R(A:BC), \end{aligned} \tag{A.107}$$

where the first inequality follows since $S_R(A:B)$ is obtained by minimizing the hybrid entropy on $\Sigma_{A:B}$, the second inequality follows from the assumption that $S_R^{(\text{eff})}$ satisfies the required inequality, and the third inequality follows from maximization.

The entanglement of purification satisfies

$$I(A:B) + I(A:C) \leq S_R(A:BC), \tag{A.108}$$

which is known to be violated by reflected entropy, at least for classically correlated states. However, this violation is often invisible in holographic theories, which include a large amount of quantum entanglement. We can prove this inequality from our islands formula by assuming that the bulk matter satisfies this inequality, as well as the monogamy of mutual information:

$$I(A:B) + I(A:C) - I(A:BC) \leq 0, \tag{A.109}$$

which is known to be satisfied by holographic matter. Then by using the inequality $S_R(A:B) \geq I(A:B)$, we confirm that this inequality is indeed satisfied.

## A.10 Null Limit of the Kink Transform

In this appendix we apply the kink transform to a Cauchy slice $\Sigma$ that has null segments. In the null limit we express the kink transform in terms of the null initial value problem. We then show that this leads to a shock in the Weyl tensor for $d > 2$. From this Weyl shock we extract the boundary stress tensor shock. This serves a two-fold purpose. The first is that it provides direct intuition for how the kink transform modifies the geometry. The second is

that, as will be evident from the calculation below, the derivation of the stress tensor shock from the Weyl shock works even for wiggly cuts of the Rindler horizon on the boundary.[2]

Let $N_k$ be a null segment of $\Sigma$ in a neighborhood of $\mathcal{R}$ and let $k^a$ be the null generator of $N_k$. We now allow the boundary anchor of $\mathcal{R}$ to be an arbitrary cut $V_0(y)$ of the Rindler horizon, as considered in Section 9.2. Lastly, denote by $P^a_\mu$ and $P^i_\mu$ the projectors onto $N_k$ and cross-sections of $N_k$ (including the RT surface $\mathcal{R}$), respectively. We can compose these to obtain the projector $P^i_a$.

By Eq. (9.51), when $\Sigma$ is spacelike in a neighborhood of $\mathcal{R}$ the kink transform can be contracted as follows:

$$x^a(K_\Sigma)_{ab} \to x^a(K_\Sigma)_{ab} - \sinh(2\pi s) x_b \, \delta(\mathcal{R}) \ . \tag{A.110}$$

In the null limit both $x^a$ and $t^\mu$ approach $k^a$. Therefore, the quantity in the LHS of Eq. (A.110) has the following null limit:

$$x^a(K_\Sigma)_{ab} \overset{\text{null}}{\to} k^a \nabla_a k_b \ . \tag{A.111}$$

The transformation of Eq. (A.110) then becomes

$$\kappa \to \kappa - \sinh(2\pi s)\delta(\lambda) \ , \tag{A.112}$$

where $\lambda$ is a null parameter adapted to $k^a$ and $\kappa$ is the inaffinity defined by

$$k^b \nabla_b k^a = \kappa k^a \ . \tag{A.113}$$

We refer to this transformation as the *left stretch*, as it arises from a one-sided dilatation along $N_k$. This transformation was originally described in [239] in the context of black hole coarse-graining.

We now show that the left stretch generates a Weyl tensor shock at the RT surface. The shear of a null congruence is defined by

$$\sigma_{ij} = P^a_i P^b_j \nabla_{(a} k_{b)} \ . \tag{A.114}$$

It satisfies the evolution equation [277]

$$\mathcal{L}_k \sigma_{ij} = \kappa \sigma_{ij} + \sigma_i{}^k \sigma_{kj} - P^\mu_i P^\mu_j k^a k^b C_{a\mu b\nu} \ . \tag{A.115}$$

Now let $\lambda$ be a parametrization of $N_k$ adapted to $k^a$, with $\lambda = 0$ corresponding to $\mathcal{R}$. In terms of $\lambda$, the evolution equation can be written as

$$\partial_\lambda \sigma_{ij} = \kappa \sigma_{ij} + \sigma_i{}^k \sigma_{kj} - C_{\lambda i \lambda j} \ . \tag{A.116}$$

[2]The results of this section do not apply when $d = 2$, as the shear and the Weyl tensor vanish identically. However in $d = 2$ there is no distinction between flat and wiggly cuts on the boundary so we gain neither additional intuition nor generality compared with the analysis in Section 9.4.

Consider now the new spacetime $\mathcal{M}_s$ generated by the left stretch. As in Section 9.4, we denote quantities in $\mathcal{M}_s$ with tildes. We can then write the evolution equation in $\mathcal{M}_s$,

$$\partial_{\tilde{\lambda}}\tilde{\sigma}_{ij} = \tilde{\kappa}\tilde{\sigma}_{ij} + \tilde{\sigma}_i{}^k\tilde{\sigma}_{kj} - \tilde{C}_{\lambda i\lambda j} \ . \tag{A.117}$$

Since $k^a$ is tangent to $N_k$, and $(N_k)_s = N_k$ as submanifolds, we can identify $k^a$ with $\tilde{k}^a$. Thus we can use the same parameter $\lambda$ in both spacetimes. Since $\sigma_{ij}$ is intrinsic to $N_k$, we can identify $\sigma_{ij}$ and $\tilde{\sigma}_{ij}$ for the same reason. Comparing Eqs. (A.116) and (A.117), and inserting Eq. (A.112), we find that there is a Weyl shock

$$\tilde{C}_{\lambda i\lambda j} = C_{\lambda i\lambda j} - \sinh(2\pi s)\sigma_{ij}\delta(\lambda) \ . \tag{A.118}$$

We now show that the Weyl shock Eq. (A.118) reproduces the near boundary shock Eq. (9.44), but now for wiggly cuts of the Rindler horizon. To do this, we evaluate both $\sigma_{ij}$ and $C_{\lambda i\lambda j}$ in Fefferman-Graham coordinates to leading non-trivial order. The Fefferman-Graham coordinates for $\mathcal{M}$ and $\mathcal{M}_s$ are defined exactly as in Section 9.4, except we now use null coordinates $(u, v)$ and $(\tilde{u}, \tilde{v})$ on the boundary as defined in Section 9.2. To start with, we note that $k_a\partial_z\bar{X}^a = 0$ since $\partial_z\bar{X}^a$ is tangent to the RT surface. Evaluating this at leading order yields the relation

$$k_z = -dz^{d-3}\mathcal{U}_{(d)} + \mathcal{O}(z^{d-4}) \ . \tag{A.119}$$

We recall that

$$\mathcal{U}_{(d)} = -\frac{4G}{d}\frac{\delta S}{\delta V}\Big|_{V_0} \ . \tag{A.120}$$

Moreover, the projector is given by

$$P_i^\mu = \partial_i\bar{X}^\mu \ . \tag{A.121}$$

From this definition, one can check that

$$P_i^z = \delta_i^z + \mathcal{O}(z^{d-1}) \ , \tag{A.122}$$

$$P_i^A = \mathcal{O}(z^{d-1}) \ . \tag{A.123}$$

Furthermore,

$$\begin{aligned} &\nabla_z k_A, \ \nabla_A k_z \sim \mathcal{O}(z^{-1}) \ , \\ &\nabla_A k_B \sim \mathcal{O}(1) \ , \\ &\nabla_z k_z = -d(d-2)\mathcal{U}_{(d)}z^{d-4} + \mathcal{O}(z^{d-5}) \ , \end{aligned} \tag{A.124}$$

where we have used that $k^A \sim \mathcal{O}(1)$. Hence to leading order we simply have

$$\sigma_{ij} = -d(d-2)\mathcal{U}_{(d)}z^{d-4}\delta_i^z\delta_j^z + \mathcal{O}(z^{d-5}) \ . \tag{A.125}$$

Finally, a straightforward but tedious calculation of the Weyl tensor yields

$$\tilde{C}_{\tilde{v}i\tilde{v}j} = C_{vivj} - 8\pi G(d-2)\left(\langle\tilde{T}_{\tilde{v}\tilde{v}}\rangle - \langle T_{vv}\rangle\right)z^{d-4}\delta_i^z\delta_j^z\delta(\tilde{v} - V_0) + \mathcal{O}(z^{d-5}) \ , \tag{A.126}$$

where we have used that $\lambda \to v, \tilde{v}$ as $z \to 0$ in $\mathcal{M}, \mathcal{M}_s$ respectively. Putting this together yields the desired shock for wiggly cuts of the Rindler horizon.

# Bibliography


[1] S. W. Hawking. "Black hole explosions". In: *Nature* 248 (1974), pp. 30–31. DOI: 10.1038/248030a0.

[2] S. W. Hawking. "Particle Creation by Black Holes". In: *Commun. Math. Phys.* 43 (1975). [,167(1975)], pp. 199–220. DOI: 10.1007/BF02345020,10.1007/BF01608497.

[3] S.W. Hawking. "Breakdown of Predictability in Gravitational Collapse". In: *Phys. Rev. D* 14 (1976), pp. 2460–2473. DOI: 10.1103/PhysRevD.14.2460.

[4] Ahmed Almheiri et al. "Black Holes: Complementarity or Firewalls?" In: *JHEP* 02 (2013), p. 062. DOI: 10.1007/JHEP02(2013)062. arXiv: 1207.3123 [hep-th].

[5] Ahmed Almheiri et al. "An Apologia for Firewalls". In: *JHEP* 09 (2013), p. 018. DOI: 10.1007/JHEP09(2013)018. arXiv: 1304.6483 [hep-th].

[6] James M. Bardeen, B. Carter, and S.W. Hawking. "The Four laws of black hole mechanics". In: *Commun. Math. Phys.* 31 (1973), pp. 161–170. DOI: 10.1007/BF01645742.

[7] Jacob D. Bekenstein. "Black holes and entropy". In: *Phys. Rev. D* 7 (1973), pp. 2333–2346. DOI: 10.1103/PhysRevD.7.2333.

[8] Jacob D. Bekenstein. "A Universal Upper Bound on the Entropy to Energy Ratio for Bounded Systems". In: *Phys. Rev. D* 23 (1981), p. 287. DOI: 10.1103/PhysRevD.23.287.

[9] Raphael Bousso. "A Covariant entropy conjecture". In: *JHEP* 07 (1999), p. 004. DOI: 10.1088/1126-6708/1999/07/004. arXiv: hep-th/9905177.

[10] Raphael Bousso et al. "Proof of a Quantum Bousso Bound". In: *Phys. Rev. D* 90.4 (2014), p. 044002. DOI: 10.1103/PhysRevD.90.044002. arXiv: 1404.5635 [hep-th].

[11] Raphael Bousso et al. "Entropy on a null surface for interacting quantum field theories and the Bousso bound". In: *Phys. Rev. D* 91.8 (2015), p. 084030. DOI: 10.1103/PhysRevD.91.084030. arXiv: 1406.4545 [hep-th].

[12] Gerard 't Hooft. "Dimensional reduction in quantum gravity". In: *Conf. Proc. C* 930308 (1993), pp. 284–296. arXiv: gr-qc/9310026.

[13] Leonard Susskind. "The World as a hologram". In: *J. Math. Phys.* 36 (1995), pp. 6377–6396. DOI: 10.1063/1.531249. arXiv: hep-th/9409089.

[14] Juan Martin Maldacena. "The Large N limit of superconformal field theories and supergravity". In: *Int. J. Theor. Phys.* 38 (1999), pp. 1113–1133. DOI: 10.1023/A:1026654312961. arXiv: hep-th/9711200.

[15] Edward Witten. "Anti-de Sitter space and holography". In: *Adv. Theor. Math. Phys.* 2 (1998), pp. 253–291. DOI: 10.4310/ATMP.1998.v2.n2.a2. arXiv: hep-th/9802150.

[16] S.S. Gubser, Igor R. Klebanov, and Alexander M. Polyakov. "Gauge theory correlators from noncritical string theory". In: *Phys. Lett. B* 428 (1998), pp. 105–114. DOI: 10.1016/S0370-2693(98)00377-3. arXiv: hep-th/9802109.

[17] Leonard Susskind and Edward Witten. "The Holographic bound in anti-de Sitter space". In: (May 1998). arXiv: hep-th/9805114.

[18] Shinsei Ryu and Tadashi Takayanagi. "Holographic derivation of entanglement entropy from AdS/CFT". In: *Phys. Rev. Lett.* 96 (2006), p. 181602. DOI: 10.1103/PhysRevLett.96.181602. arXiv: hep-th/0603001 [hep-th].

[19] Shinsei Ryu and Tadashi Takayanagi. "Aspects of Holographic Entanglement Entropy". In: *JHEP* 08 (2006), p. 045. DOI: 10.1088/1126-6708/2006/08/045. arXiv: hep-th/0605073.

[20] Veronika E. Hubeny, Mukund Rangamani, and Tadashi Takayanagi. "A Covariant holographic entanglement entropy proposal". In: *JHEP* 07 (2007), p. 062. DOI: 10.1088/1126-6708/2007/07/062. arXiv: 0705.0016 [hep-th].

[21] Thomas Faulkner, Aitor Lewkowycz, and Juan Maldacena. "Quantum corrections to holographic entanglement entropy". In: *JHEP* 11 (2013), p. 074. DOI: 10.1007/JHEP11(2013)074. arXiv: 1307.2892 [hep-th].

[22] Netta Engelhardt and Aron C. Wall. "Quantum Extremal Surfaces: Holographic Entanglement Entropy beyond the Classical Regime". In: *JHEP* 01 (2015), p. 073. DOI: 10.1007/JHEP01(2015)073. arXiv: 1408.3203 [hep-th].

[23] Daniel L. Jafferis et al. "Relative entropy equals bulk relative entropy". In: *JHEP* 06 (2016), p. 004. DOI: 10.1007/JHEP06(2016)004. arXiv: 1512.06431 [hep-th].

[24] Xi Dong, Daniel Harlow, and Aron C. Wall. "Reconstruction of Bulk Operators within the Entanglement Wedge in Gauge-Gravity Duality". In: *Phys. Rev. Lett.* 117.2 (2016), p. 021601. DOI: 10.1103/PhysRevLett.117.021601. arXiv: 1601.05416 [hep-th].

[25] Patrick Hayden and Geoffrey Penington. "Learning the Alpha-bits of Black Holes". In: *JHEP* 12 (2019), p. 007. DOI: 10.1007/JHEP12(2019)007. arXiv: 1807.06041 [hep-th].

[26] Ahmed Almheiri, Xi Dong, and Daniel Harlow. "Bulk Locality and Quantum Error Correction in AdS/CFT". In: *JHEP* 04 (2015), p. 163. DOI: 10.1007/JHEP04(2015)163. arXiv: 1411.7041 [hep-th].

[27] Daniel Harlow. "The Ryu–Takayanagi Formula from Quantum Error Correction". In: *Commun. Math. Phys.* 354.3 (2017), pp. 865–912. DOI: 10.1007/s00220-017-2904-z. arXiv: 1607.03901 [hep-th].

[28] Fernando Pastawski et al. "Holographic quantum error-correcting codes: Toy models for the bulk/boundary correspondence". In: *JHEP* 06 (2015), p. 149. DOI: 10.1007/JHEP06(2015)149. arXiv: 1503.06237 [hep-th].

[29] Patrick Hayden et al. "Holographic duality from random tensor networks". In: *JHEP* 11 (2016), p. 009. DOI: 10.1007/JHEP11(2016)009. arXiv: 1601.01694 [hep-th].

[30] Raphael Bousso. "The Holographic principle". In: *Rev. Mod. Phys.* 74 (2002), pp. 825–874. DOI: 10.1103/RevModPhys.74.825. arXiv: hep-th/0203101.

[31] Yasunori Nomura et al. "Toward a Holographic Theory for General Spacetimes". In: *Phys. Rev.* D95.8 (2017), p. 086002. DOI: 10.1103/PhysRevD.95.086002. arXiv: 1611.02702 [hep-th].

[32] Yasunori Nomura, Pratik Rath, and Nico Salzetta. "Classical Spacetimes as Amplified Information in Holographic Quantum Theories". In: *Phys. Rev.* D97.10 (2018), p. 106025. DOI: 10.1103/PhysRevD.97.106025. arXiv: 1705.06283 [hep-th].

[33] Mark Van Raamsdonk. "Comments on quantum gravity and entanglement". In: (July 2009). arXiv: 0907.2939 [hep-th].

[34] Yasunori Nomura, Pratik Rath, and Nico Salzetta. "Spacetime from Unentanglement". In: *Phys. Rev.* D97.10 (2018), p. 106010. DOI: 10.1103/PhysRevD.97.106010. arXiv: 1711.05263 [hep-th].

[35] Yasunori Nomura, Pratik Rath, and Nico Salzetta. "Pulling the Boundary into the Bulk". In: *Phys. Rev.* D98.2 (2018), p. 026010. DOI: 10.1103/PhysRevD.98.026010. arXiv: 1805.00523 [hep-th].

[36] Aitor Lewkowycz and Juan Maldacena. "Generalized gravitational entropy". In: *JHEP* 08 (2013), p. 090. DOI: 10.1007/JHEP08(2013)090. arXiv: 1304.4926 [hep-th].

[37] Chitraang Murdia et al. "Comments on holographic entanglement entropy in $TT$ deformed conformal field theories". In: *Phys. Rev. D* 100.2 (2019), p. 026011. DOI: 10.1103/PhysRevD.100.026011. arXiv: 1904.04408 [hep-th].

[38] Chris Akers and Pratik Rath. "Holographic Renyi Entropy from Quantum Error Correction". In: *JHEP* 05 (2019), p. 052. DOI: 10.1007/JHEP05(2019)052. arXiv: 1811.05171 [hep-th].

[39] Shawn X. Cui et al. "Bit Threads and Holographic Monogamy". In: (2018). DOI: 10.1007/s00220-019-03510-8. arXiv: 1808.05234 [hep-th].

[40] Tadashi Takayanagi and Koji Umemoto. "Entanglement of purification through holographic duality". In: *Nature Phys.* 14.6 (2018), pp. 573–577. DOI: 10.1038/s41567-018-0075-2. arXiv: 1708.09393 [hep-th].

[41] Phuc Nguyen et al. "Entanglement of purification: from spin chains to holography". In: *JHEP* 01 (2018), p. 098. DOI: 10.1007/JHEP01(2018)098. arXiv: 1709.07424 [hep-th].

[42] Souvik Dutta and Thomas Faulkner. "A canonical purification for the entanglement wedge cross-section". In: (May 2019). arXiv: 1905.00577 [hep-th].

[43] Chris Akers and Pratik Rath. "Entanglement Wedge Cross Sections Require Tripartite Entanglement". In: (2019). arXiv: 1911.07852 [hep-th].

[44] Geoffrey Penington. "Entanglement Wedge Reconstruction and the Information Paradox". In: (2019). arXiv: 1905.08255 [hep-th].

[45] Geoff Penington et al. "Replica wormholes and the black hole interior". In: (Nov. 2019). arXiv: 1911.11977 [hep-th].

[46] Ahmed Almheiri et al. "The Page curve of Hawking radiation from semiclassical geometry". In: (2019). arXiv: 1908.10996 [hep-th].

[47] Ahmed Almheiri et al. "The entropy of bulk quantum fields and the entanglement wedge of an evaporating black hole". In: (2019). arXiv: 1905.08762 [hep-th].

[48] Ahmed Almheiri et al. "Replica Wormholes and the Entropy of Hawking Radiation". In: (2019). arXiv: 1911.12333 [hep-th].

[49] Ahmed Almheiri, Raghu Mahajan, and Juan Maldacena. "Islands outside the horizon". In: (2019). arXiv: 1910.11077 [hep-th].

[50] Ahmed Almheiri et al. "The entropy of Hawking radiation". In: (June 2020). arXiv: 2006.06872 [hep-th].

[51] Venkatesa Chandrasekaran, Masamichi Miyaji, and Pratik Rath. "Islands for Reflected Entropy". In: (June 2020). arXiv: 2006.10754 [hep-th].

[52] Raphael Bousso et al. "Gravity Dual of Connes Cocycle Flow". In: (July 2020). arXiv: 2007.00230 [hep-th].

[53] Harold Ollivier, David Poulin, and Wojciech H Zurek. "Objective properties from subjective quantum states: Environment as a witness". In: *Physical review letters* 93.22 (2004), p. 220401.

[54] Robin Blume-Kohout and Wojciech H Zurek. "Quantum Darwinism: Entanglement, branches, and the emergent classicality of redundantly stored quantum information". In: *Physical Review A* 73.6 (2006), p. 062310.

[55] Yasunori Nomura. "Quantum Mechanics, Spacetime Locality, and Gravity". In: *Found. Phys.* 43 (2013), pp. 978–1007. DOI: 10.1007/s10701-013-9729-1. arXiv: 1110.4630 [hep-th].

[56] Fabio Sanches and Sean J. Weinberg. "Holographic entanglement entropy conjecture for general spacetimes". In: *Phys. Rev.* D94.8 (2016), p. 084034. DOI: 10.1103/PhysRevD.94.084034. arXiv: 1603.05250 [hep-th].

[57] Masamichi Miyaji and Tadashi Takayanagi. "Surface/State Correspondence as a Generalized Holography". In: *PTEP* 2015.7 (2015), 073B03. DOI: 10.1093/ptep/ptv089. arXiv: 1503.03542 [hep-th].

[58] Fabio Sanches and Sean J. Weinberg. "Boundary dual of bulk local operators". In: *Phys. Rev. D* 96.2 (2017), p. 026004. DOI: 10.1103/PhysRevD.96.026004. arXiv: 1703.07780 [hep-th].

[59] Raphael Bousso and Netta Engelhardt. "New Area Law in General Relativity". In: *Phys. Rev. Lett.* 115.8 (2015), p. 081301. DOI: 10.1103/PhysRevLett.115.081301. arXiv: 1504.07627 [hep-th].

[60] Aron C. Wall. "Maximin Surfaces, and the Strong Subadditivity of the Covariant Holographic Entanglement Entropy". In: *Class. Quant. Grav.* 31.22 (2014), p. 225007. DOI: 10.1088/0264-9381/31/22/225007. arXiv: 1211.3494 [hep-th].

[61] Matthew Headrick et al. "Causality & holographic entanglement entropy". In: *JHEP* 12 (2014), p. 162. DOI: 10.1007/JHEP12(2014)162. arXiv: 1408.6300 [hep-th].

[62] Netta Engelhardt and Aron C. Wall. "Extremal Surface Barriers". In: *JHEP* 03 (2014), p. 068. DOI: 10.1007/JHEP03(2014)068. arXiv: 1312.3699 [hep-th].

[63] Leonard Susskind, Larus Thorlacius, and John Uglum. "The Stretched horizon and black hole complementarity". In: *Phys. Rev. D* 48 (1993), pp. 3743–3761. DOI: 10.1103/PhysRevD.48.3743. arXiv: hep-th/9306069.

[64] Donald Marolf and Joseph Polchinski. "Gauge/Gravity Duality and the Black Hole Interior". In: *Phys. Rev. Lett.* 111 (2013), p. 171301. DOI: 10.1103/PhysRevLett.111.171301. arXiv: 1307.4706 [hep-th].

[65] Kyriakos Papadodimas and Suvrat Raju. "State-Dependent Bulk-Boundary Maps and Black Hole Complementarity". In: *Phys. Rev. D* 89.8 (2014), p. 086010. DOI: 10.1103/PhysRevD.89.086010. arXiv: 1310.6335 [hep-th].

[66] Kyriakos Papadodimas and Suvrat Raju. "Remarks on the necessity and implications of state-dependence in the black hole interior". In: *Phys. Rev.* D93.8 (2016), p. 084049. DOI: 10.1103/PhysRevD.93.084049. arXiv: 1503.08825 [hep-th].

[67] Raphael Bousso. "Holography in general space-times". In: *JHEP* 06 (1999), p. 028. DOI: 10.1088/1126-6708/1999/06/028. arXiv: hep-th/9906022.

[68] Yasunori Nomura. "Physical Theories, Eternal Inflation, and Quantum Universe". In: *JHEP* 11 (2011), p. 063. DOI: 10.1007/JHEP11(2011)063. arXiv: 1104.2324 [hep-th].

[69] Juan Martin Maldacena. "Eternal black holes in anti-de Sitter". In: *JHEP* 04 (2003), p. 021. DOI: 10.1088/1126-6708/2003/04/021. arXiv: hep-th/0106112.

[70] W.K. Wootters and W.H. Zurek. "A single quantum cannot be cloned". In: *Nature* 299 (1982), pp. 802–803. DOI: 10.1038/299802a0.

[71] Laurence G. Yaffe. "Large n Limits as Classical Mechanics". In: *Rev. Mod. Phys.* 54 (1982), p. 407. DOI: 10.1103/RevModPhys.54.407.

[72] Brian Swingle. "Entanglement Renormalization and Holography". In: *Phys. Rev.* D86 (2012), p. 065007. DOI: 10.1103/PhysRevD.86.065007. arXiv: 0905.1317 [cond-mat.str-el].

[73] Yasunori Nomura et al. "Spacetime Equals Entanglement". In: *Phys. Lett. B* 763 (2016), pp. 370–374. DOI: 10.1016/j.physletb.2016.10.045. arXiv: 1607.02508 [hep-th].

[74] Daniel Louis Jafferis. "Bulk reconstruction and the Hartle-Hawking wavefunction". In: (2017). arXiv: 1703.01519 [hep-th].

[75] Xiao-Liang Qi, Zhao Yang, and Yi-Zhuang You. "Holographic coherent states from random tensor networks". In: *JHEP* 08 (2017), p. 060. DOI: 10.1007/JHEP08(2017)060. arXiv: 1703.06533 [hep-th].

[76] Yasunori Nomura, Fabio Sanches, and Sean J. Weinberg. "Black Hole Interior in Quantum Gravity". In: *Phys. Rev. Lett.* 114 (2015), p. 201301. DOI: 10.1103/PhysRevLett.114.201301. arXiv: 1412.7539 [hep-th].

[77] Yasunori Nomura, Fabio Sanches, and Sean J. Weinberg. "Relativeness in Quantum Gravity: Limitations and Frame Dependence of Semiclassical Descriptions". In: *JHEP* 04 (2015), p. 158. DOI: 10.1007/JHEP04(2015)158. arXiv: 1412.7538 [hep-th].

[78] Yasunori Nomura and Nico Salzetta. "Why Firewalls Need Not Exist". In: *Phys. Lett. B* 761 (2016), pp. 62–69. DOI: 10.1016/j.physletb.2016.08.003. arXiv: 1602.07673 [hep-th].

[79] Yasunori Nomura. "A Note on Boltzmann Brains". In: *Phys. Lett. B* 749 (2015), pp. 514–518. DOI: 10.1016/j.physletb.2015.08.029. arXiv: 1502.05401 [hep-th].

[80] Kimberly K. Boddy, Sean M. Carroll, and Jason Pollack. "De Sitter Space Without Dynamical Quantum Fluctuations". In: *Found. Phys.* 46.6 (2016), pp. 702–735. DOI: 10.1007/s10701-016-9996-8. arXiv: 1405.0298 [hep-th].

[81] Matthew Headrick and Tadashi Takayanagi. "A Holographic proof of the strong subadditivity of entanglement entropy". In: *Phys. Rev.* D76 (2007), p. 106013. DOI: 10.1103/PhysRevD.76.106013. arXiv: 0704.3719 [hep-th].

[82] Daniel Kabat and Gilad Lifschytz. "Local bulk physics from intersecting modular Hamiltonians". In: *JHEP* 06 (2017), p. 120. DOI: 10.1007/JHEP06(2017)120. arXiv: 1703.06523 [hep-th].

[83] Fabio Sanches and Sean J. Weinberg. "Refinement of the Bousso-Engelhardt Area Law". In: *Phys. Rev. D* 94.2 (2016), p. 021502. DOI: 10.1103/PhysRevD.94.021502. arXiv: 1604.04919 [hep-th].

[84] Raphael Bousso and Netta Engelhardt. "Proof of a New Area Law in General Relativity". In: *Phys. Rev. D* 92.4 (2015), p. 044031. DOI: 10.1103/PhysRevD.92.044031. arXiv: 1504.07660 [gr-qc].

[85] Vijay Balasubramanian et al. "Entwinement and the emergence of spacetime". In: *JHEP* 01 (2015), p. 048. DOI: 10.1007/JHEP01(2015)048. arXiv: 1406.5859 [hep-th].

[86] Ben Freivogel et al. "Casting Shadows on Holographic Reconstruction". In: *Phys. Rev. D* 91.8 (2015), p. 086013. DOI: 10.1103/PhysRevD.91.086013. arXiv: 1412.5175 [hep-th].

[87] Veronika E. Hubeny. "Extremal surfaces as bulk probes in AdS/CFT". In: *JHEP* 07 (2012), p. 093. DOI: 10.1007/JHEP07(2012)093. arXiv: 1203.1044 [hep-th].

[88] Veronika E. Hubeny and Henry Maxfield. "Holographic probes of collapsing black holes". In: *JHEP* 03 (2014), p. 097. DOI: 10.1007/JHEP03(2014)097. arXiv: 1312.6887 [hep-th].

[89] Suvrat Raju. "Smooth Causal Patches for AdS Black Holes". In: *Phys. Rev. D* 95.12 (2017), p. 126002. DOI: 10.1103/PhysRevD.95.126002. arXiv: 1604.03095 [hep-th].

[90] G.W. Gibbons and S.W. Hawking. "Cosmological Event Horizons, Thermodynamics, and Particle Creation". In: *Phys. Rev. D* 15 (1977), pp. 2738–2751. DOI: 10.1103/PhysRevD.15.2738.

[91] Don N. Page. "Average entropy of a subsystem". In: *Phys. Rev. Lett.* 71 (1993), pp. 1291–1294. DOI: 10.1103/PhysRevLett.71.1291. arXiv: gr-qc/9305007 [gr-qc].

[92] Yasunori Nomura and Sean J. Weinberg. "Black Holes, Entropies, and Semiclassical Spacetime in Quantum Gravity". In: *JHEP* 10 (2014), p. 185. DOI: 10.1007/JHEP10(2014)185. arXiv: 1406.1505 [hep-th].

[93] Ning Bao and Aidan Chatwin-Davies. "Puzzles and pitfalls involving Haar-typicality in holography". In: *SciPost Phys.* 4.6 (2018), p. 033. DOI: 10.21468/SciPostPhys.4.6.033. arXiv: 1708.08561 [hep-th].

[94] Yuya Kusuki, Tadashi Takayanagi, and Koji Umemoto. "Holographic Entanglement Entropy on Generic Time Slices". In: *JHEP* 06 (2017), p. 021. DOI: 10.1007/JHEP06(2017)021. arXiv: 1703.00915 [hep-th].

[95] Lisa Randall and Raman Sundrum. "An Alternative to compactification". In: *Phys. Rev. Lett.* 83 (1999), pp. 4690–4693. DOI: 10.1103/PhysRevLett.83.4690. arXiv: hep-th/9906064.

[96] Juan Maldacena, Stephen H. Shenker, and Douglas Stanford. "A bound on chaos". In: *JHEP* 08 (2016), p. 106. DOI: 10.1007/JHEP08(2016)106. arXiv: 1503.01409 [hep-th].

[97] Mark Srednicki. "Chaos and quantum thermalization". In: *Physical Review E* 50.2 (1994), p. 888.

[98] Rahul Nandkishore and David A. Huse. "Many body localization and thermalization in quantum statistical mechanics". In: *Ann. Rev. Condensed Matter Phys.* 6 (2015), pp. 15–38. DOI: 10.1146/annurev-conmatphys-031214-014726. arXiv: 1404.0686 [cond-mat.stat-mech].

[99] M. Reza Mohammadi Mozaffar and Ali Mollabashi. "Entanglement in Lifshitz-type Quantum Field Theories". In: *JHEP* 07 (2017), p. 120. DOI: 10.1007/JHEP07(2017)120. arXiv: 1705.00483 [hep-th].

[100] Jose L.F. Barbon and Carlos A. Fuertes. "Holographic entanglement entropy probes (non)locality". In: *JHEP* 04 (2008), p. 096. DOI: 10.1088/1126-6708/2008/04/096. arXiv: 0803.1928 [hep-th].

[101] Willy Fischler, Arnab Kundu, and Sandipan Kundu. "Holographic Entanglement in a Noncommutative Gauge Theory". In: *JHEP* 01 (2014), p. 137. DOI: 10.1007/JHEP01(2014)137. arXiv: 1307.2932 [hep-th].

[102] Joanna L. Karczmarek and Charles Rabideau. "Holographic entanglement entropy in nonlocal theories". In: *JHEP* 10 (2013), p. 078. DOI: 10.1007/JHEP10(2013)078. arXiv: 1307.3517 [hep-th].

[103] Noburo Shiba and Tadashi Takayanagi. "Volume Law for the Entanglement Entropy in Non-local QFTs". In: *JHEP* 02 (2014), p. 033. DOI: 10.1007/JHEP02(2014)033. arXiv: 1311.1643 [hep-th].

[104] Wenbo Fu and Subir Sachdev. "Numerical study of fermion and boson models with infinite-range random interactions". In: *Phys. Rev. B* 94.3 (2016), p. 035135. DOI: 10.1103/PhysRevB.94.035135. arXiv: 1603.05246 [cond-mat.str-el].

[105] Chunxiao Liu, Xiao Chen, and Leon Balents. "Quantum Entanglement of the Sachdev-Ye-Kitaev Models". In: *Phys. Rev. B* 97.24 (2018), p. 245126. DOI: 10.1103/PhysRevB.97.245126. arXiv: 1709.06259 [cond-mat.str-el].

[106] Subir Sachdev and Jinwu Ye. "Gapless spin fluid ground state in a random, quantum Heisenberg magnet". In: *Phys. Rev. Lett.* 70 (1993), p. 3339. DOI: 10.1103/PhysRevLett.70.3339. arXiv: cond-mat/9212030 [cond-mat].

[107] Alexei Kitaev. "A simple model of quantum holography". In: *In KITP strings seminar* 12 (2015).

[108] Juan Maldacena and Douglas Stanford. "Remarks on the Sachdev-Ye-Kitaev model". In: *Phys. Rev.* D94.10 (2016), p. 106002. DOI: 10.1103/PhysRevD.94.106002. arXiv: 1604.07818 [hep-th].

[109] Yichen Huang and Yingfei Gu. "Eigenstate entanglement in the Sachdev-Ye-Kitaev model". In: *Phys. Rev. D* 100.4 (Sept. 2017), p. 041901. DOI: 10.1103/PhysRevD.100.041901. arXiv: 1709.09160 [hep-th].

[110] Ahmed Almheiri, Xi Dong, and Brian Swingle. "Linearity of Holographic Entanglement Entropy". In: *JHEP* 02 (2017), p. 074. DOI: 10.1007/JHEP02(2017)074. arXiv: 1606.04537 [hep-th].

[111] Sheldon Goldstein et al. "Canonical typicality". In: *Physical review letters* 96.5 (2006), p. 050403.

[112] Sandu Popescu, Anthony J Short, and Andreas Winter. "Entanglement and the foundations of statistical mechanics". In: *Nature Physics* 2.11 (2006), pp. 754–758.

[113] Aron C. Wall. "A proof of the generalized second law for rapidly changing fields and arbitrary horizon slices". In: *Phys. Rev. D* 85 (2012). [Erratum: Phys.Rev.D 87, 069904 (2013)], p. 104049. DOI: 10.1103/PhysRevD.85.104049. arXiv: 1105.3445 [gr-qc].

[114] Ning Bao et al. "The Holographic Entropy Cone". In: *JHEP* 09 (2015), p. 130. DOI: 10.1007/JHEP09(2015)130. arXiv: 1505.07839 [hep-th].

[115] Thomas Faulkner and Aitor Lewkowycz. "Bulk locality from modular flow". In: *JHEP* 07 (2017), p. 151. DOI: 10.1007/JHEP07(2017)151. arXiv: 1704.05464 [hep-th].

[116] Jordan Cotler et al. "Entanglement Wedge Reconstruction via Universal Recovery Channels". In: *Phys. Rev. X* 9.3 (2019), p. 031011. DOI: 10.1103/PhysRevX.9.031011. arXiv: 1704.05839 [hep-th].

[117] Sean M. Carroll and Aidan Chatwin-Davies. "Cosmic Equilibration: A Holographic No-Hair Theorem from the Generalized Second Law". In: *Phys. Rev. D* 97.4 (2018), p. 046012. DOI: 10.1103/PhysRevD.97.046012. arXiv: 1703.09241 [hep-th].

[118] Vijay Balasubramanian and Per Kraus. "Space-time and the holographic renormalization group". In: *Phys. Rev. Lett.* 83 (1999), pp. 3605–3608. DOI: 10.1103/PhysRevLett.83.3605. arXiv: hep-th/9903190.

[119] Yasunori Nomura and Nico Salzetta. "Butterfly Velocities for Holographic Theories of General Spacetimes". In: *JHEP* 10 (2017), p. 187. DOI: 10.1007/JHEP10(2017)187. arXiv: 1708.04237 [hep-th].

[120] Massimiliano Rota and Sean J. Weinberg. "New constraints for holographic entropy from maximin: A no-go theorem". In: *Phys. Rev. D* 97.8 (2018), p. 086013. DOI: 10.1103/PhysRevD.97.086013. arXiv: 1712.10004 [hep-th].

[121] Brian Swingle. "Constructing holographic spacetimes using entanglement renormalization". In: (Sept. 2012). arXiv: 1209.3304 [hep-th].

[122] Jutho Haegeman et al. "Entanglement Renormalization for Quantum Fields in Real Space". In: *Phys. Rev. Lett.* 110.10 (2013), p. 100402. DOI: 10.1103/PhysRevLett.110.100402. arXiv: 1102.5524 [hep-th].

[123] Raphael Bousso and Netta Engelhardt. "Generalized Second Law for Cosmology". In: *Phys. Rev. D* 93.2 (2016), p. 024025. DOI: 10.1103/PhysRevD.93.024025. arXiv: 1510.02099 [hep-th].

[124] Alex Hamilton et al. "Holographic representation of local bulk operators". In: *Phys. Rev. D* 74 (2006), p. 066009. DOI: 10.1103/PhysRevD.74.066009. arXiv: hep-th/0606141.

[125] Alex Hamilton et al. "Local bulk operators in AdS/CFT: A Holographic description of the black hole interior". In: *Phys. Rev. D* 75 (2007). [Erratum: Phys.Rev.D 75, 129902 (2007)], p. 106001. DOI: 10.1103/PhysRevD.75.106001. arXiv: hep-th/0612053.

[126] Idse Heemskerk et al. "Bulk and Transhorizon Measurements in AdS/CFT". In: *JHEP* 10 (2012), p. 165. DOI: 10.1007/JHEP10(2012)165. arXiv: 1201.3664 [hep-th].

[127] Raphael Bousso, Stefan Leichenauer, and Vladimir Rosenhaus. "Light-sheets and AdS/CFT". In: *Phys. Rev. D* 86 (2012), p. 046009. DOI: 10.1103/PhysRevD.86.046009. arXiv: 1203.6619 [hep-th].

[128] Bartlomiej Czech et al. "The Gravity Dual of a Density Matrix". In: *Class. Quant. Grav.* 29 (2012), p. 155009. DOI: 10.1088/0264-9381/29/15/155009. arXiv: 1204.1330 [hep-th].

[129] Emil T. Akhmedov. "A Remark on the AdS / CFT correspondence and the renormalization group flow". In: *Phys. Lett. B* 442 (1998), pp. 152–158. DOI: 10.1016/S0370-2693(98)01270-2. arXiv: hep-th/9806217.

[130] Enrique Alvarez and Cesar Gomez. "Geometric holography, the renormalization group and the c theorem". In: *Nucl. Phys. B* 541 (1999), pp. 441–460. DOI: 10.1016/S0550-3213(98)00752-4. arXiv: hep-th/9807226.

[131] Kostas Skenderis and Paul K. Townsend. "Gravitational stability and renormalization group flow". In: *Phys. Lett. B* 468 (1999), pp. 46–51. DOI: 10.1016/S0370-2693(99)01212-5. arXiv: hep-th/9909070.

[132] Jan de Boer, Erik P. Verlinde, and Herman L. Verlinde. "On the holographic renormalization group". In: *JHEP* 08 (2000), p. 003. DOI: 10.1088/1126-6708/2000/08/003. arXiv: hep-th/9912012.

[133] Lars Andersson and Jan Metzger. "The Area of horizons and the trapped region". In: *Commun. Math. Phys.* 290 (2009), pp. 941–972. DOI: 10.1007/s00220-008-0723-y. arXiv: 0708.4252 [gr-qc].

[134] Marc Mars. "Stability of Marginally Outer Trapped Surfaces and Geometric Inequalities". In: *Fundam. Theor. Phys.* 177 (2014). Ed. by Jiri Bicak and Tomas Ledvinka, pp. 191–208. DOI: 10.1007/978-3-319-06349-2_8.

[135] Ricardo Espíndola, Alberto Guijosa, and Juan F. Pedraza. "Entanglement Wedge Reconstruction and Entanglement of Purification". In: *Eur. Phys. J. C* 78.8 (2018), p. 646. DOI: 10.1140/epjc/s10052-018-6140-2. arXiv: 1804.05855 [hep-th].

[136] Ning Bao and Illan F. Halpern. "Holographic Inequalities and Entanglement of Purification". In: *JHEP* 03 (2018), p. 006. DOI: 10.1007/JHEP03(2018)006. arXiv: 1710.07643 [hep-th].

[137] Ning Bao. personal communication.

[138] Charles Fefferman and C. Robin Graham. "Conformal invariants". en. In: *Élie Cartan et les mathématiques d'aujourd'hui - Lyon, 25-29 juin 1984*. Astérisque S131. Société mathématique de France, 1985, pp. 95–116. URL: http://www.numdam.org/item/AST_1985__S131__95_0.

[139] H. Bondi, M.G.J. van der Burg, and A.W.K. Metzner. "Gravitational waves in general relativity. 7. Waves from axisymmetric isolated systems". In: *Proc. Roy. Soc. Lond. A* A269 (1962), pp. 21–52. DOI: 10.1098/rspa.1962.0161.

[140] R.K. Sachs. "Gravitational waves in general relativity. 8. Waves in asymptotically flat space-times". In: *Proc. Roy. Soc. Lond. A* A270 (1962), pp. 103–126. DOI: 10.1098/rspa.1962.0206.

[141] Masahiro Nozaki, Shinsei Ryu, and Tadashi Takayanagi. "Holographic Geometry of Entanglement Renormalization in Quantum Field Theories". In: *JHEP* 10 (2012), p. 193. DOI: 10.1007/JHEP10(2012)193. arXiv: 1208.3469 [hep-th].

[142] G. Vidal. "Entanglement Renormalization". In: *Phys. Rev. Lett.* 99.22 (2007), p. 220405. DOI: 10.1103/PhysRevLett.99.220405. arXiv: cond-mat/0512165.

[143] Yasunori Nomura and Jaime Varela. "A Note on (No) Firewalls: The Entropy Argument". In: *JHEP* 07 (2013), p. 124. DOI: 10.1007/JHEP07(2013)124. arXiv: 1211.7033 [hep-th].

[144] Ning Bao et al. "Branches of the Black Hole Wave Function Need Not Contain Firewalls". In: *Phys. Rev. D* 97.12 (2018), p. 126014. DOI: 10.1103/PhysRevD.97.126014. arXiv: 1712.04955 [hep-th].

[145] Lauren McGough, Márk Mezei, and Herman Verlinde. "Moving the CFT into the bulk with $T\overline{T}$". In: *JHEP* 04 (2018), p. 010. DOI: 10.1007/JHEP04(2018)010. arXiv: 1611.03470 [hep-th].

[146] Marika Taylor. "TT deformations in general dimensions". In: (May 2018). arXiv: 1805.10287 [hep-th].

[147] Thomas Hartman et al. "Holography at finite cutoff with a $T^2$ deformation". In: *JHEP* 03 (2019), p. 004. DOI: 10.1007/JHEP03(2019)004. arXiv: 1807.11401 [hep-th].

[148] Soumangsu Chakraborty et al. "Entanglement beyond AdS". In: *Nucl. Phys. B* 935 (2018), pp. 290–309. DOI: 10.1016/j.nuclphysb.2018.08.011. arXiv: 1805.06286 [hep-th].

[149] William Donnelly and Vasudev Shyam. "Entanglement entropy and $T\overline{T}$ deformation". In: *Phys. Rev. Lett.* 121 (2018), p. 131602. DOI: 10.1103/PhysRevLett.121.131602. arXiv: 1806.07444 [hep-th].

[150] Bin Chen, Lin Chen, and Peng-Xiang Hao. "Entanglement Entropy in $T\overline{T}$-Deformed CFT". In: (2018). arXiv: 1807.08293 [hep-th].

[151] Victor Gorbenko, Eva Silverstein, and Gonzalo Torroba. "dS/dS and $T\overline{T}$". In: *JHEP* 03 (2019), p. 085. DOI: 10.1007/JHEP03(2019)085. arXiv: 1811.07965 [hep-th].

[152] Chanyong Park. "Holographic Entanglement Entropy in Cutoff AdS". In: *Int. J. Mod. Phys. A* 33.36 (2019), p. 1850226. DOI: 10.1142/S0217751X18502263. arXiv: 1812.00545 [hep-th].

[153] Pawel Caputa, Shouvik Datta, and Vasudev Shyam. "Sphere partition functions & cut-off AdS". In: *JHEP* 05 (2019), p. 112. DOI: 10.1007/JHEP05(2019)112. arXiv: 1902.10893 [hep-th].

[154] Aritra Banerjee, Arpan Bhattacharyya, and Soumangsu Chakraborty. "Entanglement Entropy for $TT$ deformed CFT in general dimensions". In: *Nucl. Phys. B* 948 (2019), p. 114775. DOI: 10.1016/j.nuclphysb.2019.114775. arXiv: 1904.00716 [hep-th].

[155] Z Komargodski. "Aspects of renormalization group flows". In: *Lecture Notes of the Les Houches Summer School, Session XCVII, Oxford university Press* (2015). p. 255.

[156] Ling-Yan Hung, Robert C. Myers, and Michael Smolkin. "Some Calculable Contributions to Holographic Entanglement Entropy". In: *JHEP* 08 (2011), p. 039. DOI: 10.1007/JHEP08(2011)039. arXiv: 1105.6055 [hep-th].

[157] Hong Liu and Mark Mezei. "A Refinement of entanglement entropy and the number of degrees of freedom". In: *JHEP* 04 (2013), p. 162. DOI: 10.1007/JHEP04(2013)162. arXiv: 1202.2070 [hep-th].

[158] Marika Taylor and William Woodhead. "Renormalized entanglement entropy". In: *JHEP* 08 (2016), p. 165. DOI: 10.1007/JHEP08(2016)165. arXiv: 1604.06808 [hep-th].

[159] J.David Brown and Jr. York James W. "Quasilocal energy and conserved charges derived from the gravitational action". In: *Phys. Rev. D* 47 (1993), pp. 1407–1419. DOI: 10.1103/PhysRevD.47.1407. arXiv: gr-qc/9209012.

[160] Vijay Balasubramanian and Per Kraus. "A Stress tensor for Anti-de Sitter gravity". In: *Commun. Math. Phys.* 208 (1999), pp. 413–428. DOI: 10.1007/s002200050764. arXiv: hep-th/9902121.

[161] Kostas Skenderis. "Lecture notes on holographic renormalization". In: *Class. Quant. Grav.* 19 (2002). Ed. by B. de Wit and S. Vandoren, pp. 5849–5876. DOI: 10.1088/0264-9381/19/22/306. arXiv: hep-th/0209067.

[162] Joan Camps and William R. Kelly. "Generalized gravitational entropy without replica symmetry". In: *JHEP* 03 (2015), p. 061. DOI: 10.1007/JHEP03(2015)061. arXiv: 1412.4093 [hep-th].

[163] Xi Dong. "The Gravity Dual of Renyi Entropy". In: *Nature Commun.* 7 (2016), p. 12472. DOI: 10.1038/ncomms12472. arXiv: 1601.06788 [hep-th].

[164] Xi Dong. "Holographic Entanglement Entropy for General Higher Derivative Gravity". In: *JHEP* 01 (2014), p. 044. DOI: 10.1007/JHEP01(2014)044. arXiv: 1310.5713 [hep-th].

[165] Ahmed Almheiri. "Holographic Quantum Error Correction and the Projected Black Hole Interior". In: (2018). arXiv: 1810.02055 [hep-th].

[166] Xi Dong, Daniel Harlow, and Donald Marolf. "Flat entanglement spectra in fixed-area states of quantum gravity". In: *JHEP* 10 (2019), p. 240. DOI: 10.1007/JHEP10(2019)240. arXiv: 1811.05382 [hep-th].

[167] Daniel L. Jafferis and S. Josephine Suh. "The Gravity Duals of Modular Hamiltonians". In: *JHEP* 09 (2016), p. 068. DOI: 10.1007/JHEP09(2016)068. arXiv: 1412.8465 [hep-th].

[168] Xi Dong and Aitor Lewkowycz. "Entropy, Extremality, Euclidean Variations, and the Equations of Motion". In: *JHEP* 01 (2018), p. 081. DOI: 10.1007/JHEP01(2018)081. arXiv: 1705.08453 [hep-th].

[169] William Donnelly and Laurent Freidel. "Local subsystems in gauge theory and gravity". In: *JHEP* 09 (2016), p. 102. DOI: 10.1007/JHEP09(2016)102. arXiv: 1601.04744 [hep-th].

[170] William Donnelly. "Decomposition of entanglement entropy in lattice gauge theory". In: *Phys. Rev.* D85 (2012), p. 085004. DOI: 10.1103/PhysRevD.85.085004. arXiv: 1109.0036 [hep-th].

[171] Horacio Casini, Marina Huerta, and Jose Alejandro Rosabal. "Remarks on entanglement entropy for gauge fields". In: *Phys. Rev.* D89.8 (2014), p. 085012. DOI: 10.1103/PhysRevD.89.085012. arXiv: 1312.1183 [hep-th].

[172] William Donnelly. "Entanglement entropy and nonabelian gauge symmetry". In: *Class. Quant. Grav.* 31.21 (2014), p. 214003. DOI: 10.1088/0264-9381/31/21/214003. arXiv: 1406.7304 [hep-th].

[173] William Donnelly et al. "Living on the Edge: A Toy Model for Holographic Reconstruction of Algebras with Centers". In: *JHEP* 04 (2017), p. 093. DOI: 10.1007/JHEP04(2017)093. arXiv: 1611.05841 [hep-th].

[174] William Donnelly and Aron C. Wall. "Entanglement entropy of electromagnetic edge modes". In: *Phys. Rev. Lett.* 114.11 (2015), p. 111603. DOI: 10.1103/PhysRevLett.114.111603. arXiv: 1412.1895 [hep-th].

[175] William Donnelly and Aron C. Wall. "Geometric entropy and edge modes of the electromagnetic field". In: *Phys. Rev.* D94.10 (2016), p. 104053. DOI: 10.1103/PhysRevD.94.104053. arXiv: 1506.05792 [hep-th].

[176] Jennifer Lin. "Ryu-Takayanagi Area as an Entanglement Edge Term". In: (2017). arXiv: 1704.07763 [hep-th].

[177] J. B. Hartle and S. W. Hawking. "Wave Function of the Universe". In: *Phys. Rev.* D28 (1983). [Adv. Ser. Astrophys. Cosmol.3,174(1987)], pp. 2960–2975. DOI: 10.1103/PhysRevD.28.2960.

[178] Muxin Han and Shilin Huang. "Discrete gravity on random tensor network and holographic Rényi entropy". In: *JHEP* 11 (2017), p. 148. DOI: 10.1007/JHEP11(2017)148. arXiv: 1705.01964 [hep-th].

[179] Daniel Harlow. "Wormholes, Emergent Gauge Fields, and the Weak Gravity Conjecture". In: *JHEP* 01 (2016), p. 122. DOI: 10.1007/JHEP01(2016)122. arXiv: 1510.07911 [hep-th].

[180] Antony J. Speranza. "Local phase space and edge modes for diffeomorphism-invariant theories". In: *JHEP* 02 (2018), p. 021. DOI: 10.1007/JHEP02(2018)021. arXiv: 1706.05061 [hep-th].

[181] Netta Engelhardt and Aron C. Wall. "Decoding the Apparent Horizon: Coarse-Grained Holographic Entropy". In: *Phys. Rev. Lett.* 121.21 (2018), p. 211301. DOI: 10.1103/PhysRevLett.121.211301. arXiv: 1706.02038 [hep-th].

[182] Netta Engelhardt and Aron C. Wall. "Coarse Graining Holographic Black Holes". In: *JHEP* 05 (2019), p. 160. DOI: 10.1007/JHEP05(2019)160. arXiv: 1806.01281 [hep-th].

[183] Yasunori Nomura and Grant N. Remmen. "Area Law Unification and the Holographic Event Horizon". In: *JHEP* 08 (2018), p. 063. DOI: 10.1007/JHEP08(2018)063. arXiv: 1805.09339 [hep-th].

[184] Mohsen Alishahiha et al. "The dS/dS correspondence". In: *AIP Conf. Proc.* 743 (2005). [,393(2004)], pp. 393–409. DOI: 10.1063/1.1848341. arXiv: hep-th/0407125 [hep-th].

[185] Xi Dong, Eva Silverstein, and Gonzalo Torroba. "De Sitter Holography and Entanglement Entropy". In: *JHEP* 07 (2018), p. 050. DOI: 10.1007/JHEP07(2018)050. arXiv: 1804.08623 [hep-th].

[186] Masamichi Miyaji, Tadashi Takayanagi, and Kento Watanabe. "From path integrals to tensor networks for the AdS/CFT correspondence". In: *Phys. Rev.* D95.6 (2017), p. 066004. DOI: 10.1103/PhysRevD.95.066004. arXiv: 1609.04645 [hep-th].

[187] Masamichi Miyaji et al. "Continuous Multiscale Entanglement Renormalization Ansatz as Holographic Surface-State Correspondence". In: *Phys. Rev. Lett.* 115.17 (2015), p. 171602. DOI: 10.1103/PhysRevLett.115.171602. arXiv: 1506.01353 [hep-th].

[188] Ning Bao et al. "Holographic entropy inequalities and gapped phases of matter". In: *JHEP* 09 (2015), p. 203. DOI: 10.1007/JHEP09(2015)203. arXiv: 1507.05650 [hep-th].

[189] Giancarlo Camilo, Gabriel T. Landi, and Sebas Eliëns. "On the Strong Subadditivity of the Rényi entropies for bosonic and fermionic Gaussian states". In: (2018). arXiv: 1810.07070 [cond-mat.stat-mech].

[190] Mark Van Raamsdonk. "Building up spacetime with quantum entanglement". In: *Gen. Rel. Grav.* 42 (2010). [Int. J. Mod. Phys.D19,2429(2010)], pp. 2323–2329. DOI: 10.1007/s10714-010-1034-0,10.1142/S0218271810018529. arXiv: 1005.3035 [hep-th].

[191] Juan Maldacena and Leonard Susskind. "Cool horizons for entangled black holes". In: *Fortsch. Phys.* 61 (2013), pp. 781–811. DOI: 10.1002/prop.201300020. arXiv: 1306.0533 [hep-th].

[192] Vijay Balasubramanian et al. "Multiboundary Wormholes and Holographic Entanglement". In: *Class. Quant. Grav.* 31 (2014), p. 185015. DOI: 10.1088/0264-9381/31/18/185015. arXiv: 1406.2663 [hep-th].

[193] Sepehr Nezami and Michael Walter. "Multipartite Entanglement in Stabilizer Tensor Networks". In: (2016). arXiv: 1608.02595 [quant-ph].

[194] Arpan Bhattacharyya, Tadashi Takayanagi, and Koji Umemoto. "Entanglement of Purification in Free Scalar Field Theories". In: *JHEP* 04 (2018), p. 132. DOI: 10.1007/JHEP04(2018)132. arXiv: 1802.09545 [hep-th].

[195] Pawel Caputa et al. "Holographic Entanglement of Purification from Conformal Field Theories". In: *Phys. Rev. Lett.* 122.11 (2019), p. 111601. DOI: 10.1103/PhysRevLett.122.111601. arXiv: 1812.05268 [hep-th].

[196] Ning Bao et al. "Towards a Bit Threads Derivation of Holographic Entanglement of Purification". In: *JHEP* 07 (2019), p. 152. DOI: 10.1007/JHEP07(2019)152. arXiv: 1905.04317 [hep-th].

[197] Yuya Kusuki and Kotaro Tamaoka. "Entanglement Wedge Cross Section from CFT: Dynamics of Local Operator Quench". In: (2019). arXiv: 1909.06790 [hep-th].

[198] Yuya Kusuki and Kotaro Tamaoka. "Dynamics of Entanglement Wedge Cross Section from Conformal Field Theories". In: (2019). arXiv: 1907.06646 [hep-th].

[199] Koji Umemoto. "Quantum and Classical Correlations Inside the Entanglement Wedge". In: *Phys. Rev.* D100.12 (2019), p. 126021. DOI: 10.1103/PhysRevD.100.126021. arXiv: 1907.12555 [hep-th].

[200] Mark Fannes. "A continuity property of the entropy density for spin lattice systems". In: *Communications in Mathematical Physics* 31.4 (1973), pp. 291–294.

[201] Koenraad M. R. Audenaert. "Comparisons between quantum state distinguishability measures". In: *arXiv e-prints*, arXiv:1207.1197 (2012), arXiv:1207.1197. arXiv: 1207.1197 [quant-ph].

[202] Koenraad MR Audenaert. "A sharp Fannes-type inequality for the von Neumann entropy". In: *arXiv preprint quant-ph/0610146* (2006).

[203] Chris Akers et al. "The Page Curve for Reflected Entropy". In: *to appear* (2020).

[204] Barbara M. Terhal et al. "The entanglement of purification". In: *Journal of Mathematical Physics* 43.9 (2002), pp. 4286–4298. DOI: 10.1063/1.1498001. eprint: https://doi.org/10.1063/1.1498001. URL: https://doi.org/10.1063/1.1498001.

[205] Bin Chen, Lin Chen, and Cheng-Yong Zhang. "Surface/State correspondence and $T\overline{T}$ deformation". In: (2019). arXiv: 1907.12110 [hep-th].

[206] Andrea Prudenziati. "Geometry of Entanglement". In: (2019). arXiv: 1907.06238 [hep-th].

[207] Newton Cheng. "Minimizations over Geometric Extensions in Holography". In: (2019). arXiv: 1909.09334 [hep-th].

[208] Wu-Zhong Guo. "Entanglement of purification and disentanglement in CFTs". In: (2019). arXiv: 1904.12124 [hep-th].

[209] Komeil Babaei Velni, M. Reza Mohammadi Mozaffar, and M. H. Vahidinia. "Some Aspects of Entanglement Wedge Cross-Section". In: *JHEP* 05 (2019), p. 200. DOI: 10.1007/JHEP05(2019)200. arXiv: 1903.08490 [hep-th].

[210] Ning Bao, Aidan Chatwin-Davies, and Grant N. Remmen. "Entanglement of Purification and Multiboundary Wormhole Geometries". In: *JHEP* 02 (2019), p. 110. DOI: 10.1007/JHEP02(2019)110. arXiv: 1811.01983 [hep-th].

[211] Ning Bao and Illan F. Halpern. "Conditional and Multipartite Entanglements of Purification and Holography". In: *Phys. Rev. D* 99.4 (2019), p. 046010. DOI: 10.1103/PhysRevD.99.046010. arXiv: 1805.00476 [hep-th].

[212] Koji Umemoto and Yang Zhou. "Entanglement of Purification for Multipartite States and its Holographic Dual". In: *JHEP* 10 (2018), p. 152. DOI: 10.1007/JHEP10(2018)152. arXiv: 1805.02625 [hep-th].

[213] Arpan Bhattacharyya et al. "Entanglement of Purification in Many Body Systems and Symmetry Breaking". In: *Phys. Rev. Lett.* 122.20 (2019), p. 201601. DOI: 10.1103/PhysRevLett.122.201601. arXiv: 1902.02369 [hep-th].

[214] Jonathan Harper and Matthew Headrick. "Bit threads and holographic entanglement of purification". In: (2019). arXiv: 1906.05970 [hep-th].

[215] Hayato Hirai, Kotaro Tamaoka, and Tsuyoshi Yokoya. "Towards Entanglement of Purification for Conformal Field Theories". In: *PTEP* 2018.6 (2018), 063B03. DOI: 10.1093/ptep/pty063. arXiv: 1803.10539 [hep-th].

[216] Shrobona Bagchi and Arun Kumar Pati. "Monogamy, polygamy, and other properties of entanglement of purification". In: *Physical Review A* 91.4 (2015), p. 042323.

[217] Jianxin Chen and Andreas Winter. "Non-additivity of the entanglement of purification (beyond reasonable doubt)". In: *arXiv preprint arXiv:1206.1307* (2012).

[218] Donald Marolf et al. "Hot multiboundary wormholes from bipartite entanglement". In: *Class. Quant. Grav.* 32.21 (2015), p. 215006. DOI: 10.1088/0264-9381/32/21/215006. arXiv: 1506.04128 [hep-th].

[219] Alex Peach and Simon F. Ross. "Tensor Network Models of Multiboundary Wormholes". In: *Class. Quant. Grav.* 34.10 (2017), p. 105011. DOI: 10.1088/1361-6382/aa6b0f. arXiv: 1702.05984 [hep-th].

[220] Ning Bao et al. "Holographic Tensor Networks in Full AdS/CFT". In: (2019). arXiv: 1902.10157 [hep-th].

[221] Ning Bao et al. "Beyond Toy Models: Distilling Tensor Networks in Full AdS/CFT". In: (2018). arXiv: 1812.01171 [hep-th].

[222] Ning Bao, Mudassir Moosa, and Ibrahim Shehzad. "The holographic dual of Rényi relative entropy". In: (2019). arXiv: 1904.08433 [hep-th].

[223] Kotaro Tamaoka. "Entanglement Wedge Cross Section from the Dual Density Matrix". In: *Phys. Rev. Lett.* 122.14 (2019), p. 141601. DOI: 10.1103/PhysRevLett.122.141601. arXiv: 1809.09109 [hep-th].

[224] Yuya Kusuki, Jonah Kudler-Flam, and Shinsei Ryu. "Derivation of Holographic Negativity in $AdS_3/CFT_2$". In: *Phys. Rev. Lett.* 123.13 (2019), p. 131603. DOI: 10.1103/PhysRevLett.123.131603. arXiv: 1907.07824 [hep-th].

[225] Joshua Levin, Oliver DeWolfe, and Graeme Smith. "Correlation measures and distillable entanglement in AdS/CFT". In: (2019). arXiv: 1909.04727 [hep-th].

[226] Donald Marolf. "CFT sewing as the dual of AdS cut-and-paste". In: *JHEP* 02 (2020), p. 152. DOI: 10.1007/JHEP02(2020)152. arXiv: 1909.09330 [hep-th].

[227] Ning Bao and Newton Cheng. "Multipartite Reflected Entropy". In: *JHEP* 10 (2019), p. 102. DOI: 10.1007/JHEP10(2019)102. arXiv: 1909.03154 [hep-th].

[228] Jinwei Chu, Runze Qi, and Yang Zhou. "Generalizations of Reflected Entropy and the Holographic Dual". In: (2019). arXiv: 1909.10456 [hep-th].

[229] Xi Dong and Donald Marolf. "One-loop universality of holographic codes". In: (2019). arXiv: 1910.06329 [hep-th].

[230] Christopher David White, ChunJun Cao, and Brian Swingle. "Conformal field theories are magical". In: (July 2020). arXiv: 2007.01303 [quant-ph].

[231] Wolfgang Dür, Guifre Vidal, and J Ignacio Cirac. "Three qubits can be entangled in two inequivalent ways". In: *Physical Review A* 62.6 (2000), p. 062314.

[232] Samir D. Mathur. "The Information paradox: A Pedagogical introduction". In: *Class. Quant. Grav.* 26 (2009), p. 224001. DOI: 10.1088/0264-9381/26/22/224001. arXiv: 0909.1038 [hep-th].

[233] Chris Akers et al. "Quantum Maximin Surfaces". In: (2019). arXiv: 1912.02799 [hep-th].

[234] Yuya Kusuki et al. "Looking at Shadows of Entanglement Wedges". In: (Dec. 2019). arXiv: 1912.08423 [hep-th].

[235] Yasunori Nomura. "Spacetime and Universal Soft Modes — Black Holes and Beyond". In: *Phys. Rev. D* 101.6 (2020), p. 066024. DOI: 10.1103/PhysRevD.101.066024. arXiv: 1908.05728 [hep-th].

[236] Yasunori Nomura. "The Interior of a Unitarily Evaporating Black Hole". In: (Nov. 2019). arXiv: 1911.13120 [hep-th].

[237] Adam R. Brown et al. "The Python's Lunch: geometric obstructions to decoding Hawking radiation". In: (Nov. 2019). arXiv: 1912.00228 [hep-th].

[238] Tianyi Li, Jinwei Chu, and Yang Zhou. "Reflected Entropy for an Evaporating Black Hole". In: (June 2020). arXiv: 2006.10846 [hep-th].

[239] Raphael Bousso, Venkatesa Chandrasekaran, and Arvin Shahbazi-Moghaddam. "From black hole entropy to energy-minimizing states in QFT". In: *Phys. Rev.* D101.4 (2020), p. 046001. DOI: 10.1103/PhysRevD.101.046001. arXiv: 1906.05299 [hep-th].

[240] Raphael Bousso et al. "Quantum focusing conjecture". In: *Phys. Rev.* D93.6 (2016), p. 064044. DOI: 10.1103/PhysRevD.93.064044. arXiv: 1506.02669 [hep-th].

[241] Thomas Hartman. *Entanglement Entropy at Large Central Charge*. 2013. arXiv: 1303.6955 [hep-th].

[242] Thomas Hartman and Juan Maldacena. "Time Evolution of Entanglement Entropy from Black Hole Interiors". In: *JHEP* 05 (2013), p. 014. DOI: 10.1007/JHEP05(2013)014. arXiv: 1303.1080 [hep-th].

[243] Pankaj Chaturvedi, Vinay Malvimat, and Gautam Sengupta. "Holographic Quantum Entanglement Negativity". In: *JHEP* 05 (2018), p. 172. DOI: 10.1007/JHEP05(2018)172. arXiv: 1609.06609 [hep-th].

[244] Mukund Rangamani and Massimiliano Rota. "Comments on Entanglement Negativity in Holographic Field Theories". In: *JHEP* 10 (2014), p. 060. DOI: 10.1007/JHEP10(2014)060. arXiv: 1406.6989 [hep-th].

[245] Jonah Kudler-Flam and Shinsei Ryu. "Entanglement negativity and minimal entanglement wedge cross sections in holographic theories". In: *Phys. Rev. D* 99.10 (2019), p. 106014. DOI: 10.1103/PhysRevD.99.106014. arXiv: 1808.00446 [hep-th].

[246] Jonah Kudler-Flam, Yuya Kusuki, and Shinsei Ryu. "Correlation measures and the entanglement wedge cross-section after quantum quenches in two-dimensional conformal field theories". In: (2020). arXiv: 2001.05501 [hep-th].

[247] W. Dur, G. Vidal, and J.I. Cirac. "Three qubits can be entangled in two inequivalent ways". In: *Phys. Rev. A* 62 (2000), p. 062314. DOI: 10.1103/PhysRevA.62.062314. arXiv: quant-ph/0005115.

[248] Mukund Rangamani and Massimiliano Rota. "Entanglement structures in qubit systems". In: *J. Phys. A* 48.38 (2015), p. 385301. DOI: 10.1088/1751-8113/48/38/385301. arXiv: 1505.03696 [hep-th].

[249] Frank Verstraete et al. "Four qubits can be entangled in nine different ways". In: *Physical Review A* 65.5 (2002), p. 052112.

[250] Jordan S. Cotler et al. "Black Holes and Random Matrices". In: *JHEP* 05 (2017). [Erratum: JHEP 09, 002 (2018)], p. 118. DOI: 10.1007/JHEP05(2017)118. arXiv: 1611.04650 [hep-th].

[251] Phil Saad, Stephen H. Shenker, and Douglas Stanford. "A semiclassical ramp in SYK and in gravity". In: (2018). arXiv: 1806.06840 [hep-th].

[252] Phil Saad, Stephen H. Shenker, and Douglas Stanford. "JT gravity as a matrix integral". In: (2019). arXiv: 1903.11115 [hep-th].

[253] Chris Akers, Netta Engelhardt, and Daniel Harlow. "Simple holographic models of black hole evaporation". In: (Oct. 2019). arXiv: 1910.00972 [hep-th].

[254] Yiming Chen. "Pulling Out the Island with Modular Flow". In: *JHEP* 03 (2020), p. 033. DOI: 10.1007/JHEP03(2020)033. arXiv: 1912.02210 [hep-th].

[255] Chi-Fang Chen, Geoffrey Penington, and Grant Salton. "Entanglement Wedge Reconstruction using the Petz Map". In: *JHEP* 01 (2020), p. 168. DOI: 10.1007/JHEP01(2020)168. arXiv: 1902.02844 [hep-th].

[256] Thomas Faulkner et al. "Modular Hamiltonians for Deformed Half-Spaces and the Averaged Null Energy Condition". In: *JHEP* 09 (2016), p. 038. DOI: 10.1007/JHEP09(2016)038. arXiv: 1605.08072 [hep-th].

[257] Srivatsan Balakrishnan et al. "A General Proof of the Quantum Null Energy Condition". In: *JHEP* 09 (2019), p. 020. DOI: 10.1007/JHEP09(2019)020. arXiv: 1706.09432 [hep-th].

[258] Nima Lashkari. "Constraining Quantum Fields using Modular Theory". In: *JHEP* 01 (2019), p. 059. DOI: 10.1007/JHEP01(2019)059. arXiv: 1810.09306 [hep-th].

[259] Fikret Ceyhan and Thomas Faulkner. "Recovering the QNEC from the ANEC". In: (Dec. 2018). arXiv: 1812.04683 [hep-th].

[260] Aron C. Wall. "Lower Bound on the Energy Density in Classical and Quantum Field Theories". In: *Phys. Rev. Lett.* 118.15 (2017), p. 151601. DOI: 10.1103/PhysRevLett.118.151601. arXiv: 1701.03196 [hep-th].

[261] Raphael Bousso et al. "Proof of the Quantum Null Energy Condition". In: *Phys. Rev.* D93.2 (2016), p. 024017. DOI: 10.1103/PhysRevD.93.024017. arXiv: 1509.02542 [hep-th].

[262] Jason Koeller and Stefan Leichenauer. "Holographic Proof of the Quantum Null Energy Condition". In: *Phys. Rev.* D94.2 (2016), p. 024026. DOI: 10.1103/PhysRevD.94.024026. arXiv: 1512.06109 [hep-th].

[263] Jan De Boer and Lampros Lamprou. "Holographic Order from Modular Chaos". In: *JHEP* 06 (2020), p. 024. DOI: 10.1007/JHEP06(2020)024. arXiv: 1912.02810 [hep-th].

[264] Thomas Faulkner, Min Li, and Huajia Wang. "A modular toolkit for bulk reconstruction". In: *JHEP* 04 (2019), p. 119. DOI: 10.1007/JHEP04(2019)119. arXiv: 1806.10560 [hep-th].

[265] Edward Witten. "APS Medal for Exceptional Achievement in Research: Invited article on entanglement properties of quantum field theory". In: *Rev. Mod. Phys.* 90.4 (2018), p. 045003. DOI: 10.1103/RevModPhys.90.045003. arXiv: 1803.04993 [hep-th].

[266] Horacio Casini, Eduardo Teste, and Gonzalo Torroba. "Modular Hamiltonians on the null plane and the Markov property of the vacuum state". In: *J. Phys.* A50.36 (2017), p. 364001. DOI: 10.1088/1751-8121/aa7eaa. arXiv: 1703.10656 [hep-th].

[267] Srivatsan Balakrishnan and Onkar Parrikar. "Modular Hamiltonians for Euclidean Path Integral States". In: (Jan. 2020). arXiv: 2002.00018 [hep-th].

[268] Jun-ichirou Koga. "Asymptotic symmetries on Killing horizons". In: *Phys. Rev. D* 64 (2001), p. 124012. DOI: 10.1103/PhysRevD.64.124012. arXiv: gr-qc/0107096.

[269] Abhay Ashtekar, Christopher Beetle, and Jerzy Lewandowski. "Geometry of generic isolated horizons". In: *Class. Quant. Grav.* 19 (2002), pp. 1195–1225. DOI: 10.1088/0264-9381/19/6/311. arXiv: gr-qc/0111067.

[270] J. J Bisognano and E. H. Wichmann. "On the Duality Condition for Quantum Fields". In: *J. Math. Phys.* 17 (1976), pp. 303–321. DOI: 10.1063/1.522898.

[271] Robert M Wald. *General relativity*. University of Chicago press, 2010.

[272] Tadashi Takayanagi. "Holographic Dual of BCFT". In: *Phys. Rev. Lett.* 107 (2011), p. 101602. DOI: 10.1103/PhysRevLett.107.101602. arXiv: 1105.5165 [hep-th].

[273] Ioanna Kourkoulou and Juan Maldacena. "Pure states in the SYK model and nearly-$AdS_2$ gravity". In: (July 2017). arXiv: 1707.02325 [hep-th].

[274] Raphael Bousso et al. "Null Geodesics, Local CFT Operators and AdS/CFT for Subregions". In: *Phys. Rev. D* 88 (2013), p. 064057. DOI: 10.1103/PhysRevD.88.064057. arXiv: 1209.4641 [hep-th].

[275] Veronika E. Hubeny and Mukund Rangamani. "Causal Holographic Information". In: *JHEP* 06 (2012), p. 114. DOI: 10.1007/JHEP06(2012)114. arXiv: 1204.1698 [hep-th].

[276] Charles Fefferman and C. Robin Graham. "The ambient metric". In: *Ann. Math. Stud.* 178 (2011), pp. 1–128. arXiv: 0710.0919 [math.DG].

[277] Eric Gourgoulhon. "3+1 formalism and bases of numerical relativity". In: (Mar. 2007). arXiv: gr-qc/0703035.

[278] Nima Lashkari et al. "Gravitational positive energy theorems from information inequalities". In: *Progress of Theoretical and Experimental Physics* 2016.12 (2016), p. 12C109. ISSN: 2050-3911. DOI: 10.1093/ptep/ptw139. URL: http://dx.doi.org/10.1093/ptep/ptw139.

[279] William Donnelly and Laurent Freidel. "Local subsystems in gauge theory and gravity". In: *Journal of High Energy Physics* 2016.9 (2016). ISSN: 1029-8479. DOI: 10.1007/jhep09(2016)102. URL: http://dx.doi.org/10.1007/JHEP09(2016)102.

[280] Steven Carlip and Claudio Teitelboim. "The off-shell black hole". In: *Classical and Quantum Gravity* 12.7 (1995), 1699–1704. ISSN: 1361-6382. DOI: 10.1088/0264-9381/12/7/011. URL: http://dx.doi.org/10.1088/0264-9381/12/7/011.

[281] Sergio Doplicher and Roberto Longo. "Standard and split inclusions of von Neumann algebras". In: *Invent. Math.* 75 (1984), pp. 493–536. DOI: 10.1007/BF01388641.

[282] Donald Marolf. "Microcanonical Path Integrals and the Holography of small Black Hole Interiors". In: *JHEP* 09 (2018), p. 114. DOI: 10.1007/JHEP09(2018)114. arXiv: 1808.00394 [hep-th].

[283] W. Israel. "Thermo field dynamics of black holes". In: *Phys. Lett. A* 57 (1976), pp. 107–110. DOI: 10.1016/0375-9601(76)90178-X.

[284] Gary T. Horowitz and Diandian Wang. "Gravitational Corner Conditions in Holography". In: *JHEP* 01 (2020), p. 155. DOI: 10.1007/JHEP01(2020)155. arXiv: 1909.11703 [hep-th].

[285] Richard P. Woodard. "Ostrogradsky's theorem on Hamiltonian instability". In: *Scholarpedia* 10.8 (2015), p. 32243. DOI: 10.4249/scholarpedia.32243. arXiv: 1506.02210 [hep-th].

[286] Thomas Faulkner et al. "Gravitation from Entanglement in Holographic CFTs". In: *JHEP* 03 (2014), p. 051. DOI: 10.1007/JHEP03(2014)051. arXiv: 1312.7856 [hep-th].

[287] Stefan Leichenauer, Adam Levine, and Arvin Shahbazi-Moghaddam. "Energy density from second shape variations of the von Neumann entropy". In: *Phys. Rev. D* 98.8 (2018), p. 086013. DOI: 10.1103/PhysRevD.98.086013. arXiv: 1802.02584 [hep-th].

[288] William R. Kelly and Aron C. Wall. "Holographic proof of the averaged null energy condition". In: *Phys. Rev.* D90.10 (2014). [Erratum: Phys. Rev.D91,no.6,069902(2015)], p. 106003. DOI: 10.1103/PhysRevD.90.106003,10.1103/PhysRevD.91.069902. arXiv: 1408.3566 [gr-qc].

[289] Leonard Susskind. "Entanglement is not enough". In: *Fortsch. Phys.* 64 (2016), pp. 49–71. DOI: 10.1002/prop.201500095. arXiv: 1411.0690 [hep-th].